Experimental Study and Modelling of Asphaltene Precipitation Caused by Gas Injection

Verdier, Sylvain Charles Roland

Publication date:
2006

Document Version
Publisher's PDF, also known as Version of record

Experimental Study and Modelling of Asphaltene Precipitation Caused by Gas Injection

Sylvain Verdier

2006

Ph.D. Thesis

DTU

TECHNICAL UNIVERSITY OF DENMARK
DEPARTMENT OF CHEMICAL ENGINEERING
CENTER FOR PHASE EQUILIBRIA AND SEPARATION PROCESSES (IVC-SEP)

Experimental Study and Modelling of Asphaltene Precipitation Caused by Gas Injection

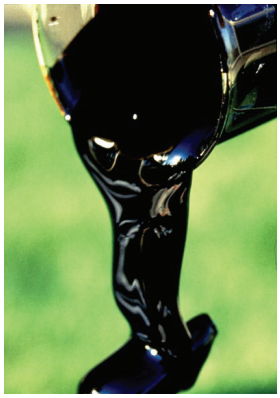

PhD Thesis

Sylvain Verdier

April 2006

IVC-SEP - Centre for Phase Equilibria and Separation Processes
Department of Chemical Engineering
Technical University of Denmark, Lyngby, Denmark

Supervisors:
Dr. Simon I. Andersen
Pr. Erling H. Stenby

ISBN 87-91435-42-0
Printed by Book Partner, Nørhaven Digital.
Copenhagen, Denmark.

Preface

This thesis is submitted as a partial fulfilment of the requirements for the PhD-degree at Danmarks Tekniske Universitet (the Technical University of Denmark). The project has been financially supported by IVC-SEP.

This PhD comprises the work carried out from May 2003 to April 2006 in the research group Centre for Phase Equilibria and Separation Processes (IVC-SEP) at the Institut for Kemiteknik (Department of Chemical Engineering). The work has been supervised by Pr. Erling H. Stenby and Dr. Simon Andersen.

The topic was the experimental study and modelling of asphaltene precipitation caused by gas injection.

Abstract

Amongst the different possible solid deposits occurring in the oil industry, asphaltenes might be the most studied and the less understood issue. The problems due to the heaviest and molar polar fraction of petroleum affect reservoirs, wells and even refinery processes, to name a few of their nuisances. The colloidal behaviour of asphaltenes in crude oil, the lack of knowledge about its structure, the complexity of the aggregation, flocculation, precipitation or deposition processes make this topic quite complex and interesting.

During the Enhanced Oil Recovery (EOR) process, gases such as carbon dioxide or nitrogen may be injected in order to decrease the viscosity of the oil or to push it towards the well, whether it is miscible or not. For instance, 20,000 tons per day of CO_2 are currently delivered to oil fields for EOR projects. Total production due to CO_2 injection is a little less than 200,000 barrel/day. However, this injection clearly modifies the composition of the oil and its conditions. Therefore, asphaltenes have the tendency to flocculate and precipitate during such modifications. There is no predictive tool so far since models are descriptive at the best. The technical solutions are expensive (injection solvent, cleaning pipes). Thus, studying asphaltene precipitation during gas injection and trying to get more knowledge about asphaltene stability seemed relevant.

In Chapter I, a brief review of asphaltene science is presented as well as the problems that petroleum industry has to cope with because of asphaltenes.

In Chapter II, some input parameters used for the modelling of asphaltene phase behaviour are determined (namely the solubility parameter of crude oils and asphaltenes as well as the critical constants of asphaltenes). The effect of pressure is emphasized.

In Chapter III, asphaltene stability in presence of carbon dioxide and methane is investigated for several crude oils over a wide range of pressures and temperatures with a novel high-pressure experimental set-up. The effects of pressure and temperature are identified.

In Chapter IV, calorimetry is used to obtain more understanding about asphaltene precipitation. Experiments are performed with dead and live oils and compared to model

systems. Two techniques were used for that matter: high-pressure scanning calorimetry and isothermal titration calorimetry.

In Chapter V, a model taking into account aggregation and based on cubic equations is presented. It is tested with several crude oils and asphaltene solutions.

Conclusions and future challenges are presented in Chapter VI. The additional information is gathered in Appendixes.

Résumé på Dansk

Af de forskellige mulige faste aflejringer, der forekommer i olieindustrien, er asfaltener måske dem, der hyppigst studeres og mindst forstås. De problemer, der skyldes den tungeste og molære, polære fraktion af jordolien, påvirker reservoirer, kilder og endog raffineringsprocesserne, for blot at nævne nogle få af generne. Asfaltenernes kolloide opførsel i råolien, manglen på viden om dens struktur, kompleksiteten af aggregeringen, flokkulationen, udfældningen eller aflejringsprocesser gør dette emne temmelig sammensat og interessant.

Under Enhanced Oil Recovery (EOR) processen kan gasser som kuldioxyd eller nitrogen injiceres for at formindske oliens viskositet eller puffe den mod kilden, enten den er blandbar eller ej. For eksempel leveres der for tiden 20.000 tons CO2 dagligt til oliefelter til EOR projekter. Den samlede produktion, der skyldes CO2 injektion er lidt under 200.000 tønder om dagen. Denne injektion ændrer imidlertid klart sammensætningen af olien og dens beskaffenhed. Derfor har asfaltener en tendens til at flokkulere og udfældes under sådanne ændringer. Så vidt er der ingen redskaber til forudsigelse, da modellerne højest er beskrivende. De tekniske løsninger er dyre (injektionsopløsningsmiddel, rengøring af rør). Således syntes det relevant at studere asfalteneudfældning under gasinjektion og forsøge at få mere viden om asfaltenestabilitet.

I kapitel I gives et kort overblik over asfaltenevidenskab og de problemer, som olieindustrien skal slås med på grund af asfaltener.

I kapitel II fastlægges nogle inputparametre, der bruges til modellering af asfaltenefaseopførslen (det vil sige opløselighedsparameteret for råolierne og asfaltenerne så vel som asfaltenernes kritiske konstanter). Virkningen af trykket fremhæves.

I kapitel III udforskes asfaltenestabilitet i nærværelse af kuldioxyd og metan for flere råolier i et bredt udvalg af tryk og temperaturer med et helt nyt højtryksekseperimentelt udstyr. Virkningerne af tryk og temperatur bestemmes.

I kapitel IV bruges kalorimetri til at få mere forståelse af asfalteneudfældning. Eksperimenter foretages med døde og levende olier og sammenlignes med modelsystemer. To teknikker blev brugt til dette formål: højtrykksscanning kalorimetri og isotermisk titreringskalorimetri.

I kapitel 5 præsenteres en model, som tager aggregering i betragtning, og som er baseret på kubiske ligninger. Den afprøves med forskellige råolier og asfalteneopløsninger.

Konklusioner og fremtidige udfordringer fremlægges i kapitel VI. Yderligere oplysninger er samlet i appendikserne.

Table of Contents

List of Appendixes

Abbreviations

Abbreviation	Description
AAD	Average Absolute Deviation
APE	Asphaltene Phase Envelope
API	American Petroleum Institute gravity
ATM	American Society for Testing and Materials
BBL	Barrel = 158.98 L
CII	Colloidal Instability Index
CMC	Critical Micellar Concentration
CNAC	Critical Nano-Aggregate Concentration
CPA	Cubic Plus Association
DSC	Differential Scanning Calorimetry
EOR	Enhanced Oil Recovery
EOS	Equation of State
FOT	Flocculation Onset Titration
FTIR	Fourier Transform Infrared Spectroscopy
GLR	Gas Liquid Ratio
GPC	Gel Permeation Chromatography
HP	High Pressure
HT	High Temperature
ITC	Isothermal Titration Calorimetry
LLE	Liquid-liquid equilibrium
MAB	Methanol-Acetone-Benzene mixtures
PPM	Parts Per Million (1 ppm = 1 mg/L)
PR	Peng-Robinson
RI	Refractive Index

SAGD	Steam Assisted Gravity Drainage
SANS	Small Angle Neutron Scattering
SARA	Saturates-Aromatics-Resins-Asphaltenes
SAXS	Small Angle X-ray Scattering
SDS	Solid Detection System
SDS	Sodium Dodecyl Sulphate
SEC	Size Exclusion Chromatography
SLE	Solid-Liquid Equilibrium
SRK	Soave-Redlich-Kwong
SPE	Society of Petroleum Engineers
SPECS	In-house PVT software
STO	Stock Tank Oil
TOAM	Thermo Optical Analysis by Microscopy
VAPEX	Vapour Extraction Process
VLE	Vapour-liquid equilibrium
VPO	Vapour Pressure Osmometry

Definitions

API: The API (American Petroleum Institute) gravity is used in the oil industry to describe the gravity of an oil and helps describing it (from "light" to "extra heavy"). The equation below links the specific gravity to the API scale:

$$Degress\ API = \frac{141.5}{specific\ gravity\ at\ 60°F/60°F} - 131.5$$

Oil	Degree API
Light	> 31.1
Medium	> 22.3
Heavy	> 10
Extra heavy	< 10

Classification of oils according to API

Asphalt: Asphalt is a type of bitumen, a highly viscous liquid that occurs naturally in most crude petroleums. Asphalt can be separated from the other components in crude oil (such as naphtha, gasoline and diesel) by the process of fractional distillation, usually under vacuum conditions..

Asphaltenes: wax-free material insoluble in n-heptane but soluble in hot benzene (IP 143)

Association: see solvation

Bitumen: fraction extractable from a sedimentary rock with organic solvents. (Tissot and Welte, 1984). Bitumen is a category of organic liquids which are highly viscous, black, sticky and wholly soluble in carbon disulfide. Asphalt and tar are the most common forms of bitumen.

Component: set of substances or cuts grouped for simulation purposes (Montel, 2004)

Constituent: pure substance which has been identified and subjected to quantitative analysis (Montel, 2004)

Cut: set of substances subjected to global quantitative analysis and presenting identical behaviour in relation to an analysis method (Montel, 2004).

First order transition: A transition in which the molar Gibbs energies or molar Helmholtz energies of the two phases (or chemical potentials of all components in the two phases) are equal at the transition temperature, but their first derivatives with respect to temperature and pressure (for example, specific enthalpy of transition and specific volume) are discontinuous at the transition point, as for two dissimilar phases that coexist

and that can be transformed into one another by a change in a field variable such as pressure, temperature, magnetic or electric field (Clark et al., 1994).

Flocculation: The process of adding reagents to facilitate the removal of suspended solids and colloidal particles (less than 1 micron). It is used in the final stage of solids-liquids separation for large water treatment systems, either via settling, flotation or filtration. The coagulant is the reagent that destabilized the solids and causes them to flocculate (come together and grow till they are heavy enough to sink).

Glass transition: A second-order transition in which a supercooled melt yields, on cooling, a glassy structure. Below the glass-transition temperature the physical properties vary in a manner similar to those of the crystalline phase (Clark et al., 1994)

Kerogen: it designates the organic constituent of the sedimentary ricks that is neither soluble in aqueous alkaline solvents nor in the common organic solvents. Sometimes, it is used for the total organic matter of sedimentary rocks but it seems to be a misuse (Tissot and Welte, 1984)

Lithology: see Petrology

Lyophilic: solvent loving

Lyophobic: solvent hating

Maltenes: mixture of the resins and oils obtained as filtrates from the asphaltene precipitation (Andersen and Speight, 2001)

Oligomer: in chemistry, an oligomer consists of a finite number of monomer units ("oligo" is Greek for "a few"), in contrast to a polymer which, at least in principle, consists of an infinite number of monomers.

Order-disorder transition: A transition in which the degree of order of the system changes. Three principal types of disordering transitions may be distinguished: (i) positional disordering in a solid, (ii) orientational disordering which may be static or dynamic and (iii) disordering associated with electronic and nuclear spin states (Clark et al., 1994).

Petrology: it is a field of geology which focuses on the study of rocks and the conditions by which they form. There are three branches of petrology, corresponding to the three types of rocks: igneous, metamorphic, and sedimentary.

Porphyrines: A porphyrin is a heterocyclic macrocycle made from 3 pyrrole subunits and one pyrroline subunit, and linked on opposite sides through 4 methine bridges.

Precipitation: The formation of a solid phase within a liquid phase (Clark et al., 1994).

Pyridine: Pyridine C_5H_5N is a simple heterocyclic aromatic organic compound that is structurally related to benzene, with one CH group in the six-membered ring replaced by a nitrogen atom.

Pyrrole: Pyrrole, or pyrrol, is a heterocyclic aromatic organic compound, a five-membered ring with the formula C_4H_5N.

Second-order transition: A transition in which a crystal structure undergoes a continuous change and in which the first derivatives of the Gibbs energies (or chemical potentials) are continuous but the second derivatives with respect to temperature and pressure (i.e. heat capacity, thermal expansion, compressibility) are discontinuous (Clark et al., 1994).

Sedimentation: Process by which solid material settles out of a suspension in a liquid medium under the opposing forces of gravitation and buoyancy.

Solvation: when specific chemical forces act between molecules, there is a possibility of complex formation. The complexes cannot be isolated usually but their existence is certain from measurements such as spectroscopic studies. Hydrogen bonding is an example as well as Lewis acid/base interactions. When **complexation** occurs between molecules that are all from the same component, the phenomenon is called **association**. When complexation occurs between molecules that are from different components, the phenomenon is called **solvation** (Elliott and Lira, 1999).

Stacking: Stacking in supramolecular chemistry refers to a stacked arrangement of aromatic molecules, which interact through aromatic interactions. The most popular example of a stacked system is found from consecutive base pairs in DNA.

Thiophene: it (C_4H_4S) is a heterocyclic aromatic organic compound. It is aromatic because one of the two lone electron pairs of the sulfur atom contributes to the delocalized pi electron system.

Wax: paraffinic waxes are n-alkanes with n greater than 17.

Literature

Andersen, S.I., Speight J.G., Petroleum resins: separation, character, and role in petroleum, Petroleum Science and Technology (2001), 19, 1 – 34

Clark J.B., Hastie J.W., Kihlborg L.H.E., Metselaar R., Thackeray M.M., Definitions of terms relating to phase transitions of the solid state, Pure &App. Chem. (1994), 66, 577-594

Elliott J.R., Lira C.T., Introductory chemical engineering thermodynamics, Prentice Hall PTR, Upper Saddle River, 1999

Montel F., Petroleum Thermodynamics, Total, 2004

Tissot B.P., Welte D.H., Petroleum formation and occurrence, Second Edition, Ed. Springer-Verlag, Berlin, 1984

University of Calgary: www.ucalgary.ca/~schramm/lyophil.htm

Wikipedia Encyclopaedia: www.wikipedia.com

Acknowledgments

A PhD is a long journey. It goes from painful to happy and thrilling moments, accompanied by hopeless instants of doubts, the main questions being “what I am doing here?” or “what is the point?”. Fortunately, one is not alone to go through this three-year expedition.

First, I thank Professor Erling Stenby for making this PhD possible and giving me the chance to work in such a creative and high-quality environment. I thank him for his continuous support and his assistance.

I express my deep and sincere gratitude to Dr. Simon I. Andersen, for leading me through the dark world of asphaltenes. His guidance, his impressive knowledge of the literature and the friendly atmosphere he initiated transformed these three years in a very rich and human experience. Tusind tak Simon! Jeg var meget stolt at arbejde med dig.

I would like to thank the administrative, technical and academic staff of IVC-SEP for helping me in many different ways, especially Annelise Lerche Kofod, Anne-Louise Biede, Zacarias Tecle or Povl Andersen to name a few. I should also express gratitude to the two Master students I worked with, Diep Duong and Veronica Torcal-Garcia, for our fruitful collaboration and their dedication.

I spent more than six months in Pau, at the Laboratoire des Fluides Complexes of the University of Pau and at the TOTAL Research Centre. The various stays I had there were incredibly rich from a scientific and personal point of view. I am grateful to all the people who helped me there, especially to Associate Professor Hervé Carrier for his guidance, his patience, his time and his friendship; to Professor Jean-Luc Daridon for his help and the fruitful discussions; to Associate Professor David Bessières and Dr. Frédéric Plantier for their priceless help in and out of the laboratory; to my fellow PhD students from Pau

for sharing these very special moments, especially Valérie Montel, Carlos Canelon and Michel Milhet.

I am very grateful to TOTAL for partially funding the various stays in Pau and giving me the opportunity to work in their research centre (CSTJF, Pau) and to attend some very useful and interesting internal courses. A very special thank to Dr. Honggang Zhou who welcome me in his office, answered all my questions (even when he was travelling around the world) and who always found time for me.

I cannot forget the ones sharing the daily life at DTU and in Denmark. Many of them are now scattered all over the world. So, friends of Denmark, Argentina, Spain, Colombia, Mexico, France, Italy, Ireland, England, Germany, Portugal, Greece and so on, I am grateful to all of you for many different reasons. You all contributed to make these three years a very, very special time of my life (with a special mention to Géraldine Vigan-Guyet and Matías Monsalvo).

Last - but not least - many thoughts to my family. Thank you for supporting all the choices I made so far. I will never be a wine-maker but I am sure you understand! A special thought for my two nephews, Antonin and the newly arrived Alexandre.

Chapter I

Introduction to Asphaltenes

Table of Contents

What are asphaltenes? How are they formed? Can they be characterized? Why do they aggregate and what are the consequences? Why do they precipitate? What happens during precipitation? What is the exact role of resins? Do asphaltenes in solution behave like in crude oil? What is the difference between flocculation and precipitation?

Most of these questions have already been discussed and studied in the literature. Nonetheless, it appears interesting to make a quick review about these issues, which are not answered for most of them.

1. Asphaltenes: definition, formation and characterization

1.1. The definition

Let us refer to the definition given by the IP 143 standard: "*the asphaltenes content of a petroleum product is the percentage by weight of wax-free material insoluble in n-heptane but soluble in hot benzene*".

This could seem like a clear and well-established definition but a quick look at the Asphaltene Standardization Discussion web site - started after the 5th International Conference on "Petroleum Phase Behaviour and Fouling" (Banff, 2004) – shows that the very definition of asphaltenes is quite controversial:

- "*I have (more or less) stopped using the term asphaltenes and instead refer to such problems as organic depositions. At least that gives me one less problem namely; explaining to the operational personnel how we can have asphaltene problems with zero asphaltene content*" (Per Fotland, Norsk Hydro AS, Bergen, Norway.)
- "*ASTM and other standards have directed our thinking toward standardized ways to isolate and quantify those materials, but after many years of testing it should be clear that what is important is not the amount of material, but its stability as a function of temperature, pressure, and composition. The continuing focus on separations illustrates the principal danger of standards: a poorly chosen standard can direct attention in the wrong direction*". (Jill Buckley, PRRC, New Mexico Tech)

These two comments summarize the questions rising even amongst experts. Why choosing n-heptane and not n-pentane? The well-known schematic representation of Long is explicit and shows the difference between those two precipitants and how they affect asphaltenes (Figure I-1). N-heptane asphaltenes are more polar and heavier than the n-pentane ones.

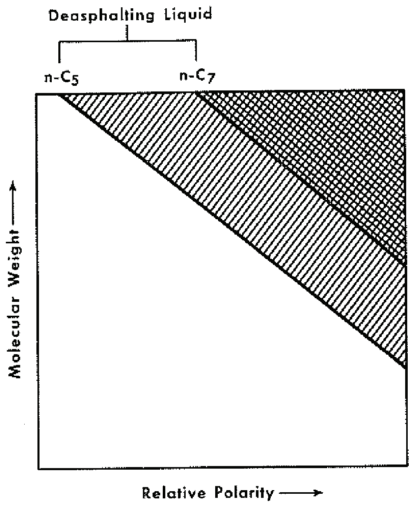

Figure I-1: Schematic representation of asphaltene composition based on molecular weight and polarity (Speight, 1994)

Furthermore, is it worth defining asphaltenes as precipitated by n-alkanes when they can also be formed by pressure depletion or temperature variations? Recent works illustrate the differences between n-heptane asphaltenes and asphaltenes caused by pressure depletion. For instance, Klein and co-workers (2005) compare n-heptane asphaltenes and the ones obtained by pressure depletion based on high resolution mass spectroscopy. They conclude that the pressure drop asphaltenes are enriched in compounds containing sulfur and oxygen, compared to the heptane insoluble asphaltenes that contain a high abundance of nitrogen-containing species. Furthermore, the heptane insoluble asphaltenes possess higher aromatic character. Aquino-Olivos et al. (2003) also investigated these differences. Size exclusion chromatography tests performed on both the live-oil-derived asphaltenes and the standard asphaltenes as precipitated by atmospheric titration on the same crude oil, revealed that the live-oil asphaltenes had apparent smaller hydrodynamic volume and narrower distributions than the standard asphaltenes for two oils. Further FTIR tests also showed large differences between standard asphaltenes and the asphaltenes obtained at high pressure filter. The latter appeared to contain more functional groups and be less saturated.

In conclusion, asphaltenes are such a vast continuum that different ways of precipitation will create different precipitated asphaltenes. Nonetheless, the definition given by the

IP143 method is the most commonly used one. Note that in this work, the asphaltenes obtained from dead oils are n-heptane precipitated as described in Appendix I-1.

The whole issue of crude oil separation is also of interest. It was reported lately that the conventional SARA separation (Saturates – Aromatics – Resins – Asphaltenes) of crude oils - which entails preliminary "deasphaltening" and subsequent separation of the soluble portion into Saturates, Aromatics and Resins - has inherent cross-contamination, and inconsistencies among reporting laboratories (Bissada et al., 2005). Besides, Andersen et al. (2001 a) submitted various crude oils to three laboratories and asked for several analysis to be performed, including the asphaltene content. The differences in asphaltene yields are strikingly large, with deviation factors up to 254.

Such results point out one of the difficulties related to asphaltenes and the lack of confidence one may have with experimental data not obtained personally. How trustful is a SARA analysis or an asphaltene content? If one works with asphaltenes precipitated by gas injection, how worthy is it to measure molar weight on n-heptane asphaltenes? These questions stress that the mere definition of asphaltenes is still an-going process.

Many well-documented monographs are available - Speight (1999), Yen and Chilingarian (1994) or Sheu and Mullins (1995) for instance- and they should be consulted for further details about the issues raised in this paragraph.

So, what is the solution if asphaltenes cannot be defined or analyzed? This will be discussed in paragraph 1.3. But, first of all, let us try to understand how asphaltenes are formed and in which oil they are present.

1.2. Asphaltene formation

This paragraph is mainly inspired by the book written by Tissot and Welte (Tissot and Welte, 1984).

The structural evolution of kerogen is due to the **burial** (increase in temperature and pressure). The temperature rise promotes the formation of bitumen and particularly of hydrocarbons. One of the proposed structures of kerogen is as follows: cyclic nuclei bearing alkyl chains and functions and linked by heteroatomic bonds and aliphatic chains. Since the conditions are changed by the burial, this structure is not anymore in

equilibrium and, hence, rearrangements take place: the **aromatization is increased** and an **ordered carbon structure** is developed. The stable structure under these conditions would be graphite but this stage is never reached in non-metamorphosed sediments. Nonetheless, the building blocks of kerogen (each nucleus made of two or more aromatic sheets) tend to become progressively parallel.

During the **diagenesis**, heteroatomic bonds are broken. Heteroatoms (especially oxygen) are partly removed as volatile compounds (H_2O, CO_2). The rupture of these bonds liberates smaller structural units made of one or several bound nuclei and aliphatic chains. The larger ones are structurally similar to kerogen but of lower molecular weight and therefore soluble: these are the asphaltenes. Here, the MAB extracts mentioned by Tissot and Welte, i.e. heavy bitumen extracted by Methanol-Acetone-Benzene mixtures, are considered as **asphaltenes**, according to the note written page 175 ("*(MAB) can be considered as being made of heavier, or more polar, asphaltenes than those extracted by chloroform or comparable solvents"*). During this first stage (the diagenesis), the larger fragments containing heteroatoms (asphaltenes and resins) are predominant.

As temperature continues to increase, the **catagenesis** starts. More bonds of various types are broken, like esters and some C-C as well, within the kerogen and within the previously generated fragments (asphaltenes, etc…). The new fragments become smaller and without oxygen. This corresponds first to the **principal phase of oil formation** and then to the stage of **wet gas and condensate** generation.
When the sediments reach the deepest part of the sedimentary basins, a general cracking of C-C occurs, both in kerogen and bitumen. Aliphatic groups that were still present in kerogen almost disappear. This is the principal phase of **dry gas formation**.

Once most labile functional groups and chains are eliminated, aromatization and polycondensation of the residual kerogen increases. Such residual kerogen is unable to generate hydrocarbons. This phase is called **metagenesis**.

Non-hydrocarbon gases – mainly nitrogen N_2 and hydrogen sulphide H_2S – may also be generated during late catagenesis and metagenesis and they are associated with methane and light hydrocarbons in certain basins. Hydrogen sulphide H_2S may be produced in large amounts by thermal cracking from kerogen and from liquid-sulphur containing compounds present in crude oils. Those two gases are of interest since they can be related to asphaltene instability.

Figure I-2 summarizes the hydrocarbon formation.

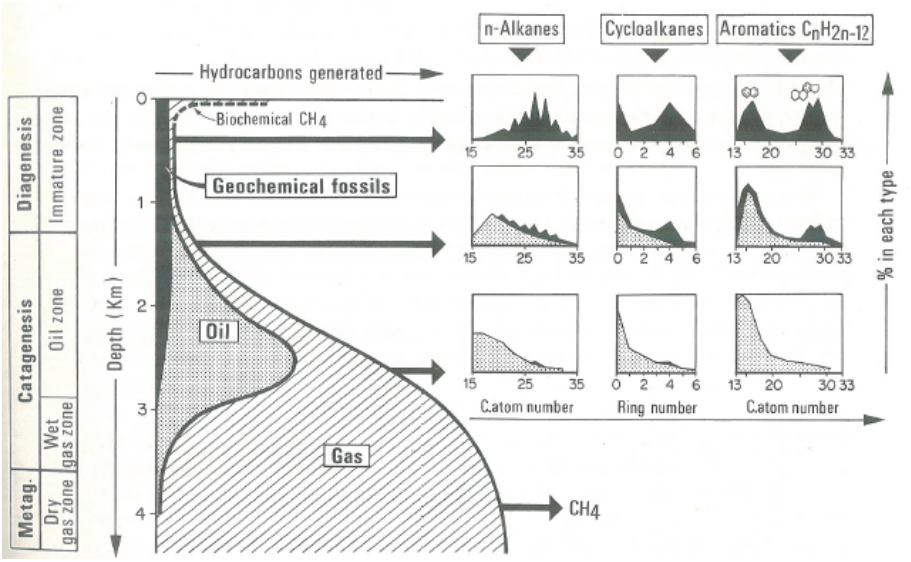

Figure I-2: General scheme of hydrocarbon formation (Tissot and Welte, 1984)

Thus, which oils contain asphaltenes? As shown in Figure I-3, **degraded crude oils** are **rich in asphaltenes**. As it was said at the beginning of this paragraph, alkanes are first removed from crude oils during biodegradation. It results in a shift towards the aromatic extremity.

Asphaltenes plus resins generally amount less than 10% in paraffinic oils and less than 20% in paraffinic-naphtenic oils. They may reach 10 to 40% in aromatic-intermediate oils. Heavy degraded oils, such as the Athabasca deposits, may contain 20 to 60% resins plus asphaltenes.

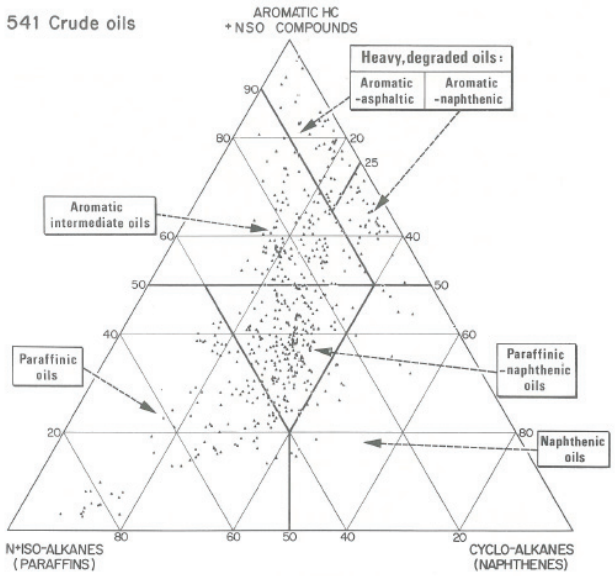

Figure I-3: Ternary diagram showing the composition of the six classes of crude oils from 541 oil fields (Tissot and Welte, 1984)

But, does it matter that much to know how much asphaltenes a crude oil contain from a production point of view? It is well-known that the asphaltene-rich oils are quite stable with respect to asphaltene precipitation. Andersen and co-workers studied several fields from Venezuela where 20 to 50 ppm were enough to cause asphaltene precipitation (Andersen et al., 2001). Per Fotland summarizes it all when he writes that "*we can have asphaltene problems with zero asphaltene content*". This issue will be further discussed in paragraph 3.5.

1.3. Asphaltene characterization

How can a molecule be characterized if its extraction is problematic and gives rise to uncertainties about its nature? What is the validity of such an analysis? This might be the most difficult dilemma about asphaltenes: extracting them from the crude oil will modify them. During the workshop about asphaltene standardization of the 5th International Conference on Petroleum Phase Behaviour and Fouling (Banff, 2004), Stig Friberg, recognized and awarded expert in colloidal science, suggested that asphaltenes should stay "*where they are*" and should be studied in situ if any results were expected. Though

this idea is very tempting, the millions of compounds present in crude oil make it difficult to obtain relevant data when asphaltenes are studied in situ. In this paragraph, several aspects of asphaltenes such as its molecular weights, composition, structure or thermophysical properties will be briefly described and commented in order to give a quick overview of the nature of asphaltenes

1.3.1. Solubility parameter of asphaltenes

Since asphaltenes are defined as a solubility class, one appealing and natural solution is the solubility parameter. The whole chapter 2 is dedicated to this tool but it can be summarized as "like dissolves like": two compounds with close solubility parameters are miscible. Hence, the distribution of asphaltenes can be done in terms of its solubility parameter in various solvents (Figure I-4).

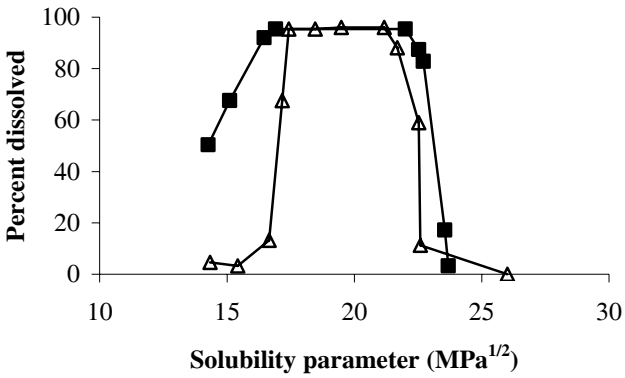

Figure I-4: Solubility parameter spectra from an asphalt (■) and its related asphaltenes (Δ) (from Yen, 1995)

Of course, in order to measure this parameter, asphaltenes have to be extracted and the issues raised in the previous paragraph are valid. A quick look at the literature shows the importance of the determination of this parameter. Amongst the families of models, which try to describe the asphaltene phase behaviour, the regular solution theory is largely represented.

Asphaltene solubility parameter is said to be between 19 and 22 $MPa^{1/2}$ (Andersen, 1999) but theoretical estimations using a group contribution method (Rogel E., 1997) found

means values between 23.1 and 26.4 $MPa^{1/2}$, depending on the molar weight. More details are available in Chapter 2, Paragraph 3.

1.3.2. Elemental composition

The choice of the precipitant and the procedure used are obviously important. For instance the H/C ratios of the n-heptane precipitate are much lower than those of the pentane precipitate, i.e. the heptane precipitate has a higher degree of aromaticity (Speight, 1994). Major differences are also observable with the N/C, O/C and S/C ratios. Asphaltene fraction contains the largest percentage of heteroatoms (N, S, O) and organometallic compounds (Ni,V, Fe) in crude oil. Table I-1 gives typical order of magnitudes for n-heptane asphaltenes.

H/C ratio	**S (w%)**	**N (w%)**	**O (w%)**	**f_a**
0.8 – 1.4	0.5 – 10.0	0.6 – 2.6	0.3 – 4.8	0.45 – 0.70

Table I-1: Composition range of n-heptane asphaltenes (Cimino et al., 1995) – f_a is the ratio of aromatic carbons in condensed rings to the total number of carbons in a molecule

The heteroatoms act as polar functional groups. The main heteroatom, sulphur, occurs in thiophenic, aliphatic structures (sulfides and disulfides) or oxidized forms (Cimino et al., 1995). Nitrogen mostly exists as pyrrolic and pyridinic and oxygen has been identified in acidic (carboxylic, phenolic) and in ketonic locations (Speight and Plancher, 1991). Most metals are in porphyrinic structures (Cimino et al., 1995).

1.3.3. Asphaltene molecules

In the literature, two structures are competing to define the asphaltene molecules: the "**continental**" (large central aromatic region with small alkyl chains on the periphery) and the "**archipelago**" models (smaller aromatic regions linked by bridging alkanes) (Figure I-5). The type of molecules will define the nature of asphaltene self-association (Yarranton, 2005):

- if asphaltenes have large aromatic cores then they are likely to form colloidal stacks held together with $\pi-\pi$ bonds.

- if the aromatic clusters in asphaltene molecules are small and dispersed, self-association is more likely to resemble polymer structures. This type of aggregate may be held together with $\pi-\pi$, acid-base, and/or hydrogen bonding. In this case, the aggregates may be considered as macromolecules. The macromolecules may freely disperse in solution or be dispersed by resins. It is also possible that resins participate in the aggregation.

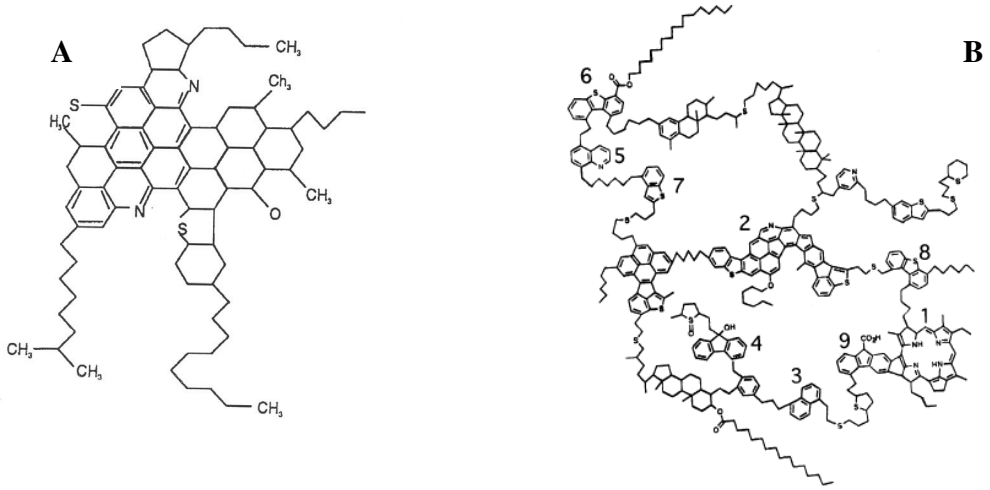

Figure I-5: Asphaltene model molecules: A, Continental structure (Speight and Moschopedis, 1981); B, Archipelago structure (Murgich et al., 1999)

Asphaltene molecular models require many approximations in their construction. Therefore, they should be used with great caution. Only semi quantitative results can be obtained from any molecular mechanics calculations (Murgich, 2005).

1.3.4. Asphaltenes in petroleum

The state of asphaltenes in crude oil and in solutions has historically been seen from a colloidal point of view (Table I-2). Yet, two views about asphaltenes are in opposition: one school of thought states that asphaltenes are colloids dispersed in crude oil and stabilized by resins and the other states that asphaltenes are dissolved in the oil. Table I-3 shows some of the arguments relative to each point of view.

Who/when	What
Nellensteyn (1923)	Introduction of colloidal theory of asphaltenes to explain the rheology of bitumens.
Sachanen (1925)	The Nellensteyn theory is extended to crude oils.
Hillman and Barnett (1937)	Asphaltenes have a chain structure formed by regions containing a number of saturated and aromatic rings connected by alkyl chains.
Pfeiffer and Saal (1940)	Asphaltenes are the centres of micelles formed by adsorption or even by absorption of resins onto the surfaces or into the interiors of asphaltene particles.
Yen at al. (1961)	Presence of C atoms of the graphitic type explained as resulting from the stacking of asphaltene molecules. Classical colloidal model assumes existence of solid particles with a core formed by stacks of asphaltenes surrounded by resins and aromatic molecules

Table I-2: Evolution of the conception of asphaltenes in petroleum (Murgich, 2005; Speight, 1994)

A recent paper explains that the colloidal models, though they were very useful in the early stages of understanding asphaltene behaviour, are overused (Sirota, 2005); indeed, the scattering data about asphaltenes in solution can also be explained by the ephemeral concentration fluctuations characteristic of a multi-component single-phase solution in the vicinity of phase separation.

Colloid	Solution
- Resins have a co-solubilization power (Porte et al., 2003) - Asphaltenes clusters in micelles (stacks from x-ray diffraction) - Aggregates in the range of colloid sizes (1 nanometre to 1 micrometre)	- Precipitation is reversible in most cases (Porte et al., 2003) - No CMC (paragraph 2.1.4) - Scattering data can also be explained with a multi-component solution (Sirota, 2005)

Table I-3: Asphaltenes in crude oil: colloidal dispersion or solution?

X-ray and neutron scattering experiments are well documented in the literature (references 2 to 19 in Sirota, 2005 for example). Various shapes and sizes were proposed (oblate or prolate cylinders, dislike shapes, fractal structures, spherical micelles…) but the analysis of scattering data depends on the model chosen, the studied regime and is based on the assumption that dissolved/dispersed asphaltenes are particles, which is still debated. So, should these results about asphaltene structures be believed?

This double nature colloid/solution is visible in the phenomena flocculation/precipitation, as it is explained in paragraph 2.3.

1.3.5. Molecular weight

Is there a more disputed, argued and controversial question than the molecular weight in the small world of asphaltene experts? This issue is still highly debated in conferences and in scientific journals these days. Already at the early stage of research about asphaltenes, the diversity of the molar weights was discussed. Thus, "*the estimation of the molecular weight of asphaltenes gives widely varying results according to the method employed. With the cryoscopic methods value ranging from 2000 to 30,000 are found.*" (Eilers, 1949).

However, nowadays, there seems to be a consensus that asphaltene monomers are relatively small and that their molecular weight should not exceed 1000 g/mol (Porte et al., 2003). The very broad range of results depends on the state of aggregation, thus depends on the technique, the temperature, the solvent and the concentration.
The results obtained by high resolution mass spectrometry (Klein et al., 2005) enable an accurate determination of the mass distribution and help understanding the composition of the different fractions. This technique is likely to bring substantial information about molecular weight and asphaltenes. But, as Irwin Wiehe recently wrote it, "*other than debating in public forums, does it really make any difference?*" (Wiehe, 2005). As a matter of fact, it does if one considers modelling, for example.

1.3.6. Thermophysical properties

There has been little work done on the thermophysical properties of asphaltenes. The most studied properties might be the solubility parameter and the density though. Both were determined experimentally or by molecular simulation. As it was said in paragraph 1.3.1, the solubility parameter of asphaltene has been reported between 19 and 26 $MPa^{1/2}$. The density is usually measured with a pycnometer and assuming that there is no excess volume. Recent values were reported between 1.17 and 1.52 g/cm^3 (Rogel and Carbognani, 2003), pointing out that the smaller the ratio H/C, the higher the density. In this study, it was also found that asphaltenes from unstable crude oils and deposits exhibit higher densities, lower hydrogen-to-carbon ratios, and higher aromaticities than asphaltenes from stable crude oils. Since density is strongly linked to the solubility parameter, this is not surprising.

Diallo et al. (2000) used molecular dynamic simulations and managed to estimate most of thermodynamic properties (molar volumes, solubility parameter, heat capacity or thermal expansivity).

Dielectric properties of asphaltenes were also investigated (Sheu et al., 1994; Pedersen, 2000). Pedersen determined static values of permittivity (dielectric constant) for various types of asphaltenes ranging between 2.48 and 2.71 at 298.15 K. He also calculated dipole moments for one type of asphaltene at 333.15 K as a function of the state of aggregation. Dipole moments could vary between 2 and 20 D.

2. Asphaltenes and Aggregation

Aggregation strongly affects asphaltenes: self-association, flocculation, precipitation, interaction with resins. This paragraph gives a brief overview of these phenomena.

2.1. Aggregation and intermolecular forces

"A most important physical property of colloidal dispersions is the tendency of the particles to aggregate. Encounters between particles dispersed in liquid media occur frequently and the stability of a dispersion is determined by the interaction between the particles during these encounters. […] The overall situation is often very complicated" (Shaw, 1992). In this paragraph, the relative importance of intermolecular forces in the asphaltene aggregation process is studied and their relationships to stability.

It is important to understand that aggregation affects asphaltenes at several levels:

- First, asphaltene monomers self-associate. Hydrogen bonds are mainly responsible for such aggregation.
- Then, flocculation and precipitation are due to the aggregation of these "macro-molecules" constituted of aggregated asphaltene monomers. Dispersion is the key force in this process.

A short summary about intermolecular forces is available in Appendix I-2.

2.1.1. The self-association: CNAC and energies

As VPO (Vapour Pressure Osmometry) and ITC (Isothermal Titration Calorimetry) measurements showed it (Wiehe, 2005; Merino-Garcia, 2003), aggregation starts at very low concentration and it is almost impossible to study the monomer since the forces driving the aggregation are quite strong. As it was mentioned in a recent paper (Porte et al., 2003), "*if the aggregation was driven by weak dispersion forces, the aggregates in solution would coexist with a noticeable concentration of free single molecules. […] Aggregation is induced by strong specific interactions (hydrogen bonds, for instance)*".

One can wonder when aggregation starts. Merino-Garcia (2003) found that aggregation started before 34 ppm by means of calorimetry measurements of asphaltenes in toluene solutions. The **Critical Nano-Aggregate Concentration** (CNAC) was found to be

around 100 ppm for asphaltenes in toluene by high-Q ultrasonic measurements (Andreatta et al., 2005). However, in these measurements, the break in ultrasonic velocity can be subject to discussion because it is of noise level. Nonetheless, absorbance measurements in toluene seem to corroborate these results since **self-association was found to start around 100 ppm** (Castillo et al., 2001). Be that as it may, one can conclude that self-association starts at very low concentration and that asphaltene monomers are hardly found in solution. Thus, the properties of asphaltenes are the ones of the aggregates, as the VPO measurements clearly show it even below 100 ppm (Wiehe, 2005).

All these measurements were done in solutions and note in crude oils. The presence of other compounds would make it difficult to detect any change or variation. For calorimetry, for instance, Merino-Garcia (2003) found quite low energies of interactions (from **-0.6 to -7.6 kJ/mol**). He used a **step-wise growth mechanism** and assumed a molar weight of 1000 g/mol. This is less than hydrogen bonding (between -10 and -40 kJ/mol). The presence of other compounds in much higher proportions would hide the self-association phenomenon. In Merino-Garcia's work, it was also suggested that a fraction of asphaltenes could be inactive and, thus, it could explain this low energy. SEC analysis of heptane-toluene fractions asphaltenes indicated that a fraction could be inactive in the self-association process (Andersen, 1994). Besides, Merino-Garcia assumed that the interaction asphaltene-toluene was negligible compared to the interaction asphaltene-asphaltene. It may also account for the low energy of interaction.

To conclude, self-association starts at very low concentrations and hydrogen bonding are believed to be mainly responsible.

2.1.2. Van der Waals forces and aggregation

Amongst the van der Waals forces, dispersion forces are believed to be responsible of the flocculation and the precipitation processes. Each of these forces will be briefly reviewed.

- **Dispersion forces**

Murgich (Murgich, 1992) claims that dispersion forces are responsible for aggregation. However, as it was mentioned at the beginning of this paragraph, self-association is rather driven by strong interaction forces. These forces are likely to be predominant during flocculation and precipitation, as it is seen in paragraph 2.3.

- **Induction forces**

They are generally small and never exceed 7% of the total forces (Kontogeorgis, 2005). This contribution is especially small when there are no ions or charged particles present in the system, which is the case in asphaltenes aggregates.

- **Electrostatic forces**

There are several ways to represent the molecular charge distribution. One of them is called the multipolar expansion and contains a monopole that reflects the total net charge plus a dipole, a quadrupole and higher multipoles (Israelachvili, 1991). The dipole moment gives a quick estimate of the polarity of a molecule. Polar forces are **significant** when the dipole moment is **larger than 1 D** (Kontogeorgis, 2005). A few experimental determinations of the dipole moment were done: it was found between 2.5 and 5 D (Maruska and Rao, 1987) and between 2 and 20 D depending on the state of aggregation (Pedersen, 2000). Pedersen also observed a clear relationship between stability in production and polarity for toluene solutions: asphaltenes from unstable crude oils were more polar than asphaltenes from crude oils without precipitation problems. Hence, it seems that not only the dispersion forces play a part during flocculation and precipitation. Amongst the van der Waals forces, **dispersion and electrostatic forces seem** to play a key role in terms of aggregation.

2.1.3. Charge transfer interactions and aggregation

First, let us investigate the role of **hydrogen bonding**. Moschopedis and Speight (Moschopedis and Speight, 1976) demonstrated that the asphaltene and resin fractions of Athabasca bitumen participate in hydrogen-bonding interactions. The role of hydrogen bonding between asphaltene and resins was also outlined by Merino-Garcia (Merino-

Garcia, 2003) with chemically altered asphaltenes. Methylated asphaltenes showed a significant reduction in heat of interaction asphaltene-resin (up to -46%). Self-association was also influenced by the methylation (Figure I-6).

At first sight, hydrogen bond is believed to promote asphaltene aggregation since it is an attractive force and, hence, destabilize the dispersion/solution. However, as Andersen and Vigild demonstrated it with chemically altered asphaltenes (Andersen and Vigild, 2005), it appears as though the **removal of hydrogen bonding** sites leads to a **decreased stability** in toluene. Intuitively, one could think that less hydrogen bongs means more stability because it would imply less attraction between asphaltene molecules. But it does affect the asphaltene-resin interaction as well, which would explain the decrease in stability.

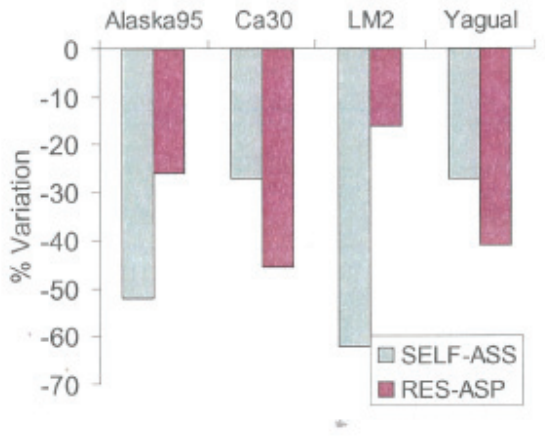

Figure I-6: Comparison of asphaltene methylation effects in self-association and interaction with resins (from Merino-Garcia, 2003)

Another type of charge transfer interaction is the **charge transfer between the π-orbitals of the aromatic rings**. This would lead to the formation of stacks, as suggested by Yen and coworkers. The model of stacked layers of asphaltenes is not fully valid though, since the alkyl branches create a steric effect and limit the chance of stacking aromatic sheets. Moreover, Andersen et al. (2005) also point out that only a fraction of the interactions among asphaltenic molecules may take place through stacking of aromatic sheets. Stacking is only one side of the issue, and more complex association schemes must be taken into account.

Electron transfer between the organic solid particles and the liquid organic phase has been mentioned as well (Siffert et al., 1994). They concluded that the more intense the transfers, the higher the charge of the particle and the better the stability of the suspension. This type of interaction is **repulsive** in this case and a higher repulsive force would improve stability.

As a conclusion, hydrogen bonds, dispersion, polar forces and $\pi - \pi$ stacking are the key forces in terms of aggregation. Nonetheless, only qualitative information has been found so far with asphaltenes. As Prausnitz et al. (1999) clearly state it, "*we must recognize at the outset that our understanding of intermolecular forces is far from complete and that quantitative results have been obtained for only simple and idealized models of real matters*". Asphaltenes are not known to be simple and idealized molecules.

2.1.4. What about the CMC?

The "CMC" (Critical Micellar Concentration) initially observed in literature by calorimetry (Andersen and Birdi, 1991) and surface tension (Rogacheva et al., 1980; Rogel et al., 2000) was an appealing idea supporting the concept of micellization to explain asphaltene aggregation.

The CMC value is between 2 and 4 g/L. Roux et al. (2001) report a change in the aggregate size for a volume fraction larger than 4% (say 5% in mass fraction, i.e. 50 g/L!) Ravey et al. (1988) observed a similar change in their SANS data when the asphaltene weight fraction was larger than 2.3% in THF. These changes cannot be attributed to the CMC. Roux and co-workers propose that the change in size is due to the interpenetration of aggregates. Indeed, when increasing the concentration, the aggregates are forces to come closer to each other (not energetically favourable). Thus rearrangement of aggregates will take place: many surfactants structures go from small micelles to long cylinders to large liposomes as the surfactant content increases above about 10% weight (Israelachvili, 1991).

So, what does happen between 2 and 4 g/L? Which phenomenon is responsible for the "pseudo-CMC"? Andreatta et al. (2005) conclude their paper saying that the reported CMC's - much higher than the CNAC's - are probably representing some higher order

aggregation. The following points bring some interesting input about the "CMC of asphaltenes" and make this concept slightly wobbly:

- Andersen et al. (2001 b) pointed out an interesting issue when they measured the influence of water on these CMC measurements. Their calorimetric titrations showed that the critical micelle concentration was highly affected by water in such a way that it must be assumed that water plays a major role in the association process.
- Sztukowski et al. (2003) could not detect any change in slope on a plot of interfacial tension versus log asphaltene concentration.
- The addition of resins (petroleum polar components) to the asphaltene system was found to eliminate the break in the curve previously assigned to CMC (Andersen et al., 2001 b).

Instead of the micellization process, asphaltene self-association rather seems to be a **step-wise process** (Merino-Garcia and Andersen, 2005). As for the "measured" CMC, if any, it is likely not to be due to the sole asphaltene structure.

2.1.5. Why is self-association not infinite?

Roux et al. (2001) used SANS measurements on asphaltene-toluene solutions, varying the asphaltene concentration. The molecular weight is stable from 0.3 to 3-4 % (volume fraction) and is around 10^5 g/mol, which means an aggregation number of 100. When the concentration is larger than 4%, the molecular weight is decreasing, which is due to repulsive forces between the aggregates.

Are chemical forces able to explain this **"saturated" behaviour**? The saturated nature of chemical forces is intimately connected with the theory of the covalent bond: once two hydrogen atoms met and have formed H_2, they are "satisfied" (or saturated). On the other hand, the purely physical force between two argon molecules, for instance, does not know such satisfaction (Prausnitz et al., 1999).

Porte et al (2003) also suggest that the **morphology and structure** of the aggregates is the key rather than the saturation of chemical forces. From scattering data, they first concluded that the dimension of the aggregates was 2 (topic that is briefly discussed in

paragraph 1.3.4). Then, the structure cannot be a fractal one since it would induce an irreversible precipitation. Here, infinite aggregation is stopped by the **high bending flexibility** of monomolecular sheets, which would sphere up and form finite vesicles. But, as they pointed it out, there is no evidence that this vesicle model is valid.

Another option to explain the limited size of aggregates - supporting this time the description of asphaltene aggregates as stacked sheets - is the **steric hindrance**. It is often advocated to be a limiting factor in the size of asphaltenes. It was suggested lately that petroleum asphaltenes have alkyl chains that act as steric hindrance for the self-association (Carbognani, 2003). These alkyl branches would limit the number of sheets per aggregate.

2.2. The role of resins

Resins and asphaltenes are usually distinguished based on the separation procedure. However, there are several ways of preparing resins and asphaltenes, resulting in slightly different compositions. Precipitation by propane separates resins and asphaltenes from the rest of the crude oil, then precipitation by n-pentane or n-heptane separates resins (soluble) from asphaltenes (insoluble) (Tissot and Welte, 1984, p 404). Resins have longer alkyl chains and smaller aromatic rings, which make them more soluble in aliphatic solvents and VPO measurements are a good tool to determine their monomeric molecular weight. VPO gave results ranging between 600 and 1000 g/mol (Speight, 1999). On the other hand, asphaltenes and resins have recently been considered an almost continuous spectrum of different polyaromatic species, each of them having its own solubility parameter (Porte et al., 2003)

The model developed by Pfeiffer and Saal in 1940 claims that asphaltenes are dispersed by the action of resins (Figure I-7). Resin-asphaltene interactions, especially through hydrogen bonding, are preferred to asphaltene association and thus they would keep these particles in suspension. The overall structure would be of a micellar type: the core of micelle is occupied by one or several asphaltene “molecules” and is surrounded by interacting resins. Then, resins are surrounded by aromatic hydrocarbons which ensure a

progressive transition to the bulk of crude oil where saturated hydrocarbons are usually predominant. (Tissot and Welte, 1984, 406-407).

As it was said in paragraph 1.3.4, this model is quite limiting but, experimentally, this stabilizing effect of resins was proved:

- 1 cm^3 of resins had the same dispersing power as 105 cm^3 of benzene (Hotier and Robin, 1983)
- Resins retard the onset flocculation point (Hammami et al, 1998; Al-Sahhaf et al., 2002)

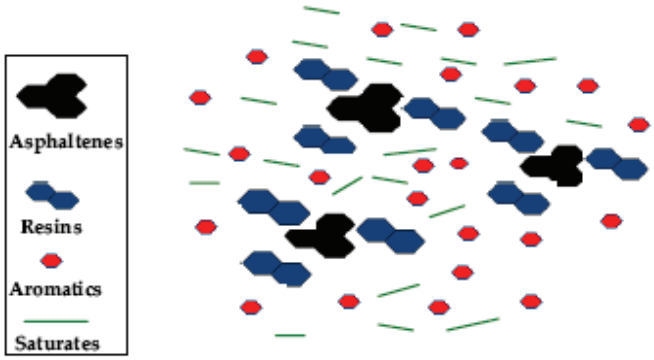

Figure I-7: State of asphaltenes in petroleum according to Pfeiffer and Saal (from Merino-Garcia, 2003)

As for the nature of the interactions between asphaltenes and resins, heats of interaction were measured for various crude oils (Merino-Garcia, 2003). They vary between -3.8 and -1.7 kJ/mol according to the type of oil and the concentration of asphaltene. This is less than hydrogen bonding and within the range of van der Waals forces. Resin interaction with asphaltenes is believed to be a combination of van der Waals, charge transfer, polar and exchange repulsion forces (Murgich, 1992). However, methylated asphaltenes showed a lower heat of interaction with resins (Merino-Garcia, 2003), which underlines the role of hydrogen bonding. Furthermore, only part of the resins are believed to interact with asphaltenes (Murgich, 2005).

Relevant literature should be consulted for further questions about resins (Merino-Garcia, 2003 or Andersen and Speight, 2001 for instance).

2.3. Asphaltene precipitation and flocculation

In this paragraph, a short introduction about colloid stability will be given as well as the difference between flocculation and precipitation and the particularities of asphaltene precipitation. But, it is important to define the difference between these processes here:

- **Flocculation** is a state of aggregation. Asphaltenes aggregates interact within each other and form "super aggregates". Flocculation is not a phase transition. Flocculation is rather related to colloids and colloidal stability than to thermodynamics and solubility.
- **Precipitation** occurs when gravity overcomes Brownian forces. The "super aggregates" are too heavy to stay in solution and, hence, they separate from the solvent phase. It is a phase separation and it can be explained in terms of solubility.

Therefore, the double nature of asphaltenes "dispersion/solution" introduced in paragraph 1.3.4 is present at this point.

2.3.1. Theory of colloid stability

Colloids can be broadly divided into two classes (Cooper, 2005):

- **Lyophilic** (solvent loving)
    - Easily dispersed by the addition of a suitable dispersing medium.
    - Usually thermodynamically stable and ΔG of formation is negative.
- **Lyophobic,** (solvent hating)
    - Require vigorous mechanical agitation to be dispersed.
    - Thermodynamically unstable, but are often metastable due to charge stabilisation through the presence of surface charges.

Colloid stability is a balance between attractive and repulsive forces: when particles collide, if the attractive forces are stronger, they aggregate and dispersion may destabilize. When repulsive forces dominate, the system will remain in a dispersed state. In general, the principal cause of aggregation is the van der Waals attractive forces between the particles, which are long-range forces. To counteract these and promote

stability, equally long-range forces are necessary. The principal stabilising options are electrostatic (the overlap of similarly charged electric double layers) and polymeric (steric stabililisation) (Shaw, 1992)

If one only considers the double-layer as source of repulsion forces, the total interaction energy is the sum of attractive forces (van der Waals forces for instance with the potential energy V_A) and repulsive forces (the double layer interaction with the potential energy V_R) and can be plotted as shown in Figure I-8:

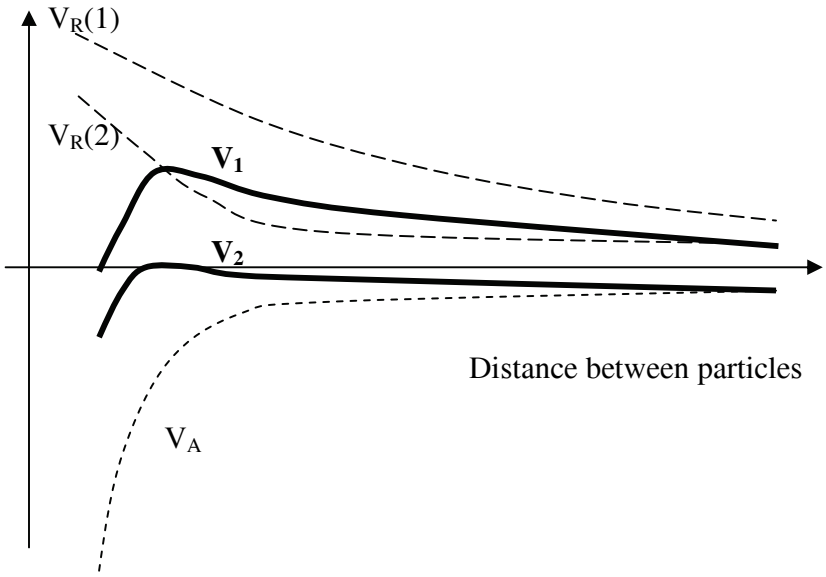

Figure I-8: Total interaction energy curve (from Shaw, 1992)

The system is **stable** if the **potential energy maximum** is large compared with the **thermal energy** kT of the particles. In the case of Figure I-8, the curve V_2 would be related to an unstable system contrary to the curve V_1. However, in many cases, steric stabilisation plays a role, especially when macromolecules are adsorbed. Quoting Shaw (Shaw, 1992): "*The adsorbed layers between the particles may interpenetatre and give a local increase in the concentration of polymer segments. Depending on the balance between polymer-polymer and polymer-dispersion medium interactions, this may lead to either repulsion or attraction.[…] If the dispersion medium is a good solvent for lyophilic moieties of the adsorbed polymer, interpenetration is not favoured and interparticle repulsion results […]. If the dispersion medium is a poor solvent, interpenetration is favoured and attraction results. The free energy change which takes place when polymer*

chains interpenetrate is influenced by factors such as temperature, pressure and solvent composition. The point at which this free energy change is equal to zero is known at the θ (theta)-point". If one reads "resins" instead of "polymers", it becomes quite familiar with the situation of asphaltenes. This is why the colloidal view of asphaltenes has been so popular over the years.

When the steric effects are added to the total interaction energy - the sum of the attractive terms V_A and the repulsive forces (electrostatic V_R and steric interactions V_S) – the potential presented in Figure I-9 can be obtained.

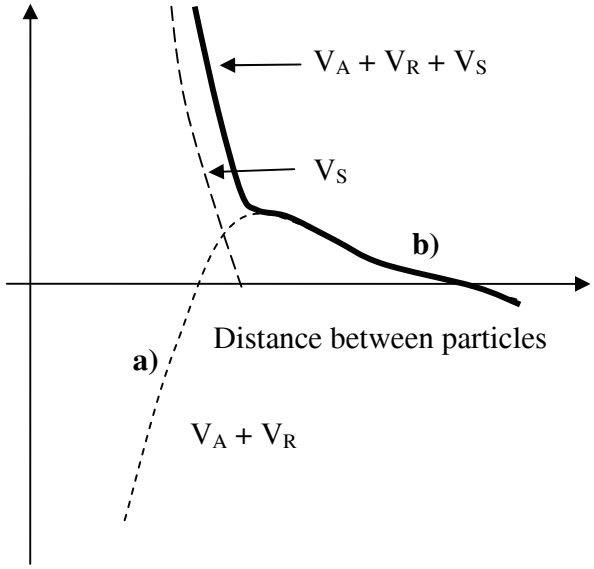

Figure I-9: Schematic interaction energy diagrams for sterically stabilised particles: a) in the absence of electric double layer repulsion; b) with electric double layer repulsion (from Shaw, 1992)

Steric interactions make the entry into a deep primary minimum virtually impossible.

An easy way to discuss the effect of temperature on stability is to study the definition of the Gibbs energy $\Delta G = \Delta H - T\Delta S$ as Napper suggested it (1977):

- If ΔH and ΔS are both positive and $\Delta H > T\Delta S$, the enthalpy change on close approach opposes flocculation (flocculation is an unstable state so with $\Delta G < 0$) whereas entropy promotes it. Because the enthalpic contribution is dominant, this

is called an **enthalpic stabilisation**. When T is increased, the entropic effect becomes more and more important and the system flocculates.

- If ΔH and ΔS are both negative and $|\Delta H| < T|\Delta S|$, this is the opposite situation: entropy favours the stability and enthalpy the flocculation. Here, flocculation occurs when T is decreased. This is an **entropic stabilisation**.
- The third scenario takes place when ΔH is positive and ΔS negative. Here, they cancel their opposite effects and, in theory, no temperature variation can induce flocculation. However, it is possible since a transition to enthalpic or entropic stabilization can happen.

Table I-4 summarises the different cases.

ΔH	ΔS	$\lvert\Delta H\rvert / T\lvert\Delta S\rvert$	ΔG	Type	Flocculation
+	+	> 1	+	Enthalpic	On heating
-	-	< 1	+	Entropic	On cooling
+	-	>, =, < 1	+	Combined	Not possible

Table I-4: Types of steric stabilization (from Napper, 1977)

Note that ΔG refers to the free energy change associated with the part of the steric barrier that is sampled during Brownian collisions. Furthermore, any physical interpretations of the signs of ΔS and ΔH must be associated with model-dependent concepts.

Table I-5 compares the steric and the charge stabilisations. Asphaltene precipitation is reversible in most cases. Therefore, steric stabilisation seems more likely to occur for asphaltene aggregates.

The DLVO theory involves estimations of the energy due to the overlap of electric double layers and the London-van der Waals energy in terms of interparticle distance. Theoretical calculations have been made for the interactions between two parallel charged plates of infinite area and thickness and between two charged spheres. As for the

steric effects, several theories have been developed over the last few decades. The work carried by Napper should be consulted for further questions related to that matter.

Steric Stabilisation	Charge Stabilisation
Insensitive to electrolyte	Coagulates on addition of electrolyte
Effective in both aqueous & non-aqueous dispersions	Effective mainly in aqueous dispersions
Effective at high and low colloid concentrations	Ineffective at high colloid concentrations
Reversible flocculation possible	Coagulation usually irreversible

Table I-5: Comparison between steric and charge stabilizations (Cooper, 2005)

The last theoretical point about colloids will be dedicated to the two types of flocculation due to steric stabilisation:

- **The depletion flocculation**: the polymer is not adsorbed, but remains free in the dispersion medium. As the colloidal particles come closer together, the inter-colloidal region consists of a region that is depleted in polymer. Solvent between the colloidal particles then tends to diffuse out to reduce the concentration gradient, causing the colloidal particles to aggregate.
- **The bridging flocculation**: a high molecular weight (i.e. very long chain) polymer is present in a very small amount (i.e. p.p.m.) and adsorbs onto the colloidal particles. The two ends of the polymer may adsorb onto different colloidal particles and then draw them together, leading to bridging flocculation.

Could asphaltene flocculation be described as the theta-point of sterically stabilized aggregates? Are resins playing the role of polymer adsorbing on asphaltene surface? Is asphaltene flocculation a bridging phenomenon due to the alkyl branches? Since flocculation and precipitation are confused most of the time, little work has effectively been achieved on asphaltene flocculation itself. Therefore, these questions will remain unanswered and as possible assumptions.

2.3.2. Asphaltene precipitation and flocculation

First, the difference between precipitation and flocculation shall be detailed: when a precipitant is added (or when a pressure or temperature modification destabilises the system), asphaltene aggregates start agglomerating: this is the **flocculation**. Then, when gravity forces can overcome Brownian forces - when particles are larger than $1\,\mu m$ (Ferworn et al., 1993) - agglomerates can settle out of solution, this is the **asphaltene precipitation**.

Let us briefly investigate this competition between diffusion (Brownian forces) and sedimentation forces (gravity and buoyancy), which is expressed by the Péclet number:

$$Pe = \frac{Gravity - induced\ motion}{Brownian\ motion} = \frac{Lv}{D} \qquad \textbf{Eq I - 1}$$

where L, v and D are respectively the characteristic length, velocity and diffusivity of the particle.

The terminal velocity is attained when the driving force on the particle and the resistance of the liquid are equal:

$$m_{particle}\left(1 - \frac{\rho_{liquid}}{\rho_{particle}}\right)g = fv \qquad \textbf{Eq I - 2}$$

where m is the mass, ρ the density, g the local acceleration due to gravity and f the frictional coefficient of the particle in the given medium.

Thus the Péclet number is:

$$Pe = m_{particle}\left(1 - \frac{\rho_{liquid}}{\rho_{particle}}\right)\frac{ag}{Df} \qquad \textbf{Eq I - 3}$$

where a is the diameter of the particle (which is assumed to be spherical).

According to the Einstein's law of diffusion, the diffusion coefficient of a suspended material at rest (i.e. no turbulence) in a steady state is related to the frictional coefficient as follows:

$$Df = kT \qquad \textbf{Eq I - 4}$$

where k is the Boltzman's constant and T the temperature.

Hence, Eq I-3 becomes:

$$Pe = m_{particle}\left(1-\frac{\rho_{liquid}}{\rho_{particle}}\right)\frac{ag}{kT} \qquad \textbf{Eq I-5}$$

A critical diameter a_c (which is the solution of $Pe=1$) can be introduced. Hence, Brownian forces take over the gravity forces when $Pe<1$ (or $a<a_c$) and vice versa. If the particle is assumed to be spherical, the diameter is easily calculated and is function of the difference in density. It slightly depends on temperature, as seen in Figure I-10. An order of magnitude of the critical diameter can be estimated for asphaltene particles. The difference in densities between the liquid medium and the particles is roughly ranging between 300 kg/m^3 (1200 – 900) and 500 kg/m^3 (1200 – 700). Of course, these values can be discussed. An average diameter of 0.7 μm can be then chosen and, hence, it is concordant with the 1 μm-value given by Ferworn and mentioned above.

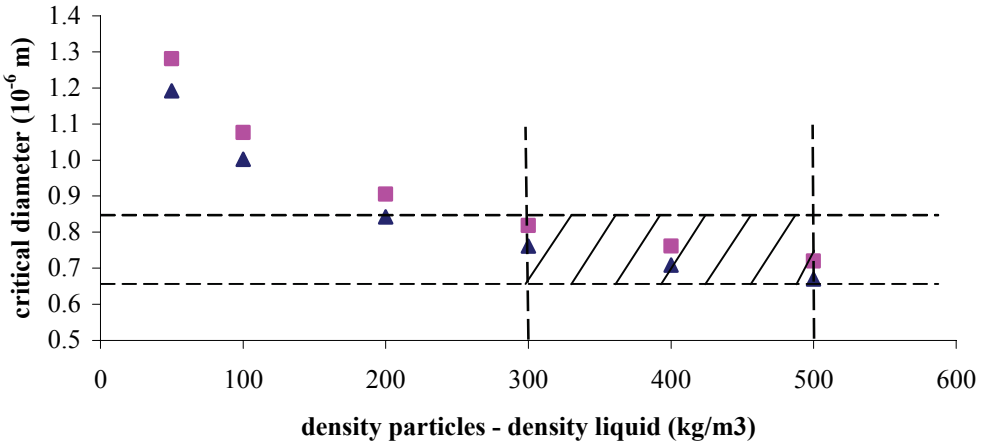

Figure I-10: Critical Sedimentation Diameter of a spherical particle (▲, 300K; ■, 400K)

Nonetheless, it is important to keep in mind that these calculations are made for individual and spherical particles at rest in a steady state. Is it the case for asphaltenes? Unfortunately, it is not. Computer simulations can be helpful to reduce these assumptions (see Padding and Louis, 2004 for the combination of hydrodynamic and Brownian forces in the sedimentation process or Odriozola et al., 2003 for the coupled aggregation and sedimentation phenomena for example).

In the literature, precipitation and flocculation are often swapped. Modelling deals with the creation of a new phase, i.e. the precipitation, but, surprisingly, this does not prevent people from modelling flocculation data as a liquid/solid or liquid/liquid equilibrium. Experimental techniques determine either flocculation or precipitation; for instance, when light scattering or light transmission techniques are used, it depends on the sensitivity of the apparatus since flocks can be detected. On the contrary, detection techniques such as the heat transfer analysis (Clarke and Pruden, 1997) or the measurement of the electrical conductivity (Fortland et al., 1993) do determine the onset of precipitation. Since flocculation precedes precipitation, the question is how distant are these two phenomena?

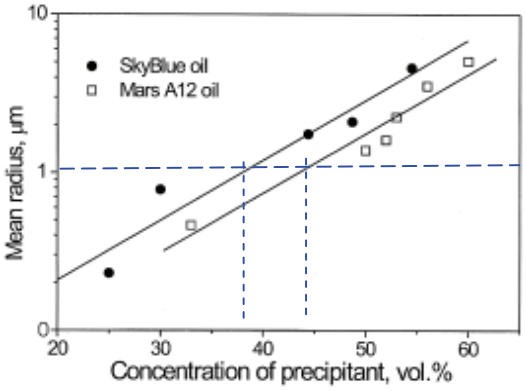

Figure I-11: Average size of asphaltenes aggregates for various concentrations of precipitants (from Burya et al., 2001)

The data obtained by Burya et al. is quite lightening (Burya et al., 2001). As seen in Figure I-11, particles with a mean diameter of 0.1 μm are detected for the SkyBlue oil at 25% precipitant but the 1 μm-size is obtained close to 40%. The same difference is observed with the MarsA12 oil. Is this 1 μm-size a reference and an agreed size as the starting point of precipitation? As it was briefly discussed above, the transition between flocculation and precipitation is quite complex since external factors such as turbulence, aggregation and size should be taken into account. Furthermore, in many experimental set-ups, there is a continuous mixing making it difficult for the particles to settle down. The transition between flocculation and precipitation is known theoretically but blurry experimentally in most cases. Thus, one should always pay attention to the use of the

terms and to the nature of experimental results when dealing with asphaltene onset determination and especially when modelling the data.

The nature of asphaltene precipitation and flocculation are not well understood in the literature: Fenistein and co-workers (Fenistein et al., 2000) explains that asphaltene flocculation is a transition between a solvated aggregation and a compaction process (compact structures were seen by radiation scattering techniques with high n-heptane contents). Asphaltene deposits are solid so is asphaltene precipitation a solid-liquid equilibrium? Precipitation is defined by the IUPAC as "*the formation of a solid phase within a liquid phase*" (Clark et al., 1994). It is modelled such as one (Chung, 1992; Lindeloff et al., 1998). Nonetheless, as Sirota states it (2005), this phase separation is **thermodynamically a liquid-liquid phase separation** which can be understood in the context of solution theory of molecules. The solid-like character of the asphaltene-rich phase which is formed is only due to the fact that the material in the heavier phase is **below its glass-transition** temperature.

2.3.3. When does asphaltene precipitation occur?

To the question "*which conditions make asphaltene precipitate?*", the answer could be "*more or less anything*" but, to be more detailed, one can mention the temperature, the pressure or the composition variations. There is no agreed explanation about the reasons of this precipitation:

- **Addition of n-alkanes** is said to depeptize the resins and the aromatics that kept the asphaltenes dispersed in solution (Ferworn et al., 1993). This is of course if one agrees with the colloidal description of asphaltenes. From the solution point of view, asphaltene precipitate when the **difference in the dispersion solubility parameters of the asphaltenes and the solvent is too high** (Zhou, 2005). Hence, weak non-specific dispersion attractions between the aggregates determine precipitation while strong interactions (hydrogen bonding for instance) govern the aggregation (Porte et al., 2003). As Figure I-12 clearly shows it, asphaltene become soluble when the dispersion part of their solubility parameter is equal to the one of the solvent. This explains why solvents such as cyclohexane, tetralin or

decalin with sole dispersion forces can be good solvents. Table I-6 attempts to explain the effects of various solvents and precipitants from a thermodynamic and a molecular point of view.

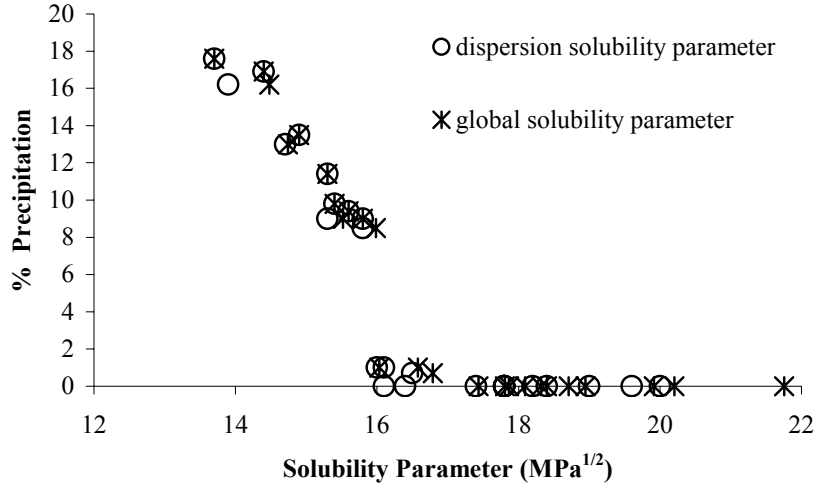

Figure I-12: Influence of dispersion forces on the amount of precipitate (adapted from Mitchell and Speight, 1973)

- Both stabilizing and destabilizing **effects of temperature** are seen in the literature (see chapter 3, paragraph 1.1). The explanations mentioned in paragraph 1.6.1 about the sterically stabilised colloids might be a key to understanding the influence of temperature on flocculation. The difference between the thermal expansion of the solvent and the one of the asphaltene might be an explanation (Gonzalez et al., 2005) Table I-7 summarizes and explains this various effects with the help of the solubility parameter and from a molecular perspective.

- The **effect of pressure** is rather agreed in the literature since asphaltene precipitate during pressure depletions (Lhioreau et al., 1967 and Hammami et al., 1998 for gas injection; Akbarzadeh, 2005 for n-alkanes). More details are given in Chapter 3, paragraph 1.2.

Solvent	Solubility parameter	Molecular level
Toluene	Asphaltenes are kept in solution since $\left\|\delta_d^{toluene} - \delta_d^{asphaltenes}\right\|$ is small	Aggregated asphaltenes are solvated and they stay away from each other.
Toluene + n-C_7	The dispersion power of the solvent is decreasing ($\delta_d^{C7} = 15.3 < \delta_d^{toluene} = 16.4 MPa^{1/2}$) and hence $\left\|\delta_d^{toluene+C7} - \delta_d^{asphaltenes}\right\|$ is increasing. Asphaltenes precipitate at one point.	The size of the aggregates is increasing (Roux et al., 2001). The aggregates are getting closer, the attractive forces between solvent and solute are weaker.
Quinoline, o-dichlorobenzene, and trichlorobenzene.	They are said to be the best solvents for breaking up asphaltene association (Wiehe, 2005). $\delta_a^{o-dichlorob.} = 7.1 > \delta_a^{toluene} = 2.5 MPa^{1/2}$ ($\delta_a = \delta_p + \delta_h$ is the associative term).	The attractive association forces are breaking the aggregates and solvating the asphaltenes.
Cyclohexane	$\delta_d^{cyclohexane} = 16.5\ MPa^{1/2}$ is toluene-like. Thus it explains why it is a good solvent (Mitchell and Speight, 1973).	See toluene
Acetone	$\delta_d^{acetone} = 15.5\ MPa^{1/2}$ which is in between octane and nonane . Acetone is a precipitant (Buenrostro-Gonzalez et al., 2002)	See toluene + n-C_7

Methanol	$\delta_d^{methanol} = 15.1\ MPa^{1/2}$ is in between hexane and heptane. Methanol is a precipitant (Andersen, 1997).	See toluene + n-C_7
Nitrogen	$\delta_d^{N_2}$ is between 1 and 4 $MPa^{1/2}$ (between 1 and 50 MPa and 293 and 383 K). The dispersion power of the solvent is highly decreased. Precipitation may occur depending on the miscibility of N_2 in the solvent.	Nitrogen is weakening the attractive forces solvent-solute. Hence, the aggregates attract each other, aggregate and flocculate.
CO_2	CO_2 has only dispersion and quadrupolar forces but the quadrupolar are assumed not to have specific influence here. $\delta_d^{CO_2}$ is varying between 3 and 16 $MPa^{1/2}$ (between 1 and 50 MPa and 293 and 383 K). These strong variations affect the solubility parameter of the solvent very much, especially since CO_2 is very soluble.	Idem as nitrogen

Table I-6: Influence of the solvent on the stability of asphaltenes

Perturbation Factor	Solubility parameter	Molecular level
Increase in T	$\left\|\delta_d^{solvent} - \delta_d^{asphaltenes}\right\|$ may increase or decrease according to their respective dependence with temperature ($d\delta_D/dT = -1.25\alpha_P\delta_D$ where α_P is the thermal expansivity). So both stabilizng and destabilizng effects can be expected.	Dispersion forces do not depend on temperature (Israelachvili, 1991) but asphaltene solution may demix if the difference in thermal expansivities between the solvent and the asphaltene is too large, i.e. the distance solvent-solute is getting bigger and aggregates can interact with each other.
Decrease in T	Idem as for increase	Idem

Table I-7: Influence of temperature on asphaltene stability

Almost all the possible techniques have been used to detect asphaltene precipitation: microscopic examination, optical transmission and light-scattering, conductivity measurements, viscosimetry, particle size analysis, fluorescence spectroscopy, density measurements or acoustic methods (see Andersen, 1999 for the different references or Chapter 3, paragraph 2). Every technique brings useful information:

- The work done by Jill Buckley with refractive index (Buckley, 1999) shows that **precipitation is strongly linked to van der Waals forces**. The refractive index only takes into account dispersion forces (Israelachvili, 1991). It corroborates what has been said previously.
- Onset titrations (Cimino et al., 1995) showed that, surprisingly, the **onset of precipitation of asphaltene solutions does not depend on the asphaltene concentration** but only on the **solvent quality**. This might suggest- that asphaltene fugacity does not depend on its molar fraction. This last piece of information does not have so much physical sense but it should be remembered if modelling is attempted.
- By means of SANS measurements and varying the n-heptane content in a toluene solution of asphaltenes, it was seen the **aggregate size is increasing but the small-scale internal structure is unchanged** (Roux et al., 2001). In the same paper, it was concluded that asphaltene precipitation is similar under temperature or composition variations, although the amplitudes and kinetics might be different. Experiments at the onset were tried but unfortunately they were not reproducible or stable. This emphasizes the need of more information about the onset of precipitation.

So, asphaltene precipitation and flocculation are distinct phenomena linked to the size of aggregates, the turbulence. It is difficult to detect the transition between these two phenomena from an experimental point of view, especially if the solution is mixed and particles cannot settle down. Flocculation is related to the colloidal nature of asphaltenes and both steric and charge stabilisations are at stake. Precipitation is a liquid-liquid transition from a thermodynamic point of view and it is linked to the dispersion forces of the solvent and the asphaltenes.

2.3.4. The reversibility

This is again a controversial issue, even in recent papers though the asphaltene community tends to agree now that asphaltene precipitation is reversible (Porte et al., 2003). Two schools of thought are in opposition; one considers that asphaltenes are dissolved in the oil in a true liquid state and that they may precipitate depending on the thermodynamic conditions. The second one states that asphaltenes are solid particles dispersed in the crude oil and stabilised by large resin molecules. Asphaltene flocculation and precipitation would be irreversible. Both views are based on experimental observations but it is believed in this work that precipitation is reversible.

When pressure is smaller than the lower pressure onset or higher than the upper pressure onset, asphaltenes are likely to go back to solution. As Hammami suggested it (2000), asphaltene precipitation is generally reversible but the kinetics of redissolution vary significantly depending on the physical state of the system. Some authors claim that the asphaltene composition has a key role in the reversibility issue (Leontaristis, 1994). Nonetheless, it is not clearly explained or proved. It was also stated that asphaltene precipitation is less likely to be reversible for crude oils subjected to conditions well beyond those of the precipitation onset (Fotland, 1996).

The hysteresis between asphaltene precipitation and redissolution has been studied (Andersen, 1992; Peramanu et al., 2001; Hammami et al., 2000). This hysteresis can be due the precipitation factor (composition, temperature or pressure). The hysteresis with temperature (Peramanu et al., 2001) seems more important than with pressure (Hammami et al., 2000). Since different oils were studied, it seems hazardous to conclude. The hysteresis may also be linked to deposition. Actually, if asphaltenes are deposited, their re-dissolution will take much longer. It is interesting to note that complete reversibility could be obtained after sonication (Mohamed et al., 1999).

2.4. Unanswered questions

Several points will be shortly introduced in this paragraph but will not be developed:

- Asphaltenes are mainly studied in solvent solutions and not in crude oils (neutron scattering, determination properties, study of interactions). But what is the validity of such measurements?
- Kinetics has a major impact on the study of phase behaviour and stability but little attention is paid to this factor. Can the results found in the literature be trusted? Is the equilibrium reached in the fields when asphaltene precipitate?
- Deposition is the problematic issue. Asphaltenes may precipitate but not deposit if the flowrate is sufficient for instance. There are very few studies about this topic. Should the efforts not be directed in this way?

3. Asphaltenes and Petroleum industry

The technical issues surrounding asphaltenes are complex, first of all because their understanding, their definition, their structures, to name a few of the problems, are partly confusing and still subject to harsh debates amongst "experts". Then, it is often when fluids have very little asphaltenes that they are problematic. Finally, asphaltenes create troubles from the production of the oil to the refinery process.

In this paragraph, the various problems encountered by the oil industry will be evocated with a special focus on gas injection. Then, the solutions used to treat and handle asphaltene problems will be briefly described.

3.1. The problems related to asphaltenes in the oil industry

The main problems caused by asphaltenes can be divided in several groups (Pineda-Flores et al., 2001):

- **The extraction**: when asphaltenes precipitate and deposit, they are likely to clock the porous space, hence reducing the permeability and the crude's exit flux. It does also affect the wettability (Cuiec, 1984). Iwere and co-workers (Iwere et al., 2002) modelled the effects of asphaltene precipitation on fluid flow and oil production from the fractured reservoirs of the Taratunich Field. The effects of asphaltene precipitation were modelled through changes in pore volume and transmissibility with reservoir pressure. The analysis of the reservoir and well performance data revealed that lithology and pore throat size played an important role in determining where asphaltene precipitates in the reservoirs. Abdulrazag and Shedid investigated the effect of fracture characteristics on reduction of permeability by asphaltene deposition in carbonate formation. They studied the influence of the flow rate and the stress, among other things (Abdulrazag and Shedid, 2004). Some simulations were also tried coupled with a thermodynamic model (Nghiem et al., 2000; Monteagudo et al., 2002). Although the results are claimed to be in agreement with experimental results, thermodynamic models are known to behave poorly when dealing with asphaltenes.

- **Transport:** blending incompatible oils that can lead to asphaltene precipitation is a well-known issue in the oil industry. Wiehe dedicated many articles to this topic. He based his work and predictions on solubility parameters. Titrations at atmospheric conditions can help finding the right proportions (Wiehe and Kennedy, 2004).
- **Processing**: Catalyst deactivation is the main problem. When hydrotreating heavy oils, both the non-asphaltenic phase and the asphaltenes undergo a chemical conversion, which may lead to unstable products as well as to increased coke lay-down on the catalyst (Bartholdi and Andersen, 2000). Fouling in heat-exchangers is also a major issue (Dickakian and Seay, 1988).
- **Crude exploitation**: economical profits related to crude exploitation depend on its chemical composition in such a way that crude with a high content of asphaltenes (18-22%) is considered as "heavy" and low quality product. Since this represents major difficulties in its extraction and refining, economical profit notably diminishes.
- **Environment**: by collecting the oil-water interface of surface equipment, such as free water knock outs and heater treaters, asphaltenes contribute to the formation of stable emulsions that make oil-water separation difficult. This contaminated water may pose problems (Stephenson, 1990).

3.2. A few words about the Enhanced Oil Recovery (EOR)

This paragraph is adapted from Morel and Roy, 2004. The term Enhanced Oil Recovery, or EOR, was first used in the 1970s and reached the height of its popularity in the 1980s. EOR methods are typically classified into three main categories:

- **Thermal**: This category covers steam injection and in-situ combustion which designates injection of air, sometimes oxygen-enriched, in viscous oils where oil/oxygen chemical reactions release large quantities of heat. These methods all cause a temperature rise in the reservoir which considerably decreases the viscosity of the oil in place.
- **Gas injection**: Not all types of gas injection are classified as EOR, and the definitions are not always precise. The following are clearly classified as EOR:

  - all injections of non-hydrocarbon gas (nitrogen, CO_2, H_2S, air…)
  - injections of miscible or partially miscible hydrocarbon gas in the oil zone
  - injections of hydrocarbon gas in zones already swept by water (this is called tertiary recovery)
  - alternating gas-water injections (Water Alternate Gas), whatever the gas may be.

- **Chemical**: Chemical methods are classified in two major families. On the one hand, injection of polymers can, enhance the macroscopic sweep efficiency of water in viscous oil (more favourable mobility ratio) by increasing the viscosity of the injection water. On the other hand, the injection of surfactants or alkaline products enhances the microscopic sweep efficiency of water.

The following points are worth mentioning:

- EOR production represents only (about) **4% of overall worldwide production**, which is still very low. A slight increase has emerged in the past few years.
- **Thermal methods** are the most often used in the EOR category, covering around **2/3 of world EOR productio**n. Gas injection follows with 25-30%, and the remainder goes to chemical EOR methods which are still quite low.
- The leading country in terms of EOR is clearly the **USA**.

These classifications and statistics should evolve perceptibly in the years to come, with the emergence of Mexico and its massive injection of nitrogen in the giant field of Akal (in the Cantarell complex), helping increase production by about one million barrels per day. It is also expected that Canada and Venezuela, which contain most of the world's heavy oil in place and are beginning to produce it, increase their production strongly using thermal processes.

3.3. The Vapex Process

Solvent-based processes for recovery of heavy oil have attracted increasing attention in the past few years as compared to steam-based processes, they may reduce the energy consumption and greenhouse gas emission. The Vapour Extraction (VAPEX) process was proposed by Butler and Mokrys for the first time in 1991 as an alternative to Steam

Assisted Gravity Drainage (SAGD) for thin reservoirs (Butler and Mokrys, 1991). The VAPEX process is closely related to the SAGD concept where the steam chamber is replaced with a chamber containing light hydrocarbon vapours close to its dew point at the reservoir pressure. The heavy oil has its viscosity reduced by dissolution of the injected solvent and is subsequently produced by a gravity drainage mechanism. Between the pure VAPEX process (cold solvent injection) and the pure SAGD process, several hybrid processes exist which combine the advantages of these two methods (Dauba et al., 2002).

Propane and ethane are considered to be the most suitable solvents for the process. However, a mixture of butane, propane and ethane can also be used, depending on the prevailing pressure in the reservoir. One can wonder what will happen in terms of asphaltene precipitation. One single study dealing with this question was found (Das and Butler, 1994). This investigation was carried out in a Hele-Shaw cell using propane and several heavy crudes. It was concluded that asphaltene deposition does not prevent the flow of oil through the reservoir for the proposed production scheme. They also observed that deasphalting takes place if the injected propane pressure is close to or higher than the vapour pressure of propane at the same temperature. However, porosity is likely to be affected by asphaltene precipitation and deposition. Asphaltene precipitation can also be seen as an in-situ upgrading of the oil and it may help producing higher quality oils. The main inconvenient of this process are the slow mixing bitumen/solvent as well as the solvent losses, its supply, storage, compression and treatment before recycling.

3.4. CO_2 injection

One of the problems of the VAPEX is the value of the hydrocarbon solvent, which is partly lost in the reservoir. For this reason other cheaper solvents may be also envisaged, particularly CO_2. Two cases are possible:

- **Miscible CO_2-EOR**: the gas aims at decreasing the viscosity and, hence, at recovering more oil. It happens in specific conditions (roughly, API>22 and depth larger than 1200 m).
- **Immiscible CO_2-EOR**: the gas is only used to re-pressurize the reservoir and to push the oil towards the well.

CO_2 EOR is a current forefront topic in the domain of sustainable development as it combines both enhanced recovery of hydrocarbons and geological storage of greenhouse gases. Another important reason for EOR development is the commitment of all the industry majors to reduce their greenhouse gas emissions. CO_2 is a highly effective enhanced recovery agent for some types of oil and we are presently witnessing the multiplication of CO_2 projects combining enhanced recovery operations and geological storage of CO_2 (Morel and Roy, 2004).

Currently, **20,000 tons per day of CO_2** are delivered to oil fields for EOR projects (Moritis 1998). A significant fraction of the injected CO_2 remains in the reservoir, but some is produced along with the oil. Generally, this CO_2 is separated from the oil, recompressed, and injected back into the reservoir. Total production is a little less than 200,000 bbl/day (3.2 x104 m^3/day) and thus roughly **10 bbl of oil are produced for every ton of CO_2 injected**. Most of the CO_2 for EOR originates from naturally occurring geologic traps, although a small fraction is from anthropogenic sources (Stevens and Gale, 2000). To date, CO_2 injection projects have focused on oil with densities between **29 and 48 °API** (855 to 711 kg/m3, respectively) and reservoir depths from 760 to 3700 m (Taber et al., 1997). Within the U.S., CO_2-EOR operations are centered in the Permian and Rocky Mountain basins (Texas, New Mexico, and Colorado). Current use of CO_2 for oil recovery is limited by cost and availability of CO_2. If substantial additional quantities of CO_2 are made available due to sequestration efforts, significant CO_2 storage capacity remains to be exploited in oil reservoirs. Screening criteria have been proposed elsewhere for selecting reservoirs where CO_2 may sustain or increase the production of oil (Taber et al., 1997). They estimate that upwards of **80% of oil reservoirs worldwide might be suitable for CO_2 injection based upon oil-recovery criteria alone**. Moreover, the process is widely applicable in both sandstone and carbonate formations with a variety of permeabilities and thickness of hydrocarbon bearing zones. The major factors limiting

CO_2 injection as an oil recovery process have been **availability of CO_2** and the **cost to build pipelines** to carry CO_2 into oil producing regions (Jessen et al., 2005).

The effect of CO_2 injection on asphaltene stability has been experienced in fields. Sarma reports several cases in with serious asphaltene deposition due to CO_2 flood: Midale (Canada), Little Creek Field (Missisipi) and West Texas (Sarma, 2003). Laboratory and simulations studies have also been carried on. In Chapter 3, paragraph 3.3, various papers studying the influence of CO_2 on asphaltene precipitation are listed.

3.5. Which oils/fields are problematic?

Field and laboratory data confirm that the lighter the oil, the lower is the asphaltene solubility. Asphaltenes tend to precipitate more easily in light oils rather than in heavy oils. For instance, the Venezuelan Boscan crude with 17.2 wt% asphaltene was produced with nearly no troubles whereas Hassi-Messaoud in Algeria has numerous production problems with only 0.15 wt% (Sarma, 2003). Since light-oil reservoirs are more often candidates to gas injection processes, the danger is even bigger.

3.6. What are the solutions so far?

3.6.1. Prevention

Chemical treatment is often the prevention method used: dispersing agents are often injected (60-70 ppm minimum at the bottom of the well). These dispersing agents are often anionic/cationic mixtures. These asphaltene inhibitors are usually prepared in the lab, by bottle tests. Since different asphaltene inhibitors work on different oils, all the possible chemistries have to be tested to select the proper additive.

An adapted management of the oilfield – by keeping the pressure constant or preventing a brutal depletion – will also avoid asphaltene precipitation, especially near the well-bore. Furthermore, incompatible oils should not be mixed.

3.6.2. The empirical tools

- **The de Boer's plot**: The de Boer's diagram is often used (Figure I-13). The difference between the reservoir pressure and the bubble point pressure is plotted as a function of the in-situ crude density and it gives evaluation of the asphaltene stability (de Boer et al., 1995). According to this graph, the lighter the oil and the farther from the bubble point, the more severe the problems will be. However, this diagram is "pessimist" and assumes that the whole reservoir is saturated in asphaltenes. This is however a very useful tool but not sufficient to make operative decisions (Zhou, 2005).

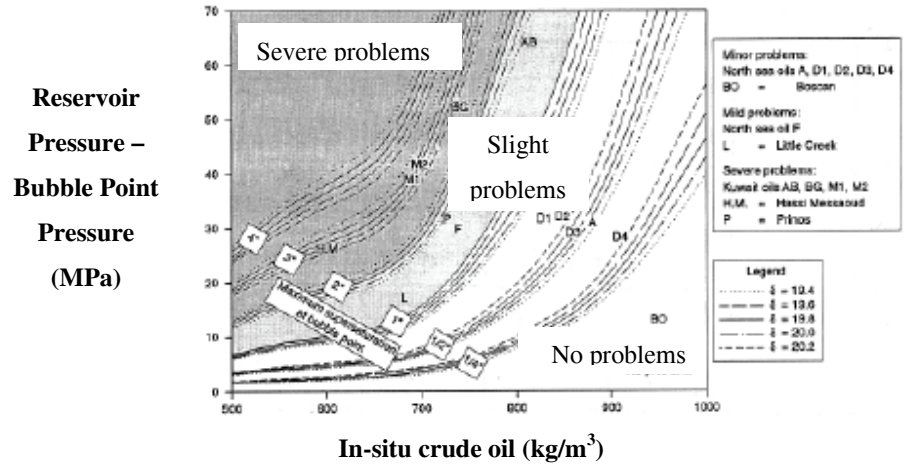

Figure I-13: Maximum supersaturation of asphalt at bubblepoint pressure (de Boer et al., 1995)

- **The Ratio Resins/Asphaltenes:** the ratio Resins/Asphaltenes is sometimes used. Indeed, resins are believed to peptpize asphaltenes and keep them in solution. Hence, the more resins, the more stable the asphaltenes. However, only a fraction of resins are active in the peptization process.Only part of the resins are able to form strong aggregates with asphaltenes (Murgich, 2005). Furthermore, the separation techniques play an important role, as it was said in paragraph 1.1. Figure I-14 clearly shows that the three techniques tested with these nine oils cannot "predict" the stability of asphaltenes.

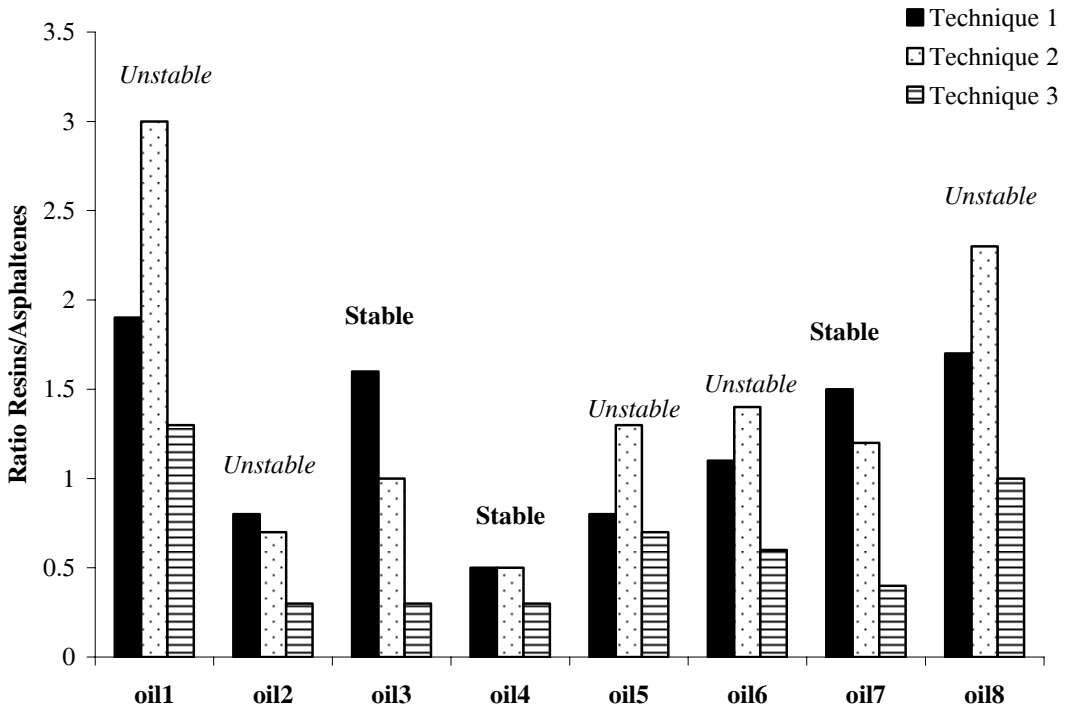

Figure I-14: Stability and the ratio Resin/Asphaltene (adapted from Zhou, 2005)

Baker Petrolite is using the Colloidal Instability Index defined by Eq I-6.

$$CII = \frac{\%\text{Saturates} + \%\text{Asphaltenes}}{\%\text{Resins} + \%\text{Aromatics}} \qquad \textbf{Eq I - 6}$$

When the index is lower than 0.7, the oil is said to be stable and when it is bigger than 0.9, it is unstable. In between the two values, further tests are required. The uncertainties related to SARA separations make such a tool not fully predictive.

- **Modelling:** Modelling is a very useful tool to predict and describe wax precipitation (Coutinho et al., 2001) or scale formation (Villafafila, 2005). Consequently, it is also applied for asphaltene precipitation. Unfortunately, since this phenomenon is not properly understood, its modelling remains dubious. Be that as it may, modelling would require the fluid characterisation and this step raises the following difficulties (Zhou, 2005):

- Complex analytical methods are required in order to characterise asphaltenes (C_{20}^+ fractions, SARA, asphaltenes molecular weight, polarity etc.).
- In addition, a special (and expensive) sampling method is necessary.
- Once the sample is available, the validity of experimental tests depends on the flocculation detection limit at reservoir conditions and on the kinetics.

This issue is discussed in more details in Chapter 5.

3.6.3. Remediation

Common approaches to the asphaltene deposition problems can be summarized as follows (Stephenson, 1990):

- **Physical cleaning and removal**: bailing, drilling or hydroblasting may be necessary when asphaltenes collect in or plug the well bore. In oil field storage tanks, precipitated asphaltenes must often be shoveled out of tank bottoms. These operations are tedious and time consuming, the necessary equipment is expensive and disposal of large volumes of washings can pose an environmental problem.
- **Solvent treatment**: although they show only slight activity, solvents such as xylene can be used to disperse/dissolve asphaltenes. This approach is often expensive due to the large dosages of solvent required. The environmental concerns over low-molecular weight aromatic solvents also must be considered
- **Treatment with low-molecular weight dispersants**: dispersant treatment is subject to the same types of difficulties as solvent treatment. Low molecular weight dispersants such as cresylic acid, have an associated toxicity which makes them less desirable to use
- **Increased emulsion breaker concentration**: asphaltenes can collect at the oil-water interface, and some have been treated with high concentrations of emulsion breakers. Sometimes this approach is effective probably due to the presence of a minor emulsion breaker component with dispersancy activity. However, excess treatment with demuslfiers is expensive.

The cost of such operations is obviously non-negligible. For instance, the shutdown and the clean-up cost for a 8-inch submarine crude pipeline was estimated around 2.5 million dollars in 1996 (Leontaritis, 1996).

4. Conclusion

This paragraph aimed at summarizing the main issues dealing with asphaltenes. Obviously, much more could be said and discussed, for both theoretical and industrial point of view. The goal was only to emphasize the complex nature of asphaltenes in order to enlighten the other parts of this thesis.

The main theoretical points about asphaltenes presented in this chapter were:

- Asphaltenes are the most polar and heavier part of petroleum. Their mere definition is still a subject of debate amongst experts. The technique used to extract them strongly influences their nature.
- Asphaltenes can be easily characterized in terms of solubility parameters.
- Asphaltene molecules are either from the archipelago or the continental type.
- Asphaltenes have a double nature: colloids and solutes in a solvent. Flocculation and precipitation are directly linked to this double nature.
- The molecular weight of asphaltene monomers is around 1000 g/mol
- Self-association starts around 100 ppm. It is mainly due to hydrogen bonding.
- Dispersion forces (and polar forces to a less extent) govern the asphaltene precipitation.
- The CMC about asphaltenes (if any) is not due to the sole asphaltene structure.
- Resins have a co-solubilizing effect on asphaltenes.
- Flocculation is a state of aggregation that precedes precipitation (which is a phase transition). Flocculation is ruled by colloidal stability whereas precipitation can be explained in terms of solubility parameters.
- Asphaltene precipitation is reversible in most cases. It is likely to be governed by kinetics.

5. Aim of this project

This project has several objectives dealing with asphaltene stability related to gas injection:

- Developing experimental methods to determine input parameters for the models, especially solubility parameters of crude oils and asphaltenes and critical constants of asphaltenes. The effect of pressure is of particular interest.
- Studying the influence of gas injection on asphaltene stability and the eventual effects of temperature and pressure.
- Investigating asphaltene precipitation by means of calorimetry for live oils, dead oils and asphaltene solutions.
- Test models based on cubic EOS and evaluate a new model taking aggregation into account.

Literature

Abdulrazag Y. Z., Shedid A. S., The effect of fracture characteristics on reduction of permeability by asphaltene precipitation in carbonate formation, J. Pet. Sci. Eng. (2004), 42, 171– 182

Akbarzadeh K., Alboudwarej H., Svrcek W., Yarranton H.W., A generalized regular solution model for asphaltene precipitation from n-alkane diluted heavy oils and bitumen, Fluid Phase Equilibr. (2005), 232, 159 - 170

Al-Sahhaf T.A., Fahim M.A., Elkilani A.S., Retardation of asphaltene precipitation by addition of toluene, resins, deasphalted oil and surfactants, Fluid Phase Equilibr. (2002), 194 – 197, 1047 - 1057

Andersen S.I., Hysteresis in precipitation and dissolution of petroleum asphaltenes, Fuel Sci. Technol. Intl. (1992), 10, 1743 - 1749

Andersen S.I., Concentration effects in HPLC-SEC analysis of petroleum asphaltenes, J. Liq. Chromatogr. (1994), 17, 4065-4079

Andersen S.I., Separation of asphaltenes by polarity using liquid-liquid extraction, Pet. Sci. Technol. (1997), 15, 185-198

Andersen S.I., Flocculation onset titration of petroleum asphaltenes, Energ. Fuel. (1999), 13, 315 – 322

Andersen S.I., Birdi K.S., Aggregation of asphaltenes as determined by calorimetry, J. Colloid. Interf. Sci. (1991), 142, 497-502

Andersen S.I., Birdi K.S., Influence of temperature and solvent on the precipitation of asphaltenes, Fuel Sci. Techn. Int. (1990), 8, 593 – 615

Andersen S.I., Hofsäss T., Kleintiz W., Rahimian I., Organic precipitates in oil production of a Venezuelan oil field, Pet. Sci. Technol. (2001 a), 19, 55- 74

Andersen S.I., del Rio J.M., Khvostitchenko D., Shakir S., Lira-Galeana C., Interaction and solubilization of water by petroleum asphaltenes in organic solution, Langmuir (2001 b), 17, 307-313

Andersen, S.I., Speight J.G., Petroleum resins: separation, character, and role in petroleum, Pet. Sci. Technol. (2001), 19, 1 – 34

Andersen S.I., Vigild M., Effect of chemical alteration on the aggregation of asphaltenes in d-toluene using SANS, Proceedings of The 6th International Conference on Petroleum Phase Behaviour and Fouling, Amsterdam, 2005

Andersen S.I., Jensen O., Speight J.G., X-ray Diffraction of Subfractions of Petroleum Asphaltenes, Energ. Fuel. (2005), 19, 2371 – 2377

Andreatta G., Bostrom N., Mullins O.C., High-Q ultrasonic determination of the critical nanoaggregate concentration of asphaltenes and the critical micelle concentration of standards surfactants, Langmuir (2005), 21, 2728 – 2736

Aquino-Olivos M.A., Andersen S.I., Lira-Galeana C., Comparisons between asphaltenes from the dead and live-oil samples of the same crude oils, Pet. Sci. Technol. (2003), 21, 1017-1041

Bartholdy J., Andersen S.I., Changes in asphaltene stability during hydrotreating, Energ. Fuel. (2000), 14, 52-55

Bissada K. K., Szymczyk E. B., Nolte D.G., Darnell L. M., Improved asphaltene and paraffin separations and quantification for crude oil and bitumen characterization, Presented at 6th International Conference on Petroleum Phase Behaviour and Fouling, Amsterdam, June 2005

de Boer R.B., Leerloyer K., Eigner M.R.P., van Bergen A.R.D., Screening of crude oils for asphalt precipitation: theory, practice, and the selection of inhibitors, SPE Prod. Facil. (1995), 55 – 61

Buckley J.S., Predicting the onset of asphaltene precipitation from refractive index measurements, Energ. Fuel. (1999), 13, 328 – 332

Buenrostro-Gonzalez E., Andersen S.I., Garcia-Martinez J.A., Lira-Galeana C., Solubility/molecular structure relationships of asphaltenes in polar and non-polar media, Energ. Fuel. (2002), 16, 732 – 741

Burya Y.G., Yudin I.K., Dechabo V.A., Anisimov M.A., Colloidal properties of crude oils studied by dynamic light-scattering, Int. J. Thermophys. (2001), 22, 5, 1397 – 1410

Butler, R.M., Mokrys, I.J., A new process (VAPEX) for recovering heavy oils using hot water and hydrocarbon vapour", J.C.P.T. (Jan. 1991), 97

Carbognani L., Solid petroleum asphaltenes seem surrounded by alkyl layers, Pet. Sci. Technol. (2003), 21, 537-556

Castillo J., Hung J., Fernandez A., Mujica V., Nonlinear optical evidences of aggregation in asphaltene-toluene solutions, Fuel (2001), 80, 1239 - 1243

Chung F.T.H., Thermodynamic modelling for organic solid precipitation, SPE 24851 (1992), 869 – 878

Cimino R., Correra S., Del Bianco A., Lockart T.P., Solubility and Phase Behaviour of asphaltenes in hydrocarbon media, Asphaltenes: Fundamentals and Applications, Sheu E.Y., Mullins O.C., Ed., Plenum Press, NY, 97 - 130 (1995)

Clark J.B., Hastie J.W., Kihlborg L.H.E., Metselaar R., Thackeray M.M., Definitions of terms relating to phase transitions of the solid state, Pure & App. Chem. (1994), 66, 577-594

Clarke P.F., Pruden B.P, Asphaltene precipitation: detection using heat transfer analysis, and inhibition using chemical additives, Fuel (1997), 76, 7, 607 – 614

Cooper S., Course Notes, Department of Chemistry, University of Durham, England (http://www.dur.ac.uk/sharon.cooper/lectures/colloids/interfacesweb1.html), 2005

Coutinho J.A.P., Pauly J., Daridon J.L., A thermodynamic model to predict wax formation in petroleum fluids, Braz. J. Chem. Eng. (2001), 18, 411 - 422

Cuiec L., Rock/crude oil interactions and weattbility: an attempt to understand their interaction, Proceedings of SPE Annual Technical Conference and Exhibition (1984),

Das S.K., Butler R. M., Effect of Asphaltene Deposition on the Vapex Process: A Preliminary Investigation Using a Hele-Shaw Cell, J. Can. Petrol. Technol. (1994), 33, 39-45

Dauba C., Quettier L., Christensen J., Le Goff C., Cordelier P., An Integrated Experimental and Numerical Approach to Assess the Performance of Solvent Injection into Heavy Oil, Proceedings - SPE Annual Technical Conference and Exhibition (2002), 1131-1140

Diallo M.S., Cagin T., Faulon J.L, Goddard III W.A., Thermodynamic properties of asphaltenes: a predictive approach base don computer assisted structure elucidation and atomistic simulations, in "Asphaltene and asphalts, 2. Developments in Petroleum Science, 40 B", Edited by T.F. Yen and G.V. Chilingarian, chap. 5, 2000

Dickakian G., Seay S., Asphaltene precipitation primary crude exchanger fouling mechanism, Oil Gas J. (1988), 86, 47-50

Dickie J.P., Yen T.F., Anal. Chem. (1967), 39, 1847

Eilers H., The colloidal structure of asphalt, J. Phy. Chem. (1949), 53, 1195 – 1211

Fenistein D., Barré L., Frot D., Oil Gas Sci. Technol. (2000), 55, 123 – 128

Ferworn K.A., Svrcek W.Y., Mehortra A.K., Measurement of asphaltene particle size distribution in crude oils diluted with n-heptane, Ind. Eng. Chem. Res. (1993), 32, 955 – 959

Fotland P., Precipitation of asphaltenes at high-pressures; Experimental technique and results, Fuel Sci. Techn. Int. (1996), 14, 313 - 325

Fotland P., Anfindsen H., Fadnes F.H., Detection of asphaltene precipitation and amounts precipitated by measurement of electrical conductivity, Fluid Phase Equilibr. (1993), 82, 157 – 164

Hammami A., Ferworn K.A:, Nighswander J.A., Overå S., Stange E., Asphaltenic crude oil characterization: an experimental investigation of the effect of resins on the stability of asphaltenes, Pet. Sci. Technol. (1998), 16, 227 – 249

Hammami A., Phelps C.H., Monger-McClure T., Little T.M., Asphaltene precipitation from live oils: an experimental investigation of onset conditions and reversibility, Energ. Fuel. (2000), 14, 14 – 18

Hotier G., Robin M., Action de divers diluants sur les produits pétroliers lourds : mesure, interprétation et prévision de la floculation des asphaltenes, Rev. I. Fr. Petrol. (1983), 38, 1, 101 – 120

Israelachvili J., Intermolecular and surface forces, 2nd edition, Academic Press, London, 1991

Iwere, F.O., Apaydin, O.G., Moreno, J.E., Simulation of asphaltene precipitation in fractured reservoirs: a case study, SPE 74373, SPE International Petroleum Conference and Exhibition, Mexico, Villahermosa, Mexico, 10– 12 February 2002

Jessen K., Kovscek A.R., Orr F.M. Jr., Increasing CO_2 storage in oil recovery, Energ. Conve. .Manag. (2005), 46, 293–311

Klein G.C., Yen A., Asomaning S., Rodgers R.P., Marshall A.G., High resolution mass spectrometry compositional comparison of the heptane precipitated asphaltenes and asphaltenes induced from reduction of pressure, Proceedings of the 6th International Conference on Petroleum Phase Behaviour and Fouling, Amsterdam, June 2005

Kontogeorgis G., Intermolecular Forces & Hydrogen Bonding, Course Notes, Department of Chemical Engineering, Technical University of Denmark, 2005

Leontaritis K.J., Amaefule J.O., Charles R.E., A systematic approach for the prevention of formation damage caused by asphaltene precipitation, SPE Prod. Facil. (1994), 9, 157-164

Leontaritis K.J., Offshore asphaltene and wax deposition: problems/solutions, World Oil (1996), 217, 57-63

Lhioreau C., Briant J., Tindy R., Influence de la pression sur la floculation des asphaltenes, Rev. I. Fr. Petrol. (1967), 22, 797 - 806

Lindeloff N., Heidemann R.A., Andersen S.I., Stenby E.H., A thermodynamic mixed-solid asphaltene precipitation model, Pet. Sci. Technol. (1998), 16, 3&4, 307 - 321

Maruska H.P., Rao B.M.L., The role of polar species in the aggregation of asphaltenes, Fuel. Sci. Tech. Int. (1987), 5, 119 - 168

Merino-Garcia D., Calorimetric investigations of asphaltene self-association and interaction with resins, Ph.D. Thesis, IVC-SEP, Department of Chemical Engineering, Denmark, Technical University, Lyngby, Denmark, 2003

Merino-Garcia D., Andersen S.I., Calorimetric evidence about the application of the concept of CMC to asphaltene self-association, J. Dispers. Sci. Technol. (2005), 26, 217-225

Mitchell D.L., Speight J.G., The solubility of asphaltenes in hydrocarbon solvents, Fuel (1973), 52, 149 – 152

Mohamed R.S., Loh W., Ramos A.C.S., Delgado C.C., Almeida V.R., Reversibility and inhibition of asphaltene in Brazilian crude oils, Pet. Sci. Technol. (1999), 17, 877 – 896

Monteagudo J.E.P., Rajagopal K., Lage, P.L.C., Simulating oil flow in porous media under asphaltene deposition, Chem. Eng. Sci. (2002), 57, 323-337

Morel D., Roy C., EOR: high-potential technologies for mature fields, Technoscoop (2004), 28, 34 – 41

Moritis, G., 1998 Worldwide EOR Survey, Oil Gas J. (Apr. 1998), 20, 49-97

Moschopedis S.E., Speight J.G., Hydrogen bonding by oxygen functions in Athabasca bitumen, Fuel (1976), 55, 187 - 192

Müller-Dethlefs K., Hobza K., Noncovalent interactions: a challenge for experiment and theory, Chem. Rev. (2000), 100, 143 – 167

Murgich J., Intermolecular forces in aggregates of asphaltenes and resins, Pet. Sc. Technol. (2002), 20, 983 - 997

Murgich J., Molecular mechanics study of the selectivity in the interaction between some typical resins and asphaltenes, Proceedings of the 6th International Conference on Petroleum Phase Behaviour and Fouling, Amsterdam, June 2005

Nagel R.G., Hunter B.E., Peggs J.K., Fong D.K., Mazzocchi E., Tertiary application of a hydrocarbon miscible flood. Rainbow Keg River 'B' pool, SPE Reservoir Eng. (1990), 5, 301-308

Napper D.H., Steric stabilization, J. Colloid. Interf. Sci. (1977), 58, 390 - 407

Nghiem L.X., Kohse B.F., Ali S.M.F., Doan Q., Asphaltene precipitation: Phase behaviour modelling and compositional simulation, Proceedings of the SPE Asia Pacific Conference on Integrated Modelling for Asset Management, 283-296, 2000

Odriozola G., Leone R., Schmitt A., Moncho-Jorda A., Hidalgo-Alvarez R., Coupled aggregation and sedimentation processes: the sticking probability effect, Phys. Rev. E. (2003) 67, 031401, 1-5

Padding J.T., Louis A. A., Hydrodynamic and brownian fluctuations in sedimenting suspensions, Phys. Rev. Letters (2004), 93, 220601, 1-4

Pedersen C., Asphaltene characterization: permittivity measurements and modelling, Ph.D. Thesis, IVC-SEP, Department of Chemical Engineering, Denmark, Technical University, Lyngby, Denmark, 2000

Peramanu S., Singh C., Agrawala M., Yarranton H.W., Investigation on the reversibility of asphaltene precipitation, Energ. Fuel. (2001), 15, 910 – 917

Pineda-Flores G., Mesta-Howard A.M., Petroleum asphaltenes: generated problematic and possible biodegradation mechanism, Rev. Lat. Microbiologia (2001), 43, 3, 143 – 150

Porte G., Zhou H., Lazzeri V., Reversible description of asphaltene colloidal association and precipitation, Langmuir (2003), 19, 40 – 47

Prausnitz J.M., Lichtenthaler R.N., Gomes de Azevedo E., Molecular thermodynamics of Fluid-Phase Equilibria (3rd edition), Prentice Hall PTR, New Jersey, 1999

Ravey J.C., Ducouret G., Espinat D., Asphaltene macrostructure by small-angle neutron-scattering, Fuel (1988), 67, 1560 - 1567

Rogacheva O.V., Rimaev R.N., Gubaidullin V.Z., Khazimov D.K., Investigation of the surface activity of the asphaltenes of petroleum residues, Colloid J. USSR (1980), 42, 586 - 589

Rogel E., Theoretical estimation of the solubility parameter distributions of asphaltenes, Energ. Fuel (1997), 11, 920-925

Rogel E., Carbognani L., Density estimation of asphaltenes using molecular dynamic simulations, Energ. Fuel. (2003), 17, 378 – 386

Rogel E., Leon O., Torres G., Espidel J., Aggregation of asphaltenes in organic solvents using surface tension measurements, Fuel (2000), 79, 1389- 1394

Roux J.N., Brosseta D., Demé B., SANS study of asphaltene aggregation: concentration and solvent quality effects, Langmuir (2001), 17, 5085 - 5092

Sallamie N., Shaw J.M., Heat capacity prediction for polynuclear aromatic solids using vibration spectra, Fluid Phase Equilb. (2005), 237, 100 – 110

Speight J.G., Moschopedis S.E., On the molecular nature of petroleum asphaltenes, Adv. Chem. Ser. (1981), 195, 1 – 15

Sarma H.K., Can we ignore asphaltene in a gas injection project for light oils?, Proceedings - SPE International Improved Oil Recovery Conference in Asia Pacific (2003), 193-199

Shaw D.J., Introduction to colloid and surface chemistry, 4th edition, Butterworth-Heinemann Publications, Oxford, 1992

Sheu E.Y., Mullins O.C., Asphaltenes: Fundamentals and Applications, Ed., Plenum Press, NY (1995)

Sheu E.Y., De Tar M.M., Storm D.A., Dielectric properties of asphaltene solutions, Fuel (1994), 73, 1, 45 - 50

Siffert B., Kuczinski J., Papirer E., Relationship between electrical charge and flocculation of heavy oil distillation residues in organic medium, J. Coll. Int. Sci. (1990), 135, 107 – 117

Sirota E.B., Physical structure of asphaltenes, Energ. Fuel. (2005), 19, 1290-1296

Speight J.G., Plancher H., Molecular models for petroluemasphaltenes and implications for asphalt science and technology, Proc. Int. Symp. On Chemistry of Bitumens (1991), 154

Speight, J.G., The Chemistry and Technology of Petroleum, 3rd ed., Marcel Dekker, NY (1999)

Speight J.G., Chemical and Physical studies of petroleum asphaltenes, in Asphaltenes and asphalts, 1. Developments in petroleum science, 40, Ed. by Yen T.F., Chilingrian G.V., Elsevier Science, Amsterdam, 7 – 65 (1994),

Stephenson W.K., Producing asphaltenic crude oils: problems and solutions, Petrol. Eng. Int. (1990), 24 - 91

Stevens S.H., Gale, J., Geologic CO_2 Sequestration May Benefit Upstream Industry, Oil Gas J. (2000), 15, 40-44

Sztukowski D.M., Jafari, J., Alboudwarej H., Yarranton H.W., Asphaltene self-association and water-in-hydrocarbon emulsions, J. Colloid. Interf. Sci. (2003), 265, 179–186

Taber J.J., Martin F. D., Seright R.S., EOR Screening Criteria Revisited—Part 1: Introduction to Screening Criteria and Enhanced Recovery Field Projects, Soc. Pet. Eng. Res. Eng. (1997), 189-198

Tissot B.P., Welste D.H., Petroleum formation and occurrence, Second Edition, Ed. Springer-Verlag, Berlin, 1984

Villafafila A., Measurement and Modelling of Scaling Minerals, PhD Thesis, Department of Chemical Engineering, Technical University of Denmark, 2005

Wiehe I.A., In Defense of Vapor Pressure Osmometry for Measuring Molecular Weight, Proceedings of the 6th International Conference on Petroleum Phase Behaviour and Fouling, Amsterdam, June 2005

Wiehe I.A., Kennedy R.J., Oil compatibility model and crude oil incompatibility, Energ. Fuel. (2000), 14, 56-59

Yarranton H.W., Issues in characterizing asphaltenes and other heavy fraction components, Proceedings of the 6th International Conference on Petroleum Phase Behaviour and Fouling, Amsterdam, June 2005

Yen T.F., Asphaltenes: types and sources, in “Structures and Dynamics of Asphaltenes”, Ed. by Mullins O.C., Sheu E.Y., Plenum Press, NY (1995), 1 - 20

Yen T.F., Chilingrian G.V., Asphaltenes and asphalts, 1. Developments in petroleum science, 40, Elsevier Science, Amsterdam (1994)

Zhou H., Total Research Centre, Pau, France, Personal communication (2005)

Websites:

The asphaltene standardization discussion:
http://asphaltenes.syncrude-research.karo.com/users/folder.asp

Chapter II

Characterization of Crude Oils and Asphaltenes

Table of Contents

Can solubility parameters or critical parameters of asphaltenes – widely employed to model the phase behaviour of asphaltenic fluids – be measured? How trustful would such measurements be? Can the effect of pressure and temperature be taken into account?

This chapter describes several techniques developed for crude oils and asphaltenes in order to characterize them. First, a brief overview of oil characterization is given and is followed by the definition of the solubility parameter and its various properties. Then, an alternative approach using internal pressure to determine the solubility parameter of crude oil is presented. Finally, solubility parameters and critical constants of asphaltenes are determined with various techniques.

1. Introduction

1.1. A brief overview about characterization of crude oil

This paragraph is mainly inspired by Montel, 2004.

The characterization of a reservoir fluid constitutes a chain as shown in the diagram below. Each link of this chain is vital to ensure the reliability of the results provided by the model. The main operations are summarized in Figure II-1.

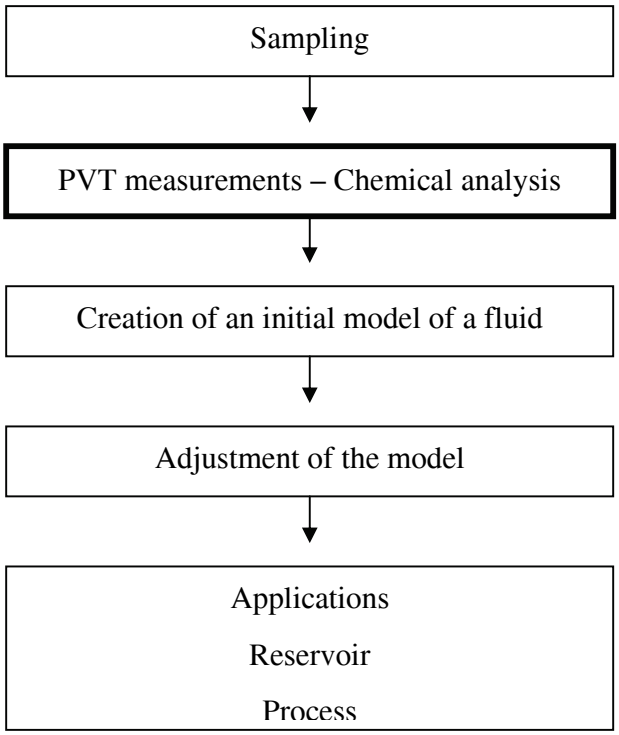

Figure II-1: Characterization of a crude oil (Montel, 2004)

The sampling of petroleum effluents is the weak link in the modelling chain. It can occur at various stages in the life of a field, in an exploration, appraisal or production well before or after production start-up.

The first problem encountered in simulating the behaviour of a petroleum fluid is the selection of an analytical description suitable for the model chosen. This choice is made

difficult by the major constraint applicable to all models: the limit on the number of fluid components.

This constraint is especially crucial in the case of compositional reservoir models intended to avoid prohibitive calculation times. Thus it is often necessary to group together constituents or cuts in the basic analysis to reduce the number of components under the limit imposed.

There is no universal analysis process: each laboratory issues its own specific description. As a result, petroleum "cuts" may comply with one or more varying criteria (Table II-1).

Criteria	Techniques
Boiling point	Distillation or gas chromatography
Molecular weight	Gel permeation chromatography
Chemical family	Liquid chromatography
Functional group	Absorption spectrometry

Table II-1: Criteria and methods used to define the cuts (Montel, 2004)

Petroleum cuts are used in general from 11 atoms of carbon but some laboratories cease identification beyond 7 atoms of carbon, others give only the main components between 7 and 11 carbons.

Gases do not give rise to problems in that they contain only small quantities of heavy constituents. Analysis by gas chromatography is exhaustive and all constituents are identified and quantitatively analysed. For liquids, the accuracy of the measurement of the specific fractions of the identified constituents depends on the accuracy of weighing of the internal standard, calibration of the Flame Ionisation Detector and of the integrator. Around 1% relative is accepted for the main components up to 10% relative for the minor ones. Thus cluttering up the results with insignificant decimals is not justified, but the great contrast in contents between major and minor components sometimes results in the retention of an excessive number of decimals for high concentrations. To convert the specific fractions to molar fractions, it is necessary either to analyse all the fluid down to

the heaviest cuts or to measure the molecular weight of the part which could not be analysed.

The use of gel permeation chromatography (GPC) allows extending analysis of liquids heavier constituents found in petroleum fluids. Laboratories which do not use this method employ cryometric or tonometric methods to measure the molecular weights in cuts or the liquid as a whole. Whatever analysis methods are used, the linking of the various results always implies a problem of overlap since the criteria are not the same. However, GPC is not an appropriate technique for asphaltenes because of the sizes of its molecules. These various problems explain why analyses are not accompanied by an evaluation of the uncertainties; in addition, the conversion of specific fractions to molar fractions introduces coupling resulting in error matrixes, not to mention the successive recombining to arrive at reservoir fluids.

The issue about the molar distribution (exponential or gamma distribution) will not be discussed here. The monograph by Whitson and Brulé should be consulted for that matter (Whitson and Brulé, 2000).

When a cubic equation of state is used, three parameters are needed: the critical temperature T_c, the critical pressure P_c and the acentric factor ω. Many correlations are present in the literature and they are based on different measurable parameters:

- Boiling points and specific densities (Kesler-Lee, 1976; Cavett, 1962; Riazi and Daubert, 1980; Nokay, 1959),
- NMR spectra (Alexander et al., 1985)
- Structure with the group contribution method (Marrero and Gani, 2001)

Twu (1984) developed correlations based on perturbation expansions: first, classical correlations are used for normal paraffins and then the “expanded” correlations are applied to the petroleum fractions.

Nevertheless, what will be the impact of a wrong estimation of these critical parameters? Figure II-2 shows the influence of T_c on physical properties (liquid density, vapour pressure, liquid enthalpy, etc.) and on phase envelope. Obviously, determining accurately such parameters is of great importance and relevance.

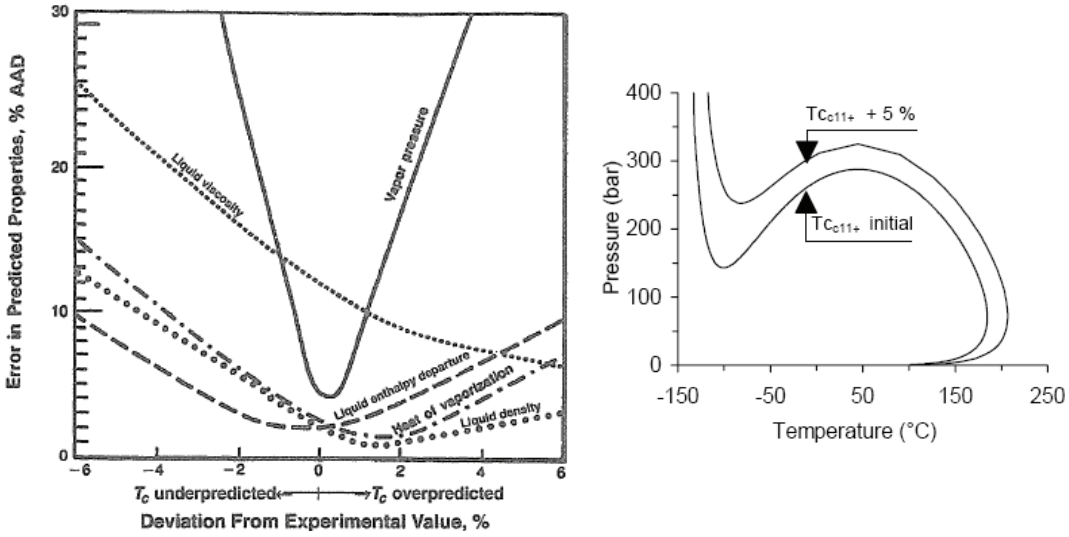

Figure II-2: Deviations due to improper estimation of critical temperature (left-hand side from Whitson and Brulé, 2000; right-hand side from Montel, 2004)

When it comes to asphaltenes, the determination of critical parameters is problematic. They are often fitted to titration experiments or to other properties (Szewczyk and Béhar, 1999; Nghiem et al., 1993). Hence, another characterization parameter is usually employed for asphaltenic fluids: the solubility parameter. Chapter 5 presents the different models used to describe asphaltene precipitation. Many of them are based on the regular solution theory using, for instance, the Flory-Huggins or Scatchard-Hildebrand equations. The coming paragraphs will deal with the definition of the solubility parameter, its determination for crude oil and asphaltenes as well as its modelling by means of cubic EOS.

1.2. Solubility parameter: definition and determination

1.2.1. Definition

The solubility parameter, δ, was defined by Hildebrand and Scott (1950) as follows:

$$\delta = \left(\frac{-E}{V} \right)^{1/2} \qquad \textbf{Eq II-1}$$

where $-E$ is the cohesive energy of the liquid and V the molar volume.

However, several interpretations of the "cohesive energy" are available in the literature, as seen in Table II-2 .

Source	Definition	Thermodynamic path
Hildebrand and Scott (1950)	$\delta = \left(\frac{-E}{V_{liq}(T,P)} \right)^{1/2}$	
Barton (1983)	$\delta = \left(\frac{U_{liq}(T,P=0) - U_{vap}(T,P_{sat})}{V_{liq}(T,P)} \right)^{1/2}$	liquid(P_{sat}, T) → vapour (P_{sat}, T,) → vapour(P = 0, T)
Maloney and Prausnitz (1974)	$\delta = \left(\frac{U_{liq}(T,P=0) - U_{vap}(T,P)}{V_{liq}(T,P)} \right)^{\frac{1}{2}}$	liquid(P, T) → liquid(P_{sat}, T) → vapour (P_{sat}, T,) → vapour(P = 0, T)
Lyckman et al. (1965)	$\delta = \left(\frac{U_{liq}(T,P=0) - U_{vap}(T,P_{sat})}{V_{liq}(T,P_{sat})} \right)^{\frac{1}{2}}$	liquid(P_{sat}, T) → vapour (P_{sat}, T,) → vapour(P = 0, T)
Hoy (1970)	$\delta = \left(\frac{-U_{liq}(T,P)}{V_{liq}(T,P)} \right)^{\frac{1}{2}}$	(T,P)

Table II-2: Some definitions of the solubility parameter

The first approach is presented by Barton (1983): he states that the cohesive energy is a saturation property and can be written as:

$$-E = \Delta_l^g U + \Delta_g^\infty U = U_{vap}\left(T, P=0\right) - U_{liq}\left(T, P_{sat}\right) \qquad \textbf{Eq II-2}$$

where $\Delta_l^g U$ is the molar vaporization energy that is required to vaporize one mole of the liquid to its saturated vapour and $\Delta_g^\infty U = \int_{V=V^g}^{V=\infty} \left(\frac{\partial U}{\partial V}\right)_T dV$ is the energy required to expand the saturated liquid to infinite volume at constant temperature.

At temperatures below the normal boiling point, $\Delta_g^\infty U$ is usually negligible compared to $\Delta_l^g U$. Hence, Eq II-2 becomes:

$$-E = \Delta_l^g H - RT = U_{vap}\left(T, P_{sat}\right) - U_{liq}\left(T, P_{sat}\right) \qquad \textbf{Eq II-3}$$

This last approximation is by far the most used one to describe and calculate the cohesive energy since the enthalpy of vaporisation is measurable in most cases for pure compounds.

However, it is believed in this work that the cohesive energy depends on pressure (since the cohesion of a liquid is affected by pressure). Thus, a more appropriate definition would rather be:

$$-E\left(T,P\right) = U_{vap}\left(T, P=0\right) - U_{liq}\left(T,P\right) = -U_r \qquad \textbf{Eq II-4}$$

This definition specifies that the cohesive energy is equal to the residual internal energy $-U_r$. As a result, the definition of δ used in this work is:

$$\delta\left(T,P\right) = \left(\frac{U_{vap}\left(T, P=0\right) - U_{liq}\left(T,P\right)}{V_{liq}\left(T,P\right)}\right)^{1/2} \qquad \textbf{Eq II-5}$$

This definition was used by Maloney and Prausnitz (1974).

However, the definition of δ does not seem to be so clear because many other definitions can be found in the literature, as shown with the following three examples. Lyckman et al. (1965) use the same definition except that the volume is at the saturation pressure:

$$\delta = \left(\frac{U_{vap}\left(T, P=0\right) - U_{liq}\left(T, P_{sat}\right)}{V_{liq}\left(T, P_{sat}\right)} \right)^{\frac{1}{2}} \qquad \textbf{Eq II-6}$$

In this case, δ does not depend on pressure.

Another widespread definition is the one used by Hoy (1970) for instance, i.e. the cohesive energy is said to be equal to the internal energy U :

$$\delta = \left(\frac{U_{liq}\left(T, P\right)}{V_{liq}\left(T, P\right)} \right)^{\frac{1}{2}} \qquad \textbf{Eq II-7}$$

Hildebrand and Scott (1950), Allen et al. (1960) and Amoros et al. (1984) amongst others used this definition when they linked solubility parameter to internal pressure, which will be further investigated. This description is just a "snapshot" at a given $\left(T, P\right)$. This definition is also regularly chosen for modelling δ with an equation of state (Utracki and Simha, 2004 for instance).

These few examples show that the definition of δ is varying in function of the needs. And, since pressure is taken into account in this work, Eq II-5 appears to be the most relevant one for our purpose.

Most of the data available in literature about the solubility parameter are calculated at 298.15 K and at atmospheric pressure using the approximation made with Eq II-3:

$$\delta = \left(\frac{\Delta_l^g H - RT}{V_{liq}} \right)^{1/2} \qquad \textbf{Eq II-8}$$

The difference between Eq II-1 and Eq II-8 can be emphasized here: the molar cohesive energy $-E$ of n-heptane is 29.33 kJ.mol^{-1} at its normal boiling point whereas its molar energy of vaporization $\Delta_l^g U$ is 28.93 kJ.mol^{-1} at the same temperature (Barton, 1983), i.e. a deviation of 0.13%. This apparently slight deviation can have a big impact later on, when the solubility parameter is used.

The notion of cohesive energy density (CED) is sometimes introduced:

$$CED = \delta^2 \qquad \textbf{Eq II-9}$$

If it is assumed that the cohesive energy is made up of a linear combination of contributions from dispersion interactions (d), polar interactions (p) and hydrogen bonding (h), then the solubility parameter can be written as follows, as suggested by Hansen (1967):

$$\delta^2 = \delta_d^2 + \delta_p^2 + \delta_h^2 \qquad \textbf{Eq II-10}$$

1.2.2. Determination and measurement

Since the solubility parameter is extensively used in fields as different as paints, pharmaceuticals, polymers and petroleum, many techniques and correlations are available to determine it. However – and this is its main drawback – it cannot be measured directly. Thus, it is not surprising to see solubility parameters of pure compounds reported with deviations up to 0.5 $MPa^{1/2}$ according to the database used (n-heptane for instance, Barton, 1983).

If one works at ambient conditions (conditions for which the solubility parameter was initially designed for), Eq II-8 is usually valid. But what happens for non-volatile compounds? What happens when pressure is taken into account?

Many empirical correlations exist and link measurable physical properties to the solubility parameter: viscosity, permittivity, refractive index or surface tension to name a few. All the details about these techniques are available in Barton, 1983. But those methods have limitations. For example, refractive index only takes into account dispersion forces (Israelachvili, 1992).

For crude oils, many correlations are based on molar weight (Won et al., 1986; Chung, 1992; Zhou et al., 1996). Not only do they not depend on temperature but they do not work properly when polar forces or hydrogen bonds are present (Torcal-Garcia, 2004).

Group contribution methods also enable the determination of solubility parameters (Lyckman et al., 1965 and more recently Laux, 1992). The structure of the molecules is hence required, which is problematic for asphaltenes for instance.

Ensley (1994) listed some different ways to obtain the solubility parameter for unknown compounds (Table II-3). If one wants to take into account the effect of pressure and temperature and work with non-volatile compounds without making assumptions (no equations), the internal pressure seems the more relevant method to use for crude oils.

Methods	Advantages	Drawbacks
Measurement of the heat of vaporization	Easy and fast	Not possible for non volatile compounds
Vapour pressure measurements and application of the Clausius-Clapeyron or the Antoine equation	Easy and fast	Idem
Boiling point measurements and application of the Hildebrand-Scott relationship	Easy and Fast	Idem
Heat of Mixing	Can be done at different T	Depends on the equation
Polymer swelling measurements	Easy and fast	Not accurate
Measurements of the internal pressure	T and P dependence	Heavy experimental set-up
Measurements of the thermal pressure	Idem	Idem

Table II-3: Different ways to determine solubility parameters

The very complete handbook written by Barton should be consulted for more details about the different techniques and correlations mentioned in this paragraph.

1.3. Influence of pressure and temperature

1.3.1. Solubility parameter from PR EOS

Solubility parameter is defined by Eq II-5 as:

$$\delta^2 = \frac{-U_r(T,P)}{v(T,P)} = \int_v^{\infty}\left(\frac{\partial U}{\partial V}\right)dV \qquad \textbf{Eq II-11}$$

where U is the internal energy, U_r the residual energy, v the molar volume.

With the Peng-Robinson equation of state (PR EOS), it becomes:

$$\delta^2 = \frac{\sqrt{2}}{4b}\left(a - T\frac{da}{dT}\right)\left[\ln\left(\frac{v(T,P)+b\left(\sqrt{2}+1\right)}{v(T,P)-b\left(\sqrt{2}-1\right)}\right)\right]\cdot\frac{1}{v(T,P)} \qquad \textbf{Eq II-12}$$

where a the attractive term of the PR EOS and b the co-volume.

Since cubic EOS are known not to give accurate evaluations of volumes, experimental volumes can be used in Eq II-12 instead.

1.3.2. Influence of temperature

Both molar volumes and cohesion energy are affected by temperature. Barton (1991) suggested the following linear relationship between δ and T:

$$\delta(T) = \delta^0 - m(T - T_0) \qquad \textbf{Eq II-13}$$

The coefficient m is listed for pure compounds (p 304 in Barton, 1991) and varies between 2.00 and $3.00\cdot10^{-2}$ $MPa^{1/2}.K^{-1}$ for the studied hydrocarbons ($2.70\cdot10^{-2}$ for n-pentane, $1.83\cdot10^{-2}$ for n-nonane and $1.98\cdot10^{-2}$ for n-decane for instance). Figure II-3 presents the dependence of m with respect to the molar weight. It seems that the higher the molar weight, the less δ depends on temperature.

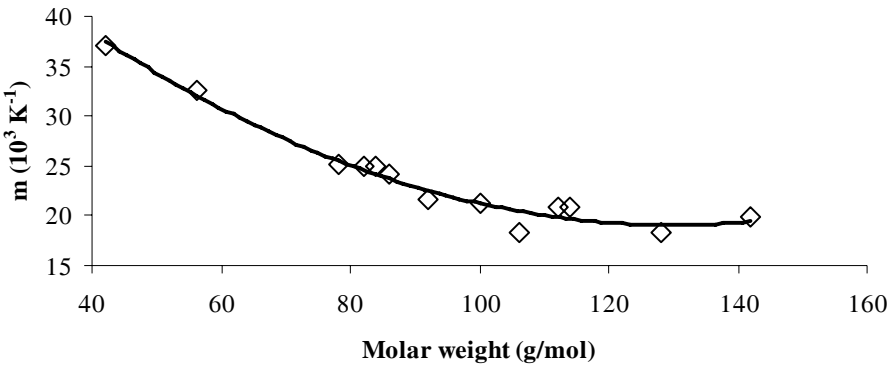

Figure II-3: Dependence of m with respect to molar weight (adapted from Barton, 1991)

Nonetheless, it is interesting to use some of the definitions of δ given in Table II-2 to evaluate the influence of temperature. Three definitions of the cohesive energy were tested in addition to the correlation given by Barton (1991). Calculations were performed for n-heptane at 0.1 MPa. The liquid density was calculated from the DIPPR correlation as well as the heat of vaporisation.

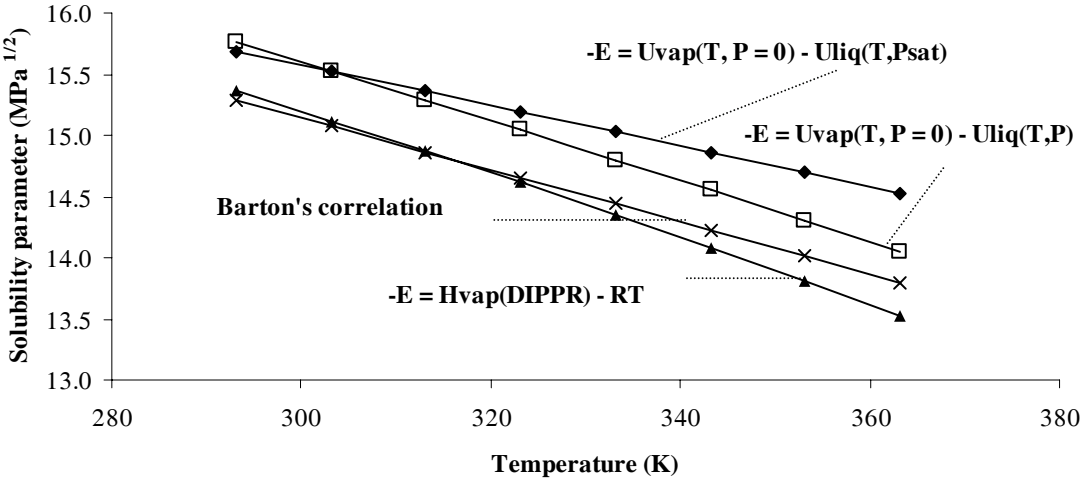

Figure II-4: Influence of temperature on the solubility parameter of n-heptane at 0.1 MPa

Solubility parameter strongly depends on temperature. Furthermore, the choice of cohesive energy highly affects this dependence. As it is seen on Figure II-4, the DIPPR and the Barton's correlations give close results (deviation within 0.01 and 0.28 $MPa^{1/2}$). With the two other definitions of cohesive energy, solubility parameters are higher

(deviation between 0.40 and 0.53 $MPa^{1/2}$ for the cohesive energy function of pressure and 0.32 and 1.00 $MPa^{1/2}$ for the second one). Similar results were obtained for toluene and ethanol (Appendix II-1). The correlation given by Barton for the temperature dependency is also close to the calculations performed with the DIPPR heat of vaporisation.

Heat of vaporisations can be calculated from PR EOS as follows:

$$H_{vap} = \frac{\sqrt{2}}{4b}\left(a - T\frac{da}{dT}\right)\left[\ln\left(\frac{v_{liq}(T,P_{sat}) + b\left(\sqrt{2}+1\right)}{v_{liq}(T,P_{sat}) - b\left(\sqrt{2}-1\right)}\right) - \ln\left(\frac{v_{vap}(T,P_{sat}) + b\left(\sqrt{2}+1\right)}{v_{vap}(T,P_{sat}) - b\left(\sqrt{2}-1\right)}\right)\right] + RT \qquad \textbf{Eq II-14}$$

At 303.15 K, the saturated volume of the vapour phase is 0.321 m^3/mol (NIST website). Hence, the heat of vaporisation of n-heptane at 303.15 K and the respective saturated pressure (7.75 10^{-3} MPa) is 38 141 J/mol whereas the DIPPR correlation gives 36 334 J/mol. When the solubility parameter is calculated with this energy of vaporisation, it follows curve calculated with $-E = U_{vap}(T, P=0) - U_{liq}(T, P_{sat})$. Hence, the deviation seen between the DIPPR correlation and the PR EOS is due to the inaccurate ability of PR to estimate heat of vaporisation.

Another striking result was that PR EOS combined with experimental volumes managed to calculate the total solubility parameter for ethanol and toluene. Indeed, it was only expected to give the dispersion term.

Therefore, is there a correct definition of the cohesive energy? In this work, it is believed that the cohesive energy should depend on pressure. Hence, it should be equal to the residual internal energy. Note that an accuracy of 0.1 $MPa^{1/2}$ is required for modelling, as it is explained in Chapter 5.

1.3.3. Influence of pressure

The different solubility parameters presented in Table II-2 were calculated for n-heptane with experimental densities at 303.15 K (Figure II-5). The modified Tait equation used by Cibulka and Hnedkovsky (1996) was employed to describe density with respect to pressure. The saturated density, the heat of vaporization and the saturated pressure were calculated from the DIPPR correlations.

The solubility parameter of n-heptane at 303.15 K and 0.1 MPa is 15.07 $MPa^{1/2}$ (Barton, 1991). The heat of vaporisation gives a very accurate estimation of it but it is likely that the solubility parameters from literature have been evaluated that way. Calculations were performed with Eq II-14 for n-heptane and it appeared that $U_{vap}(T, P=0) - U_{vap}(T, P_{sat})$ did not affect cohesive energy (the impact on the solubility parameter is less than 0.01 $MPa^{1/2}$).

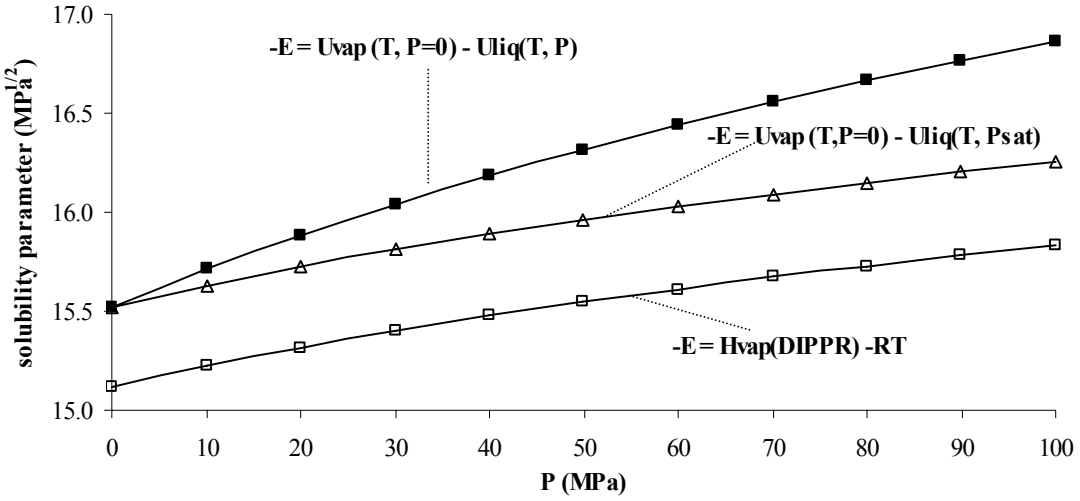

Figure II-5: Influence of pressure on the solubility parameter of n-heptane at 303.15 K

The most interesting fact is the effect of pressure on cohesive energy. $U_{liq}(T, P) - U_{liq}(T, P_{sat})$ strongly affects the solubility parameter and the difference reaches 0.6 $MPa^{1/2}$ at 100 MPa. Similar calculations were carried out for ethanol and

toluene (Appendix II-2). Similar results were found except that the differences reached 1 $MPa^{1/2}$ at 100 MPa and 303.15 K for both compounds.

Hence, the assumption that cohesive energy does not depend on pressure is rather wrong since pressure induces large differences that will greatly affect modelling.

1.3.4. Solubility parameters of gases

In this work, the effect of gas injection on asphaltene stability is studied. Hence, the solubility parameters of carbon dioxide, nitrogen and methane are now calculated over a wide range of temperatures and pressures. Densities were given by NIST website (www.webbook.nist.gov) and solubility parameters were calculated according to Eq II-5.

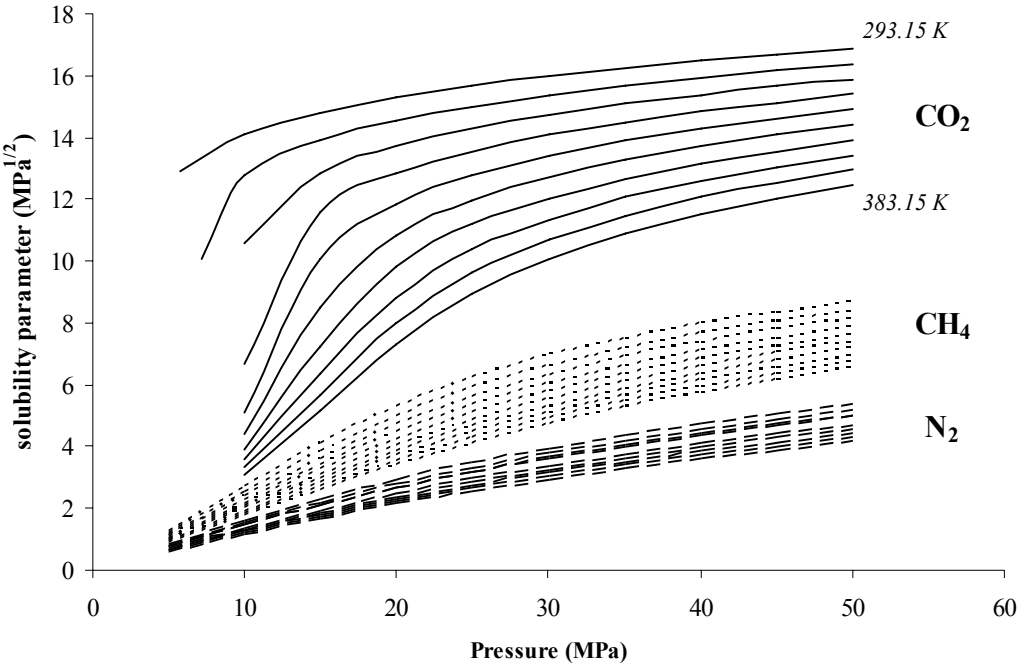

Figure II-6: Solubility parameters of carbon dioxide, methane and nitrogen (calculated every 10 K, starting at 293.15 K for the top curves)

The strong variations of δ_{CO_2} are due to its density. Note that the three compounds are supercritical fluids under these conditions.

1.4. Conclusion

The various definitions of cohesive energy induced many definitions and databases of solubility parameters for pure compounds. The heat of vaporisation can be used if it is the one given at the saturated pressure. The effects of temperature and pressure are both important and should be taken into account. When PR EOS is combined to experimental molar volumes, the total δ is believed to be properly estimated.

2. Solubility parameter of crude oil

2.1. Internal pressure, an alternative

The internal pressure π is defined as follows:

$$\pi = \left(\frac{\partial U}{\partial V}\right)_T = T\left(\frac{\partial P}{\partial T}\right)_V - P = T\frac{\alpha_P}{\kappa_T} - P \qquad \textbf{Eq II-15}$$

where $\alpha_P = \frac{1}{V}\left(\frac{\partial V}{\partial T}\right)_P$ is the thermal expansivity and $\kappa_T = -\frac{1}{V}\left(\frac{\partial V}{\partial P}\right)_T$ the isothermal compressibility.

The difference between internal pressure and solubility parameter is not that simple: these two notions describe the same phenomenon, i.e. the cohesion of a liquid but not in the same way. The cohesive energy density is a measure of the total molecular cohesion per unit volume contrary to the internal pressure, which is a measure of the change in internal energy of a liquid as it experiences a small isothermal expansion. Such a differential change in volume does not necessarily disrupt all intermolecular interactions to an equal extent. The interactions most affected include repulsion, dispersion and weak dipole processes. In other words, a small volume expansion has a disruptive effect on these interactions, which may be equivalent to that of vaporisation (Barton, 1983).

One can attempt to link these two notions using the typical Mie's form of the intermolecular potential:

$$U = U_A + U_R = -\frac{a}{V^n} + \frac{b}{V^m} \qquad \textbf{Eq II-16}$$

where U_A is the attractive energy, U_R the repulsive term, V the molar volume, a, b, m and n are constants. The repulsive term U_R is only significant for highly compressed liquids so, at low pressures, we have:

$$U = U_A = -\frac{a}{V^n} \qquad \textbf{Eq II-17}$$

Using Eq II-7 and Eq II-17, one obtains:

$$\delta = \left(\frac{1}{n} \pi \right)^{1/2} \qquad \textbf{Eq II-18}$$

The factor n is listed for the most common compounds (Allen et al., 1960; Amoros et al., 1984) and it is around the unity. When n is equal to 1, the fluid is a Van der Waals fluid. Figure II-7 shows the variations of n with respect to the carbon number.

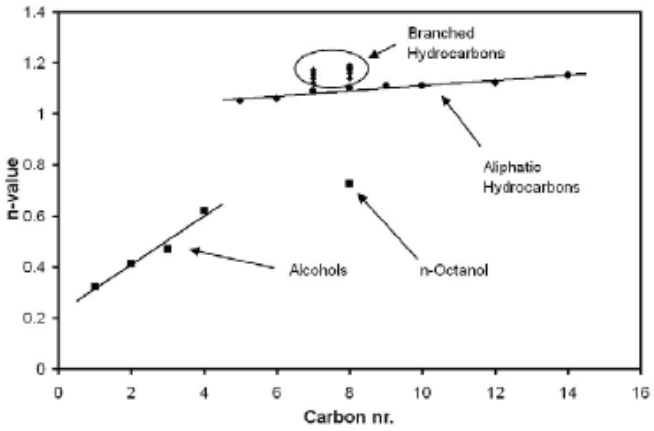

Figure II-7: n-value as function of the carbon number (from Duong, 2004)

Internal pressure is usually not known accurately. For instance, π of toluene is 307.1MPa (Cibulka and Takagi, 1999), 322.0 MPa (Verdier and Andersen, 2005) or 347.1 MPa (Sun et al., 1991) at 303.15 K and 0.1 MPa. Figure II-8 shows the n-values calculated with other sets of data. Internal pressure was calculated from thermal expansivities and isothermal compressibilites as Eq II-15 explains it and data were taken from Perry et al. (1997). As for solubility parameters, they were taken from Barton (1983). For these calculations, the n-value of n-alkanes does not increase with the carbon number contrary to the trend shown in Figure II-7. Eq II-18 is based on the assumption that cohesive energy is equal to internal energy. However if cohesive energy is defined as $-U_r$, the following relationship is found:

$$\delta^2 = \pi + A/\rho \qquad \textbf{Eq II-19}$$

where A is a constant determined for any reference condition and ρ is the density (see the Appendix II-3 for the derivation).

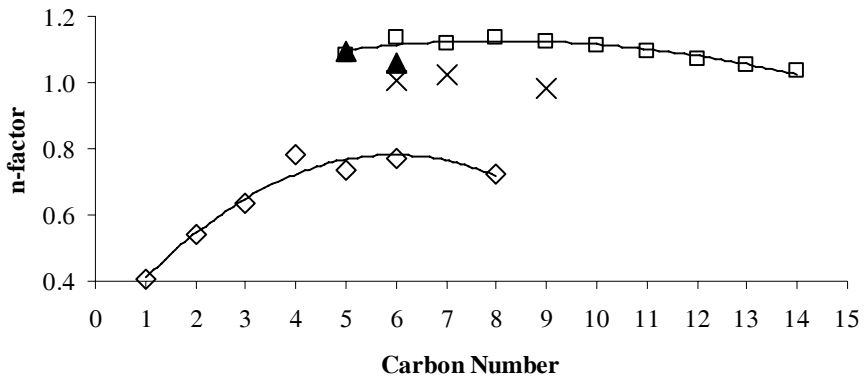

Figure II-8: n-value as function of the carbon number (□, n-alkanes; ◇, alcohols; ▲; cycloalkanes; ×, aromatics)

Nevertheless, although internal energy gives a good approximation of δ for hydrocarbons and aromatics, compounds exhibiting hydrogen bonding cannot be represented by π. Therefore Bagley et al. (1971) subdivided the solubility parameter in two parts for interacting systems:

- one part corresponding to the "physical" or "non-chemical" effects that is called the volume-dependent cohesion parameter defined by:

$$\delta_V^2 = \pi \qquad \textbf{Eq II-20}$$

- the other component is a residual parameter, arising from the "chemical" effects:

$$\delta_R^2 = \frac{\left(\Delta_l^g U - \pi V\right)}{V} \qquad \textbf{Eq II-21}$$

Hence, solubility parameter can be estimated by internal pressure using Eq II-15:

$$\delta_v = \pi^{1/2} = \left(T\frac{\alpha_p}{\kappa_T} - P \right)^{1/2} \qquad \textbf{Eq II-22}$$

Such a division of the solubility parameter resembles the Hansen parameter and is validated by Eq II-19. In this work, thermal expansivites and isothermal compressibilities have been measured up to 30 MPa at 303.15 K for pure compounds as well as dead and recombined crude oils.

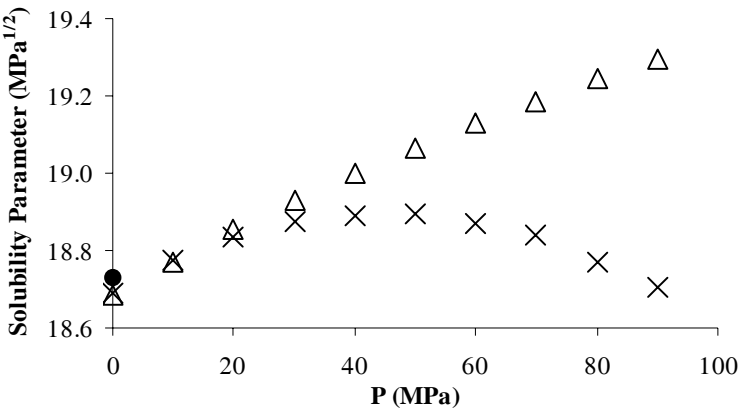

Figure II-9: Solubility parameter of benzene as function of pressure at 303.15 K (△, from heat of vaporisation; ×, from internal pressure (Sun et al.,1987); ●, 1 bar (Hildebrand et al., 1970))

Moreover, the fundamental difference between internal pressure and cohesive energy density is emphasized when pressure is taken into account. Figure II-9 shows the solubility parameter of benzene calculated in two ways at 303.15 K:

- from heat of vaporisation with Eq II-8, using the DIPPR correlation for ΔH_l^g and experimental molar volumes (Sun et al., 1987)
- from internal pressure with Eq II-18 with n=1.06. Isothermal compressibilities and thermal expansivities were determined by speed-of-sound measurements (Sun et al., 1987)

The description at atmospheric pressure is quite good (difference of 0.04 $MPa^{1/2}$ compared to δ given by Hildebrand et al. (1970) at 293.15 K). The two curves have a similar shape up to 30 MPa and then, they start diverging. Indeed, for internal pressure, resultant forces under low-pressure conditions are attractive and, as the pressure increases, the repulsive forces become preponderant.

Pressure (MPa)	20	79	197	523	717	908	1095
Internal pressure (MPa)	275	280	250	199	4	-157	-432

Table II-4: Internal pressure of diethylether at 298.15 K as function of pressure (Moore, 1959)

Table II-4 illustrates this effect of pressure on internal pressure for diethyl ether at 298.15 K (Moore, 1959) For moderate increases in pressure, the internal pressure first increases only slightly and then decreases slowly but as P exceeds 500 MPa, the internal pressure begins to decrease rapidly, and goes to large negative values as the liquid is further compressed.

Therefore, though internal pressure and solubility parameter are related to the cohesive energy, they behave differently when hydrogen bonding or pressure are at stake for instance.

2.2. Internal pressure of pure compounds

The experimental procedure is detailed in Verdier and Andersen (2005) (presented in Appendix II-4). Nevetheless, a short description will be given.

Scanning transitiometry was used to measure thermal expansivities. This method was proposed by Randzio in 1985. A fluid is isothermally compressed or decompressed in a calorimeter and the heat released is proportional to its thermal expansivity as follows:

$$\left.\frac{\delta Q}{dt}\right|_T = -(\alpha_P - \alpha_V) V T \frac{dP}{dt} \qquad \textbf{Eq II-23}$$

where $\left(\delta Q/dT\right)_T$ is the rate of heat measured by the microcalorimeter, α_p the thermal expansivity of the fluid under investigation, α_V the thermal expansivity of the stainless steel, V the volume of the cell, T the temperature and dP/dT the rate of increase in pressure.

In this work, a LKB 2277 Bio Monitor calorimeter was modified to stand high-pressures. An automatic high-pressure syringe pump (ISCO 260 D) was used to compress and decompress the fluid. Unfortunately, this calorimeter does not permit scanning in temperatures. Thermal expansivities of several pure compounds were measured up to 30 MPa and at 303.15 K. The deviation to literature data was within 2%.

Isothermal compressibility was determined indirectly through density. A high-pressure Anton Paar densimeter DMA 512 was employed to measure densities with respect to pressure. A syringe pump ISCO 260D was used to control pressure. Then, using a modified Tait equation, density was fitted as follows:

$$\rho = \frac{\rho_0(T)}{1 - C(T)\ln\left(\frac{B(T)+P}{B(T)+P_0}\right)} \qquad \textbf{Eq II-24}$$

where $\rho_0(T)$ is the density at $P = P_0$, C and B are functions of temperature and P the pressure.

The densimeter was calibrated according to the method developed by Lagourette et al. (1992). Densities of pure compounds were measured with an AAD of 0.1% over the pressure range at 303.15 K. Finally, isothermal compressibility was calculated with the modified Tait equation:

$$\kappa_T = -\frac{1}{V}\left(\frac{\partial V}{\partial P}\right)_T = \frac{1}{\rho}\left(\frac{\partial \rho}{\partial P}\right)_T = \frac{C}{B+P}\cdot\frac{1}{1 - C\ln\left(\frac{B+P}{B+P_0}\right)} \qquad \textbf{Eq II-25}$$

For the five pure compounds studied, the average absolute deviation was within 2.7%.

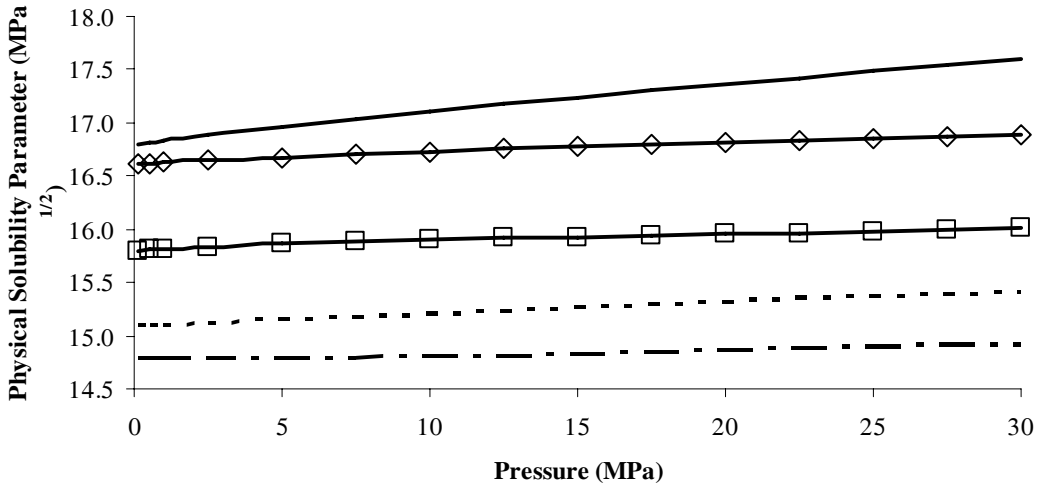

Figure II-10: Physical solubility parameter as a function of pressure at 303.15 K

(– —, n-hexane; —, cyclohexane; - - -, n-heptane; —□—, n-decane; —◇—, ethanol)

Hence, internal pressures (i.e. "physical" solubility parameters) could be determined up to 30 MPa (Figure II-10). One can see that pressure does not affect much solubility parameter, except for cyclohexane. Indeed, the pressure is quite limited.

Table II-5 presents the comparison of this work with literature data at atmospheric pressure. The references can be found in Appendix II-4.

Compound	n-hexane	cyclohexane	n-heptane	n-decane	ethanol
$\delta_{\text{literature}}$	14.70	16.62	15.07	15.60	26.05
$\left(\pi_{this\ work}\right)^{\frac{1}{2}}$	15.16	16.86	15.62	16.52	16.61
$\delta_{lit} - \left(\pi_{this\ work}\right)^{\frac{1}{2}}$	- 0.46	- 0.24	- 0.55	- 0.90	9.49
$\pi_{\text{literature}}$	236.7	315.6	250.4	-	291.0
$\pi_{\text{this work}}$	229.8	284.3	243.99	272.4	275.9
$\pi_{\text{literature}} - \pi_{\text{this work}}$	6.9	31.3	6.4	-	15.1

Table II-5: Solubility Parameters (in $MPa^{1/2}$) and Internal Pressures (in MPa) at 303.15 K and 0.1 MPa

The deviation between δ and δ_v is up to 1 $MPa^{1/2}$ for hydrocarbons but, as expected, it reaches 10 $MPa^{1/2}$ for ethanol. As a matter of fact, hydrogen bonds are not taken into account by the "physical" solubility parameter.

As a conclusion, internal pressure can be successfully measured with respect to pressure but it does not give results accurate enough for modelling. The high deviation related to isothermal compressibility may be one of the reasons. Furthermore, "chemical" forces are not taken into account by internal pressure.

2.3. Internal pressure of crude oils

Though accuracy was not good enough for modelling, dead crude oils as well as recombined ones were investigated. Indeed, solubility parameter has never been measured for live oils and over a pressure range.

Figure II-11 shows δ_v of the dead crude oil A at 303.15 K. In this case, pressure has a strong impact. The impact of the factor n introduced by Eq II-18 was tested here. Even a small factor highly affects the results.

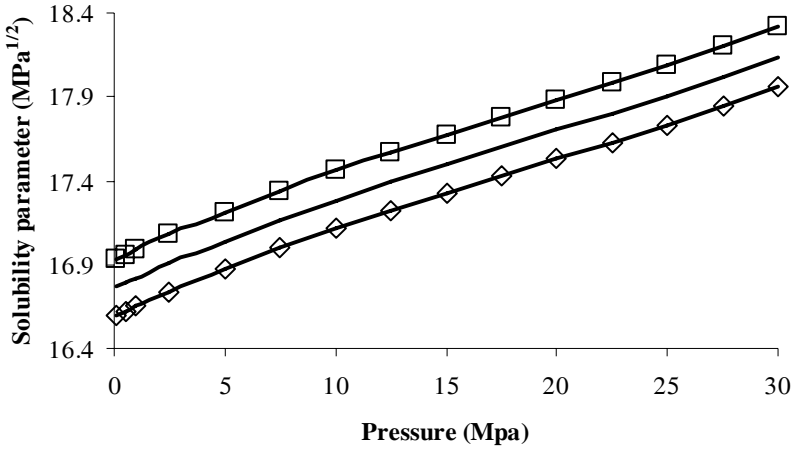

Figure II-11: Solubility parameter of a dead oil A at 303.15 K (—, n = 1; □ , n = 0.98; ◇ , n = 1.02)

Afterwards, a dead oil was recombined with 2.5 w% methane. Its thermal expansivity was successfully measured (Figure II-12). A fast decompression induced a break in the calorimetric signal. It is supposed to be the bubble point. It was confirmed by the PV curve performed with the ISCO pump.

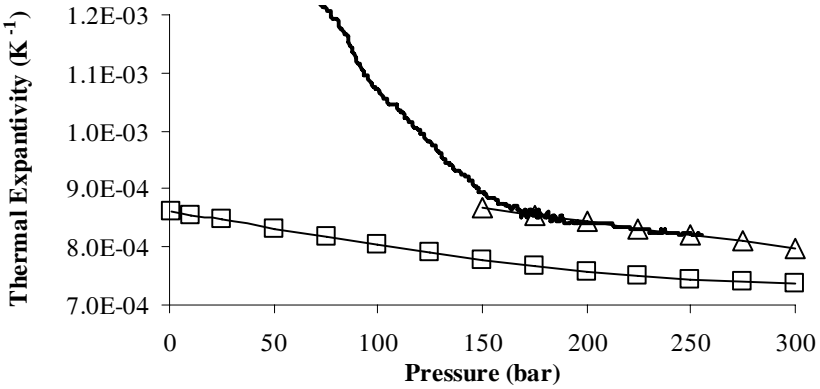

Figure II-12: Thermal expansivity of oil 1 at 303.15 K (— , live oil B; fast decompression; Δ , live oil B, slow decompression; □, dead oil B)

Once densities were measured, the respective solubility parameters of oil B were calculated. As it is visible in Figure II-13, the solubility parameter of the live oil is lower.

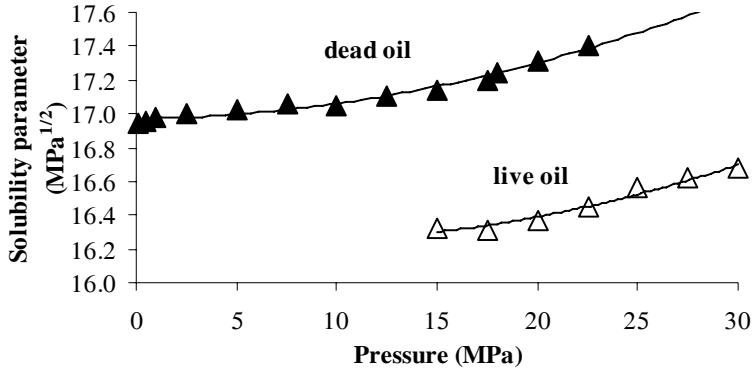

Figure II-13: Solubility parameter of oil 1 at 303.15 K (Δ, live oil B, from internal pressure; ▲, dead oil B, from internal pressure)

One can "predict" $\delta_{live\ oil}$ from $\delta_{dead\ oil}$ and the methane content with the following mixing rule:

$$\delta_{live\ oil} = \varphi_{dead\ oil}\delta_{dead\ oil} + \varphi_{gas}\delta_{gas} \qquad \textbf{Eq II-26}$$

where φ is the volume fraction.

The calculations performed in paragraph 1.3.4 shows that the solubility parameter of methane at 303.15 K varies within 3.84 and 6.63 $MPa^{1/2}$ between 15 and 30 MPa. The 2.5 w% corresponds to a volume fraction of 6.5% for methane. The calculated solubility parameter of live oil B turns out to fit the experimental one (Table II-6).

Pressure (MPa)	δ_{CH4}	$\delta_{dead\ oil}$	$\delta_{live\ oil}$	$\delta_{mixing\ rule}$	Difference
15	3.84	17.10	16.24	16.33	0.09
20	4.99	17.19	16.40	16.36	0.03
25	5.91	17.31	16.57	16.57	0.00
30	6.63	17.41	16.70	16.68	0.03

Table II-6: Solubility parameters (in $MPa^{1/2}$) related to live oil and calculated with the mixing rule

2.4. Conclusion

Internal pressures of dead and live oils can be successfully measured up to 30 MPa. However, by definition, solubility parameter and internal pressure are different. Hence, such measurements turn out to be incompatible with modelling since a high accuracy is expected. Nonetheless, it is the first time that solubility parameters of oils have been measured. Modelling of the solubility parameter has been performed with PR EOS for this crude oil after it has been characterised but the deviation was quite high (up to 4.9 $MPa^{1/2}$). More details are available in Appendix II-5 about this modelling.

3. Characterization of asphaltenes

The issues about asphaltene characterisation were introduced in Chapter 1, paragraph 1.3. The polydisperse nature of asphaltenes makes any characterisation difficult. However, in this paragraph, solubility parameters and critical constants were determined for several asphaltenes in solution.

3.1. Solubility parameter of asphaltenes

3.1.1. Literature survey

The determination of the solubility parameters of asphaltenes is uncertain in most cases. Hirschberg et al. (1984) used titration experiments to determine asphaltene solubility parameters, assuming a molar volume. They found a value of 19.50 $MPa^{1/2}$ and a small temperature dependence when fitting their data. Wang and Buckley (2001) used asphaltene molar volume and solubility parameter as adjustable parameters in their asphaltene solubility model. As for Yarranton and Masliyah (1996), they determined it by fitting the model to one set of asphaltene-n-heptane-toluene titration curve. Could it be done otherwise? Can a complex and polydisperse system be represented by a single parameter? Nevertheless, several techniques are available to determine this parameter for asphaltenes. They are based on:

- **Miscibility** (Lian, 1994): here, the miscibility of asphaltenes is measured in various solvents and a solubility profile is obtained. Hence, a range of solubility parameters is obtained. Lian reports solubility parameters ranging between 17.6 and 21.3 $MPa^{1/2}$.

- **Titration** (Hirschberg et al., 1984; Andersen, 1999): Andersen states that, if one plots $V_{\text{precipitant}}/V_{\text{oil}}$ vs. $V_{\text{solvent}}/V_{\text{oil}}$, both the intercept and the slope give access to the solubility parameter of the crude oil δ_o and to a critical one δ_{cr}. Empirically, in polymer chemistry, the solubility parameter of asphaltenes is such as $\delta_a = \delta_{cr} + 4$ (in $MPa^{1/2}$). Eighteen crude oils were investigated and the calculated δ_a are within 19 and 22 $MPa^{1/2}$ at room conditions.

- **Inverse gas chromatography** (Mutelet et al., 2004): only asphaltenes from a single oil were tested. It was found that δ_a depends on the n-heptane fraction. Although a solubility parameter is assumed to be a property of the "pure compound" and no to depend on the mixture, such a variation is not surprising. Indeed, the structure of asphaltenes and its state of aggregation is known to be affected by n-heptane content (Fenistein et al., 1998). They studied the size of aggregates by SANS measurements and they found out that, when asphaltenes are diluted in a toluene-heptane mixture, the average aggregate sizes increase with the heptane content. However, the calculated solubility parameter at the onset of precipitation is 29.9 $MPa^{1/2}$ and, apparently, onset titrations gave a value of 31.9 $MPa^{1/2}$. These values exceed the usual ranges of δ_a. The temperature is quite high (523 K for the injector and the detector which is above the reported glass transition temperature). It seems that further tests should be performed to validate this technique.

- **Refractive index** (Christiansen, 1999): as it was said in paragraph 1.2.2, dispersive solubility parameter and refractive index are correlated. Wang and Buckley (2001) proposed the following correlation:

$$\delta = 52.042\left(\frac{RI^2-1}{RI^2+2}\right)+2.904 \qquad \textbf{Eq II-27}$$

where RI is the refractive index.

This correlation is widely used for crude oils. Torcal-Garcia (2004) compared the results obtained for crude oils with both onset titration and refractive index. Results are usually of the same order of magnitude but deviations can reach up to 2 $MPa^{1/2}$ as it is visible in Figure II-14.

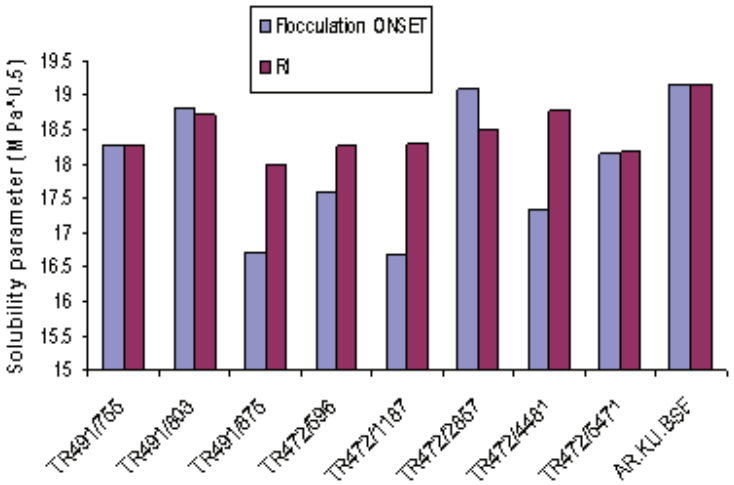

Figure II-14: Solubility parameters of several crude oils from onset titrations and refractive index measurements at room conditions (Torcal-Garcia, 2004)

This technique based on refractive index was not directly applied to asphaltene solutions but both refractive index and density of asphaltenes were determined by Christiansen. He used a volume mixing rule between solvents and asphaltenes. He also assumed that there were no excess properties (ideal mixture). Furthermore, he performed onset titration experiments and calculated δ_a combining the onset titrations and the regular solution theory. His results are presented in Table II-7 for two of the asphaltenes that have been investigated in this work. δ_a calculated from refractive index may seem low at first sight but refractive index only takes into account dispersion forces. If one adds the polar and the hydrogen bonding terms, δ_a reaches the usual order of magnitude. Note that the uncertainty is about 1.5% for refractive index measurement and 13.8% for density measurements.

Asphaltenes	Refractive Index	δ from RI (in $MPa^{1/2}$)	Density (in kg/m^3)	δ from titration (in $MPa^{1/2}$)
OLEO D	1.716 – 1.723	17.1 – 17.6	0.973	20.4
A 95	1.7063 – 1.7628	17.2 – 18.5	1.003	20.8

Table II-7: Properties of asphaltenes A95 and OLEOD from refractive index measurements and onset titrations (adapted from Christensen, 1999)

- **Correlations** (Laux, 1992): Laux developed a correlation taking into account the hetero-atom content, the carbon number and the hydrogen deficit. Two asphaltenes were tested with this method and the respective solubility parameters are 18.68 and 19.35 $MPa^{1/2}$, which is in the expected range. This method has not been very much used. Indeed, a complete chemical analysis is required and the temperature dependence is not taken into account.

So, a few techniques exist to evaluate the solubility parameter of asphaltenes. However, they are either inaccurate (miscibility) or based on strong assumption (ideal solution for the refractive index) or seem to give high results (chromatography).

3.1.2. Partial volumes and regular solution theory

In this work, a simple and fast technique, based on density measurements of asphaltenes dissolved in several solvents, was applied to determine the solubility parameter of asphaltenes. The input parameters are the internal and solubility parameters of the pure solvents at 0.1 MPa and the desired temperature. This procedure had been used by Liron and Cohen (1983) for compounds of pharmaceutical relevance such as cholesterol in various solvents (toluene, carbon tetrachloride, chlorobenzene, chloroform and nitrobenzene).

Consider a binary constituted of a solvent 1 and a solute 2. According to Hildebrand and Dymond (1967), introducing molecules of solute in the solvent causes microscopic regions of weakness and expansion until enough energy has been absorbed to restore the local internal pressure to the bulk internal pressure. Accordingly, it can be written:

$$\left(\overline{v_2} - v_2^0\right)\pi_1 = \overline{E_2} - E_2^0 \qquad \textbf{Eq II-28}$$

where $\overline{v_2}$ is the partial molar volume, v_2^0 is the molar volume of the pure solute, π_1 the internal pressure of the solvent 1 and $\overline{E_2} - E_2^0$ is the partial molar energy of transferring a mole of liquid solute 2 from pure liquid to solution.

It is assumed that internal pressure is unchanged by the small amount of solute introduced (Hildebrand et al., 1970). This equation has no theoretical background but, quoting

Hildebrand and Dymond (1967), "*the best we have been able to do is to rely somewhat upon intuition to produce a rough-and-ready relation that withstands the test of experiment amazingly well*".

The regular solution theory can be applied and it gives:

$$\overline{E_2} - E_2^0 = \overline{v_2}\,\varphi_1^2\left(\delta_1 - \delta_2\right)^2 \qquad \textbf{Eq II-29}$$

where δ_i is the solubility parameter of the compound i and ϕ_1 is the volume fraction of the solvent. The key assumption in the regular theory is that, in a regular solution, there is no entropy change when a small amount of one of its components is transferred to it from an ideal solution of the same composition, the total volume remaining unchanged, i.e. there is no excess entropy when mixing occurs at constant volume (Hildebrand et al., 1970).

Since the solutions are highly diluted (mass fractions of solute below 10^{-2}), φ_1 is approximately equal to 1. Thus, combining Eq II-27 and Eq II-28, one obtains:

$$\frac{\overline{v_2} - v_2^0}{\overline{v_2}} = \frac{\left(\delta_1 - \delta_2\right)^2}{\pi_1} \qquad \textbf{Eq II-30}$$

After dividing each member of Eq II-29 by the molecular weight of the solute 2 M_{w2}, one can write:

$$\frac{\overline{V_{s2}} - V_{s2}^0}{\overline{V_{s2}}} = \frac{\left(\delta_1 - \delta_2\right)^2}{\pi_1} \qquad \textbf{Eq II-31}$$

where $\overline{V}$ is the specific partial volume (expressed in m^3/kg).

Nevertheless, when dealing with non-crystalline solids (like asphaltenes), two solvents are necessary (Liron and Cohen, 1983). Indeed, if the solvents are named 1 and 3 and the solute 2, Eq II-30 can be written:

$$\frac{\overline{V_{s21}} - V_{s2}^0}{\overline{V_{s21}}} = \frac{\left(\delta_1 - \delta_2\right)^2}{\pi_1} \qquad \textbf{Eq II-32}$$

$$\frac{\overline{V_{s23}} - V_{s2}^0}{\overline{V_{s23}}} = \frac{(\delta_3 - \delta_2)^2}{\pi_3} \qquad \textbf{Eq II-33}$$

where $\overline{V_{s2i}}$ is the partial specific volume of 2 in solvent i and V_{s2}^0 is the specific volume of the pure solute (i.e. the reciprocal of its pure density). After rearrangement, a 2nd order polynomial is obtained:

$$A\delta_2^2 + B\delta_2 + C = 0 \qquad \textbf{Eq II-34}$$

where $A = \frac{\overline{V_{s23}}}{\pi_3} - \frac{\overline{V_{s21}}}{\pi_1}$, $B = 2\left(\delta_1 \frac{\overline{V_{s21}}}{\pi_1} - \delta_3 \frac{\overline{V_{s23}}}{\pi_3}\right)$ and $C = \overline{V_{s21}}\left(1 - \frac{\delta_1^2}{\pi_1}\right) - \overline{V_{s23}}\left(1 - \frac{\delta_3^2}{\pi_3}\right)$

Two roots are obtained and the most relevant one is chosen (within the usual range).

3.1.3. Experimental procedure, calibration and results

An Anton-Paar densimeter DMA 58 was used. This high-precision densimeter contains a U-shaped sample tube electromagnetically excited. The period of oscillation T is related to the density of the sample. The claimed precision of the temperature-controlled system is better than ± 0.005°C and the display resolution is 0.01°C. The sample volume is approximately 0.7 cm^3. The constants were calculated with the solvent itself and air. The DIPPR correlations were used. Appendix II-6 presents the origin of the compounds and their respective purities.

Solute	$\overline{v_s}(this\ work)$	$\overline{v_s}(literature)$ [a]	**Deviation (%)**
n-heptane	156.01	152.63	2.2
n-decane	205.54	203.88	0.8

Table II-8: Partial molar volumes of n-decane and n-heptane in methanol at 298.15 K and 0.1 MPa (in cm^3/mol) (a: Barbosa et al., 2001)

First, molar volumes of known compounds were measured. Densities of several dilutions of n-heptane and n-decane in methanol were measured. Then, partial molar volumes were calculated and compared to literature (Barbosa et al., 2001). The maximum deviation is 2.2%, which is found acceptable (Table II-8).

The asphaltenes used were obtained with a modified IP 143 method from the oils OLEO D and A95 (see Appendix I-1). The mixtures were prepared by mass using the balance Sartorius Analytic A210P (accuracy: 0.0005 g, display resolution: 0.0001 g). These asphaltenes were mixed with the different solvents (toluene, m-xylene and carbon disulfide) by 15 minutes of ultrasonication. Each sample was injected in the oscillating tube with a 2 mL-syringe. Excess fluid was overflowed past the vibrating tube. Once the thermal equilibrium was reached, the measurement was made, the cell was cleaned with toluene, then ethanol and finally dried with air (by means of the small pump included in the densimeter) until the period reached the one of the empty tube. Each sample was measured twice. The dilutions were prepared between 0 and 0.3 wt. %. Table II-9 gives the different specific partial volumes with respect to the various solvents.

Solvent	**Toluene**	**Carbon disulfide**	**m-xylene**
	Partial specific volumes (m^3/kg)		
OLEOD	$9.48.10^{-4}$	$9.20.10^{-4}$	$9.42.10^{-4}$
A95	$9.22.10^{-4}$	$8.78.10^{-4}$	$9.14.10^{-4}$

Table II-9: Partial specific volumes of the asphaltenes at 303.15 K

Internal pressure was calculated using thermal expansivity and isothermal compressibility. As for the solubility parameter, cohesive energy was approximated with heat of vaporization. DIPPR correlations were used for both molar volumes and heats of vaporization. These values and the relevant references are presented in Table II-10.

	Toluene	**m-Xylene**
Internal pressure (MPa)	322.0 [a]	343.4 [b]
Solubility parameter ($MPa^{1/2}$)	18.20	17.94

Table II-10: Internal pressures and solubility parameters of the solvents at 303.15K and 0.1 MPa (a: Verdier et al., 2005 ; b: Taravillo et al., 1994 for thermal expansivity; Weast and Selby, 1966 for isothermal compressibility)

Table II-11 presents the solubility parameters of the asphaltenes under investigation, as well as their densities. The second root of Eq II-33 is also mentioned for the pair toluene/m-xylene. In this case, the solubility parameter is too small but the density is in the expected order of magnitude. The deviations between m-xylene/CS_2 and toluene/CS_2 are within 3.5% for the solubility parameter and within 1% for the density. The average properties are calculated with the last two pairs of solvents since the first one gives irrelevant results.

Solvents	**Solubility parameter ($MPa^{1/2}$)**		**Density (g/cm^3)**	
	OLEO D	**A 95**	**OLEO D**	**A 95**
Toluene/m-xylene	28.2 (15.2)	28.7 (14.5)	1.53 (1.08)	1.66 (1.13)
Toluene/Carbon disulfide	21.5	22.8	1.09	1.16
Carbon disulfide/m-xylene	20.8	22.0	1.09	1.15
Average Property	21.1	22.4	1.09	1.16
Difference with Christensen, 1999	0.7 $MPa^{1/2}$	1.6 $MPa^{1/2}$	0.12 g/cm^3	0.15 g/cm^3

Table II-11: Solubility parameter and densities of the asphaltenes OLEO D and A 95 (at 303.15 K and 0.1 MPa)

The deviation with the results obtained by Christiansen (1999) for the same asphaltenes is surprisingly quite low considering the numerous assumptions made for such calculations. But, is such an accuracy good enough for modelling?

3.1.4. Conclusion

The method used in this work was applied for the first time to asphaltenes. It is based on the assumptions of the regular solution theory and it requires little experimental work. Two pairs of solvents out of the three tried turned out to give solubility parameters in the usual range. The deviation between the two solvents is about 3% for solubility parameter and 1% for the density. When compared to results obtained by titrations, the measured solubility parameters exceed the accuracy expected for modelling. However, input parameters such as internal pressure and solubility parameters have a big impact on the

results. Nonetheless, considering the wide deviations about internal pressures in literature, this method is not likely to give exact enough solubility parameters.

3.2. Critical parameters of asphaltenes

3.2.1. Method based on partial volumes

The main idea is to use partial volume measurements combined with a cubic equation of state (EOS) and to determine the critical coordinates.

The partial molar volume is defined as:

$$\overline{v_i} = \left(\frac{\partial V}{\partial n_i}\right)_{T,P,n_j} \qquad \textbf{Eq II-35}$$

where V is the volume and n_i the mole numbers of component i.

It can also be written as follows:

$$\overline{v_i} = \frac{-\left(\frac{\partial P}{\partial n_i}\right)_{T,V,n_j}}{\left(\frac{\partial P}{\partial V}\right)_{T,n}} \qquad \textbf{Eq II-36}$$

Each term of this ratio is function of the reduced residual Helmholtz energy, $F = A^r\left(T,V,n\right)/RT$.

$$\left(\frac{\partial P}{\partial n_i}\right)_{T,V,n_j} = -RT\left(\frac{\partial^2 F}{\partial V \partial n_i}\right)_{T,n_j} + \frac{RT}{V} \qquad \textbf{Eq II-37}$$

$$\left(\frac{\partial P}{\partial V}\right)_{T,n} = -RT\left(\frac{\partial^2 F}{\partial V^2}\right)_{T,n} - \frac{nRT}{V^2} \qquad \textbf{Eq II-38}$$

Each of these derivatives is easily determined analytically if the method developed by J. Mollerup is followed (Michelsen and Mollerup, 2004). Thus, knowing $\overline{V_i}$ should enable the determination of T_C, P_c and ω suitable for a defined equation.

The Peng-Robinson EOS was chosen. The method was first tested with two pure and heavy compounds (n-tetradecane and n-octadecane) mixed in the solvents of interest

(toluene, m-xylene and carbon disulfide) at 298.15 K and 0.1 MPa. Partial volumes are given in Table II-12.

	Toluene	Carbon disulfide	m-xylene
n-C_{14}	$2.70.10^{-4}$	$4.70.10^{-4}$	$2.68.10^{-4}$
n-C_{18}	$3.35.10^{-4}$	$5.50.10^{-4}$	$3.33.10^{-4}$

Table II-12: Partial molar volumes of pure compounds in the various solvents at 298.15 K and 0.1 MPa (m^3/mol)

The partial molar volumes calculated with the EOS and the respective critical parameters are then compared to experimental values. The deviations are as follows:

- **For n-tetradecane**: -12.8% in toluene, -10.1% in m-xylene and 12.3% in carbon disulfide.
- **For n-octadecane**: 8.5% in toluene, -26.1% in m-xylene and-7.8% in carbon disulfide.

The absolute average deviation is 13%. If one wants to reduce this deviation by fitting the critical parameters, a similar deviation has to be made on the critical parameters (i.e. T_c of n-tetradecane should be modified of 13% to fit its molar volume in toluene). But, as it was shown in Figure II-2, such a large deviation would induce large error in results of modelling.

	T_c (K)	P_c (atm)	omega	Mw (g/mol)
OLEOD	980	7.2	2.90	1000
OLEOD	1650	3.1	2.90	4000
A95	947	7.0	2.98	1000
A95	1500	3.0	3.07	4000

Table II-13: Critical parameters of asphaltenes calculated from partial volume measurements and with PR EOS

Furthermore, a major issue rises when dealing with asphaltenes: the molecular weight. Indeed, specific volumes are determined and a molecular weight has to be measured or

assumed. Table II-13 presents the critical parameters calculated with two assumed molecular weights (1000 and 4000 g/mol). As expected, the bigger the molecule, the higher T_c and the smaller P_c. However, the acentric factor has a very small influence on the calculated partial volume.

Hence, although the idea appeared appealing to use partial volumes and EOS to determine critical parameters, the uncertainty of the measurements and the issue about molar weight make such a technique too inaccurate for modelling purpose.

3.2.2. Method based on NMR data

Alexander et al. (1985) developed correlations in order to estimate a, b and m for SRK EOS from NMR data. Alexander and co-workers correlated these SRK parameters to composition using the number of carbons, the types of hydrogen atoms as well as the contents of nitrogen, oxygen and sulphur. The details of the method are presented in Appendix II-7.

Gupta (1986) used these correlations to estimate the critical parameters for asphaltene molecules (rather aggregates since he measured molecular weight). In this work, the Alexander's correlations have been tested for 10 different asphaltenes obtained by a modified IP 143 method (presented in Appendix I-1). Elemental analysis was performed as well as molecular weight determination by VPO in pyridine at 333.15 K. NMR analysis was conducted by Miknis/Netzel at the Western Research Institute (Wyoming). Data are available in Appendix II-8. In this work, the N-content was assumed to be due to (NH_2)-groups and the O-content due to (OH)-groups. As for Np, it was set to zero. The two sets of equations were tested (for "pure" hydrocarbons and with heteroatoms). The equations are available in Appendix II-6.

The names of the asphaltenes were built as follows: "xxc7yy" means "Oil xx precipitated in n-C_7 at temperature yy" and "xxc7tozz" means "Oil xx precipitated in a mixture of n-C_7 -and toluene with zz volume % of toluene". Table II-14 presents the results. Heteroatoms have a huge impact on T_c and P_c (up to 238% deviation for T_c and 213% for P_c) as it is seen in Figure II-15 and Figure II-16. Note that Gupta (1986) used the correlations made for "pure" hydrocarbons.

		Hydrocarbons		With hetero-atoms	
Asphaltenes	M_w (g/mol)	T_c (K)	P_c (atm)	T_c (K)	P_c (atm)
b1c725	2000	1324	3.6	1771	4.5
b1c760	5800	1412	1.3	3066	2.6
b1c780	7300	1431	1.0	3491	2.3
b1c7to10	5800	1435	1.3	2993	2.5
b1c7to20	9300	1300	0.8	4397	2.4
k1c725	4300	1564	2.0	2226	2.6
k1c760	5900	1527	1.5	2797	2.5
k1c780	6800	1550	1.3	2959	2.3
k1c7to10	4700	1603	1.8	2571	2.8
k1c7to20	3800	1528	2.1	2049	2.7

Table II-14: Critical parameters obtained with Alexander's correlations with measured Mw

The expected trends are visible: the bigger the molecule, the higher Tc and the smaller Pc. Since the equation related to the acentric factor only had imaginary roots, no ω could be calculated.

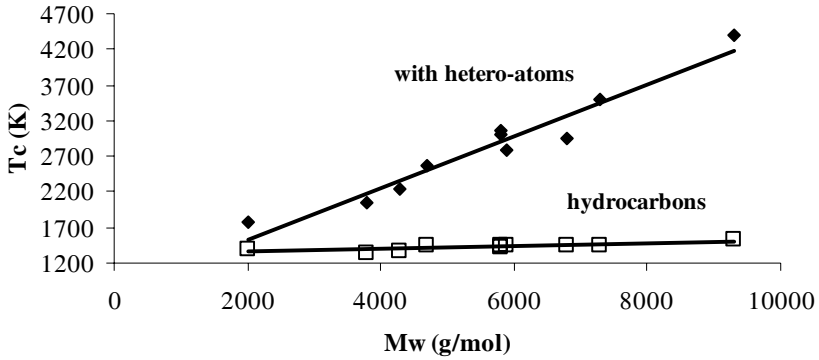

Figure II-15: Tc of asphaltenes with respect to molecular weight

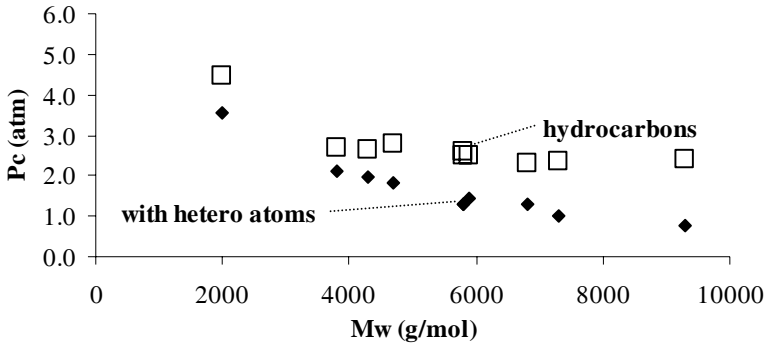

Figure II-16: P_c of asphaltenes with respect to molecular weight

The measured molecular weight is the one of aggregates. Therefore, it was decided to assign a fixed value (1000 g/mol) in order to get the critical properties of the monomer. Table II-15 shows the results obtained with the various correlations in this case.

	Hydrocarbons			With hetero-atoms	
Asphaltenes	**T_c (K)**	**P_c (atm)**	**omega**	**T_c (K)**	**P_c (atm)**
b1c725	1194	6.9	2.113	1393	7.4
b1c760	1215	7.2	2.090	1454	8.0
b1c780	1213	7.2	2.112	1448	7.9
b1c7to10	1201	7.0	2.130	1424	7.6
b1c7to20	1235	7.6	2.042	1517	8.6
k1c725	1253	7.5	2.142	1372	7.7
k1c760	1276	8.1	2.070	1453	8.6
k1c780	1283	8.1	2.066	1447	8.6
k1c7to10	1261	7.5	2.124	1433	8.0
k1c7to20	1243	7.3	2.146	1342	7.4

Table II-15: Critical parameters obtained with Alexander's correlations with Mw = 1000 g/mol

The critical temperatures are very similar for all the asphaltenes. Indeed, the average of the absolute deviation is 25 K for the correlation "hydrocarbon" and 36 K for correlation "with hetero-atoms" whereas it is 86 and 549 K respectively with the experimental molecular weights. As a matter of fact, the compositions of these different asphaltenes are very similar in C and H. Note that the acentric factors could only be calculated with the hydrocarbon correlation.

It seems quite adventurous to draw any conclusions from these various correlations. Alexander's correlations depend very much on the molecular weight and the hetero-atom content. Though fixing a molecular weight reduces the choice of the correlation and the influence of hetero-atoms, the calculated critical parameters are much higher.

So, is the solution the one proposed by Szewczyk and Béhar (1999)? They used a group contribution method (Avaullée's method) to estimate critical parameters. However, they assumed a molecular weight of 1000 g/mol. Furthemore, the structure of asphaltene molecules has to be known.

3.2.3. Comparison between the two methods

Partial volumes of asphaltenes K1C7to20 were measured at 298.15 K and 0.1 MPa as it was explained in paragraph 3.1.3. Then, critical parameters were calculated in order to fit experimental partial volumes to the calculated ones. The acentric factor was set to 3. Both measured and hypothetical molar weights were used for the calculations.

Table II-16 compares the results obtained with the two methods (partial volumes and NMR data). Both Alexander's correlations were used.

When the molar weight is set to 1000 g/mol, the critical parameters obtained from partial volumes are relatively "close" to the ones obtained from NMR data (AAD = 4% for T_c and 17% for P_c) whereas the deviation is much larger with the measured molar weight (AAD = 13% for Tc and 45% for Pc).

These results confirm that both techniques are not accurate enough and are based on too many assumptions to be used for modelling purpose for asphaltenic fluids.

	Partial volumes	**NMR, correl. hydrocarbon**	**NMR, correl. hetero-atoms**	**Partial volumes**	**NMR data, correl. hydrocarbon**	**NMR, correl. hetero-atoms**
M_w (g/mol)	1000	1000	1000	3800	3800	3800
T_c (K)	1300	1243	1342	1988	1528	2049
P_c (atm)	8.7	7.3	7.4	3.7	2.1	2.7
omega	3	2.146	-		-	-

Table II-16: Critical parameters of asphaltenes K1C7to20 determined by different methods

4. Conclusion

Solubility parameters are widely used but their definition is often up to the user. When pressure and temperature are studied, cohesive energy should be defined as the residual internal energy. Indeed, pressure strongly affects cohesive energy - contrary to the usual belief – as it was checked for three pure compounds up to 100 MPa.

Internal pressure is an alternative to measure the solubility parameter of complex liquid compounds and with respect to pressure and temperature. However, its determination is not accurate enough to give proper results with modelling (1 $MPa^{1/2}$). In addition, hydrogen bonds are not taken into account by this physical property.

Solubility parameters of asphaltenes can be measured by various techniques but none of them seem accurate enough. The method applied here for the first time to asphaltenes gave results in agreement with another technique. However, the deviation (between 0.7 and 1.6 $MPa^{1/2}$) is not compatible with modelling.

Critical parameters were also determined with two techniques: a new one (based on molar volumes) and another one (based on NMR data). None of these methods give exact enough critical properties.

Hence, the characterisation of crude oil and asphaltenes was investigated but the complex and polydisperse nature of these systems induces large uncertainties in any technique used. Are parameters related to asphaltenes bound to remain fitting parameters?

Literature

Alexander G.L., Schwarz B.J., Prausnitz J.M., Phase Equilibria for high-boiling fossil-fuel distillates. 2. Correlation of equation of state constants with characterization data for phase equilibrium calculations, Ind. Eng. Chem. Fundam. (1985), 24, 311 – 315

Allen G., Gee G., Wislon G.J., Intermolecular forces and chain flexibility in polymers: internal pressures and cohesive energy densities of simple liquids, Polymer (1960), 456 – 466

Amoros J., Solana J.R., Vilar E., Behaviour of the internal pressure of liquids in accordance with variations in temperature, volume and cohesive energy density, Mat. Chem. Phys. (1984), 10, 6, 557 – 578

Andersen S.I., Flocculation onset titration of petroleum asphaltenes, Energ. Fuel. (1999), 13, 315 – 322

Bagley E.B., Nelson T.P., Scigliano J.M., Three dimensional solubility parameters and their relationship to internal measurements in polar and hydrogen bonding solvents, J. Paint Technol. (1971), 43, 35 – 42

Barbosa E.F.G., Sousa S.M.C., M.S.C.S. Santos, I.M.S. Lampreia, Partial molar volumes of linear hydrocarbons in methanol in the very dilute region. Intermolecular interactions. H-bond effects, Phys. Chem. Chem. Phys. (2001), 3, 556 – 561

Barton A.F.M., CRC Handbook of solubility parameters and other cohesion parameters; CRC Press, Inc., 1983

Barton A.F.M., CRC Handbook of solubility parameters and other cohesion parameters; CRC Press, Inc., 1991

Buckley J.S., Hirasaki G.J., Liu Y., Von Drasek S., Wang J.-X., Gill B.S., Asphaltene precipitation and solvent properties of crude oils, Pet. Sci. Technol.(1998), 16, 251 – 285

Cavett R.H., Physical Data for Distillation Calculations-Vapor-Liquid Equilibria, Proc., 27th API Meeting, San Francisco 351, 1962

Christiansen S.D., Properties of Asphaltenes, Master Thesis, Department of Chemical Engineering, Technical University of Denmark, February 1999

Chung F.T.H., Thermodynamic modelling for organic solid precipitation, SPE 24851 (1992), 869 – 878

Cibulka I., Hnedkovsky L., Liquid densities at elevated pressures of n-alkanes from C_5 to C_{16}. A critical evaluation of experimental data, J. Chem. Eng. Data (1996), 41, 657 – 668

Cibulka I., Takagi T., P-rho-T data of liquids: summarization and Evaluation. 5 – Aromatic hydrocarbons, J. Chem. Eng. Data (1999), 44, 411 - 429

Duong D., Determination of Solubility Parameters for Crude Oils, Master Thesis, Department of Chemical Engineering, Technical University of Denmark, Sept. 2004

Ensley K.E., Thermodynamics of asphalt intermolecular interactions and asphalt-aggregate interactions, in: T.F. Yen and G.V. Chilingarian (Ed), Asphaltenes and asphalts, 1. Developments in petroleum science, 40, 401 – 426, 1994

Fenistein D., Barré L., Broseta D., Espinat D., Livet A., Roux J.N., Scarsella M., Viscosimetric and neutron scattering study of asphaltene aggregates in mixed toluene/heptane solvents, Langmuir (1998), 14, 1013 – 1020

Gupta A.K., A model for asphaltene flocculation using an equation of state, Master Thesis, University of Calgary, Calgary, Canada, 1986

Hansen C.M., The three dimensional solubility parameter and solvent diffusion coefficient, Danish Technical Press, Copenhagen, 1967

Hildebrand J.H., Dymond J., Partial molal volumes in regular solutions, J. Chem. Phys. (1967), 46, 2, 624 – 626

Hildebrand J.H., Prausnitz J. M., Scott R.L., Regular and related solutions, Van Nostrand Reinhold Company, New-York, 1970

Hildebrand J.H., Scott R.L., The solubility of nonelectrolytes, Reinhold, New York, 1950

Hirschberg A., deJong L.N.J., Schipper B.A., Meijer J.G., Influence of temperature and Pressure on asphaltene flocculation, paper SPE 11202, SPEJ (1984) 283 – 293

Hoy K.L., New values of the solubility parameters from vapor pressure data, J. Paint. Technol.(1970), 42, 1, 76 – 118

Israelachvili J.N., Intermolecular and surface forces, 2nd edition, Academic Press (1992)

Kesler M.G., Lee B.I., Improve Predictions of Enthalpy of Fractions, Hydro. Proc. (1976), 55, 153

Lagourette B., Boned C., Saint-Guirons H., Xans P., Zhou H., Densimeter calibration method versus temperature and pressure, Meas, Sci. technol. (1992), 3, 699 - 703
Laux H., Löslichkeitsparameter und Verteiliugn von Erdölrückstands-Komponenten, Erdöl Erdgas Kohle (1992), 108, 5, 227 – 232

Lian L., Peptization studies of asphaltene and solubility parameter spectra, Fuel (1994), 73, 3, 423 – 428

Liron X., Cohen S., Densitometric determination of the solubility parameter and molal volume of compounds of medicinal relevance, J. Pharm. Sci. (1983), 72, 499 - 504

Lyckman E.W., Eckert C.A., Prausnitz J.M., Generalized liquid volumes and solubility parameters for regular solution application, Chem. Eng. Sci. (1965), 20, 703 – 706

Maloney D.P., Prausnitz J.M., Thermodynamic properties of liquid polyethylene, Journal of applied polymer science (1974), 18, 2703 - 2710

Marrero J., Gani R., Group-contribution based estimation of pure component properties, Fluid Phase Equilibr. (2001), 183-184, 183-208

Michelsen M.L., Mollerup J.M., Thermodynamic models: fundamentals and computational aspects, Tie-Line Publications, Holte, 2004

Montel F., Petroleum Thermodynamics, Notes, Total, 2004

Moore W.J., Physical Chemistry, 3rd edition, Longmans, London, 1959, pp 423-424

Mutelet F., Ekulu G., Solimando R., Rogalski, Solubility parameters of crude oils and asphaltenes, Energ. Fuel. (2004), 18, 667 - 673

Nghiem L.X., Hassam M.S., Nutakki R., George A.E.D., Efficient modelling of asphaltene precipitation, SPE 26642 (1993)

Nokay R., Estimate Petrochemical Properties, Chem. Eng. (1959), 147

Null H.R., Palmer D.A., Predicting Phase Equilibria, Chem.Eng.Prog. (1969), 65, 47 – 51

Perry, R.H., Green, D.W., Maloney, J.O., Perry's chemical engineers' handbook (7th edition), McGraw-Hill, New-York, 1997

Randzio S.L., Scanning calorimeters controlled by an independent thermodynamic variable: definitions and some metrological problems, Thermochim. Acta (1985), 89, 215 – 241

Riazi M.R., Daubert, T.E., Simplify Property Predictions, Hydro. Proc. (1980), 115

Sun T.F., Bominaar S.A.R.C., Ten Seldam C.A., Biswas S.N., Evaluation of the thermophysical properties of toluene and n-heptane from 180 to 320 K and up to 260 Mpa from speed-of-sound data, Berich. Bunsen Gesell. (1991), 95, 696 – 704

Sun T.F., Kortbeek P.J., Trappeniers N.J., Biswas S.N., Acoustic and thermodynamic properties of benzene and cyclohexane as a function of pressure and temperature, Phys. Chem. Liq. (1987), 16, 163 – 178

Szewczyk V., Behar E., Compositional model for predicting asphaltenes flocculation, Fluid Phase Equilibr. (1999), 158, 459 – 469

Taravillo M., Castro S., Garcia Baonza V., Caceres M., Nunez J., Thermophysical properties of liquid m-xylene at high pressures, Chem. Soc. Faraday. Trans. (1994), 90, 1217 – 1221

Torcal-Garcia V., Asphaltene phase stability after hydrotreatment and heat treatment of heavy feedstocks, Master Thesis, Department of Chemical Engineering, Technical University of Denmark, 2004

Twu C.H., An internally consistent correlation for predicting the critical properties and molecular weights of petroleum and coal-tar liquids, Fluid Phase Equilibr. (1984), 137 – 150

Utracki L.A., Simha R., Statistical thermodynamics predictions of the solubility parameter, Polym. Int. (2004), 53, 279 – 286

Verdier S., Andersen S.I., Internal pressure and solubility parameter as a function of pressure, Fluid Phase Equilibr. (2005), 231, 125–137

Verdier S., Duong D., Andersen S.I., Experimental determination of solubility parameters of oils as function of pressure, Energ. Fuel. (2005), 19, 1225 - 1229

Wang J.X., Buckley J.S., A two-component solubility model of the onset of asphaltene flocculation in crude oils, Energ. Fuel. (2001), 15, 1004 – 1012

Weast R.C., Selby S.M., Handbook of chemistry and physics, 47th edition, The Chemical Rubber Co., Cleveland, 1966

Whitson C.H., Brulé M.R., Phase Behaviour, SPE Monograph, Vol. 20, Richardson, Texas, 2000

Won K.W., Thermodynamics for solid solution-liquid-vapor equilibria: wax phase formation from heavy hydrocarbons mixtures, *Fluid Phase Equilibr.* (1986), 30, 265 – 279

Yarranton H.W., Masliyah J.H., Molar mass distribution and solubility modeling of asphaltenes, AIChE (1996), 42, 12, 3533 - 3543

Zhou H., Thomas F.B., Moore R.G., Modelling of solid precipitation from reservoir fluid, J.C.P.T. (1996), 35, 10, 37 - 45

List of symbols

Latin letters

a	Attractive term of a cubic EOS
b	Co-volume
B	Coefficient of the modified Tait equation
C	Coefficient of the modified Tait equation
CED	Cohesive Energy Density
E	Cohesive energy
H	Enthalpy
m	Temperature dependence of the solubility parameter
n	ratio between internal pressure and the cohesive energy density
P	Pressure
R	Gas constant
RI	Refractive index
T	Temperature
U	Internal energy
V	Molar volume

Greek letters

α_P	Isobaric thermal expansivity
δ	Solubility parameter
κ_T	Isothermal compressibility
π	Internal pressure
ρ	Density
ω	Acentric factor

Subscripts and Superscripts

A	Attractive
c	Critical
d	Dispersion
h	Hydrogen bonding
liq	Liquid
p	Polar
R	Repulsive
r	Residual
sat	Saturation
v	Volume-dependent
vap	Vapour
0	Reference

Chapter III

Asphaltene Stability and Gas Injection

Table of Contents

What is the influence of pressure and temperature on asphaltene stability? Does temperature equally affect precipitation induced by n-heptane, CO_2 or methane? Are there factors influencing reversibility? How can the onset be accurately determined?

First, the influence of pressure and temperature as it is reported in the literature will be given. Then, the different techniques used to determine asphaltene precipitation and flocculation will be briefly described. Finally, the experiments carried out with a novel experimental set-up developed at the University of Pau will be presented. The effect of pressure, temperature, gas nature and composition will be investigated for two crude oils.

1. Influence of pressure and temperature on asphaltene stability

1.1. Temperature and Asphaltene Precipitation

In the literature, the influence of temperature on asphaltene stability has been studied in two ways:

- Onset of precipitation vs. *T*
- Amount of precipitated asphaltenes vs. *T*

The last one has been preferred because it is easier to measure. It has been mainly performed with n-alkanes as precipitants. Table III-1 lists some of the effects found in the literature for STO (Stock Tank Oils) with n-alkanes.

Method	Precipitant	T range	Effect of T on Solubility	Reference
Amount	propane		Increase	Bushnell and Ryan, 1976
Onset	n-heptane	60 to 120°C	Increase and decrease	Peramanu et al., 1999
Amount	n-C_5 to n-C_8	4°C to 100°C	Increase and decrease	Andersen and Birdi, 1990
Amount	n-C_5 to n-C_7	0°C to solvent reflux T	Increase and decrease for heavy oil. Decrease for light oil	Ali and Ghannam, 1981
Amount	n-heptane	-2 to 80°C	Decrease	Andersen, 1994
Amount	n-heptane	40 to 200°C	Decrease	Andersen et al., 1998
Amount	n-C_5 to n-C_{12}	20 to 65°C	Decrease	Hu and Guo, 2001

Table III-1: Influence of temperature on the solubility of asphaltenes in crude oils

In many cases, the yield of precipitated asphaltenes decreases with temperature. In some cases, there is a maximum in yield (i.e. a minimum in solubility) and then a decrease. As for low n-alkanes (below n-pentane), they may induce an increase in asphaltene yields as Andersen suggests it (Andersen, 1994). But, do asphaltenes behave with carbon dioxide, methane or nitrogen as they do with n-heptane? Are these titrations with respect to temperature useful for live oils? Are there any general rules?

Idem and Ibrahim (2002) state that, in presence of CO_2, asphaltene stability in crude oils improves with temperature for two of the three different samples they studied. However, they compare volumes at different temperatures (from 300.4 to 337.7 K) and they observe different trends. The density of CO_2 varies between 882.9 and 633.1 kg/m3 at 17.2 MPa within this temperature range (see http://webbook.nist.gov/chemistry/ for the densities). Thus, on a mass-based scale, it is seen that asphaltenes are less stable with temperature since less amount of CO_2 is required to initiate precipitation (Figure III-1).

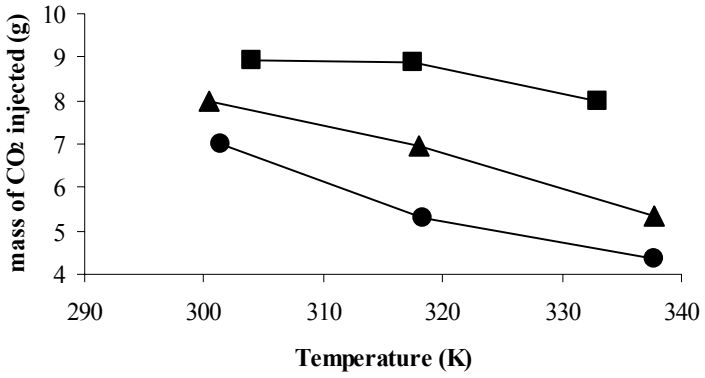

Figure III-1: Onset of precipitation of three crude oils in presence of CO_2 as function of temperature (■, oil 1; ▲, oil 2; ●, oil 3) (data from Idem and Ibrahim, 2002)

Kokal et al. (1992) studied the influence of various gases on two oils and found opposite results for the CO_2 injection: the Suffield oil was more stable with a temperature increase whereas the Lindbergh oil was not. They explain these effects by the competition

between temperature (affecting the solubility parameter of asphaltenes) and composition (influencing the solubility of the solvent).

As a brief conclusion for the effect of temperature, one can say that temperature is reported as having both stabilizing and destabilizing impact with any precipitant.
To the author's knowledge, there is no proof of a possible link between the effect of temperature with n-alkanes and gases. As for the usefulness of titrations at atmospheric conditions, it still remains to be proven.

1.2. Pressure and Asphaltene Precipitation

Pressure depletions do destabilize asphaltenes. As a matter of fact, this is the main reason why asphaltenes are studied. Any work in the literature dealing with gas injection and crude oil shows that a decrease of pressure may induce asphaltene precipitation (Lhioreau et al., 1967; Hamammi et al., 2000; Fotland, 1996; Joshi et al., 2001).
Akbarzadeh et al. (2005) studied the influence of pressure with n-heptane as a precipitant (Figure III-2). In this case as well, the yield of precipitate decrease with pressure, i.e. asphaltenes are more soluble at higher pressures.

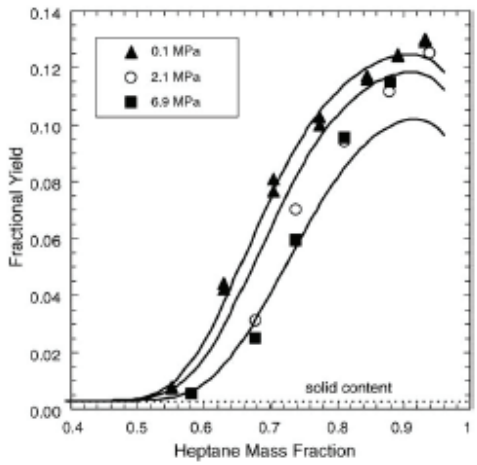

Figure III-2: Influence of pressure on n-heptane induced precipitation (from Akbarzadeh et al., 2005)

Hence, it seems that pressure only has one effect with both gas and n-alkanes as precipitants.

1.3. Asphaltene Phase Envelopes

The notion of Asphaltene Phase Envelopes (APE) was first introduced by Leontaritis in 1996. However, it was initially named "Asphaltene Deposition Envelope", which is not correct since precipitation and deposition are two different processes. Such an envelope is presented in Figure III-3 and it consists of:

- the bubble point curve (appearance of vapour phase)
- the upper onset curve (or precipitation curve)
- the lower onset curve (or dissolution curve)

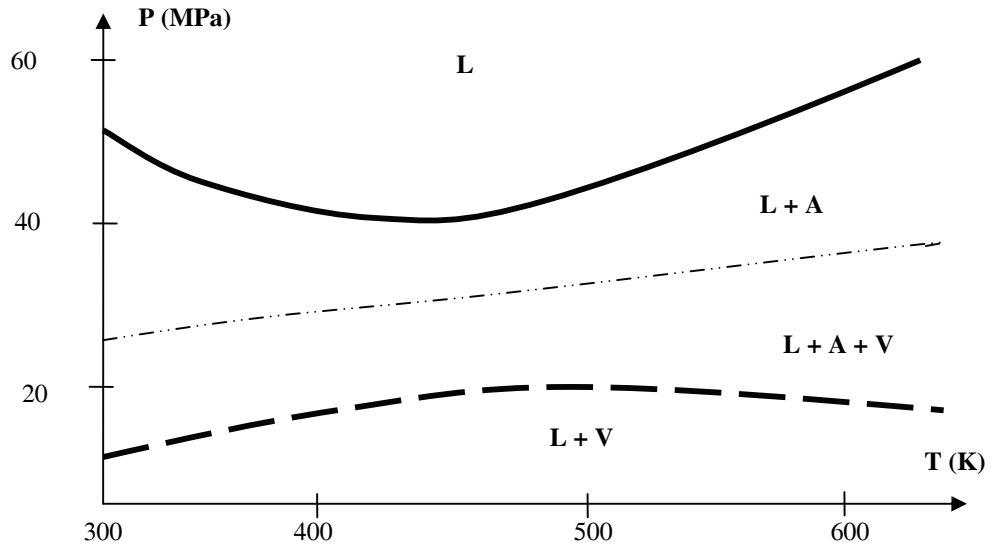

Figure III-3: Typical APE of a live oil (L: Liquid; A: Precipitated Asphaltenes; V=Vapour)

Note that the word "deposit" is sometimes used instead of "precipitated asphaltenes" and "precipitation" is referred as "flocculation" (Szewczyk and Béhar, 1999 for instance). Both are incorrect.

Few APE's are reported in the literature since they are difficult to obtain. Buenrostro-Gonzalez et al. (2004) listed the few APE they could find (less than 10 papers in total since 1949). The same authors determined the APE's of live oils by an optical technique and saw little effect of temperature on the upper onset curve of the oil C1 $\left(dP/dT = -0.08\ MPa.K^{-1}\right)$ and stronger effect on the oil Y3 $\left(dP/dT = -0.29\ MPa.K^{-1}\right)$.

Jamaluddin et al. (2002) recombined a dead oil with nitrogen and measured both bubble points and onset pressures in a Near-Infra-Red high pressure Jeffri Cell (Figure III-4).

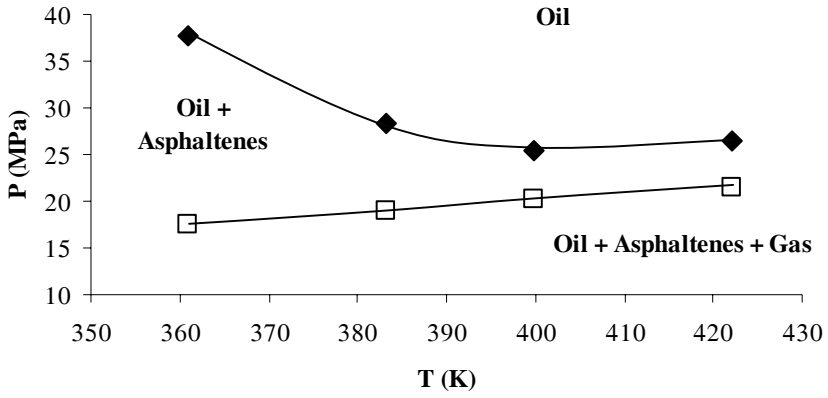

Figure III-4: APE of a live oil (◆, onset point; □, bubble point) (from Jamaluddin et al., 2002)

In this case, pressure has a stabilizing effect and temperature has both (stabilizing until 400 K and destabilizing above). The lower onset curve was not determined. Indeed, it strongly depends on reversibility and the ability of asphaltenes to go back to solution.

Of course, APE's, as any measurements related to asphaltenes, are subjects to doubts. Was the equilibrium reached? How sensitive is the technique? How is this sample representative of an in-situ oil? Could other phases be present? Indeed, as Shaw and Béhar pointed it out, SLLV behaviour should be expected for asymmetric mixtures especially in presence of waxes and asphaltenes (Shaw and Béhar, 2003). Can the ordinary techniques used for the determination of asphaltene onsets of precipitation detect these SLLV equilibria?

These issues should be considered, especially when one tries to model such data.

1.4. Le Châtelier's principle

Both effects of pressure and temperature can be explained by the Le Châtelier's principle. Indeed, it states that "*every change of one of the factors of an equilibrium occasions a rearrangement of the system in such a direction that the factor in question experiences a change in a sense opposite to the original change*." (Le Châtelier, 1888)

The equilibrium we are interested in is the following one:

$$Asphaltene(solution) \rightleftharpoons Asphaltene(precipitated) \qquad (1)$$

Andersen and Speight (1999) listed two other reactions:

- the aggregation:

$$Asphaltenes_{\,i} + Asphaltenes_{\,l} \rightleftarrows Asphaltenes_{\,i+l} \qquad (2)$$

- the interaction with the resins:

$$Asphaltenes + \text{resins} \rightleftarrows Asphaltenes - \text{resins} \qquad (3)$$

Aggregation only takes place at low concentration as it was said in chapter 1, paragraph 1.4.1. Hence, equilibrium (2) can be neglected since the onset conditions are investigated here. As for the interactions with resins, they can be seen as part of the asphaltene continuum.

- **The effect of pressure**

If pressure is increased, the position of equilibrium will move so that the pressure is reduced again, i.e. the number of molecules decreases or the volume is reduced. Experimentally, it is seen that solubility of asphaltenes in oil increases with increasing pressure. Thus, it means that the system decreases its volume when pressure is increased, i.e. the volume of the two-phase region is larger than the one of the one-phase region. To the authors' knowledge, there is no experimental evidence of a gain in volume during precipitation in the open literature except one recent work relating a decrease in a reduced density with precipitation (Ekulu et al., 2004). The authors plotted the density of (crude oil + solvent+ flocculant) – density (deasphalted oil + solvent + precipitant) as function of the precipitant content. The break corresponds to asphaltene flocculation, as an optical method confirmed it. In addition, as it is explained in Chapter 4, paragraph 3.3, a gain in volume was observed on a recombined oil after precipitation.

Furthermore, by means of various equations of state (EOS) (CPA in Knudsen, 2001 and SAFT in Christensen et al., 2005), an increase of 10 cm^3 per mole at 400 K was calculated between the onset and the bubble point as follows:

$$v_{1\,phase} = \frac{RTZ_1}{P} \qquad \textbf{Eq III-1}$$

$$v_{2\,phases} = \frac{RT}{P}\left(x_{oil}Z_{oil} + x_{asphaltene}Z_{asphaltene}\right) \qquad \textbf{Eq III-2}$$

where v is the molar volume, T the temperature, P the pressure, x the mole fraction and Z the compressibility factor.

The difference $v_{2\ phases} - v_{1\ phases}$ gives the volumetric variations due to asphaltene precipitation and the increase due to asphaltene is approximately 50% of the total change. Similar calculations with a cubic EOS are presented in Chapter 5, paragraph 2.4. It is concluded that, for 1 mole of a system (99% oil+1% asphaltenes) with average densities and molecular weights, the volume change due to the asphaltene phase itself is less than 0.05 cm^3, which is very little to be detected.

Hence, pressure seems to stabilize asphaltenes and precipitation seems to be followed by an increase in volume, as the Le Châtelier's principle predicted it.

- **The effect of temperature**

If temperature is increased, the Le Châtelier's principle states that the position of equilibrium (1) will move so that the temperature is reduced again. If the reaction is exothermic, the equilibrium will go to the left side when temperature is increased, i.e. asphaltenes will be more soluble. If not, the asphaltenes will be less soluble. As it was said previously, both stabilizing and destabilizing effects are found in the literature. Could it be that some asphaltene precipitations are exothermic and some others endothermic? Is it due to the solvent properties or to the asphaltenes themselves?

The calorimetric aspect of precipitation is detailed in Chapter 4. In the literature, precipitation induced by n-alkanes is reported to be endothermic whereas it is exothermic for live oils and by pressure depletion. Our work presented in chapter 4 confirmed the second result but not the first one. So far, there are not enough experimental evidences to relate the exo- or endothermy of asphaltene precipitation to the impact of temperature on stability.

The Le Châtelier's principle can also be explained by equations as shown in Appendix 3-1 (influence of pressure and temperature on the equilibrium constant). The effect of temperature on the equilibrium is related to the heat of reaction and the effect of pressure to the molar volume of asphaltene in the different phases.

2. The Onset Determination

As it was said in Chapter 1, paragraph 1.6.2, almost all the possible techniques have been used to detect asphaltene precipitation: microscopic examination, optical transmission and light-scattering, conductivity measurements, viscosimetry, particle size analysis, fluorescence spectroscopy, density measurements or acoustic methods. Several questions raises: do they determine the onset of precipitation or flocculation? How accurate are they? Can they be applied to live oil systems? Could they eventually determine SLLV phase behaviour?

This paragraph aims at studying these different techniques and list their advantages and drawbacks. A closer look will be given to filtration since this technique has been applied in this work.

2.1. Determination of the onset of precipitation

Few methods determine onsets of precipitation: **viscosity measurements** (El-Mohamed et al., 1988; Escobedo and Mansoori, 1994), **filtration techniques** (Leontaritis et al., 1994), methods based on **heat transfer** (Clarke and Pruden, 1997), **electrical conductivity** (Fotland et al., 1993) and **density**-based procedures (Ekulu et al., 2004). Indeed, asphaltene precipitation is the formation of a solid-like phase and hence the mentioned techniques render the appearance of such a phase. On the contrary, flocculation is a state of aggregation and asphaltenes are still in solution.

- **Viscosity**

El-Mohamed et al. (1988) studied the effect of viscosity next to the onset point with a horizontal Ostwald viscometer. The asphaltenic solutions shifted from Newtonian behaviour to non-Newtonian across the onset.

Escobedo and Mansoori (1994) extended this method to crude oils but still at room conditions. Note that they claimed developing a new technique.

- **Heat Transfer**

Clarke and Pruden (1997) developed an interesting technique based on heat transfer through a precipitate layer. N-heptane induced precipitation was investigated at room conditions. It is likely that an important quantity of precipitate is formed before detecting

any change in the transfer. No comparison with other onset detection method was achieved

- **Electrical conductivity**

Fotland et al. (1993) mixed crude oil and precipitant and followed the electrical conductivity vs. the amount of precipitant. First, conductivity increases upon addition of n-alkanes and a maximum is reached. This maximum corresponds to the point of precipitation. Microscopy and gravimetric techniques were used to check this method. The amount of precipitates were also estimated. This technique was then extended to high pressures and temperatures with success (Fotland, 1996). This technique is believed to be reliable.

- **Density**

Lately, density was also applied to the determination of asphaltene precipitation (Ekulu et al., 2004). Crude oil was mixed with n-heptane and its density was measured. A reduced density was plotted and the break was assumed to be due to asphaltene precipitation (though it is referred as flocculation). This technique should be further studied and extended to live oils.

- **Filtration**

Leontaritis and co-workers (1994) measured the weight of material deposited on 0.1, 0.45 and 1 μm membrane filters at atmospheric conditions. This gravimetric method enables the mass of asphaltenes to be plotted against the solvent/sample ratio from which the onset can be found. Negahban et al. (2005) performed HP/HT filtration with a $0.22\,\mu m$ filter-paper size. High-pressure microscopy and a spectral-analysis system combined with the filtration showed that the precipitated asphaltene particle size was ranging between 0.5 μm at the onset and up to 1.5 μm at the bubble point. Peramanu et al. (1999) developed a flow-loop with an in-line filter detecting asphaltene precipitation when a pressure drop occurs across the filter. However, the nominal size of the filter was $60\,\mu m$. Thus, the pressure drop will occur only once the filter is plugged with such a pore size. Edmonds et al. (1999) used a high-pressure PVT cell connected to a 0.5 μm filter to determine the asphaltene concentration as a function of pressure. Fahim et al. (2004) studied the influence of various gases (CO_2, C_1, C_2, C_3, C_4 as well as natural gas) on the

amount of asphaltenes precipitating using a PVT system with optical fibre detection of bubble point regimes with a filter attachment. The filter porosity was $0.5\,\mu m$. A study by Burya et al. (2001) with Dynamic Light Scattering confirms these results about size: the precipitated asphaltenes were ranging between 0.4 and 5 μm for one oil and 0.7 to 1.6 μm for a second one. Furthermore, Briant and Hotier (1983) observed particles in the range of 0.1-3 μm at the onset of asphaltene precipitation.

Table III-2 lists the different techniques used to detect the onset of precipitation with their respective characteristics.

2.2. Determination of the onset of flocculation

As Clarke and Pruden (1996) state it, most of the methods determine the onset of flocculation. Indeed, many methods do follow the state of aggregation and help determining the onset of flocculation.

The optical methods are the core of these methods: **refractive index** (Buckley, 1996; Buckley et al., 1998; Buckley, 1999), **microscopy** (Heithaus, 1962; Hirschberg et al., 1984), **light scattering** (Hotier and Robin, 1983; Hu and Guo, 2001), **light transmittance** (Hammami et al., 1995; Hammami et al., 2000), **light reflexion** (Castillo et al., 2006), **UV–vis spectro-photometry** (Andersen, 1999).

Another technique using speed-of-sound was developed by Carrier et al. (2000). They studied the phase gap between two coherent signals, one being the reference and the other one going through the fluid. This technique was successfully used to measure LLE transitions (Lu et al., 1999). It was applied at atmospheric conditions and with n-hexane as a precipitant.

The transition between precipitation and flocculation is rather blurry and, as it was shown in Chapter 1, paragraph 1.6.2, there can be a great difference in precipitant composition between those two phenomena. Thus, the techniques measuring variations of physical properties such as viscosity or density should rather be used since they are related to the creation of a new phase.

Technique	System	Conditions	Advantages	Drawbacks	Reference
Viscosity	Asphaltene solutions	293 K, 0.1 MPa	Fast	Limited working conditions Not tested with crude oils Strongly time-dependent	El-Mohamed et al., 1988
Heat Transfer	Crude oil	301 K, 0.1 MPa		Tested with n-heptane Not compared to other onset techniques Important precipitate necessary to detect a change	Clarke and Pruden, 1997
Electrical conductivity	Crude oil	Until 70 MPa and 393 K	Reliable Wide working conditions Checked with other methods		Fotland et al., 1993 Fotland, 1996
Density	Crude oil	Room conditions	Easy To be extended and checked	Limited conditions	Ekulu et al., 2004
Filtration	Crude oil	HP/HT	Reliable	Size of precipitated asphaltenes is assumed	Negahban et al. (2005)

Table III-2: Examples of techniques used for the determination of the onset of precipitation

2.3. Possible uncertainties

The DB Robinson solid detection system (SDS) is generally used to determine APE's (Hammami et al., 1995; Hammami et al., 2000; Aquino-Olivos et al., 2003). The SDS detects the asphaltene deposition onset by light scattering of a laser light beam shining through the windows of a PVT cell. Upon formation of particles, the light is scattered and less light will be transmitted and the transition or deposition pressure can be evaluated from abrupt changes in the detector signal vs. pressure curve. However, as it was observed by Aquino-Olivos et al. (2003), some difficulties can occur in assessing the right transition for some oils as the light transmission versus pressure curve may be non-trivial and show several inflection points (Figure III-5). Therefore, in that case, an accurate determination of the onset point is not possible with the sole SDS system and could be combined with filtration as Aquino-Olivos and co-workers did (2003).

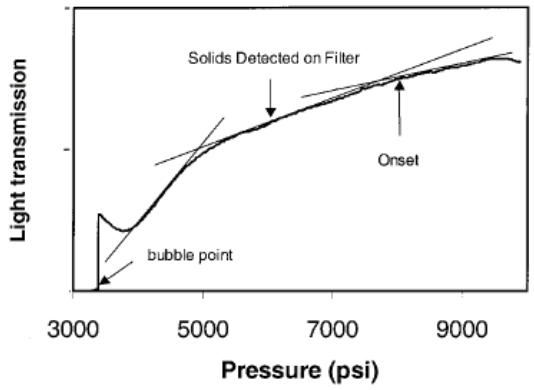

Figure III-5: Example of optical signal obtained during the pressure depletion of a live oil with a DB Robinson solid detection system (Aquino-Olivos et al., 2003)

Co-precipitation of waxes with asphaltenes is often mentioned as a drawback of any of the techniques used to determine onsets. Aquino-Olivos and co-workers (2001) determined the APE of a live oil using SDS. The obtained upper curve exhibited a S-shape (Figure III-6). The low temperature contribution to this was probably caused by the presence of waxes. However, one should expect that a decrease in pressure above the fluid bubble point should redissolve wax crystals according to ordinary wax phase diagrams. On the other hand, the large spread in the data points obtained at 60°C talks in

the favour of a different mechanism from that at higher temperatures. Therefore, the S-shape behaviour is assumed to result from overlaying of two mechanisms of asphaltene and wax precipitation.

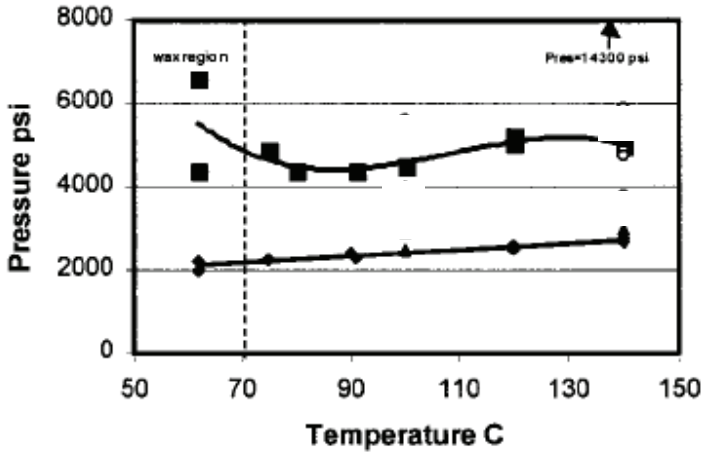

Figure III-6: Upper Precipitation Curve (solid squares) and Bubble point line (solid diamonds) (Aquino-Olivos et al., 2001)

Therefore, can one be sure that the phase transition is not due to waxes at low temperatures? A simple analysis of the precipitated solid would help answering such a question. But, depending on the technique and on the PVT cell, sampling solids is not always possible.

3. Measurement of APE of recombined oil

A novel high-pressure cell was developed at the Laboratoire des Fluides Complexes (University of Pau, France). Its main advantages are the following ones:

- A small sample is required (5 g).
- The injection of the precipitant is done at the conditions of investigation.
- The sample is mixed continuously.
- The dead volume is almost non-existent.
- A filtration technique under pressure enables the determination of asphaltene precipitation.

This new apparatus was tested with two different crude oils and two gases. The influence of temperature, pressure and gas composition on asphaltene stability was investigated.

3.1. Sampling and recombining method

Before presenting the set-up and the results, a very brief explanation of the differences between bottom-hole and recombined samples will be given. Obtaining a representative quantity of fluid is a very difficult operation. Several sampling methods exist (Montel, 2004):

- **Surface sampling**: a given number of gas and liquid samples are taken from the test separator. In presence of solid phase deposition in the test installations, tubing or separator, there is a risk that these deposited constituents (heavy paraffins or asphaltenes) will not be sampled quantitatively. Hence, the samples are not representative of the in-situ oil. Wellhead sampling is sometimes performed when fluids are single phase under wellhead conditions (which is rarely the case except for HP/HT reservoirs).
- **Bottom-hole sampling**: there are two broad categories of bottom-hole testers; those which sample the reservoir fluid during the drilling phase and those which sample the fluid from the production tubing of a fully-equipped well. The testers in the first category are generally used for surveying fluids and measuring pressure; those in the second for studying the thermodynamic behaviour of dluids.

Thanks to advanced monitoring of the formation testers, the samples can also be used for PVT characterisation.

Bottom-hole samples are much more expensive that surface samples. Furthermore, their transport must be done at constant temperature and pressure. Therefore, working with surface samples is often preferred. If one assumes that there was no deposit in the installations and that the fluid is representative of the in-situ oil, recombination can occur. There are two possible experimental recombination techniques:

- Conditioning the separator gas bottles at the test separator temperature and transferring the gas in equilibrium for recombination. The transferred gas corresponds to the separator gas in thermodynamic equilibrium
- Conditioning the gas bottles at temperature higher than the one of the separator and transfer of the whole fluid for recombination. The gas transferred no longer corresponds to the separator gas in thermodynamic equilibrium.

The first technique uses the correct gas with an incorrect GLR (Gas Liquid Ratio) whereas the second one recombines an incorrect gas with an incorrect GLR.

In this chapter, Stock-Tank Oils were used and recombined with pure gases.

3.2. Experimental set-up

A simplified scheme of the experimental setup used to study asphaltene stability with addition of gas is shown in Figure III-7. The experimental device consists of three main parts: a PVT cell (used to mix the crude oil and the precipitant), a filtration part (enabling filtration under pressure) and an injection cell**.** The filtration cell is a piston cell able to function under a pressure of 70 MPa from 253 to 473 K and allowing the homogenization of the fluids by means of a magnetic stirrer. The injection cell is also a piston cell with an operating pressure of 70 MPa, a maximum temperature of use of 423.15 K and a total volume of 50 cm^3.

- **The PVT cell**

The PVT cell is a 2.6 to 13 cm^3 variable piston cell, designed to work under a maximum pressure of 70 MPa and up to 473 K. This cell was machined so that one can mix and

homogenize the fluids by means of a magnetic stirrer (the presence of the agitator imposes an incompressible volume of 2.6 cc).

Note that the incompressible volume is not a dead volume since the whole interior of the cell is stirred. A proper cleaning is possible by means of two sapphire windows, associated to a camera. The cleaning procedure is as follows:

- The cell is filled with toluene and stirring is switched on.
- The cell is emptied and, if the toluene is not colourless, the operation is repeated.

Once it is done, the inside of the cell is checked with the camera through the sapphire windows to see whether or not asphaltene particles are sticking on the inner walls. If it is the case, toluene is injected until all the deposited asphaltenes are dissolved.

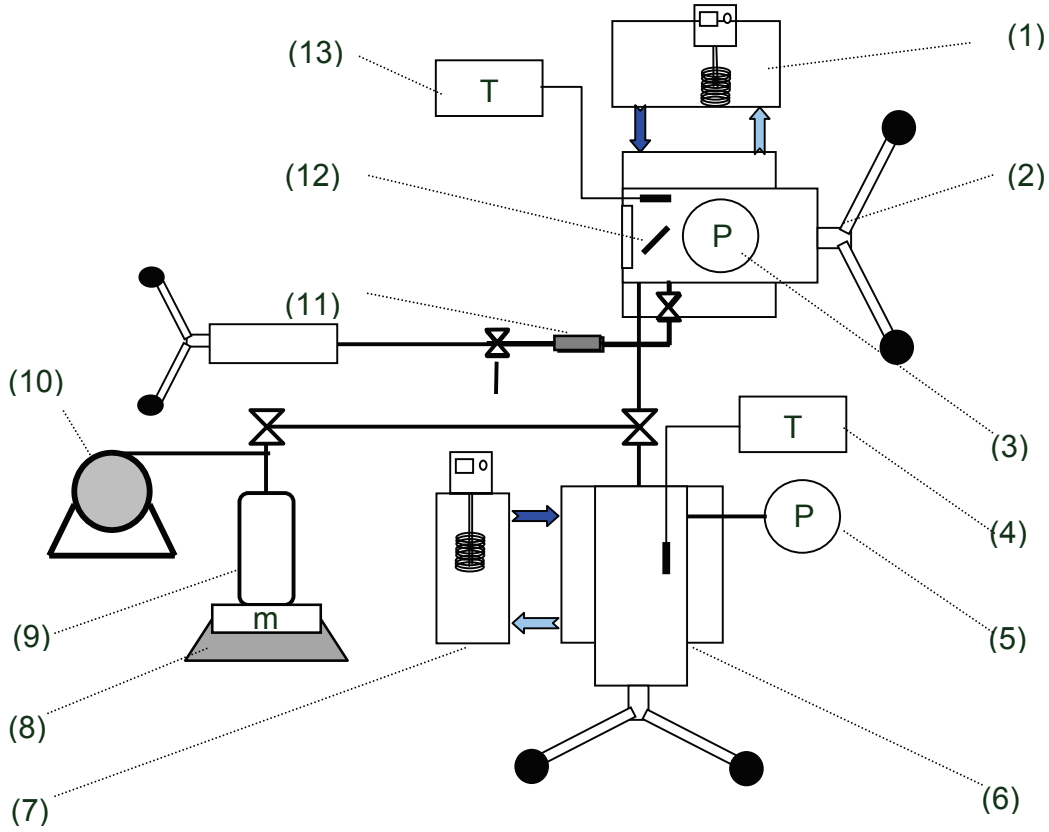

Figure III-7: Scheme of the asphaltene cell (1, thermostat; 2, high pressure cell; 3, pressure gauge; 4, thermometer; 5, pressure gauge; 6, injection pump; 7, thermostat; 8, balance; 9, crude oil sample; 10, vacuum pump; 11, filter; 12, magnetic stirrer; 13, thermometer) (Carrier, 2005)

The temperature of the system, controlled using a Huber Unistat DC cryothermostat, is determined by a probe (Pt 100, of an accuracy of 0.1 K). Three valves are connected to this cell and are used to introduce the crude oil, the precipitant and to filter the mixture, respectively. A Kulite pressure gauge (HEM 375), operational between 1 and 100 MPa and compensated in the temperature range 298.15- 505.15K, measures the pressure within 0.1 MPa. Moreover, this transducer is a flush pressure gauge, which considerably reduces dead volumes.

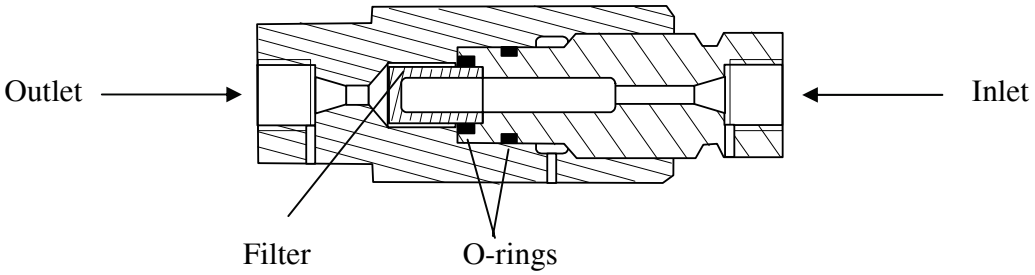

Figure III-8: Sketch of the filter holder (Carrier, 2005)

- **The high-pressure filter**

The inlet part of the filtering system, which consists of a 0.5 μm porosity filter (Swagelok) fixed in a filter holder that can stand up to 100 MPa, is connected to PVT cell whereas the outlet part is connected to a manual high pressure pump (Figure III-8). This size of pores is believed to be the one of the precipitated asphaltenes as it was reported earlier (paragraph 2.1). It might be that precipitated asphaltenes have smaller sizes but this pore size of 0.5 μm is widely used (see references given in paragraph 2.1). This will be the criterion we use to determine whether or not precipitation occurred.

Then, before filtration starts and to avoid asphaltene precipitation caused by pressure depletion, it is filled with nitrogen up to the pressure of the mixture. This last pump enables isobaric transfers of the fluids through the filter during the filtration. Pictures of the filter before and after precipitation are presented in Figure III-9.

Figure III-9: Filter before precipitation (on the left) and after (on the right) (Carrier, 2005)

- **The injection cell**

The last part of the set-up is an injection cell. Its operating pressure is 70 MPa, the maximum temperature is 423.15 K and the total volume is 50 cm^3. The volume injected per round was determined after calibration versus temperature and pressure with n-heptane [26]. It was found equal to 0.7608 cm^3. This cell is equipped with a sliding gauge, which gives access to its volume with a precision of 0.01 round (7.6 mm^3). The temperature of the injection cell is kept constant within 0.1 K using a cryothermostat Huber Unistat DC. A similar temperature probe is used (PT 100, precision of 0.1 K). An operational pressure gauge Kulite, (HEM 375) operating between 0 and 100 MPa, is used for pressure determination (uncertainty below 0.1 MPa).

3.3. Experimental procedure

Prior to any study, high vacuum is made in the filtration cell and in all the connecting lines. The sample is stirred for half an hour before injection in the PVT cell. The weighted asphaltenic oil is introduced at atmopsheric pressure in the cell, regulated at the desired temperature. The oil is then pressurized by displacement of the piston. The precipitant, maintained at the temperature and pressure of study, is then injected in the filtration cell where the mixture is continuously stirred, at constant pressure. Once the system is stable (no need to modify the volume to keep the pressure constant), the mixture is filtered at the studied pressure and temperature. Hence, the filter is closely analyzed to see whether or not traces of asphaltenes can be detected on the filter. It is

important to notice that the filtration is operated by displacement of the mixture through the filter at constant pressure (ΔP less than 1 bar). A new filter is used for each experimental run to preserve a constant pore size of the filtration medium.

CO_2 and CH_4 were provided by Messer and their purity are respectively 99.998% and 99.995% (in volume).

This study has been conduced with two asphaltenic crude oils: one from South America and the other one from Middle-East. Some properties of the two investigated crude oils are presented in Table III-3 (SARA analysis and degree API). The aromatic and resin contents differ whereas the other properties are very similar.

	South American crude oil	Middle East crude oil
Saturates	35 %	34 %
Aromatics	24 %	41 %
Resins	32 %	16 %
Asphaltenes	9 %	9 %
Degree API	27	29

Table III-3: SARA analysis (weight %) and degree API of the two studied crude oils

3.4. Influence of carbon dioxide

Many studies report the impact of CO_2 on asphaltene precipitation (Monger, 1985; Novosad and Costain, 1990; Srivastava et al., 1995; Idem and Ibrahim, 2002). However, a minimum amount has to be injected. Figure III-10 shows the experimental data obtained by Srivastava and co-workers (1995) and at least 40 % in mole are necessary to start precipitation for this Weyburn fluid at 16 MPa and 332.15 K. For the fluid from Middle-East, weight fractions between 15 and 20% were tried and all of them induced asphaltene precipitation. For the crude oil from South America, at 20 MPa and for temperatures ranging between 303 and 383 K, a minimum of 18 w% had to be injected to initiate precipitation.

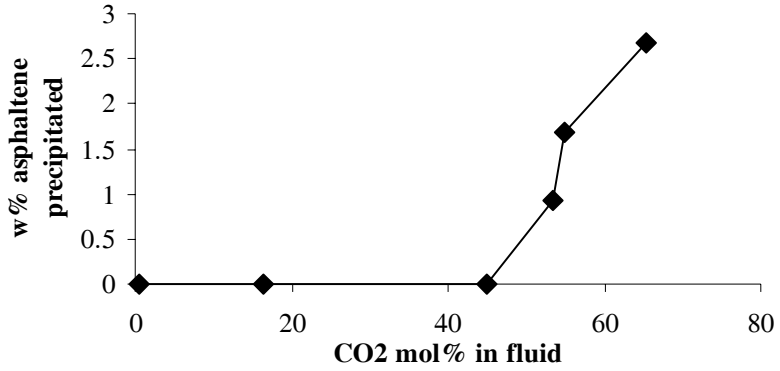

Figure III-10: Influence of CO_2 on the amount of precipitated asphaltenes (from Srivastava et al., 1995)

The first study was made on the South American crude oil with a single composition (19 w% CO_2 – 81 w% crude oil). The onset curve and the bubble point curve from 293.15 up to 383.15 K are given in Figure III-11.

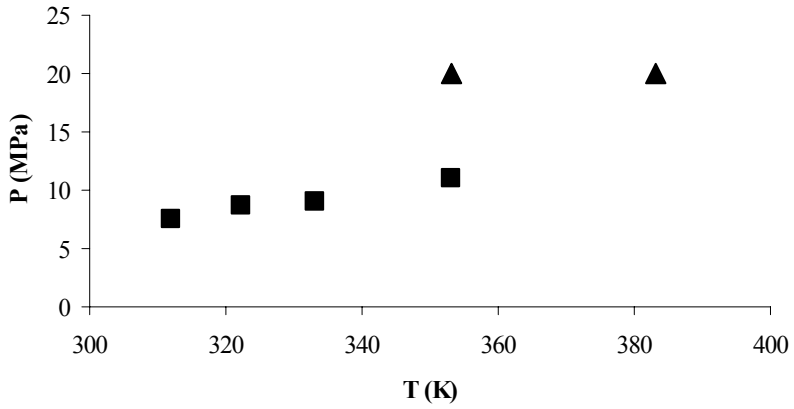

Figure III-11: **Asphaltene Phase Envelope of the South American crude (▲, onsetpoint; ■, bubble point)**

The bubble point was determined by means of the PV curve of the mixture. Figure III-12 shows one of them at 353.15 K.

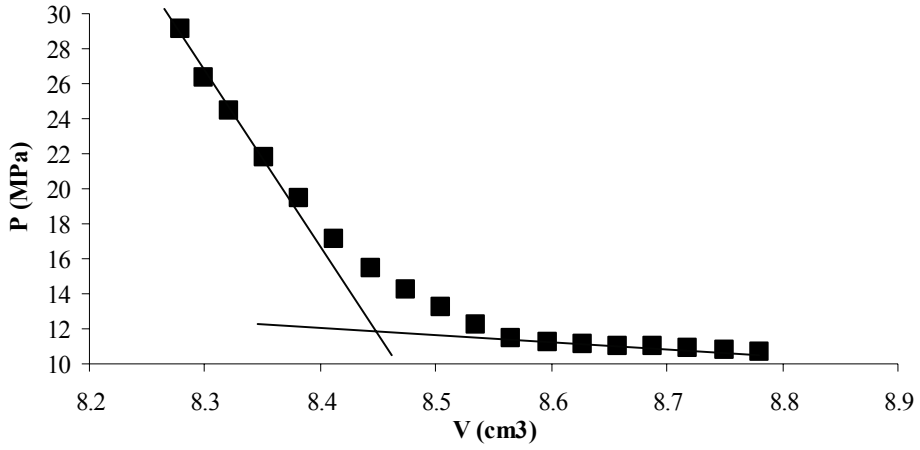

Figure III-12: PV curve of the South American crude oil at 353.15 K

In order to determine it more accurately, isothermal compressibility $\kappa_T \left(= -1/V\left(\partial V/\partial P\right)_T \approx -1/V\left(\Delta V/\Delta P\right)_T\right)$ was plotted with respect to pressure (Figure III-13). There was no volumetric evidence of the asphaltene precipitation. Indeed, the equipment should be much more accurate in terms of volume to be able to detect any sign of precipitation, if any.

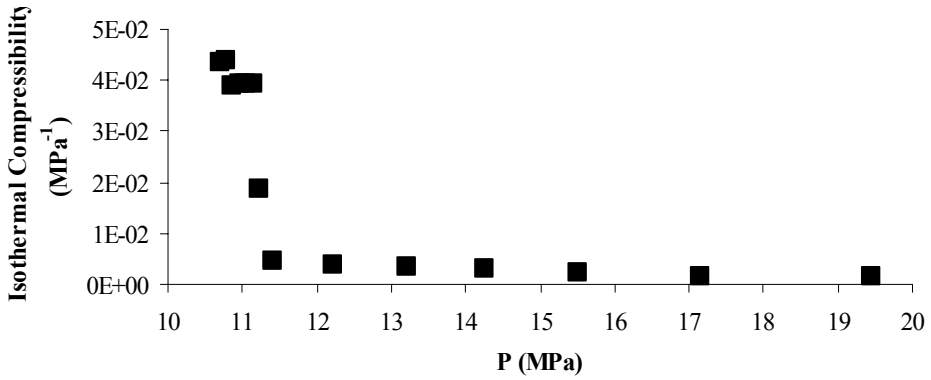

Figure III-13: Isothermal compressibility at 353.15 K of the South American crude oil

As for the precipitation envelope, small pressure steps combined with filtrations were carried. Very little sample is required for each experiment (5 g of crude usually) and this is one of the major advantages of this high-pressure system. However, with the first crude oil, only two points were obtained because there was no more available oil. Furthermore, the effect of temperature is not visible on this plot.

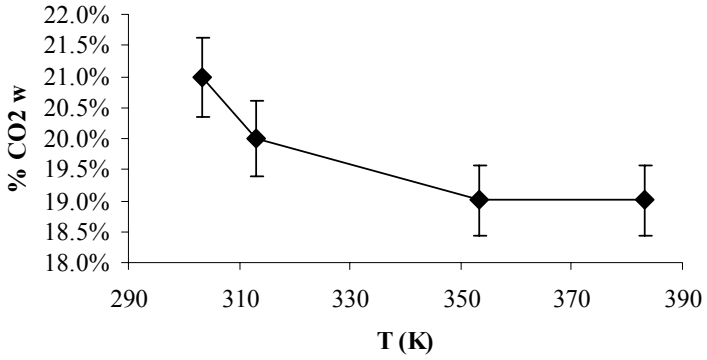

Figure III-14Influence of temperature on the onset (South American crude oil at 20 MPa)

Nonetheless, stability was studied at 20 MPa and up to 383 K for the same crude oil. Figure III-14 clearly shows that less CO_2 is required to precipitate asphaltenes when temperature is increased, i.e. the higher the temperature, the less soluble the asphaltenes.

The second crude (from Middle-East) was also investigated and its phase envelope was determined for a fixed CO_2 content (18% in weight), as seen on Figure III-15. The same conclusions were found:

- The higher the pressure, the more soluble the asphaltenes.
- The higher the temperature, the lower the solubility.

Hence, the two investigated oils seem to behave in the same way with respect to pressure and temperature.

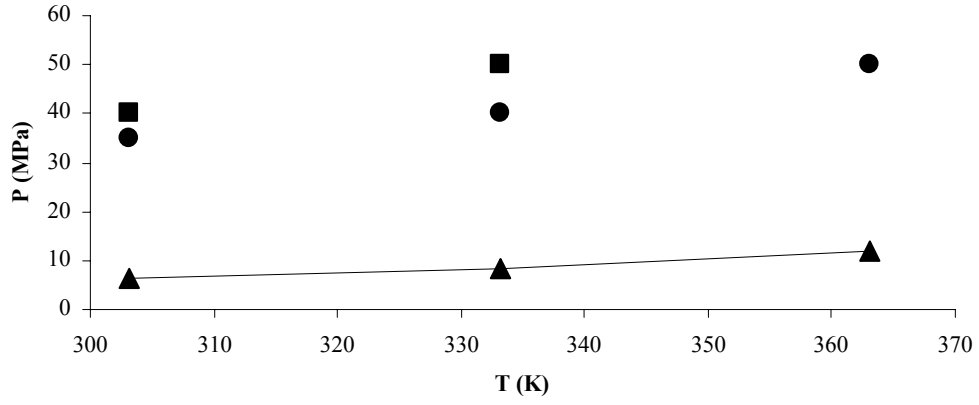

Figure III-15: Asphaltene Phase Envelope of the Middle-East crude oil (18% CO_2). (■, no precipitated asphaltenes; ●, precipitated asphaltenes; ▲, bubble point)

For the South American crude oil, the re-dissolution was observed for all the investigated conditions and the kinetics was quite fast (a few hours at high pressure were sufficient after the depletion). As for the crude oil from Middle East, it was not seen, even after a 72 hour continuous mixing. The resin content could be an explanation (32% for the South American crude oil and 16% for the Middle East one). Indeed, resins are assumed to peptize asphaltenes and keep them in solution.

3.5. Influence of methane

The same tests were carried with the crude oil from Middle-East but with methane as the gas agent. Methane does have dispersion forces and is known to induce asphaltene precipitation (Gonzalez et al., 2005). However, its solubility is much lower than the one of carbon dioxide. Figure III-16 shows solubilities of methane (Srivastan et al, 1992), nitrogen (Azarnoosh and McKetta, 1963) and carbon dioxide (Shaver et al., 2001) in n-decane at 344 K. Carbon dioxide is almost fully miscible whereas methane and nitrogen solubilities are much lower (less than 20%).

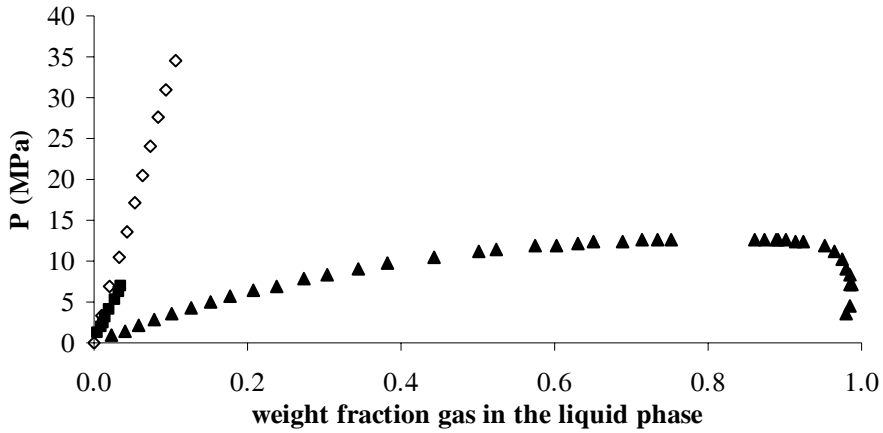

Figure III-16: Solubility of various gases in n-decane (▲, CO2; ■, CH4; ◇, N2) (see below for the references)

This difference of solubility between methane and carbon dioxide was observed for the crude oil from Middle-East. Indeed, above 6w% of methane, the bubble point curves behaved differently. As a matter of fact, the usual and expected break took place at lower pressures, which means the oil is saturated in gas and that the system has more than one phase.

The effect of temperature was studied for two methane concentrations (10 and 14 w%). For those two concentrations, at 50 MPa, there were precipitated asphaltenes at 333.15 K and none at 373.15 K. It means **temperature has a stabilizing effect** whereas it was the contrary with CO_2 for the same crude oil. Kokal and co-workers (Kokal et al., 1992) mixed several light gases with two crude oils and measured the onset pressures between 298 and 373 K. With CO_2, temperature had both stabilizing and destabilizing effect according to the oil under investigation. On the contrary, with light gases (ethane and propane), there was a maximum in stability around 323 K for both oils. Methane had no effect in terms of asphaltene precipitation. Hence, it is not unheard of for an oil to exhibit different stability behaviours with different gases as it was found in this work.

The effect of concentration was also studied (at 333.15 K). The P-x diagram plotted in Figure III-17 shows the experimental onset and bubble points. The full line represents one possible phase envelope. It was chosen because no precipitate was detected with 2w% at any pressure whereas precipitated asphaltenes were detected at 4 and 6 w%.

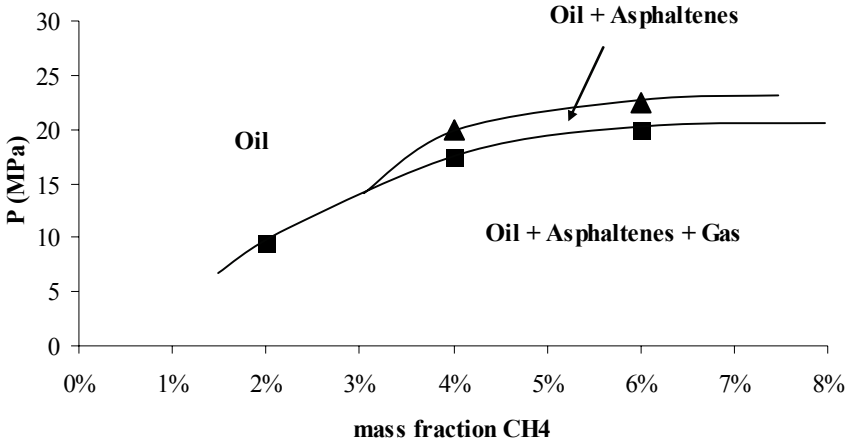

Figure III-17: P-x diagram of the system crude oil Middle-East + Methane at 333.15 K (▲, onset point; ■, bubble point)

It is seen that the higher the methane content, the higher the bubble point pressure and the onset pressure. The gap between the onset and the bubble point curves is quite small. The re-dissolution curve (or lower onset curve) was not detected.

This diagram is similar to the one reported by Szewczyk and Béhar but with carbon dioxide and presented in Figure III-18 (Szewczyk and Béhar, 1999).

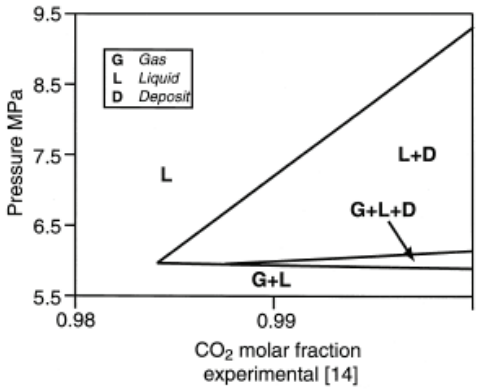

Figure III-18: Phase envelope of a crude oil + CO_2 at 303 K (from Szewczyk and Béhar, 1999)

As for the effect of pressure, it is a stabilizing one as it has always been reported in the literature so far.

Reversibility was observed for 10, 12 and 14 w% of methane. In these situations, asphaltenes were precipitated. Then, temperature was increased and asphaltenes happened to go back to solution. This was noticed for this oil with carbon dioxide. The kinetics is much faster. Is it because there is less gas component (14 w% at the most instead of 18w%)?

3.6. Conclusions

This novel HP cell combined with the filtration under pressure enabled the stability analysis of two crude oils with respect to pressure, temperature and composition.

- **Effect of temperature**

With CO_2, increasing temperature had a destabilizing effect for both oils. With CH_4, only the crude from Middle-East was investigated and temperature stabilizes it.

- **Effect of composition**

A minimum amount of gas had to be present to initiate asphaltene precipitation: between 2 and 4 w% for CH_4 (varying pressures at 323.15 K) and 19 w% for CO_2 (varying temperatures at 20 MPa).

- **Effect of pressure**

The higher the pressure, the more soluble the asphaltenes for any gas injected.

This apparatus has a promising future since its working conditions are wide, the required sample is small, the dead volume is inexistent, its cleaning is easy and the technique used to determine asphaltene precipitation is not subject to doubts. Few apparatus dedicated to the study of asphaltene solubility with pressure and temperature offer such advantages.
Furthermore, an optical device was developed lately on this cell. It brings interesting input about the phase transitions (Castillo et al., 2006). The combination of both techniques (filtration+ laser) will for sure improve the understanding of asphaltenic fluids. Note that an automatic control and regulation of the pressure would improve this experimental set-up. Appendix III-2 presents the article related to this work that will be published in Energy & Fuels in 2006.

3.7. Unanswered issues and future work

Of course, several issues are still raising questions. A few of them are listed below:

- **The pore size:** a size of 0.5 μm was chosen to detect the precipitated asphaltene as it was done in several studies. Some analyses confirm such a size but a careful study with a range of filters (from 0.1 to 1 μm) for instance would bring very useful information. As a matter of fact, when does precipitation start? When the size of the solids is 0.5 or 0.1 μm? The size-distribution studies carried by Montel (2006) seem promising for that matter.

- **Kinetics:** is the thermodynamic equilibrium reached? In this work, filtration was carried out once pressure was stable. It usually took between 5 and 24 hours. But, kinetics can be very slow for asphaltenic fluids. It might be that asphaltenes were not present in this work for some conditions but that they could have been a few hours later. The use of the new laser system will permit to follow what "happens" in the cell a bit more instead of working with a "black box" system.

- **Exact onset:** in this work, filtrations were carried at different pressures to detect the onset. The pressure difference between two tests was varying between 2.5 and 10 MPa. Smaller differences should be tested to obtain more accurate phase envelopes.

- **Reversibility:** reversibility is highly related to kinetics. Precipitation was reversible with methane and not carbon dioxide with the crude oil from Middle-East. As it was said, the use of the laser with help detecting the reversibility and obtaining the lower onset curves.

- **Nitrogen:** nitrogen is reported as a precipitant but no careful study presents its effects on asphaltene stability. This experimental set-up should be used to perform such an investigation.

4. Conclusion

Gas injection was studied with a new high-pressure cell for two crude oils and two gases. This technique detects precipitation and not flocculation (like many techniques do). The determination of APE appeared to be time-consuming at the beginning but a better knowledge of the experimental set-up enables fast measurements now (say 1-2 weeks to obtain the PT-phase envelope of one defined mixture if nothing goes wrong).

The main issue is kinetics. But, this issue is valid for any measurements related to live oils and asphaltene precipitation. How can one be 100% sure that the equilibrium is reached? Hence, modelling of APE should be taken with care and perspective, especially when the technique detects flocculation and not precipitation. Is it worth spending time and money modelling “unreliable” data?

And last, but not least: even if a proper determination of an APE can be performed, how representative is the studied sample?

Literature

Akbarzadeh K., Alboudwarej H., Svrcek W., Yarranton H.W., A generalized regular solution model for asphaltene precipitation from n-alkane diluted heavy oils and bitumen, Fluid Phase Equilibr. (2005), 232, 159 - 170

Ali L.H., Al-Ghannam K.A., Investigations into asphaltenes in heavy crude oil. I. Effect of temperature on precipitation by alkane solvents, Fuel (1981), 60, 1043 – 1046

Andersen S.I., Effect of precipitation temperature on the composition of n-heptane asphaltenes, Fuel Sci.Techn. Int. (1994), 12, 51 – 74

Andersen S.I., Birdi K.S., Influence of temperature and solvent on the precipitation of asphaltenes, Fuel Sci.Techn. Int. (1990), 8, 593 – 615

Andersen S.I., Speight J.G., Thermodynamic models for asphaltene solubility and precipitation, J. Petrol. Sci. Eng. (1999), 22, 53 – 66

Andersen S.I., Flocculation onset titration of petroleum asphaltenes, Energ. Fuel. (1999), 13, 315 – 322

Aquino-Olivos M.A., Andersen S.I., Lira-Galeana C., Comparisons between asphaltenes from the dead and live-oil samples of the same crude oils, Pet. Sci. Technol. (2003), 21, 1017 – 1041

Aquino-Olivos M.A., Buenrostro-Gonzalez E., Andersen S.I., Lira-Galeana C., Investigations of inhibition of asphaltene precipitation at high pressure using bottomhole samples, Energ. Fuel.(2001), 15, 236-240

Azarnoosh A., McKetta J.J, Nitrogen-n-decane system in two-phase region, J. Chem. Eng. Data (1963), 8, 494-496

Briant J., Hotier G., Research on the state of asphaltenes in hydrocarbon mixtures – size of molecular clusters, Rev. I. Fr. Pet. (1983), 38, 83 – 100

Buckley J.S., Microscopic investigation of the onset of asphaltene precipitation (1996), Fuel Sci.Techn. Int. (1996), 14, 55 - 74

Buckley J.S., Predicting the onset of asphaltene precipitation from refractive index measurements, Energ. Fuel. (1999), 13, 328 – 332

Buckley J.S., Hirasaki G.J., Liu Y., Von Drasek S., Wang J.-X., Gill B.S., Asphaltene precipitation and solvent properties of crude oils, Pet. Sci. Technol. (1998), 16, 251 – 285

Buenrostro-Gonzalez E., Lira-Galeana C., Gil-Villegas A., Wu J., Asphaltene precipitation in crude oils: theory and experiments, AIChE J. (2004), 50, 2552 – 2570

Burya Y.G., Yudin I.K., Dechabo V.A., Anisimon M.A., Colloidal properties of crude oils studied by dynamic light-scattering, Int. J. Thermophys. (2001), 22, 5, 1397 – 1410

Bushnell J.D., Ryan D.G., United States Patent No. 3976396, 1976

Carrier H., Laboratoire des Fluides Complexes, University of Pau, Personal communication (2005)

Carrier H., Plantier F., Daridon J.-L., Lagourette B., Lu Z., Acoustic method for measuring asphaltene flocculation in crude oils, J. Petrol. Sci. Eng. (2000), 27, 111 - 117

Castillo J., Acevedo S., Canelon C.E., Carrier H., Daridon J.L., High pressure and high temperature investigations of asphaltene stability using an extrinsic refractometer, Energ. Fuel. (2006), accepted for publication

Christensen A.A., Hadsbjerg C., Vestager-Tybjerg P.C., A study of the perturbed chain statistical associating fluid theory, Midterm Project: Technical University of Denmark, Department of Chemical Engineering, 2005

Clarke P.F., Pruden B.P, Asphaltene precipitation: detection using heat transfer analysis, and inhibition using chemical additives, Fuel, (1997), 76, 7, 607 – 614

Edmonds B., Moorwood R. A. S., Szczepanski R., Zhang X., Heyward M., Hurle R., Measurement and prediction of asphaltene precipitation from live oils, Proceedings of the third international symposium on colloid chemistry in oil production, asphaltenes and waxes deposition (ISCOP'99), Mexico, November (1999)

Ekulu G., Magri P., Rogalski M., Scanning aggregation phenomena in crude oils with density measurements, J. Dispers. Sci. Technol (2004), 25, 321 – 331

El-Mohamed S., Hardouin F., Gasparoux H., Floculation des produits lourds du pétrole, J. Chim. Phys. (1988), 85, 135 - 144

Escobedo J., Mansoori G.A.. Theory of viscosity as a criterion for detection of onset of asphaltene flocculation, Proceedings of the SPE International Petroleum Conference and Exhibition of Mexico, SPE 28729 (1994), 585 - 596

Fahim M.A., Dang T., Verdier S., Andersen S.I., Measurements of Precipitation of Asphaltenes from Live Oil Systems using a Filtration Technique, Presented at the 5th International Conference on Petroleum Phase Behaviour and Fouling, Banff, June 13 - 17, 2004.

Fotland P., Anfindsen H., Fadnes F.H., Detection of asphaltene precipitation and amounts precipitated by measurement of electrical conductivity, Fluid Phase Equilibr. (1993), 82, 157 – 164

Fotland P., Precipitation of asphaltenes at high-pressures; Experimental technique and results, Fuel Sci.Techn. Int. (1996), 14, 313 – 325

Gonzalez D.L., Ting P.D., G.J. Hirasaki, Chapman W.G., Prediction of asphaltene instability Ander gas injection with the PC-SAFT equation of state, Energ. Fuel (2005), 19, 1230 - 1234

Hammami A., Phelps C.H., Monger-McClure T., Little T.M., Asphaltene precipitation from live oils: an experimental investigation of onset conditions and reversibility, Energ. Fuel. 2000, 14, 14 – 18

Hammami A., Chang-Yen D., Nighswander J.A., Stange E., An Experimental Study of the Effect of Paraffinic Solvents on the Onset and Bulk Precipitation of Asphaltenes, Fuel Sci.Techn. Int. (1995), 13, 1167-1184

Heithaus J.J., Measurement and significance of asphaltene peptization, J. Inst. Pet. (1962), 48, 45 – 53

Hirschberg A., deJong L.N.J., Schipper B.A., Meijer J.G., Influence of temperature and Pressure on asphaltene flocculation, paper SPE 11202, SPE J. (1984) 283 – 293

Hotier G., Robin M., Action de divers diluants sur les produits pétroliers lourds : mesure, interprétation et prévision de la floculation des asphaltenes, Rev. I. Fr. Petrol. (1983), 38, 1, 101 – 120

Hu Y.-F., Guo T.-M., Effect of temperature and molecular weight of n-alkane precipitants on asphaltene precipitation, Fluid Phase Equilibr. (2001), 192, 13 – 25

Knudsen L. B., Modelling of asphaltene precipitation; Master's thesis: Technical University of Denmark, Department of Chemical Engineering, 2001.

Idem R.O., Ibrahim H.H., Kinetics of CO_2-induced asphaltene precipitation from various Saskatchewan crude oils during CO_2 miscible flooding, J. Pet. Sci. Eng. (2002), 35, 233 – 246

Jamaluddin A.K.M., Creek J., Kabir C.S., McFadden J.D., D'Cruz D., Manakalathil J., Joshi N., Ross B., J. Can. Pet. Technol. (2002), 41, 44 - 52

Jamaluddin A.K.M., Joshi N., Iwere F., Gurpinar O., An Investigation of Asphaltene Instability under Nitrogen Injection, Proceedings of the SPE International Petroleum Conference and Exhibition of Mexico (2002), 427 – 436

Joshi N.B., Mullins O.C., Jamaluddin A., Creek J., McFadden J., Asphaltene precipitation from live crude oil, Energ. Fuel. (2001), 15, 979 – 986

Kokal S.L., Najman J., Sayegh S.G., George A.E., Measurement and correlation of asphaltene precipitation from heavy oils by gas injection, J. Can. Petrol. Technol. (1992), 31, 24-30

Le Châtelier, H. L. Ann. Mines (1888), 13, 157

Laux H., Rahimian I., Browarzik D., Floculation of asphaltenes at high pressure. I – Experimental determination of the onset of flocculation, Pet. Sci. Technol. (2001), 19, 1155 – 166

Leontaritis K.J., The asphaltene and wax deposition envelopes, Fuel Sci.Techn. Int. (1996), 14, 13 – 39

Leontaritis K.J., Amaefule J.O., Charles R.E., Systematic approach for the prevention and treatment of formation damage caused by asphaltene deposition, SPE Prod. Facil. (1994), 9, 157-164

Lhioreau C., Briant J., Tindy R., Influence de la pression sur la floculation des asphaltenes, Rev. I. Fr. Petrol. (1967), 22, 5, 797 – 806

Lu Z., Daridon J.L., Lagourette B., Ye S., Phase comparison technique for measuring liquid-liquid phase equilibrium, Rev. Sci. Instrum. (1999), 70, 2065-2068

Monger T.G., The impact of oil aromaticity on carbon dioxide flooding, SPE J. (1985), 25, 371 – 378

Montel F., Petroleum Thermodynamics, Notes, Total, 2004

Montel V., Laboratoire des Fluides Complexes, University of Pau, Personal communication (2006)

Negahban S., Bahamaish J.N.M., Joshi N., Nighswander J., Jamaluddin A.K.M., An experimental study at an Abu Dhabi reservoir of asphaltene precipitation caused by gas injection, SPE Prod. .Facil. (2005), 20, 115-125

Novosad Z., Costain T.G., Experimental and modelling studies of asphaltene equilibria for a reservoir under CO2 injection, SPE 20530 (1990), 599 - 607

Peramanu S., Clarke P.F., Pruden B.B., Flow loop apparatus to study the effect of solvent, temperature and additives on asphaltene precipitation, J. Petrol. Sci. Eng. (1999), 23, 133–143

Shaver R.D., Robinson R.L., Gasem K.A.M., An automated apparatus for equilibrium phase compositions, densities, and interfacial tensions: data for carbon dioxide + decane, Fluid Phase Equilibr. (2001), 179, 43–66

Shaw J.M., Béhar E., SLLV phase behavior and phase diagram transitions in asymmetric hydrocarbon fluids, Fluid Phase Equilibr. (2003), 209, 185 – 206

Srivastan S., Darwish N.A., Gasem K.A.M., Robinson R.L. Jr., Solubility of methane in hexane, decane, and dodecane at temperatures from 311 to 423 K and pressures to 10.4 MPa, J. Chem. Eng. Data (1992), 37, 516 - 520

Srivastava R.K., Huang S.S., Dyer S.B., Mourits, F.M., Quantification of asphaltene flocculation during miscible CO_2 flooding in the Weyburn reservoir, J. Can. Pet. Tech. (1995), 34, 31 – 42

Stachowiak C., Grolier J.-P.E., Randzio S.L., Transitiometric investigation of asphaltenic fluids under in-well pressure and temperature conditions, Energ. Fuel. (2001), 15, 1033 – 1037

Szewczyk V., Béhar E., Compositional model for predicting asphaltenes flocculation, Fluid Phase Equilibr. (1999), 158, 459 – 469

Chapter IV

Asphaltene Precipitation and Calorimetry

Table of Contents

What is asphaltene precipitation about in terms of calorimetry? Can calorimetry help predicting the influence of temperature on stability, as the Le Châtelier's principle predict it? What has been done in that area so far? Can calorimetry help understanding precipitation and other aggregation phenomena?

First, a brief literature review will explain the different works done with dilution and precipitation of asphaltenic systems. Then, the attempt to follow asphaltene precipitation induced by n-heptane by Isothermal Titration Calorimetry will be presented. Finally, some experiments carried out will live oils in a HP calorimeter will be described and explained.

1. Review

Little work has been done with calorimetry and asphaltenes. This paragraph is a short summary of the relevant articles found in the literature

1.1. Brief note about exo- and endothermy

Why is the dissolution of phenanthrene in quinoline endothermic whereas the dissolution of tetraphenylporphine in the same solvent is exothermic (Zhang et al., 2003)? What kind of information about interactions can be retrieved from heats of dilution? The structures of these molecules are presented in Figure IV-1.

The variation of enthalpy can be expressed as follows in terms of creation or breaking of bonds:

$$\Delta H = \begin{pmatrix} \text{energy used in} \\ \text{bond breaking} \end{pmatrix} - \begin{pmatrix} \text{energy released} \\ \text{in bond making} \end{pmatrix} \qquad \textbf{Eq IV-1}$$

Let us consider the sole case of dissolution. It can be viewed as occurring in three steps:

- Breaking solute-solute attractions (endothermic)
- Breaking solvent-solvent attractions (endothermic)
- Forming solvent-solute attractions (exothermic)

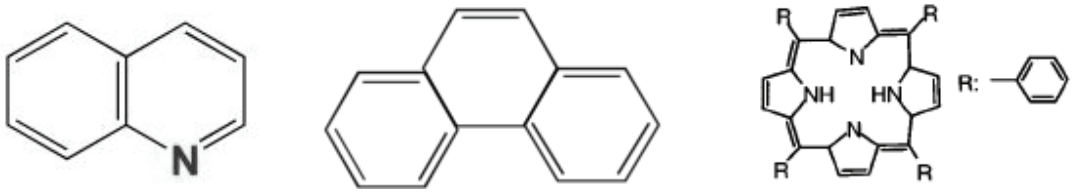

a) Quinoline **b) Phenanthrene** **c) Tetraphenylporphine**

Figure IV-1: Structure of quinoline, phenanthrene and tetraphenylporphine

So, to answer the question starting this paragraph, the heat absorbed by the breaking of the phenanthrene and quinoline self-interactions is larger than the heat released by the formation of the quinoline-phenathrene attractions. Indeed, hydrogen bonds are present between quinoline molecules. It gives a total heat of solution of 93.5 J/g whereas it is -5.9 J/g for the system tetraphenylporphine/quinoline. In the latter case, the solute-solvent

interaction is very strong since hydrogen bonds can be created thanks to the nitrogen atoms present in both types of molecules. Hence, the number of bonds, as well as their nature (dispersion, polar, hydrogen bonding) explains this difference between the two solutes. When a chemical reaction occurs, the same scheme can be applied: the breaking of the reactant molecules (endothermic) and the formation of the product molecules (exothermic).

1.2. Mixtures of Asphaltenes and crude oils with aromatics and n-alkanes

Few calorimetric studies of the systems (solvents + asphaltenes/crude oils) are available. They are summarized in Table IV-1.

Solute	Solvent	Experiment	Heat signal	Reference
Asphaltenes	Toluene	Titration Calorimetry	Endothermic	Andersen and Birdi, 1991
Asphaltenes	Toluene	Titration Calorimetry	Endothermic	Andersen and Christensen, 2000
Asphaltenes	Aromatics	Titration Calorimetry	Endothermic	Merino-Garcia, 2004
Asphaltenes	Aromatics	Enthalpy of mixing (DSC + microcalorimetry)	Exothermic (between -6 and -16 J/g)	Zhang et al. , 2005
Asphaltenes	n-alkanes	Enthalpy of mixing	Exothermic	Mahmoud et al., 2005
Crude oil	n-alkanes (C_6 to C_{16})	Titration calorimetry	Exothermic except for C_6 (endothermic)	Stachowiak et al. , 2005
Crude oil	Toluene and n-heptane	DSC	Endotherms between 300 and 400 K	Ekulu et al., 2005

Table IV-1: Heat of mixing between asphaltenic systems and various solvents

1.2.1. Dilution of asphaltene solutions

First, let us consider the dilution of asphaltenes with aromatics. Two phenomena are competing when aromatics are added, as summarized in Table IV-2:

- The solvation, i.e. the creation of solvent-asphaltene interactions (exothermic)
- The dissociation of the aggregates (endothermic)

Zhang et al. (2005) report **exothermic** heats of mixing for two asphaltenes tested in three solvents. In this case, it seems that the **solvent-asphaltene interaction** is much **stronger** than the **asphaltene-asphaltene attraction**. These interactions are likely to be van der Waals forces.

Bond-breaking (endothermic)	**Bond-making (exothermic)**
Asphaltene – Asphaltene	Asph.-Toluene

Table IV-2: Bond breaking and making during dilution of asphaltene solution with toluene

On the contrary, Merino-Garcia studied self-association of tens of asphaltene in toluene and he only got **endothermic signals**, i.e. dissociation of the aggregates. He assumed that the energy of interaction asphaltene-toluene was negligible. Indeed, the self-association is believed to be due to hydrogen bonding that are stronger than van der Waals forces. The calculated asphaltene-asphaltene energies were ranging between -7.6 to -0.6 kJ/mol. Considering that this energy is lower than the usual range of hydrogen bonding (-40 to -10 kJ/mol), he concluded that part of the asphaltenes were inactive. However, could it be that the exothermic interaction toluene/asphaltene was "cancelling" the heat of dissolution? Endothermic signals were also obtained by dilution of concentrated asphaltenes solutions (30 g/L) in toluene (Andersen and Birdi, 1991; Andersen and Christensen, 2000)

Nonetheless, Roux et al. (2001) studied the size of asphaltene particles with respect to dilution in toluene by SANS. They found that both radius of gyration and molecular weights are stable with an asphaltene volume fraction between 0.3 and 3-4% and steadily decrease above 3-4%. These results raise serious questions. Indeed, the change in the

state of aggregation occurs for a volume fraction higher than 4%, i.e. **40 g/L** but no change in the structure is visible below this value and down to 0.03% (0.3 g/l). So, what are the measured calorimetric signals if they are not due to the dissociation of the asphaltene aggregates? So, either the asphaltenes studied by Roux and co-workers have very specific properties or the model they used to analyze the data are not proper for such systems. Indeed, Sirota explains that SANS is "overinterpreted" because asphaltene particles are assumed to be micelles or colloids (Sirota, 2005). Therefore, SAXS and SANS measurements can be explained as the result of ephemeral dynamically fluctuating compositional inhomogenieties similar to those observed in any one-phase liquid mixture of unlike molecules.

As a brief conclusion about the dilution of asphaltenes by aromatics, one can say that:

- The interaction asphaltene-toluene is not always negligible since exothermic heats of mixing can be found.
- The energy asphaltene-asphaltene can not be measured without strong assumptions.
- A combined measure of the state of aggregation and heats of dilution with the same system would enable a better understanding of the dilution process.

The dilution of asphaltene solutions by n-alkanes has also been investigated in the past by Mahmoud (1999, 2005). Mixing of asphaltenes with n-alkanes produces exothermic effects whether asphaltenes are precipitated or in solution. Table IV-3 summarizes the state of the bonds when n-heptane is mixed with an asphaltene solution.

Bond-breaking (endothermic)	**Bond-making (exothermic)**
Asphaltene -Toluene	Asphaltene – Asphaltene
Heptane-heptane	Toluene- heptane
Toluene-Toluene	Asphaltene-heptane

Table IV-3: Bond breaking and making during addition of n-heptane in asphaltene solutions

Hence, it seems that the bond-making process overcomes the bond-breaking one. Indeed, when n-heptane is added, the aggregates grow as neutron-scattering data confirm it (Fénistein et al., 1998; Roux et al., 2001). In addition, n-heptane molecules are believed to be "immobilized" in the protecting shell formed by aliphatic lateral chains of asphaltenes (Mahmoud, 2005). Such results are in agreement with an exothermic heat of mixing due to n-alkane injection.

1.2.2. Dilution of crude oils

The influence of toluene on asphaltenic crude oils was studied by Ekulu et al. (2005). Thermal analysis of two oils was conducted by DSC between 293 and 473 K with different ratios of toluene. Large endotherms were found and the authors conclude that they are due to the disintegration of the aggregates. Furthermore, they also ran experiments with de-asphalted oils and no signal was observed. Neutron-scattering experiments confirm that the size of the aggregates is affected by temperature variations. As a matter of fact, Roux et al. (2001) found that the higher the temperature, the smaller the aggregates (the aggregate size decreased from 70 to 50 Å when temperature varied from 293 to 346 K). It could have been interesting to plot the heat of dissolution of the aggregate vs. the toluene concentration but such calculations were not performed by Ekulu and co-workers (2005).

Dilution of crude oils with n-alkanes was also attempted. Stachowiak et al. (2005) tested two crude oils with various n-alkanes and they found that n-hexane induced endothermic effects whereas higher n-alkanes released exothermic heat. The endothermic heat of mixing is due to interactions with the crude oils (breaking of bonds) while the exothermic effect results from physical interactions between long aliphatic chains and asphaltenes. Ekulu and co-workers also mixed crude oils and n-heptane. However, they did find endothermic effects (Ekulu et al., 2005). It is so because the energy due to bond breaking is higher than the energy of bond-making. Indeed, the solvent is a mixture toluene/heptane. However, for both studies, n-alkane injection occurred before the onset of precipitation. Nonetheless, Ekulu and co-workers related the heat of dilution to the propensity to precipitate. Indeed, the oil F_1 is more likely to precipitate than oil F_2 and it

exhibits a higher heat of mixing (129 J/g vs. 5 J/g). Can it be explained? When n-heptane is added to a mixture toluene-asphaltenes, two processes compete: the breaking of the toluene-asphaltene interactions and the creation of the asphaltene-asphaltene bond (the toluene-toluene, heptane-heptane and asphaltene-heptane interactions are assumed to play a minor role since no specific interactions are at stake). Let us write in equations this difference in heat of mixing:

$$\Delta H_{mix}^{F_1} < \Delta H_{mix}^{F_2} < 0$$

$$\Delta H_{breaking}^{F_1} - \Delta H_{bonding}^{F_1} < \Delta H_{breaking}^{F_2} - \Delta H_{bonding}^{F_2} < 0$$

$$\Delta H_{breaking\ tol/asph}^{F_1} - \Delta H_{bonding\ asph/asph}^{F_1} < \Delta H_{breaking\ tol/asph}^{F_2} - \Delta H_{bonding\ asph/asph}^{F_2} < 0$$

So, with stronger toluene/asphaltene attractions and weaker asphaltene/asphaltene interactions, asphaltenes will indeed be more stable and, hence, they will be less likely to precipitate. This might be the case for asphaltenes F_2 and a lower heat of mixing would exactly fit this explanation.

1.3. Precipitation

Most of the experiments with n-alkanes reported in the literature are performed below the onset of precipitation. In fact, such measurements can be difficult, especially because of the lack of reproducibility. Roux et al. (2001) attempted to find the narrow composition for which the flocculation process was sufficiently slow to be observed conveniently but they could not succeed. Only one work about calorimetry refers specifically to asphaltene precipitation (Stachowiak, 2001; Stachowiak et al., 2001) and several ones indirectly (Ekulu et al., 2005; Mahmoud et al., 2005).

First, it was found that precipitation induced by n-hexane and n-heptane was endothermic for several crude oils (Stachowiak, 2001). Table IV-3 can be analyzed with care for that matter: exothermy means that the infinite aggregation of asphaltene molecules and the asphaltene-alkanes interactions do not overcome the solvent-asphaltene breaking. Note that Table IV-3 deals with asphaltene solutions and not crude oils and, hence, “toluene” should be replaced by “solvent”. It is then quite likely that a more complex solvent – such as deasphaltened oil - has much stronger interactions with asphaltenes than pure toluene.

For instance, resins have strong interactions with asphaltenes since 1 cm^3 of resins had the same dispersing power as 105 cm^3 of benzene (Hotier and Robin, 1983).

When precipitation is caused by pressure depletion (Stachowiak et al., 2001), exothermic signals are found. Table IV-4 lists the different bonds broken and created.

Bond-breaking (endothermic)	Bond-making (exothermic)
Asphaltene -solvent	Asphaltene – Asphaltene
	Solvent-solvent

Table IV-4: State of the interactions during pressure depletion of crude oils

Since more bonds are created than broken, it does seem logical that precipitation caused by pressure depletion is exothermic. As a matter of fact, precipitation is often described as an infinite aggregation (Fénistein, 1998).

In terms of Le Châtelier's principle (Chapter 3, paragraph 1.4), what can be learnt from such experiments? As it was concluded in Chapter 3, an endothermic precipitation means that an increase temperature would destabilize solubilised asphaltenes. Unfortunately, in the mentioned works, the impact of temperature on stability was not studied. Nonetheless, it would mean that the n-heptane induced asphaltenes (Stachowiak, 2001) would precipitate with temperature. On the contrary, the live oil (Stachowiak et al., 2001) would be more stable with higher temperatures.

1.4. Other calorimetric studies

Andersen et al. (2001) studied the interaction between water and asphaltenes in solutions. It appeared that the CMC could be assigned to the water content. Indeed, after drying the toluene used for titration calorimetry, the break that was assumed to be due to a CMC disappeared.

Merino-Garcia (2004) studied the interaction asphaltene-resin. He found that stable oils had more interaction with a model resin (nonylphenol) than unstable crude oils. The

number of sites was estimated as well (no more heat of interaction). Furthermore, no correlation between heat of interaction asphaltene-resins and stability was found.

Glass transitions have also been measured for asphaltenes by DSC. Zhang et al. (2004) list the work done previously on that matter. The glass transition range is reported between 100 and 180°C.

1.5. Conclusion

No solvent is inert and, hence, determination of interactions energy requires assumptions. Obviously, calorimetric data show that precipitation caused by pressure or temperature variations is different from the one caused by n-alkanes. Indeed, the same interactions are not involved. As a matter of fact, as it was said in chapter 1, paragraph 1.1, the differences between "pressure-depleted asphaltenes" and n-heptane asphaltenes are massive (distribution, composition, etc…).

Furthermore, calorimetry has not been used very much for asphaltenic systems whereas it has great potentials to understand aggregation and precipitation. However, the time when calorimetry will enable predictions about asphaltene precipitations is out of reach with today's work. Do heats of mixing contain information about stability? The following paragraphs will be focused on this question.

2. Asphaltene precipitation and Isothermal Titration Calorimetry

Isothermal titration calorimetry (ITC) is widely used in the study of ligand-protein interactions or micellar behaviour of surfactants for instance. Andersen and Birdi used ITC for asphaltene solutions in order to measure CMC of asphaltenes (Andersen and Birdi, 1991). Then, Merino-Garcia applied it for the first time to asphaltene systems (Merino-Garcia, 2004). He focused on self-association and the asphaltene-resin interaction. In this paragraph, asphaltene precipitation is investigated with ITC.

2.1. Description of the ITC equipment

Experiments have been performed with a VP-ITC 2000 Microcal© calorimeter. The principle is the one of a twin-calorimeter: two cells (a sample and a reference), a change in the sample cell modifies temperature and this difference is converted into an electric and then calorimetric signal after proper calibration.

In our work, a mixture solvent-solute is usually placed in the sample cell and a precipitant is injected with a syringe. The volume of the cell is 1.4615 mL and the syringe has a capacity of 294 μL. The smallest injected volume can be 0.1 μL. The equipment is kept in a glove box to minimize the influence of external conditions (temperature and humidity mainly). For that purpose, silica gel is used to keep the atmosphere dry.

The sample cell is filled with pure solvent. The stirrer spins at 300 rpm. Between each injection, there is sufficient time to reach thermal equilibrium. The first injection is not used since the tip of the cell is in contact with the solution during the equilibration time.

The full experimental procedure is described in Appendix IV-1.

The main drawback of this system is that the cell has to be filled from the beginning in order to have a constant baseline. Then, when precipitant is injected, the excess volume flows over. Hence, the heat of mixing is not the one of the whole system but only of the volume of the cell.

All the experiments have been performed at 303.15 K ± 0.01 K and atmospheric pressure.

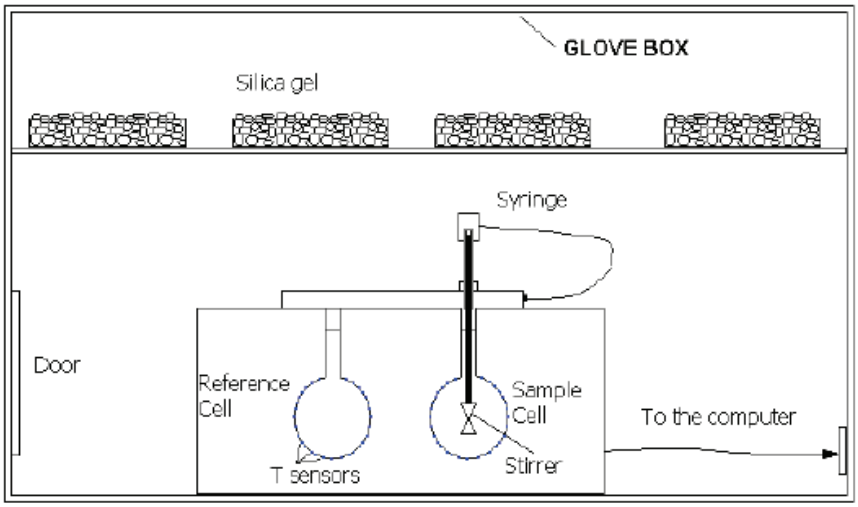

Figure IV-2: Schematic view of the ITC (from Merino-Garcia, 2004)

2.2. ITC and Phase transitions

What happens during a phase transition such as a LLE? A solute breaks its interactions with the solvent (endothermic) and both solute and solvents interact with themselves (exothermic). According to the energies of interactions, the signal can be either endothermic or exothermic.

Such an experiment was tried with the mixture n-heptane/methanol. Indeed, a phase split happens for $x_{methanol} = 0.88$ at 303.15 K and 0.1 MPa (Figure IV-3)

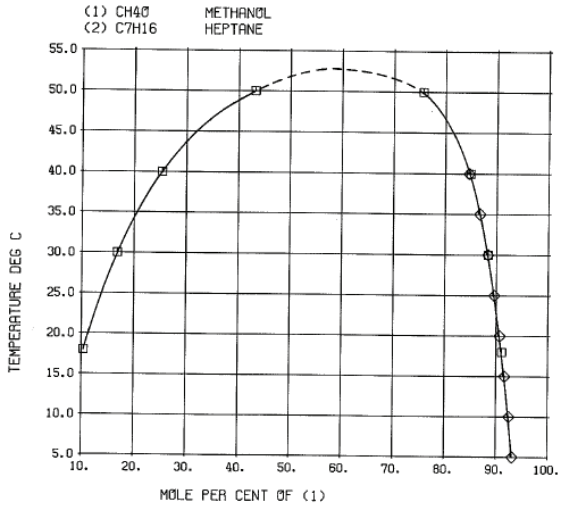

Figure IV-3: T-x diagram of the system methanol/n-heptane (Sørensen and Arlt, 1995)

In terms of volume fraction, it is equivalent to $\varphi_{methanol} = 0.67$ (the mixture was assumed ideal and densities were taken from the DIPPR correlations). The cell was filled with a mixture methanol/n-heptane of $\varphi_{methanol} = 0.73$ and, after the injection of n-heptane, the volume fraction is $\varphi_{methanol} = 0.61$. Note that the volume fraction is the global one and is similar to the one of the feed for a flash.

The heat/injection as function of the volume fraction is presented in Figure IV-4. It is found to be more representative than cumulated heats because the change in heat may be too small to be detected. Nonetheless, cumulated signals do show the LLE of this system. When the system goes over the phase transition, an exothermic change is seen (negative enthalpy). It means that the breaking of bonds n-heptane/methanol (van der Waals forces) has less thermal effects than the creation of n-heptane/n-heptane (dispersion forces) but, above all, methanol/methanol (hydrogen bonds). Between $\varphi = 0.69$ and 0.67, hydrogen bonds are created between methanol molecules, as spectroscopy data show it (Jensen and Lyberg-Kofod, 2005).

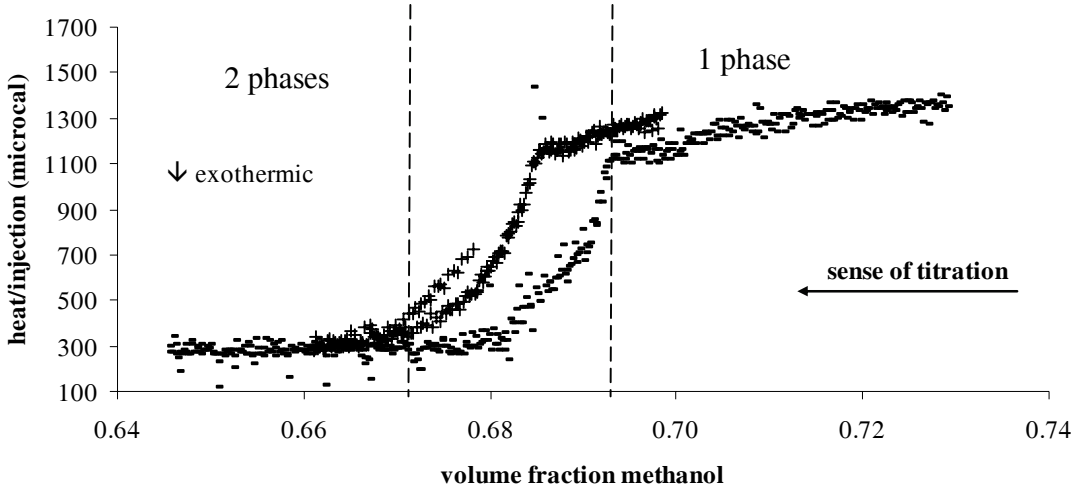

Figure IV-4: LLE detected by ITC (methanol/n-heptane at 303.15 k) (-, data 1; +, data 2)

Several experiments have been tried and they all successfully show the same trend. Only two are presented here. The transition is observed over a range of volume fraction (between 0.67 and 0.69). Does the LLE start when the curve breaks for the first time or is it complete at the second plateau? Does it start when the first drop of the n-heptane-rich

phase appear? What is the solubility limit? Any onset determination has to cope with this dilemma. However, in this work, only qualitative results are expected so this issue will not be further debated.

This was a phase transition seen by ITC. But can this technique also detect structural changes such as aggregation? As it was said in the introduction, ITC is employed to determine CMC. A CMC is a Critical Micellar Concentration. Solutions of highly surface-active materials exhibit unusual physical properties. In dilute solution, the surfactant acts as a normal solute. However, at a certain concentration, abrupt changes in physical properties occur (osmotic pressure, turbidity, surface tension, conductivity). It can be explained in terms of organised aggregates (or micelles) of the surfactant ions in which the lyophilic hydrocarbon chains are oriented towards the interior of the micelle, leaving the hydrophilic groups in contact with the aqueous medium (Shaw, 1992). Indeed, intermolecular attractions between hydrocarbon chains in the interior of the micelle represent an energetically favourable situation.

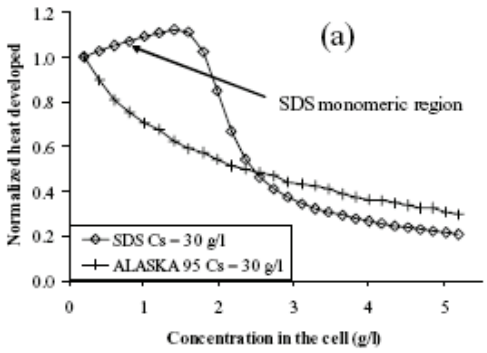

Figure IV-5: Enthalpograms of SDS and asphaltenes (both at 30 g/L in the syringe) normalized by the heat developed at the first injection (from Merino-Garcia, 2004)

Merino-Garcia tried to check whether asphaltenes exhibited such a CMC. Hence, he diluted concentrated asphaltenes in toluene and compared the signals to the ones obtained with SDS (Sodium Dodecyl Sulphate, a well-studied surfactant exhibiting a CMC). No break in the curve was seen with asphaltenes whereas the exothermic formation of aggregates with SDS could be detected (Figure IV-5).

However, aggregation can be both exothermic or endothermic. For instance, Dzwolak et al. (2003) explain that aggregation of polypeptides and proteins may have either endothermic or exothermic character, or, as for insulin, an exothermic aggregation may follow after an endothermic intermediate transition. The key factors are obviously the strengths of the bond solute-solvent and solute-solute.

So, ITC can detect LLE and aggregate formation. One last test was made with the formation of a solid, AgCl(s). A solution of $AgNO_3$(aq) is added to a solution of NaCl(aq). A precipitate forms according to the following reaction:

$$Ag^+ + Cl^- \rightleftarrows AgCl(s) \qquad K = \frac{1}{K_s} = 10^{9.75}$$

Appendix 4-2 presents the various concentrations used and the calculations related to the minimum volume to inject for the precipitation to start. The heat of precipitation is −127.1 kJ/mol at 298.15 K and 0.1 MPa. As it is visible on Figure IV-6, there is an exothermic signal from a certain volume (150 microliter for this experiment). However, the repeatability of these experiments was very poor (see Appendix 4-3 for more details). It might be due to the cleaning of the cell though it was done intensively. Indeed, the interior of the cell cannot be checked. It might be that solid AgCl deposited on the inner walls of the cell and, hence, was modifying the solubility. As a consequence, no proper estimation of the heat of the formation could be done but, as it was said previously, only qualitative information are of interest for this study.

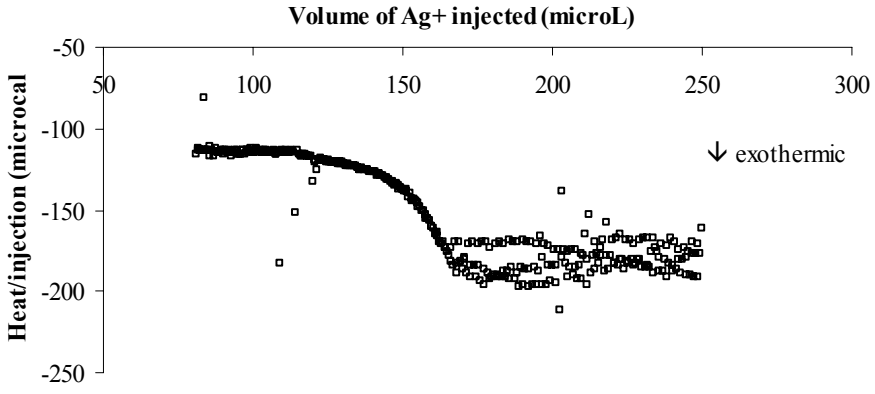

Figure IV-6: Enthalpograms of the titration $Ag^+ + Cl^- \rightarrow AgCl(s)$

Be that as it may, it appears that ITC is able to detect some phase transitions such as LLE or SLE and structural changes such as aggregation and CMC. But, will it be able to detect asphaltene precipitation if the energy of the broken bonds asphaltene-solvents is equivalent to the energy of formation asphaltenes-asphaltenes since most of them are believed to be dispersion forces?

2.3. ITC and Asphaltene Precipitation

2.3.1. Asphaltene solutions

Asphaltene solutions in toluene were tested at different concentrations (1.4 g/L and 10 g/L) for asphaltenes extracted from a Boscan crude oil with the modified IP143 method presented in the appendix 1.1. Onset titrations were performed at atmospheric conditions and the onset ratio $V_{toluene}/V_{n-C7}$ is 0.78. Several concentrations were tested and the onset occurred at the same ratio toluene/n-heptane, as reported in the literature (Porte et al., 2003).

Figure IV-7 shows the enthalpograms obtained during the titrations of the Boscan solution with n-heptane at 303.15 K and 0.1 MPa. All the enthalpograms are presented in Appendix IV-4. First, it is seen that the dilution of this asphaltene solution with n-alkanes is endothermic contrary to the results obtained by Mahmoud et al. (2005). The explanation lies in the various strengths of attractions listed in Table IV-3. The delay between each injection was at least 300 s and the maximum injection rate was 0.8 microL/injection.

Furthermore, all the experiments showed exactly the same trend:

- **Phase 1**: at low n-heptane content, low noise perturbs the main signal.
- **Phase 2**: there is no perturbation of the signal of the dilution.
- **Phase 3**: much stronger disturbances appear.

The assumptions are numerous to explain such behaviour. Is phase 1 due to local precipitation? Are the precipitated asphaltenes redissolving in zone 2? Is zone 1 due to flocculation? Is zone 3 the “real” precipitation?

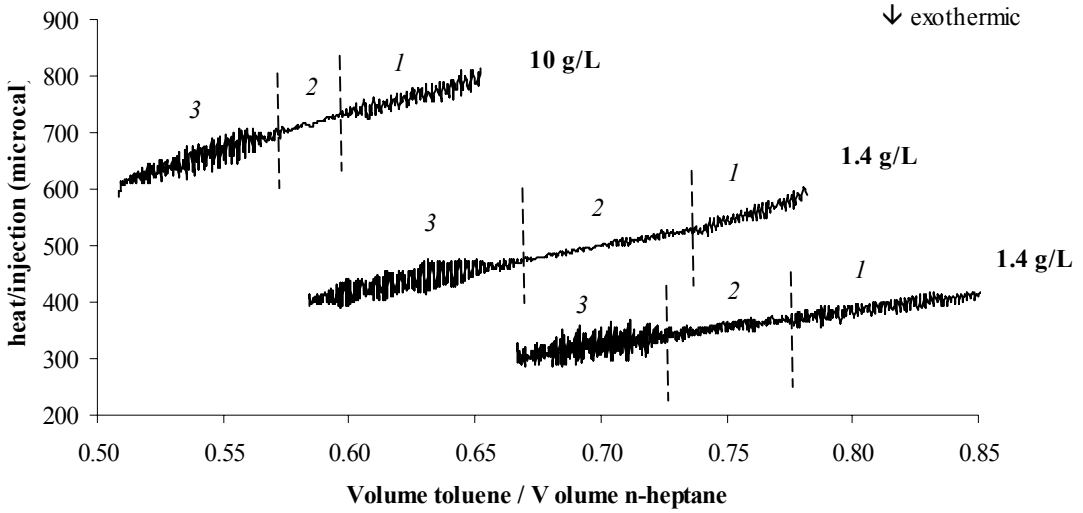

Figure IV-7: Enthalpograms obtained during the addition of n-heptane in asphaltene solution

Since the onset determined by Flocculation Onset Titration is done by optical measurements, it is possible that the "real" onset starts at lower n-heptane concentrations. Furthermore, flocculation is known to happen before precipitation. Hence, in order to know what was the state of the asphaltenes, the samples before and after titration were analyzed with a microscope usually used for thermo optical analysis by microscopy (TOAM). It appeared that some aggregates are present at the lowest n-heptane concentrations but there are many more at the end of the titration. Thus, it is believed that precipitation starts during the studied range of n-heptane fraction. It is worth noting that asphaltene concentration did affect the onset since more n-heptane was necessary. Indeed, the phase 3 starts for $V_{toluene}/V_{n-C7}$ around 0.65-0.70 for the low concentrations whereas it starts around 0.55 for the 10 g/L solutions. The deviation between "similar" experiments has several sources: the difficulty to repeat such experiments mentioned by Roux et al. (2001), the possible presence of deposited asphaltenes on the inner walls at the beginning of the experiments, a difference in the initial amount of solution (accuracy of the syringe: 0.1 mL).

Figure IV-8 shows more precisely one enthalpogram obtained during the titration (squares) as well as an average of the signal (full line). It is not possible to say whether or not precipitation (if it is what happens in phase 3 as we believe it) is endo- or exothermic.

If the energy of the broken interactions asphaltene-toluene (possibly polar and dispersion forces) is equivalent to the formation of the asphaltene-asphaltene interactions (polar and dispersive as well), such disturbances make sense. The bond making and bond breaking processes cancel each others in a way.

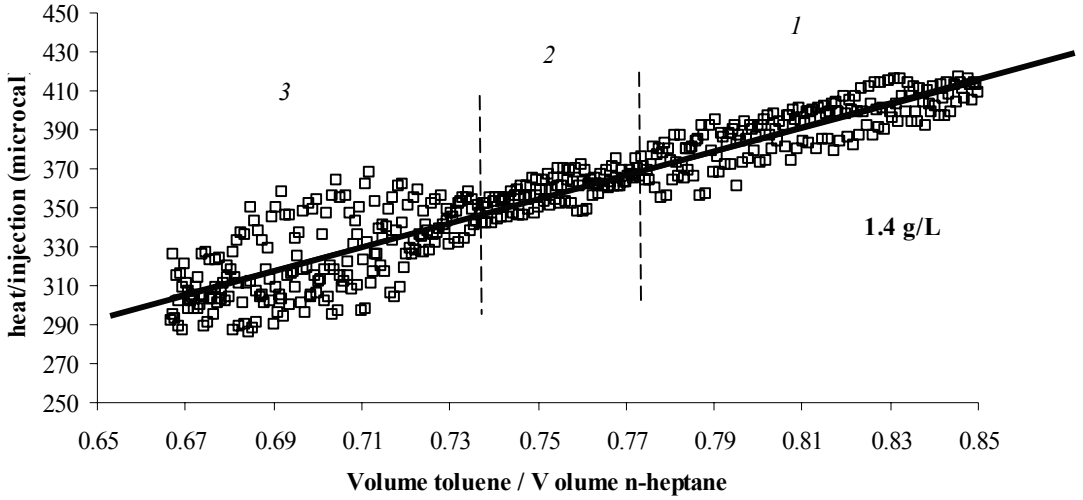

Figure IV-8: One enthalpogram of the titration of Boscan asphaltene with n-heptane

A close analysis of the peaks may bring useful information. Figure IV-9 shows three peaks obtained during the three different phases of the titration (0.7 microL/injection). The three of them have a similar shape: a first and large endothermic peak followed by a smaller one. The second peak is narrower, which means that the re-arrangement is faster.

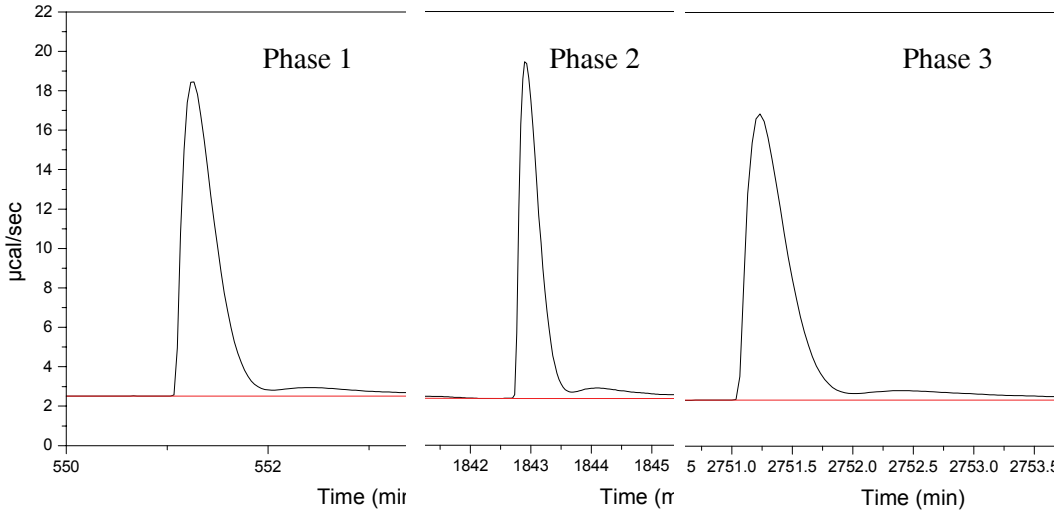

Figure IV-9: Peaks obtained during the titration of a solution of Boscan asphaltenes

In terms of Le Châtelier's principle, such an athermal behaviour would mean that precipitation is not affected by temperature. It may be possible as it explained in Chapter 3, paragraph 1.Note that, at one point, it was thought that the time between injections was not sufficient for the system to reach its thermal equilibrium. It was duly checked and it was not the case.

2.3.2. Crude oil

Two crude oils were investigated: Boqueron 2 and the crude oil from Middle East studied in Chapter 3 and in Paragraph 3.

The onset of flocculation was determined with the usual FOT method (Andersen, 1999). The onset ratios $V_{toluene}/V_{n-C7}$ are respectively 0.65 and 0.32 for Boqueron and the crude from Middle-East. We assumed that the onset did not depend on the asphaltene concentration. Figure IV-10 and Figure IV-11 shows the enthalpograms obtained during the titrations of these two crude oils. Different orders of magnitude of concentrations were tested. On Figure IV-11, two titrations of the same solution are presented. The reasons for such deviation were presented in the previous paragraph.

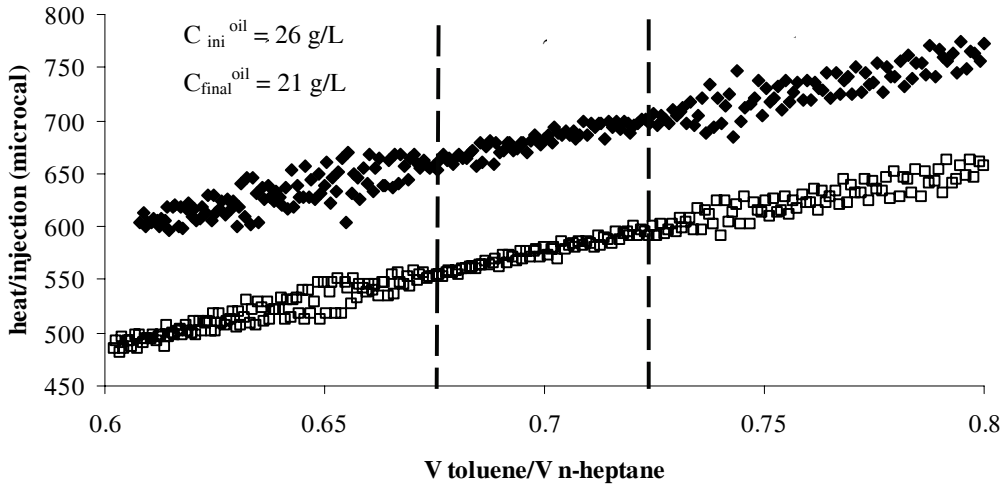

Figure IV-10: Enthalpograms of the titration of Boqueron with n-heptane at 303.15 K

The trend is very similar to the one observed for asphaltene solutions for both crude oils:

- Endothermic heat of mixing
- Three phases in the signals

If the third phase is indeed precipitation, the almost athermal behaviour means that the broken and created bonds have the same nature, i.e. van der Waals forces.

According to the Le Châtelier's principle, temperature does not affect much asphaltene stability in that temperature range for this system.

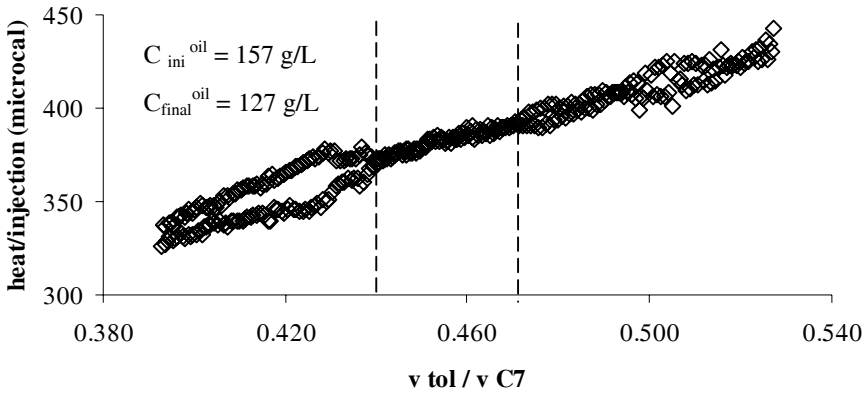

Figure IV-11: Enthalpogram of the titration of crude oil Middle-East with n-heptane at 303.15 K

3. Asphaltene precipitation and high pressure calorimetry

The issue whether or not asphaltene precipitation caused by gas injection or n-alkane injection are the same phenomena is quite relevant. Indeed, the common study in most of the laboratories dealing with asphaltenes is to perform titrations on a dead crude oil (no gas) with n-alkanes at atmospheric conditions. Then, those results are extrapolated to live oils by means of modelling. Is this procedure really relevant? Since the asphaltenes are not the same, what is the point?

In order to gain understanding about precipitation caused by gas injection, it was decided to use high-pressure calorimetry and to perform temperature or pressure variations.

Such experiments have been performed successfully once in the past (Stachowiak et al., 2001). In this work, two live oils were introduced under pressure in a calorimeter and the fluid was decompressed and compressed several times. Figure IV-12 shows the heat flow obtained during a re-compression of one of the fluids. Pressure is known to stabilize asphaltenes. Hence this signal would represent the re-solubilization of asphaltenes. However, this process is usually quite slow.

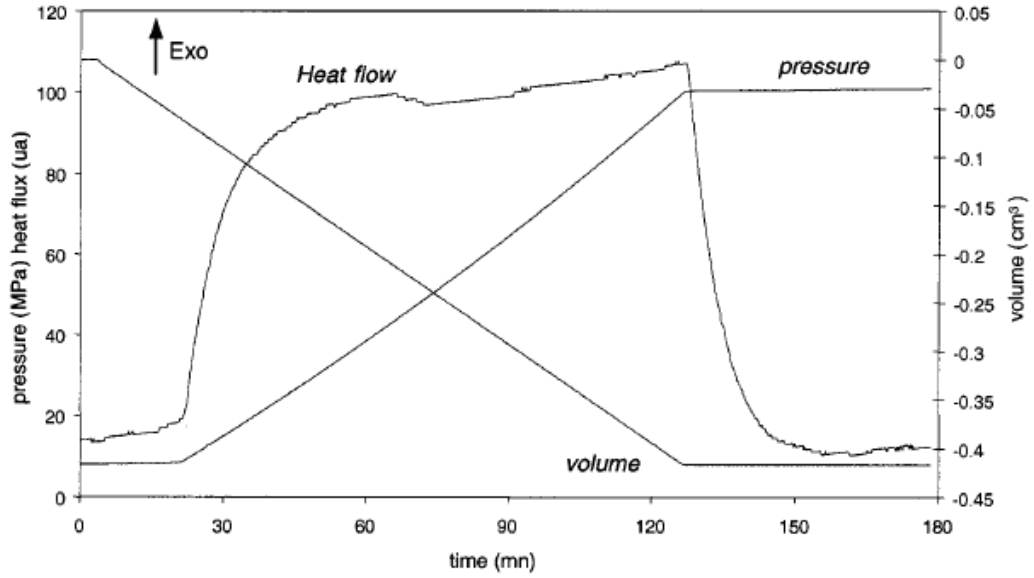

Figure IV-12: Typical results obtained with an asphaltenic fluid during a compression at 430.7 K (Stachowiak et al., 2001)

Decompressions showed exothermic signals on both samples and they were believed to be related to asphaltene precipitation. The reproducibility is quite poor since decompression of a live asphaltenic oil is almost a one-time process because of the reversibility issue, especially with no mixing. Before presenting our results, the experimental set-up as well as the experimental procedure will be briefly described. These experiments have been performed at the Laboratoire des Fluides Complexes, Université de Pau, France..

3.1. Experimental set-up

The calorimeter is a PVT Calorimeter (calorimetric detector: Setaram C80) presented in Figure IV-13. Further details about the experimental set-up can be found in Bessières et al., 2005.

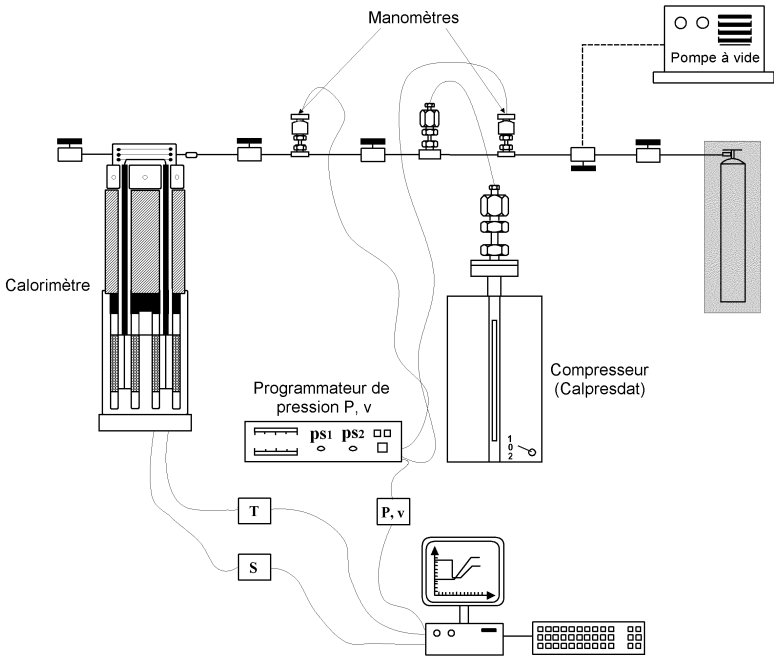

Figure IV-13: Schematic representation of the PVT Calorimeter (Setaram C80) (Bessiéres et al., 2005)

The experimental procedure is as follows:

- The calorimeter is cleaned, dried and vacuumed
- The temperature of the calorimeter is set to the studied temperature.

- The whole system (calorimeter + connections) is filled with N_2 at the pressure of study.
- The cylinder containing the live oil is connected to the calorimeter.
- The valve connecting the calorimeter and the live oil container is opened. A microvalve located at the end of the calorimeter is opened. Hence, the live oil is allowed to flow through the calorimeter and to fill it.

The nitrogen contained in the calorimeter is expelled and once oil flows at the end of the system, all valves are closed. Hence, by following this procedure, the sample is not flashed and asphaltenes do not precipitate. The main assumption is that nitrogen does not mix with the oil. According to our experience, it does not if the filling procedure is fast enough. Furthermore, even if some asphaltenes are precipitated at the contact oil/gas, the first millilitres of oil are expelled from the calorimeter. Nonetheless, in order to check the state of the asphaltenes, the high-pressure filter used in the PVT cell described in Chapter 3 is employed.

3.2. The system under investigation

The crude oil from Middle-East was studied. Its SARA composition is as follows: Saturates: 34%, Aromatics: 41 %, Resins: 16 %, Asphaltenes: 9%. Its API degree is 29 (medium oil). It was recombined with a recombined natural gas as follows: 20.8 w% natural gas – 79.2 w% crude oil. The composition of the gas is presented in Table IV-5.

Compounds	CO_2	N_2	Methane	Ethane	n-C3	n-C4	n-C5	nC6	nC7
Weight fraction	13%	5%	14%	13%	24%	18%	7%	3%	2%

Table IV-5: Mass composition of the natural gas

This mixture was prepared in IVC-SEP and sent to Pau in a high-pressure cylinder at 40 MPa. Unfortunately, a filtration was carried out in Pau and asphaltenes turned out to be precipitated. Thus, the mixtures was transferred the calorimeter, compressed at 80 MPa and the mixture rested two weeks. However, no filtration was carried out at that pressure since the amount of sample did not allow it.

3.3. Variations of temperature

The first series of experiments was a temperature scanning between 30 and 90°C at 80 MPa with the smallest temperature rate possible with this calorimeter (0.05 °C/min). The volumetric and calorimetric signals are recorded simultaneously. The first experiment showed variations in both signals around 350 K: an increase in thermal expansivity (the slope of volume with respect to temperature) and an exothermic signal (Figure IV-14).

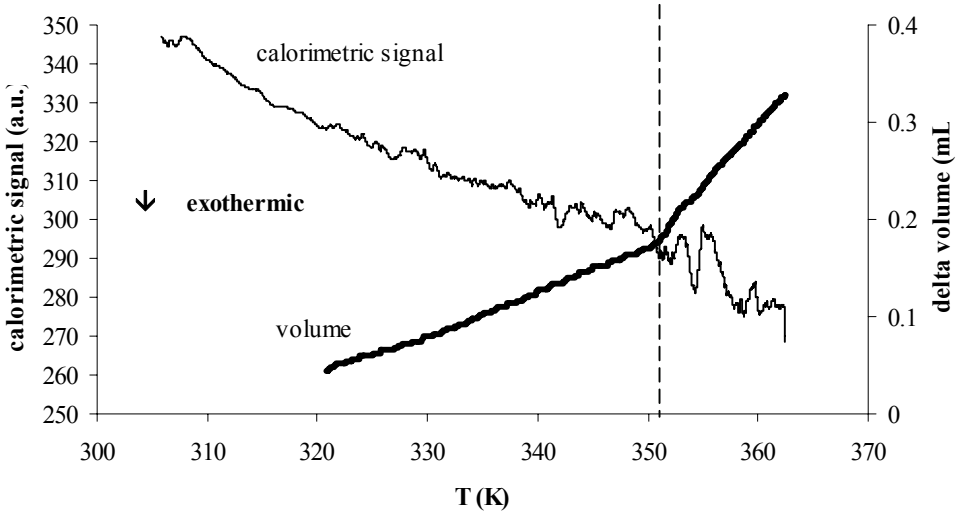

Figure IV-14: Volumetric and calorimetric signals during the first temperature variation at 80 MPa (system: crude oil from Middle-East recombined 20.8w% of natural gas)

The phase transition is believed to be a precipitation since there is a "gain in volume" (about 0.1 mL for a total volume of 30 mL). An exothermic precipitation means that temperature would stabilize asphaltenes. On the contrary, asphaltenes seem to precipitate with an increase of temperature. So, is the Le Châtelier's principle not used properly or is it the understanding of the experimental results? No filtration was carried out but the gain in volume gives to understand that a new phase is created. As for the Le Châtelier's principle, as it was said in Chapter 3, paragraph 1.4, only one equilibrium was taken into account. Could it be that the other reactions are not negligible as it was assumed?

Before 350 K, the signal is slightly perturbed. It might be that flocculation – which precedes precipitation – affects the calorimetric signal since it is change in the state of aggregation. Nonetheless, since both volumetric and calorimetric signals exhibit strong variations at the same temperature, the phase transition is believed to happen at 350 K.

The second run only showed a variation in thermal expansivity around 370 K (Figure IV-15) and no calorimetric signal. The short exothermic peak in Figure IV-15 is probably due to the electronic equipment.

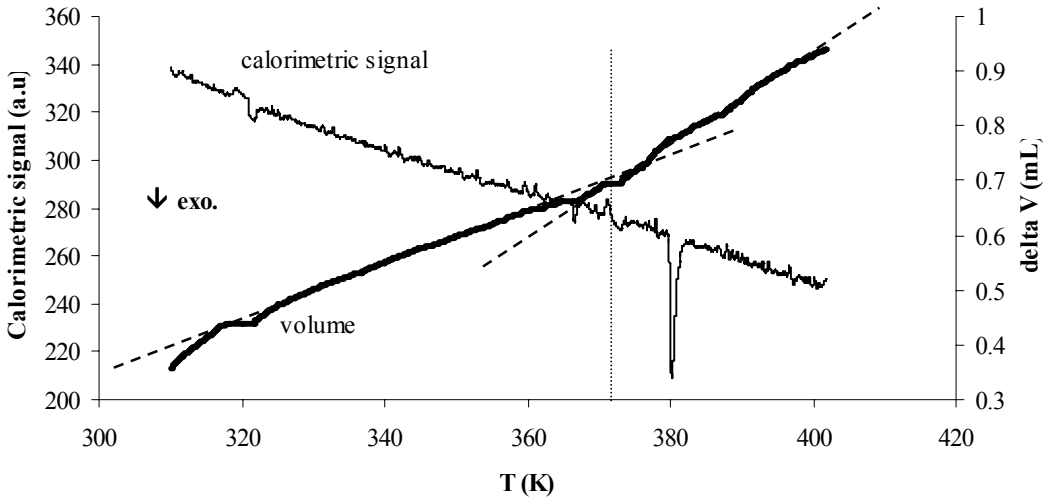

Figure IV-15: Signals obtained during the second temperature run at 80 MPa (system: crude oil from Middle-East recombined 20.8w% of natural gas)

The first perturbation observed around 320 K is due to a problem of the pressure regulation. At 380 K, the perturbation is believed to be a problem of the electrical system. In between the two experiments, the system was re-pressurized and rested for several days. Nonetheless, re-dissolution is known to be very slow. Hence, it might be that only a part of the asphaltenes went back to solution but not enough to give a "heat of precipitation" as it was visible for the first run. It would also explain the difference in the onset temperature (350 K for the first run and 370 K for the second one). As a matter of fact, it is a system with less asphaltenes in solution that precipitates.

It is also interesting to note that an increase of temperature has a destabilizing effect on this oil with both natural gas and CO_2 (see chapter 3 and the APE of this oil). Furthermore, the conditions of the onset with the natural gas (350 K and 80 MPa for 20.8 w%) are in the same order of magnitude as the ones obtained with 19 w% CO_2.

The observed phase transition is related to a change in thermal expansivity and heat capacity. It reminds the notion of second-order transition.

LLE were determined by DSC for polymer systems (Maderek and Wolf, 1983). A slight endothermic signal was detected around 505 K for the system a solution of 20 w% poly(decyl methacrylate) in iso-octane. Turbidimetry confirmed the results with a demixing temperature of 507 K. The signals presented in Figure IV-16 are very similar to Figure IV-12 obtained for asphaltenes varying temperature.

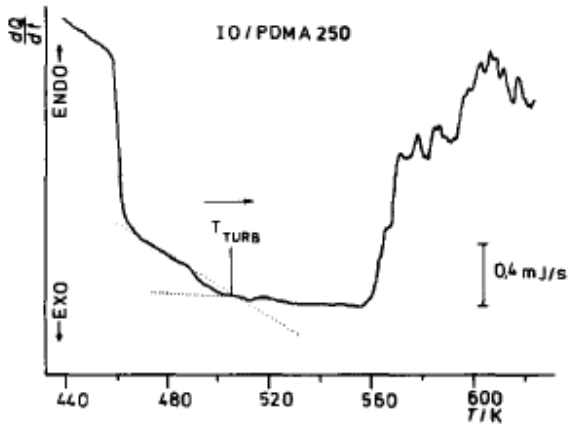

Figure IV-16: DSC signal of the demixing of 20 wt-% solution of poly(decyl methacrylate) in iso-octane, Mw = 250 000 (Maderek and Wolf, 1983)

3.4. Pressure depletion

The same fluid was recompressed up to 80 MPa and kept at rest for two weeks. This time was meant to let some of the precipitated asphaltenes to go back to solution. The second series of experiments was pressure depletions with a controlled volume decrease at 303.15 K (Figure IV-17).

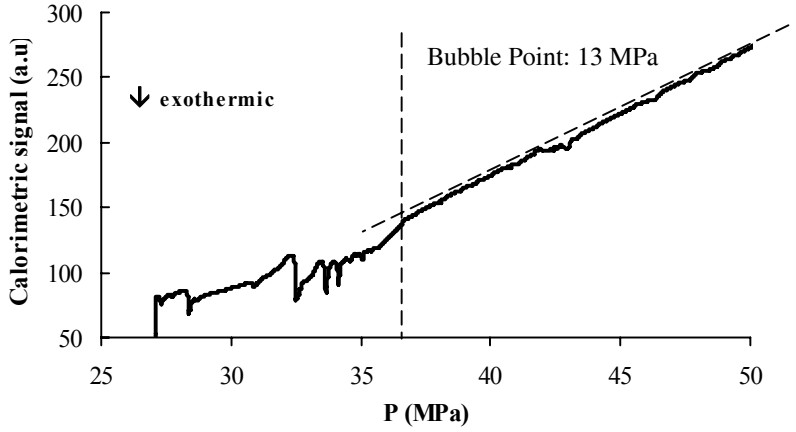

Figure IV-17: Calorimetric signals obtained during the pressure depletion at 303.15 K

An exothermic signal was detected at 37 MPa. Note that the onset of the same oil + 19% CO_2 occurs between 35 and 40 MPa at this temperature. One could think that the change of the calorimetric signal is due to the creation of a vapour phase. However, the PV curve of this fluid shows that the bubble point of this system is at 13 MPa at 303.15 K.

Such a signal could not be repeated during runs 2, 3 and 4 even though the pressure went down to the bubble point (where precipitation is said to be maximum). The time between each run was likely not to be sufficient for the asphaltenes to dissolve. This was also seen by Stachowiak et al. (2001).

3.5. Discussion and Conclusion

Asphaltene precipitation of crude oil recombined with a natural gas was caused by pressure and temperature variations. This phase transition was followed by calorimetry and has apparently the same characteristics as a second-order transition: changes of thermal expansivity and heat capacity.

Precipitation caused by temperature and pressure variations was detected as slightly exothermic as Stachowiak et al. (2001) reported it for pressure depletions. Table IV-4 listed the interactions broken and created during such transitions and it makes sense that it is exothermic (more created bonds than broken).

The onsets determined by calorimetry are very close to the ones determined by filtration though the gases are different. Precipitations of live oils followed by calorimetry should

be combined with filtration to be sure of the obtained signals. But, it would mean that each sample could only be used once and recombination is quite heavy and time-consuming. Furthermore, the amount of available crude oil did not allow it.

Hence, with enough crude oil, a complete APE (Asphaltene Phase Envelope) including onset and bubble points could be determined thanks to HP calorimetry. Indeed, bubble points can be determined by calorimetry (Verdier et al., 2005).

4. Conclusion about calorimetry

Two asphaltene precipitations were tested: the one induced by n-alkanes and the one due to gas and variations of T and P.

The first one did not exhibit any strong exothermic or endothermic signals but precipitation was rather athermal contrary to what has been observed for model systems (LLE, SLE, micellization). Therefore, it appears the energy of the broken bonds is balanced by the energy of the created ones. The n-heptane content was increased but no difference was observed. The enthalpograms of the crude oils were similar to the ones of the asphaltene solutions.

The second series of tests was performed with HP calorimeter and recombined oils. Both pressure depletions and temperature variations induced asphaltene precipitations. The increase in volume confirms these results but no filtration was performed. The re-dissolution of asphaltenes was very slow and was not seen. Hence, such experiments can be performed once. An accurate high-pressure pycnometer would enable the onset determination without the difficult of calorimetry.

Literature

Andersen S.I., Birdi K.S., Aggregation of asphaltenes as determined by calorimetry, J. Coll. Int. Sci. (1991), 142, 497 – 502

Andersen S.I., Christensen S.D., The critical micelle concentration of asphaltenes as measured by calorimetry, Energ. Fuel (2000), 14, 38-42

Andersen S.I., del Rio J.M., Khvostitchenko D., Shakir S., Lira-Galeana C., Interaction and solubilization of water by petroleum asphaltenes in organic solution, Langmuir (2001), 17, 307 – 313

Bessieres D., Saint-Guirons H, Daridon J.-L., J. Therm. Anal. Calorim. (1999), 58, 39-49

Bessières D., Lafitte T., Daridon J.-L., Randzio S., High pressure thermal expansion of gases: Measurements and calibration, Thermochim. Acta (2005), 428, 25-30

Dzwolak W., Ravindra, R., Lendermann J. Winter R., Aggregation of bovine insulin probed by DSC/PPC calorimetry and FTIR spectroscopy, Biochemistry (2003), 42, 11347-11355

Ekulu G., Nicolas C., Achard C., Rogalski M., Characterization of aggregation processes in crude oils using differential scanning calorimetry, Energ. Fuel. (2005), 19, 1297-1302

Fenistein D., Barré L., Broseta D., Espinat D., Livet A., Roux J.N., Scarsella M., Viscosimetric and neutron scattering study of asphaltene aggregates in mixed toluene/heptane solvents, Langmuir (1998), 14, 1013 – 1020

Hotier G., Robin M., Action de divers diluants sur les produits pétroliers lourds : mesure, interprétation et prévision de la floculation des asphaltenes, Rev. I. Fr. Petrol. (1983), 38, 101 – 120

Jensen L., Lyberg-Kofod J., Investigation of Hydrogen bonding in Associating Compounds Using IR Spectroscopy, Midterm Project, Department of Chemical Engineering, Technical University of Denmark, January 2005

Lundberg G. W., Thermodynamics of Solutions, XI. Heats of Mixing of Hydrocarbons, J. Chem. Eng. Data (1964), 9, 193-198

Maderek E., Wolf B.A., Detection of liquid-liquid demixing by differential scanning calorimetry, Polym. Bull. (1983), 10, 458 - 463

Mahmoud R., PhD Thesis, Nancy, 1999

Mahmoud R., Gierycz P., Solimando R., Rogalski M., Calorimetic probing of n-alkane-petroleum asphaltene interactions, Energ. Fuel. (2005), 19, 2474 - 2479

Merino-Garcia D., Calorimetric investigations of asphaltene self-association and interaction with resins, Ph.D. Thesis, IVC-SEP, Department of Chemical Engineering, Denmark, Technical University, Lyngby, Denmark, 2004

Porte G., Zhou H., Lazzeri V., Reversible description of asphaltene colloidal association and precipitation, Langmuir (2003), 19, 40 – 47

Roux J.N., Broseta D., Demé B., SANS study of asphaltene aggregation: concentration and solvent quality effects, Langmuir (2001), 17, 5085 – 5092

Shaw D.J., Introduction to colloid and surface chemistry, 4th edition, Butterworth-Heinemann Publications, 1992

Sirota E.B., Physical structure of asphaltenes, Energ. Fuel. (2005), 19, 1290-1296

Stachowiak L., Diagrammes de phases : fluides supercritiques-hydrocarbures lourds. Etudes des phénomènes de floculation des fluides asphalténiques, PhD Thesis, Clermont-Ferrand, 2001

Stachowiak Ch., Grolier J.-P. E., Randzio S.L., Transitiometric investigation of asphaltenic fluids under in-well pressure and temperature conditions, Energ. Fuel. (2001), 15, 1033 – 1037

Stachowiak C., Viguié J.R., JPE Grolier, Rogalski M., Effetc of n-alkanes on asphaltene structuring in Petroleum Oils, Langmuir (2005), 21, 4821 – 4829

Sørensen J.M., Arlt W., Liquid-liquid equilibrium data collection, Binary Systems, Chemistry Data Series, vol. V, Part 1, Dechema, Frankfurt, 1995

Verdier S., Duong D., Andersen S.I., Experimental determination of solubility parameters of oils as a function of pressure, Energ. Fuel. (2005), 19, 1225 - 1229

Zhang Y., Takanohashi T., Sato S., Saito I., Observation of glass transition in asphaltenes, Energ. Fuel. (2004), 18, 283 - 284

Zhang Y., Takanohashi T., Shishido T., Sato S., Saito I., Estimating the interaction energy of asphaltene aggregates with aromatic solvents, Energ. Fuel. (2005), 19, 1023 – 1028

Chapter V

Modelling of Asphaltene Precipitation

Table of Contents

The petroleum industry needs models to predict asphaltene precipitation. However, a dilemma arises: asphaltenic fluids are complex and need complex models to be described, i.e. they require many parameters and the more parameters, the more fitting procedures are necessary. Furthermore, although models are able to describe asphaltene phase envelopes, prediction remains a chimera out of reach so far. Nonetheless, all these efforts done through the years helped shaping the experimental research about asphaltenes, pointing out which characteristics were necessary (molecular weight, solubility parameters and critical parameters for example).

Though the understanding of asphaltene precipitation is relatively poor, a lot of efforts have been put into modelling since it is much less cost-dissuasive than experiments, especially at high pressure and temperature conditions. The modelling of asphaltenic fluids followed the evolution of thermodynamics, starting with the simple solubility parameters and the regular solutions and ending up with various versions of SAFT nowadays. Most of the papers dealing with asphaltene modelling claim that they successfully described experimental results. Obviously, it is not the case. The determination of input parameters remains the key issue to move from the description phase to the prediction one.

In this chapter, the various models used over the years will be briefly presented. Then, examples of phase equilibria calculations with a cubic equation of state will be shown for asphaltenic systems in order to evaluate the influence of the input parameters. Finally, a model developed by Total will be presented. This model takes into account aggregation and modifies fugacities. A second approach - based on the same assumptions but modifying the a and b parameters of asphaltenes - will also be introduced and some results will be shown.

1. The different families of models

Asphaltenes are said to be either peptized by resins or solvated by the liquid medium. Hence, two families of models exist in the literature (Cimino et al., 1995):

- **The lyophobic models**: asphaltenes are lyophobic colloids (solvent-hating). They are peptized by resins and the dispersion is a two-phase system. This co-called "colloidal model" has strongly influenced the way of thinking of scientists since Nellesteyn, Pfeiffer and Saal claimed that asphaltenes were micelles composed of an insoluble, aromatic core with adsorbed resin molecules, providing steric stabilization and thereby preventing flocculation and precipitation. This description of the asphaltene also implies that asphaltene precipitation is irreversible.
- **The lyophilic models**: asphaltenes are lyophilic colloids (solvent-loving) surrounded and solvated by the liquid medium. It is a true solution, hence reversible. In this model, asphaltene monomers and aggregates are in thermodynamic equilibrium. The role of resins on the stabilization is due to their influence on the solvation power of the liquid medium. Destabilization occurs when the solvation power of the liquid medium is too poor.

These models will be discussed now as well as their various versions.

1.1. The steric-stabilization model

Leontaritis and Mansoori mainly developed this model (Leontaritis and Manssori, 1987). They used the picture promoted by Nellensteyn, i.e. that asphaltenes are insoluble, solid particles peptized by resins adsorbed onto their surfaces.

According to them, the asphaltene fraction is stable when the chemical potential of resins $\Delta\mu_2$ is lower than a critical one $\Delta\mu_2^{CR}$. $\Delta\mu_2$ is expressed as follows:

$$\Delta\mu_2 = RT\left[\ln\varphi_2 - (r-1)(1-\varphi_2) + r\chi(1-\varphi_2)^2\right] \qquad \textbf{Eq V-1}$$

where $\Delta\mu_2$ is the difference between the chemical potentials of the resins in solution and in their reference state, R the gas constant, T the temperature, φ_2 the volume fraction of the resins, χ the interaction parameter between resins and solvents and r the ratio between the molar volumes of the resins and the solvent.
The critical chemical potential $\Delta\mu_2^{CR}$ refers to the value when the number of resins adsorbed on the surface of the asphaltene aggregates is the minimum required for their peptization.

This model has been further developed but it has only been employed for data regression. Furthermore, the concepts behind this model still need to be proved: are resins physically present at the interface between the asphaltene micelles and the crude oil? Isolated asphaltene fractions can be stable in some solvents. Hence, it emphasizes that the presence of resins is not a necessary condition for the stabilization of asphaltene aggregates (Cimino et al., 1995). The reversibility – discussed in Chapter 1 paragraph 1.6.3. - does not support this model neither.

Victorov and Firoozabadi developed a micellization model: it uses the "Nellensteyn assumptions", like the previous model (Victorov and Firoozabadi, 1996). Three major contributions to the process of micelle formation are taken into account:

- **The lyophobic contributions**: they represent the free energy gain upon transferring asphaltene and resin molecules from an indefinitely diluted crude to a micelle.
- **The interfacial contribution**: a definite positive interfacial tension is attributed to the micellar core in the crude
- **The electrostatic contribution**

The Peng-Robinson EOS was used to describe the properties of the bulk-phase. Some of the parameters were estimated and some fitted. The model was able to describe the asphaltene precipitation but with a low degree of accuracy. Furthermore, the issue of reversibility was not discussed. This approach was further investigated by Fahim and co-workers who used a group-contribution method to estimate the critical properties of the

asphaltenes, resins and oil (Fahim et al., 2001). The amount of precipitated asphaltenes was predicted within 0.57% according to the authors, which seems even better than the experimental accuracy of such experiments.

So, as tempting as this model can appear, it seems quite unlikely to be able to describe or predict asphaltene precipitation properly since it has not be proved so far.

1.2. The thermodynamic models

1.2.1. The Flory-Huggins equation

The first model treating asphaltenes as solvated in a liquid medium was the Flory theory for polymer solutions. This method decouples the vapour-liquid equilibrium from the liquid-solid one. The vapour-liquid calculations are first done and then a correction is applied to the liquid phase accounting that the vapour phase remains unchanged. Hirschberg and co-workers treated asphaltenes as monodispersed solvated macromolecules without considering resins especially but only as a part of the solvent (Hirschberg et al., 1984). After several simplifications, the maximum volume fraction of soluble asphaltenes in the crude $\varphi_a^{\max}$ was expressed as follows:

$$\varphi_a^{\max} = \exp\left[\frac{v_a}{v_l}\left(1-\frac{v_l}{v_a}-\frac{v_l}{RT}\left(\delta_a-\delta_l\right)^2\right)\right] \qquad \textbf{Eq V-2}$$

where v is the molar volume, δ the solubility parameter, R the gas constant and T the temperature. The subscripts a and l respectively refer to the asphaltenes and the liquid medium.

The solubility parameter of the liquid was calculated with the SRK EOS after the fluid was characterized. The asphaltene properties were estimated from titration experiments. The work they achieved is quite impressive since the effects of pressure, gas injection and temperature were investigated. This is the reason why this work remains as a reference.

If one takes the logarithm of the maximum solubility and its derivative with respect to temperature, one obtains the following equation:

$$\left(\frac{\partial \ln \varphi_a^{\max}}{\partial T}\right)_P = \frac{v_a}{v_l}\left(\alpha_{P.a} - \alpha_{P,l}\right) + \frac{v_a}{RT}\left(\delta_a - \delta_l\right)^2 \times \left[\frac{1}{T} - \alpha_{P.a} - 2\frac{\partial\left(\delta_a - \delta_l\right)/\partial T}{\delta_a - \delta_l}\right] \quad \textbf{Eq V-3}$$

where α_P is the isobaric thermal expansivity.

Thus, the evolution of the maximum solubility with temperature is ruled by:

- **The difference in thermal expansivities:** thermal expansivity of a liquid is around 10^{-3} K^{-1} whereas the one of a solid is lower (10^{-4}-10^{-5} K^{-1}). It was calculated for asphaltenes by means of a computer assisted structure elucidation software (Diallo et al., 2004) and, at 300 K, it was estimated to be 1.9 10^{-4} K^{-1}. As for the one of the oil, it was measured at 303.15 K for several oils but these results were not published (see Chapter 2, paragraph 2.3). The technique used is similar to the one explained in Verdier and Andersen, 2003. The thermal expansivities were ranging between 6.8 10^{-4} K^{-1} and 7.8 10^{-4} K^{-1} at 303.15 K and 0.1 MPa.
- **The molar volumes:** once more, the molecular weight is a problematic issue. Densities of asphaltenes can be measured if one assumes there is no excess volume (Rogel and Carbognani, 2003; Rogel et al., 2003). The reported values are ranging between 1.17 and 1.52 g/cm^3. With a molecular assumed to be 1000 g/mol, the molar volume of asphaltenes is approximately 7.6 10^{-4} m^3/mol. As for the oil, with a density ranging between 600 and 800 kg/m^3 and a molar weight between 200 and 300 g/mol, the molar volume is approximately 3.6 10^{-4} m^3/mol at room conditions.
- **The difference in solubility parameters:** as it was said in chapter 1, paragraph 1.3.1, the solubility parameter of asphaltenes has been reported between 19 and 26 MPa$^{1/2}$. As for the one of the oil, it is lower and say is ranging between 16 and 18 MPa$^{1/2}$.

- **The parameter** $\partial(\delta_a - \delta_l)/\partial T$ **:** Barton proposed a linear dependence of δ with temperature:

$$\delta(T) = \delta^0 - m(T - T_0) \qquad \textbf{Eq V- 4}$$

The coefficient m is listed for pure compounds (Barton, 1991) and varies between 2.00 and $3.00 \cdot 10^{-2}$ $MPa^{1/2}.K^{-1}$ for hydrocarbons ($2.70 \cdot 10^{-2}$ for n-pentane, $1.83 \cdot 10^{-2}$ for n-nonane and $1.98 \cdot 10^{-2}$ for n-decane for instance). As for asphaltenes, its temperature-dependent coefficient has been fitted to titration experiments by Hirschberg et al. and was found equal to $2.1 \cdot 10^{-2}$ $MPa^{1/2}.K^{-1}$. It was also calculated by means of a computer assisted structure elucidation software (Diallo et al., 2004) and it was much smaller this time ($4 \cdot 10^{-3}$ $MPa^{1/2}.K^{-1}$). The influence of these parameters can be briefly studied. A hypothetical dead oil with the following initial characteristics is studied:

	asphaltene	**oil**
expansivity (K^{-1})	$2.0\ 10^{-4}$	$7.0\ 10^{-4}$
δ ($MPa^{1/2}$)	21.0	17.0
Molar volume (m3/mol)	$8.3\ 10^{-4}$	$3.3\ 10^{-4}$
m ($MPa^{1/2}.K^{-1}$)	$4.0\ 10^{-3}$	$3.0\ 10^{-2}$
Molar mass (g/mol)	1000	200
density (kg/m3)	1200	600

Table V-1: Characteristics of the oil and asphaltenes

The influence of the solubility parameter of the asphaltenes is presented in Figure V-1.

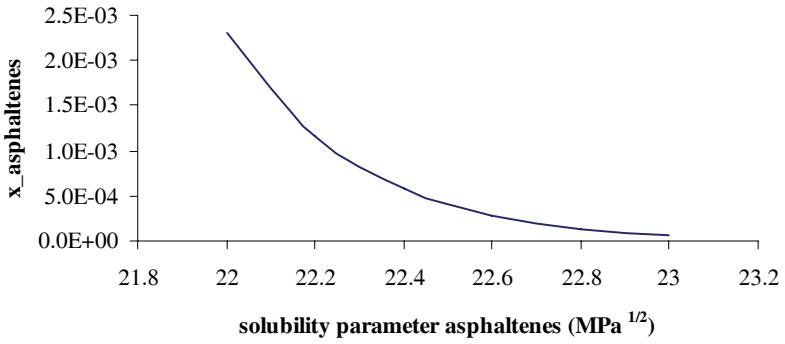

Figure V-1: Influence of the solubility parameter of the asphaltenes on their solubility

The variations of the solubility are huge (4000% of deviation for a difference of 1 $MPa^{1/2}$). As it was said in Chapter 2, solubility parameters cannot be determined directly and, even for pure compounds, results commonly differ from 0.2 $MPa^{1/2}$. No experimental method can give accurate enough results for such a sensitive model.

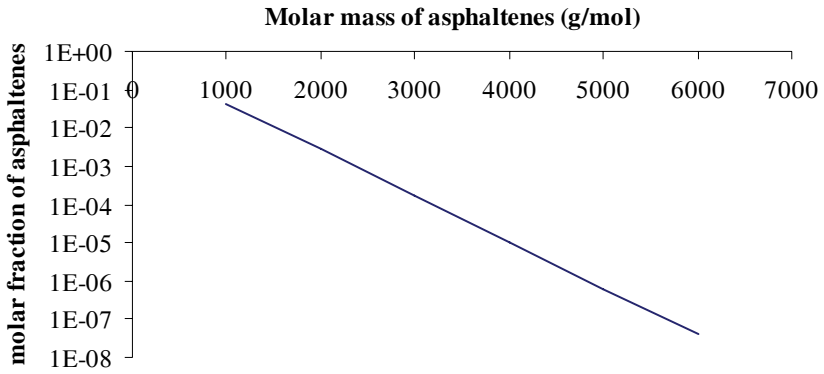

Figure V-2: Influence of molar mass of asphaltenes on their solubility

Figure V-2 presents the impact of molar mass in the model since it affects the molar volume. So, according to the state of aggregation, the solubility varies massively because the logarithmic dependence. Obviously, the molar mass of asphaltenes has to be fitted or assumed, which reduces the possibility of prediction of such a model.

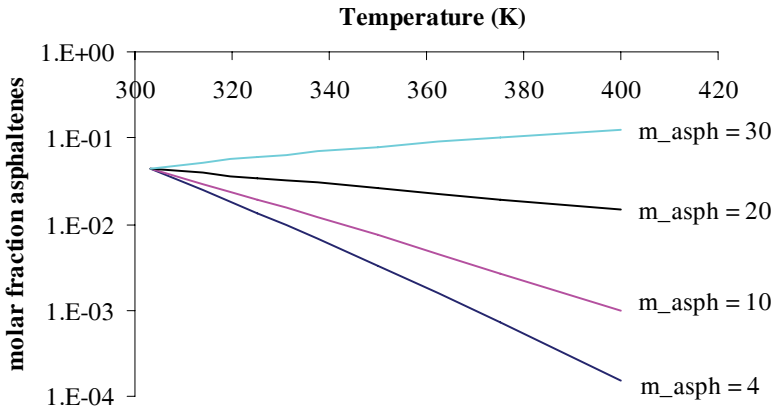

Figure V-3: Influence of temperature on the solubility of asphaltenes (m is in $Pa^{1/2}.K^{-1}$)

The last parameter studied here is the temperature-dependence of the solubility parameter of asphaltenes. The factor *m* can either increase or decrease the solubility with respect to

temperature (Figure V-3). When rough estimations are made, the first term of Eq V-3 is within 10^{-3} whereas the second one is 10^{-1}. Hence, it is assumed to be negligible. In this case, the solutions satisfying $\left(\partial \ln \varphi_a^{\max} / \partial T\right)_P = 0$ are either $\delta_a = \delta_l$ or $\left(m_a - m_l\right) = 1/2\left(1/T - \alpha_{P,a}\right)\left(\delta_a - \delta_l\right)$. Therefore, according to this model, temperature increases the maximum solubility if $\left(m_a - m_l\right) > 1/2\left(1/T - \alpha_{P,a}\right)\left(\delta_a - \delta_l\right) \approx \left(\delta_a - \delta_l\right)/2T$ and decreases otherwise. This means that if one was able to measure properly the solubility parameter of both asphaltenes and oil as a function of temperature, it would be possible to predict the influence of temperature on asphaltene solubility. However, one should keep in mind that this theory has been developed for non-associated compounds and who could say when parameters stops having a physical sense and when their determination becomes a fitting exercise to make a model perform "properly"? That is the reason why such relationships should be used with caution.

As it was said in Chapter 1, paragraph 1.6.2, precipitation is due to dispersion forces and is due to the difference of the dispersive part of the solubility parameters $\delta_l^d - \delta_a^d$. Thus, Eq V-2 and Eq V-3 could be written in terms of dispersive solubility parameters and not with the "total" one. In addition, Hansen reports the following dependence with temperature for δ^d (Hansen, 2000):

$$\left.\frac{\partial \delta^d}{\partial T}\right|_P = -1.25\,\alpha_P\,\delta^d \qquad \textbf{Eq V-5}$$

Assuming that thermal expansivity is constant with temperature – which is not correct -, one gets:

$$\delta^d = \delta_0^d\; e^{-1.25\,\alpha_P T} \qquad \textbf{Eq V-6}$$

Eq V-3 becomes:

$$\left(\frac{\partial \ln \varphi_a^{\max}}{\partial T}\right)_P = \frac{v_a}{RT}\left(\delta_a^d - \delta_l^d\right)^2 \times \left[\frac{1}{T} - \alpha_{P,a} - 2.5\frac{\left(\alpha_{P,l}\delta_l - \alpha_{P,a}\delta_a\right)}{\delta_a - \delta_l}\right] \qquad \textbf{Eq V-7}$$

Here again, this equation should be used with care and perspective.

The effect of pressure can be studied in the same way. Indeed, δ can be written:

$$\delta(T,P)^2 = \frac{-U^r(T,P)}{v(T,P)} \approx \frac{-U^r(T)}{v(T,P)} = \frac{-U^r(T)}{M}\rho(T,P) = A(T)\rho \qquad \textbf{Eq V-8}$$

Furthermore, assuming a constant isothermal compressibility κ_T, density is such as:

$$\rho(T,P) = \rho(T,P_0)e^{\kappa_T(P-P_0)} \qquad \textbf{Eq V-9}$$

Hence, the solubility parameter is:

$$\delta = \left[A(T)\rho(T,P_0)\right]^{\frac{1}{2}} e^{\frac{\kappa_T(P-P_0)}{2}} = \delta(T,P_0)e^{\frac{\kappa_T(P-P_0)}{2}} \qquad \textbf{Eq V-10}$$

Compressibility of oils was measured by high-pressure density measurements for several oils according to a method detailed elsewhere (Verdier and Andersen, 2005). The compressibilities of oils were ranging between 5 and 9 10^{-4} MPa^{-1}. As for asphaltenes, molar volumes were once reported as function of pressure (Diallo et al., 2004) and, from this data between 200 and 800 bar, compressibility is estimated to be $1.7\,10^{-4}$ MPa^{-1} at 300 K. Figure V-4 shows the influence of pressure on the solubility of asphaltenes as function of the compressibility of asphaltenes.

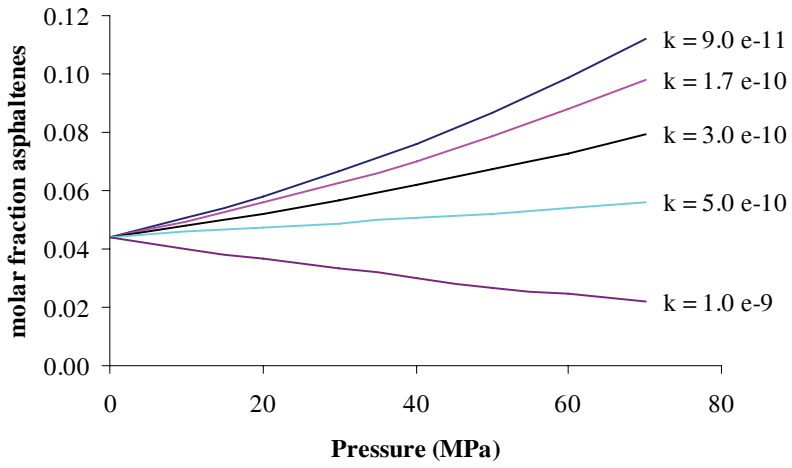

Figure V-4: Influence of pressure on the solubility of asphaltenes (the compressibility of asphaltenes is in Pa^{-1})

The influence of pressure in much less than temperature on the solubility and the equation is hence much less dependent on the input factors relevant to pressure, i.e. the compressibilities. Pressure increases the solubility as it is known experimentally. If the compressibility of asphaltenes is larger than the one of the solvent, pressure happens to decreases solubility. This has of course not much physical sense.

Many more calculations could be made with such a model, especially with the effect of gas on the solubility parameter of the solvent. However, as Andersen and Speight spotted it, it is necessary to recognize the lack of resemblance between this model and the true nature of asphaltenes (Andersen and Speight, 1999). Many other groups worked with the Flory-Huggins theory: for instance, Yarranton's group from the University of Calgary combined it with a mass distribution of the asphaltenes and developed correlations of the different parameters (see Alboudwarej et al., 2005 for instance). The system is characterized and the equilibrium is solved with the Rachford-Rice equation. The amount of precipitated asphaltenes can be fitted with good accuracy.

1.2.2. The Scatchard-Hildebrand equation

This approach assumes that the regular solution theory applies to the crude oil (Griffith and Siegmund, 1985). Assuming that the activity of asphaltenes is unity,

$$\ln x_a = -\frac{RT}{v_a}\varphi_l^2\left(\delta_l - \delta_a\right)^2 \qquad \textbf{Eq V-11}$$

where x_a is the fraction of soluble asphaltenes and φ_l the volume fraction of the liquid medium.

The same derivations with temperature as in the previous paragraph can be done and the same conclusions drawn. In addition, this model does not take aggregation into account since it states that there is no specific interaction.

1.2.3. The Scott-Magat equation

One other important feature of asphaltenes is their molar distribution (chapter 1, paragraph 1.3). Kawanaka and co-workers applied this distribution by means of the Scott-Magat equation (Kawanaka et al., 1991). The Flory interaction parameter was modified

with the introduction of an interaction parameter l_{12} and with a statistical entropic term l/z. The experimental fit turned out to be good thanks to the additional parameters but the predictions remained poor. Phase diagrams of mixtures CO_2-oils were also investigated. In total, six parameters were tuned to experimental data in order to fit the results.

1.2.4. Cubic equations of state

Cubic equations of state were not so much investigated. Gupta coupled a solid phase fugacity with a Peng-Robinson model (Gupta, 1986). The critical parameters are obtained from the Alexander's correlations combining NMR data and the SRK EOS. However, as seen in Chapter 3, paragraph 3.2.2, the heteroatom content and the choice of the molar weight are crucial and can give irrelevant results. The interaction parameters k_{ij} were the key parameters to fit in order to get the proper trends in solubility. However, they had to be fitted for every n-alkane used during the titrations thought they should be constant (Andersen and Speight, 1999).

Szewczyk and Béhar desribed the flocculation as the formation of a new liquid phase with a high asphaltenic content (Szewczyk and Béhar, 1999) (note that they used the word "flocculation" and not "precipitation" to describe the phase transition and the term "deposit" instead of "precipitated asphaltenes"). The crude oil is represented by a light fraction (F_{11}-F_{20}) and the F_{20+} heavy fraction is divided into four pseudo-components. The critical properties are estimated by a group contribution method and the PR EOS is used in combination with specific mixing rules. The critical pressures of the fraction are fitted to the density at atmospheric conditions and the properties of the asphaltenes are fitted to the amount of precipitated asphaltenes at 303.15 K. This fitting procedure enables a proper description of the saturation pressures, the relative volumes and the flocculation curves.

The Computer Modelling Group (Calgary, Canada) modelled the precipitated asphaltene as a dense phase, either liquid or solid (Nghiem et al., 1993). The asphaltene fraction is

divided into two: a precipitating and a non-precipitating component. The PR EOS was used as well with interaction parameters. However, they do not explain how the critical parameters were obtained and what their values are. Hence, they might have slightly more than two or three fitting parameters, as they claim. The interaction parameters were used to fit the precipitation curve.

To conclude, the cubic EOS are very popular in the calculation of phase equilibria and especially in the oil industry. However, the determination of the critical parameters and the characterization of the oil – especially the heavy fraction – prevent this approach from being anything else but a good fitting exercise of parameters. The absence of specific interactions also makes this approach not that physical.

1.2.5. The association EOS

Associating EOS like SAFT are the most advanced EOS, the last branch of the tree. It seemed quite natural to apply these equations to asphaltene precipitation. Many groups and famous scientists in the world of chemical engineering tried to apply them: Chapman (Ting et al., 2003), Prausnitz (Wu et al., 1998; Wu et al., 2000), Firoozabadi (Wu et al., 1998; Wu et al., 2000), Gil-Villegas (Buenrostro-Gonzalez et al., 2004) or Michelsen (Christensen et al., 2005) to name a few.

The same problems as for the cubic EOS rise: characterization of the oil (the heavy fraction particularly) and determination of the parameters. Andersen and Speight summarized it all: "*The more realistic the model becomes, the more complex it will be. The complexity as well gives rise to an increase in unknown parameters which in turn will have to be estimated or fitted to experimental data*". (Andersen and Speight, 1999).

Though their respective work is impressive as well as the fitting curves obtained, especially for gas injection and phase envelopes, the use of SAFT raises fundamental questions. The two main issues are **the absence of the dilution effect and the co-solubilizing effect of resins** (Zhou, 2005).

A few ppm of a given asphaltene seems to have the same stability as 1% of the same asphaltene in a given solvent mixture. There is one way to represent this: use very high molecular weights or consider finite size aggregation even in good solvent (it is important that the size is finite since, if it is not, no asphaltenes will ever be dissolved in any solvent). Figure V-5 shows the influence of dilution on the onset from an experimental point of view and modelled with SAFT (Zhou, 2005). As expected, the SAFT EOS, even with fitted parameters, cannot describe the data properly since fugacity of asphaltenes depends on its molar fraction.

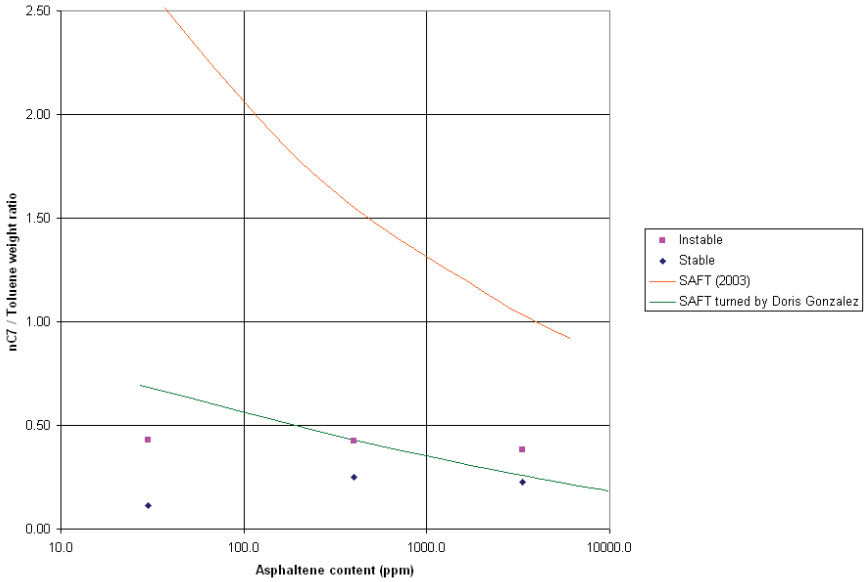

Figure V-5: Dilution of asphaltenes and its modelling (from Zhou, 2005)

Then, addition of a few ppm of resins will increase hugely the stability of a few ppm of asphaltenes (Porte et al., 2003). Such a small quantity does not affect the solvent power of the liquid medium. This effect can only be attributed to the **co-solubilizing effect of resins.** This behaviour supports the idea that resins or asphaltenes with lower solubility parameters can interact with asphaltenes with higher solubility parameters and act as co-solubilizing agents. In other words, resin and asphaltene molecules are part of the same aggregates in solution and a model with a single huge asphaltene molecule can then be rejected. In association models, a strong interaction is required to take into account this effect. If this energy is too strong, the association will be infinite and no asphaltene

molecules will be soluble. On the contrary, if the energy is too low, there will be no association. So, what about choosing an intermediate interaction energy? **No energy-based model can give a centred distribution of the molecules, as it is the case for asphaltenes.** There would be many monomers, a few dimers, a few trimers but less and so on. Thus, this energy-based model is not sufficient (and SAFT is energy-driven) (Zhou, 2005).

CPA (Cubic Plus Association, Kontogeorgis et al., 1996) was also used to model asphaltene precipitation (Knudsen, 2001; Fahim and Andersen, 2005). Fahim and Andersen found that the error in constructing asphaltene precipitation envelope by SRK EOS (untuned) has been dropped from 19% to 10% by using the CPA EOS. However, the final match depends on the initial tuning of SRK. In most cases, the improvement is within 5%. As Fahim and Andersen said it, "*is it technically reasonable?*", i.e. are all these efforts made to use CPA worth the results for asphaltenic systems?

1.3. Scaling equations

Scaling equations were proposed in 1996, similarly to the ones used in aggregation and gelation phenomena (Rassamdana et al., 1996). Such a method successfully described the amount of precipitated asphaltenes as function of the solvent-to-crude oil ratio and the molar weight of the solvent. A correlation was also proposed for the onset of precipitation. The same authors wrote several papers, including studies about gas injection, molecular weight or the structure of the aggregates. Their work about scaling equations was also further investigated.

1.4. Conclusion

Though thermodynamic models are the solution to model asphaltene precipitation, they face a dilemma: when they are too complex, the parameters to fit are too numerous and prevent the modelling from being relevant and when they are too simple, though they can render some of the properties, they cannot describe all the necessary features. Unless, the input parameters can be measured or calculated very accurately, all models are bound to remain fitting exercises.

2. Asphaltene precipitation and cubic EOS

The approach using cubic EOS seemed fruitful and promising in the few cases it was used (see paragraph 1.2.4). Obviously, the characterization step is of major importance, especially the choice of the critical parameters of asphaltenes. Are these parameters bound to remain fitting parameters or can they be predicted? If yes, what is the required accuracy? Does a cubic EOS have enough degrees of freedom to describe all the thermodynamic properties of asphaltenes? This paragraph is a brief attempt to answer some of these questions.

2.1. The model

In this work, the Peng-Robinson EOS is used. The interactions parameters are set to zero unless stated otherwise, the same model is used for all the phases, there is no Peneloux correction for the volume and the Poynting factor is not used neither. Asphaltene precipitation is treated as liquid-liquid transition. A multiphase flash developed by Michael Michelsen was used in a Fortran environment. The method to solve the Rachford-Rice equation as well as the stability analysis is fully described in Michelsen's monograph (Michelsen and Møllerup, 2004). The same calculations can be made with the in-house software SPECS if asphaltenes are entered as a new compound with its respective parameters. Note that the asphaltene phase is not a pure phase.

2.2. The dilution effect

As Porte et al. (2003) reported it, one of the few known facts about asphaltenes is that dilution of asphaltene solutions (i.e. asphaltenes in toluene) does not affect the onset. In order to model such behaviour, it would require that fugacity does not depend on molar fraction, which is not the case for a cubic EOS.

The system studied here is composed of n-heptane, toluene and asphaltenes (seen as a pseudo-component). Table V-2 gives the respective critical parameters. The working conditions are 300 K and 0.1 MPa. For the conversion in ppm (mg/L), the density of toluene and n-heptane were calculated with the DIPPR correlations. Density of asphaltenes was assumed to be 1200 kg/m^3 and with a molar mass of 1000 g/mol.

	Tc (K)	Pc (atm)	omega
asphatene	1300	7	3
toluene	591.8	40.523	0.2621
nC7	540.2	27.042	0.3495

Table V-2: Critical parameters of the system

Figure V-5 shows that the onset does depend on the asphaltene concentration with PR. The ratio $m_{n-C7}/m_{toluene}$ for the onset conditions is indeed affected by the dilution.

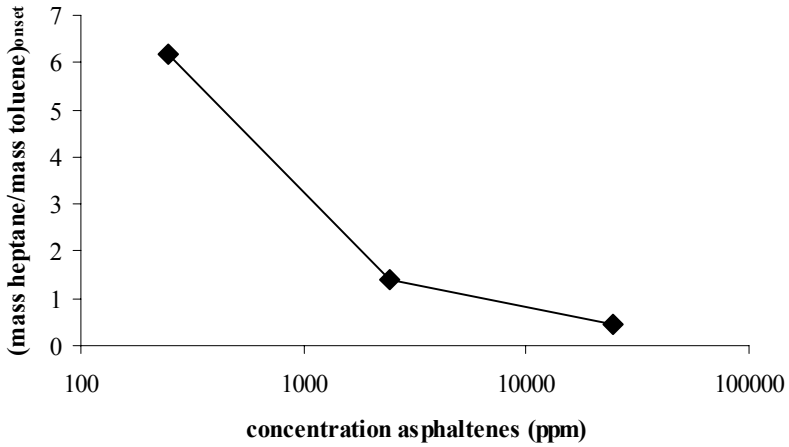

Figure V-6: Influence of dilution on the onset conditions (here, the mass ratio n-heptane/toluene)

More complex systems could be tested (crude oil, other solvents and precipitants) but the purpose was only to show the inability of EOS to model this characteristic behaviour of asphaltenes.

2.3. Phase envelopes

The effects of pressure and temperature on asphaltene stability are of great importance and they are easily seen on a phase envelope. The same system as above was used but with the following molar fractions: $x_{asphaltenes} = 0.0034$, $x_{toluene} = 0.7035$ and $x_{n\text{-}C7} = 0.2930$. The phase envelope was determined varying temperature and pressure and following the appearance of the asphaltene-rich phase (Figure V-7).

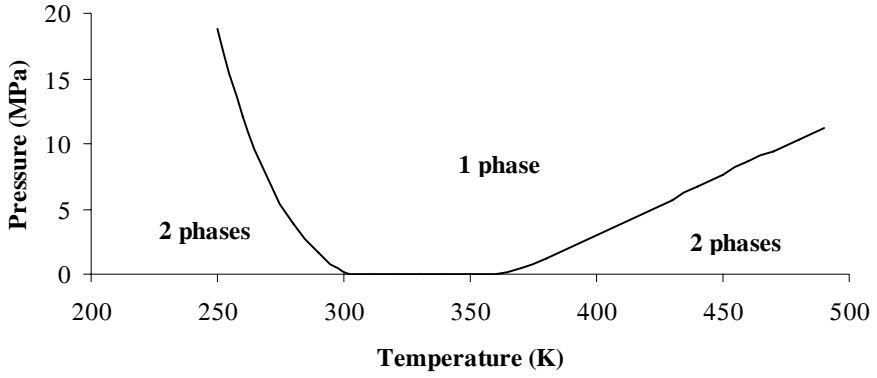

Figure V-7: P-T diagram for a system toluene/n-heptane/asphaltene with PR

Pressure has only one effect, i.e. increasing asphaltene stability whereas temperature first increase and then decrease their stability. Between 300 and 360 K, asphaltenes are always soluble. This results concord with some experimental facts, i.e. that temperature can increase and/or decrease stability and that pressure increases stability (see chapter 3, paragraph 1).

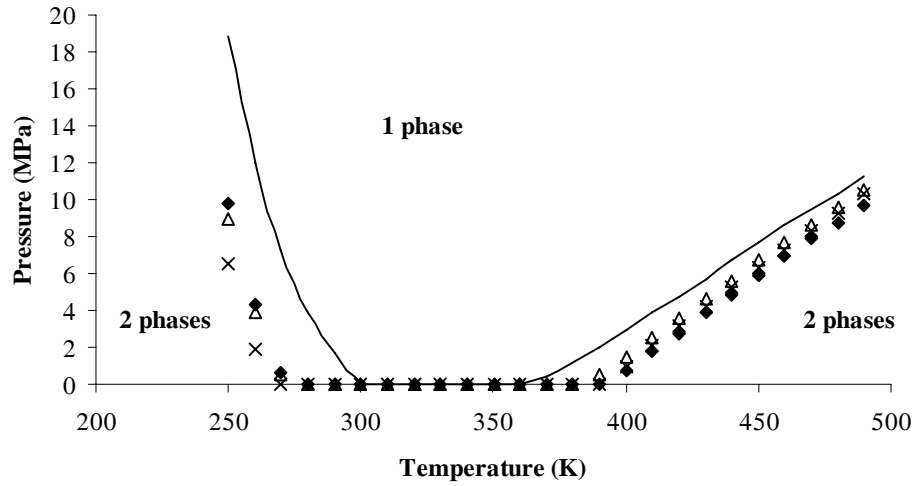

Figure V-8: Influence of the critical parameters on the phase envelope (Δ, 1%- modified Pc; ×, 1% - modified omega; ◆, 1% - modified Tc)

However, one can wonder how sensitive the model is to the parameters related to asphaltenes. The original critical parameters presented in Table V-2 are now decreased by a 1% factor. As seen in Figure V-8, a simple modification of 1% can induce variations

up to 30 K or 12 MPa for the onset conditions. Such changes are very large from a production point of view. However, at higher temperatures (above 400 K), the differences are not as important. It is interesting to notice that the three critical parameters are equally sensitive to modifications.

2.4. Volumetric calculations

It is worth investigating whether or not a cubic EOS predicts a gain in volume once asphaltenes precipitate. Similarly to what was done with PC-SAFT for a crude oil recombined with gas (Christensen et al., 2005), the output of the multiphase flash enable the calculation of volumetric changes:

$$v_{1\,phase} = \frac{RTZ_1}{P} \qquad \textbf{Eq V-12}$$

$$v_{2\,phases} = \frac{RT}{P}\left(x_{oil}Z_{oil} + x_{asphaltene}Z_{asphaltene}\right) \qquad \textbf{Eq V-13}$$

The difference $v_{2\,phases} - v_{1\,phases}$ gives the volumetric variations due to asphaltene precipitation. The system described in Figure V-7 was used. The calculations were made at constant T as if the system was going through a pressure depletion. $v_{1\,phase}$ was chosen to be the volume at $\left(T, P = P_{onset} + 1\,bar\right)$.

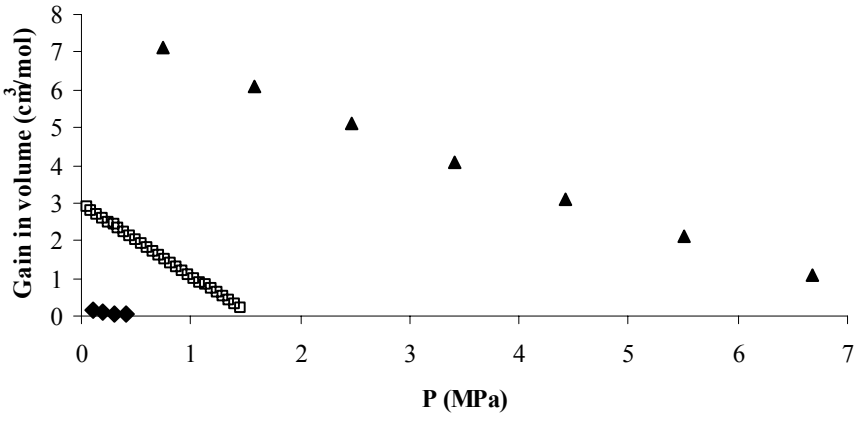

Figure V-9: Volume difference per mole between the two-phase and the one-phase zones (◆, 370 K; □, 400 K; ▲, 450 K)

The gain is very small since the asphaltene fraction is 3.10^{-3} and reaches at the most 7 cm^3/mol. The further the system is from the onset, the more asphaltenes precipitate, as expected. The gain due to the asphaltene fraction reaches 3.4 cm3/mol at the most (at 370 K and 1 MPa). Hence, for 1 mole of a system (99% oil+1% asphaltenes) with average densities and molecular weights, the volume change due to the asphaltene phase itself is less than 0.05 cm^3, which is very little to be detected.

2.5. Gas injection

Though the model is very parameter-dependent, the effect of gas injection is interesting. In this part, a system asphaltene/toluene/n-heptane/CO_2 was used. The molar fractions are respectively 3.43 10^{-2}, 0.698, 0.199 and 0.100. The same critical parameters are the ones presented in Table V-2.

First, the interactions parameters were set to zero. The onset curve and the bubble point curve are presented in Figure V-10. The three-phase zone (gas + asphaltene + oil) is below 3 MPa at the best (at 490 K) and the two-zone phase can reach 90 MPa at 250 K. For the onset curve, it reaches a plateau from 350 K around 30 MPa. Temperature has little effect on the asphaltene stability though the slope is slightly increasing (i.e. an increase of temperature may destabilize the solution).

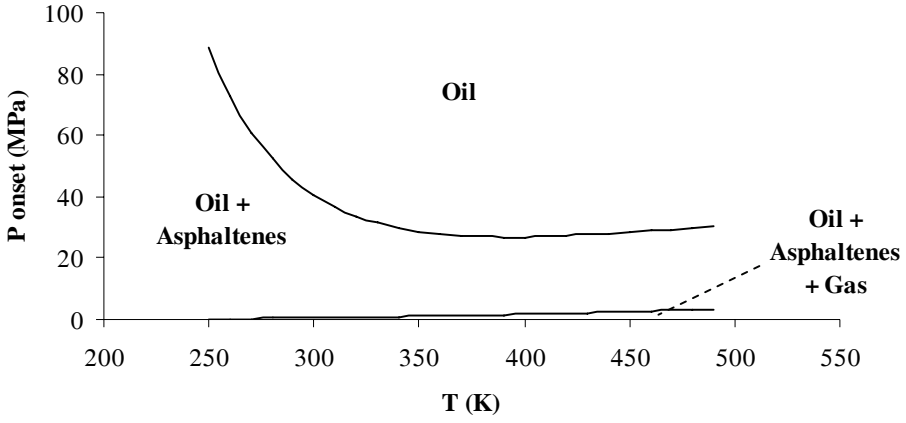

Figure V-10: Phase Envelope of a mixture (toluene+asphaltene+n-heptane) with 10% CO_2

In Figure V-11, the impact of interaction parameters between CO_2 and the compounds is visible. This parameter was set to 0.12 as advised in the literature (Li et al., 2001). The difference in onset pressures at the same temperature is ranging between 2.4 and 23.8 MPa. This is quite a lot from an experimental point of view.

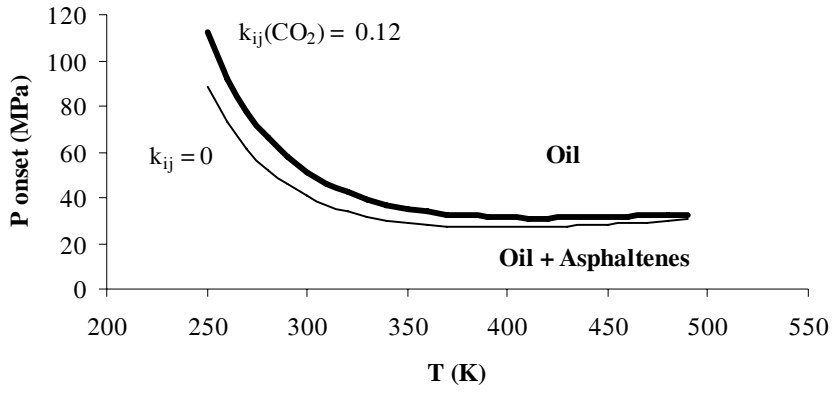

Figure V-11: Influence of the interaction parameters on the onset curve

During EOS recovery, other gases such as nitrogen or methane can be used and, though this model is quite flexible, the trends are of interest. The composition of the system is the same one as previously: 3.43 10^{-2} for asphaltenes, 0.698 for toluene, 0.199 for n-heptane and 0.100 for the gas component. Figure V-12 clearly shows that, at low temperatures, the onset pressures are very different according to the gas used. For the three gases, the influence of temperature becomes weaker when it reaches 350 K.

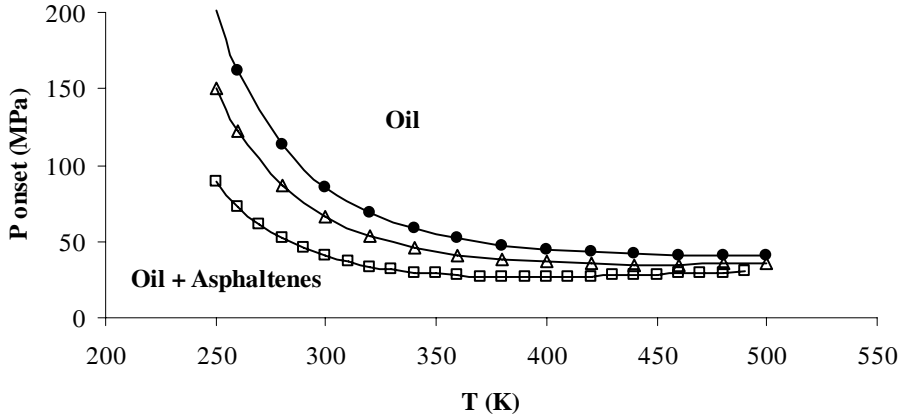

Figure V-12: Asphaltene Precipitation curves for various gases (●, N_2; Δ, CH_4; □, CO_2)

Both the three gases, pressure does increase the solubility of asphaltenes at constant temperature. The influence of temperature at constant pressure varies according to the temperature. If $\left(\Delta P/\Delta T\right)_{onset}$ is plotted as function of temperature, one can easily see whether or not temperature as stabilizing or destabilizing effect on the stability.

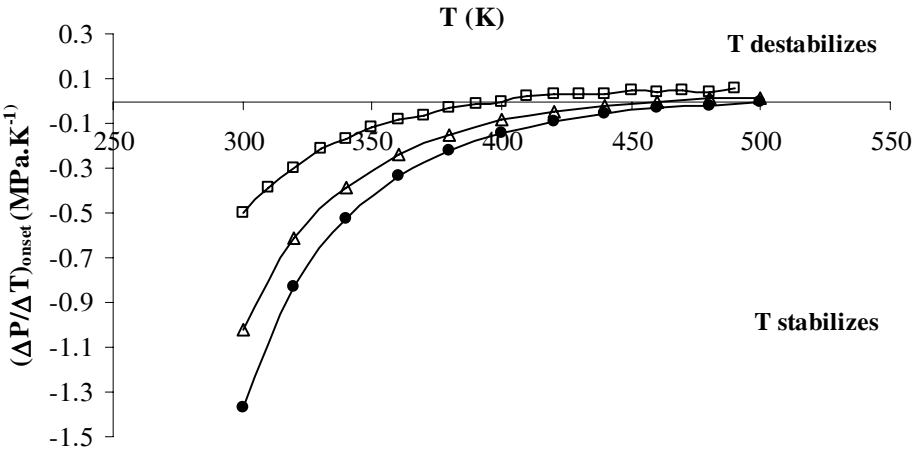

Figure V-13: Influence of temperature on asphaltene stability (●, N_2; Δ, CH_4; □, CO_2)

Indeed, if $\left(\Delta P/\Delta T\right)_{onset}$ is positive, it means that an increase in temperature is likely to make the system cross the precipitation curve in the sense $Oil \rightarrow Oil + Asphaltenes$ at constant pressure, i.e. temperature will destabilize the system. As seen in Figure V-13, from 400 K, with CO_2, temperature will destabilize the system though the effect is small. As for methane, the slope is slightly positive from 480 K but the effect is almost non-existent. When the system contains nitrogen, temperature only seems to stabilize the system. Of course, these results should be analyzed with care since no interaction coefficients were used and the trends highly depend on the critical parameters of asphaltenes. For instance, Figure V-14 was plotted for the CO_2-system but with a critical pressure of asphaltenes equal to 6.5 atm instead of the original 7 atm. It is indeed a large variation but, considering how critical parameters of asphaltenes are obtained in the literature, it is not unseen to consider such a case. The phase behaviour has now little to do with Figure V-10.

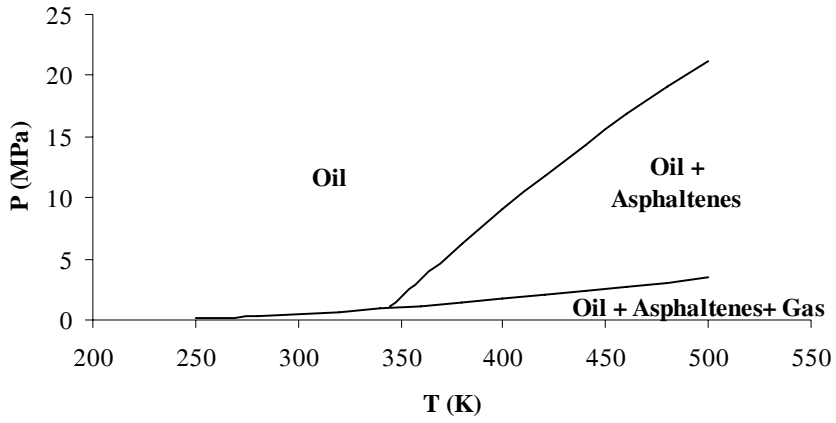

Figure V-14: Influence of P_c(asphaltene) on the phase envelope in presence of CO_2

So, what are the conclusions of such modelling?

- The cubic EOS can not render the absence of dilution effect.
- Obviously, any phase envelope can be described considering the dependence to the critical parameters of asphaltenes.
- The model can detect asphaltene precipitation due to gas injection
- The interaction coefficients can be used as additional fitting parameters
- Pressure increases asphaltene stability whereas temperature can both destabilize and stabilize asphaltenic fluids.

Much more could be done with this model but the objective was not to evaluate the model but rather to show how sensitive and flexible it is when dealing with asphaltenes.

3. A new approach combining aggregation and cubic EOS

The idea is to establish a model able to describe and predict asphaltene precipitation, taking into account the association of asphaltene molecules into nano-aggregates (Zhou et al., 2005). The precipitation occurs when the asphaltene phase is in equilibrium with the bulk phase (the crude oil).

In spite of an often complex scheme and a large number of fitting parameters, most of models invoking association do not allow representation of the simple fact that the asphaltene nano-aggregates in terms of size are insensitive to dilution in good solvents or a change in solvent quality when the solution is far from the precipitation threshold. The description of the mechanism of nano-aggregation by these models depends on the balance between the energy of association in opposition to the dispersive term. Thus, in some cases, the aggregates tend to grow indefinitely or, in other cases, to disappear completely. The geometry of the nano-aggregates is very difficult to take into account by these models.

Regarding this difficulty, a description proposed lately seems to be an attractive alternative (Porte et al., 2003). This description is based on a simple idea: on one side, the forces involved in the colloidal aggregation and on the other side, those driving the precipitation are different in nature and strength. The aggregation is driven by strong specific forces and the size of the aggregates is limited for geometric reason; therefore the aggregates are insensitive to the quality of the apolar solvent. The precipitation is determined by the weaker and non-specific dispersion forces. Using this picture, any equation of state can be modified for the description of asphaltene dissolution – precipitation.

3.1. The TOTAL model

The assumptions are as follows:

- Asphaltene molecules are associated into aggregates having an equal number of asphaltene molecules. This number, noted N, is called the **aggregation number**
- There can be several types of asphaltenes but every molecule has the same number of "binding sites" N_S

- The association energy per bonding is equal for any asphaltene molecule
- The number of free asphaltene molecules is very small regarding the number of associated asphaltene molecules.

Let us consider the following reaction:

$$\sum N_i \cdot molecules \Leftrightarrow aggregate$$

Therefore, one can write the relation between the concentration of associated molecules of asphaltenes and free molecule. The first case-scenario is the mono-dispersed asphaltene. In this case, the chemical reaction is:

$$N\,molecules \Leftrightarrow aggregate$$

The thermodynamic equilibrium of a chemical reaction is described by:

$$\Delta_r G^0 + RT \ln K = 0 \qquad \textbf{Eq V-14}$$

where $\Delta_r G^0 = \mu^{o,aggr} - N\mu^{o,free}$ is the standard reaction Gibbs energy and K the equilibrium constant.

This constant can be written as follows:

$$K = \prod_i a_i^{\nu_i} \qquad \textbf{Eq V-15}$$

where a_i is the activity coefficient and ν_i is the stoichiometric coefficient (positive integer for products, negative integer for reactants).

Thus, taking into account the chemical reaction mentioned above, the thermodynamic equilibrium is such as:

$$\Delta_r G^0 + RT \ln \left[\frac{\gamma_a^{agg} x_a^{agg}}{\left(\gamma_a^{free} x_a^{free} \right)^N} \right] = 0 \qquad \textbf{Eq V-16}$$

$$\Delta_r G^0 + RT \ln \left[\frac{\gamma_a^{agg}}{\left(\gamma_a^{free} \right)^N} \right] + RT \ln \left[\frac{x_a^{agg}}{\left(x_a^{free} \right)^N} \right] = 0 \qquad \textbf{Eq V-17}$$

The superscript *agg* and *free* refers respectively to the aggregated and free asphaltenes.

$\Delta_r G^0$ is function of the number of binding sites N_s as follows:

$$\Delta_r G^0 = N_s \Delta G^0_{agg} / 2 \qquad \textbf{Eq V-18}$$

where ΔG^0_{agg} corresponds to Gibbs energy of a bonding between two asphaltene or resin molecules (between -40 and -10 kJ/mol for hydrogen bonding for instance). The factor 2 is due to the fact that the binding energy is "shared" by two molecules.

The activity coefficient is model-dependent but, since an asphaltene molecule has the same environment in the aggregate or the free form (Zhou et al., 2005), one can write:

$$\frac{(\gamma_a^{free})^N}{(\gamma_a^{agg})} \approx 1 \qquad \textbf{Eq V-19}$$

Hence, the molar fractions of the aggregated and free asphaltenes are such as:

$$\frac{(x_a^{free})^N}{(x_a^{agg})} = \exp\left(\frac{\Delta_r G^0}{RT}\right) = \frac{1}{K} \qquad \textbf{Eq V-20}$$

It is important to count properly the number of asphaltene molecules. Table V-3 presents the number of moles according to the progress of the reaction, noted ξ.

Progress	$N\,molecules \Leftrightarrow aggregate$	**Total of asphaltenes molecules**		**Mole fraction asphaltenes**
$\xi = 0$	n_a	0	n_a	$n_a \Big/ \left[n_a + \sum_{j \neq a} n_j \right]$
ξ	$n_a(1-\xi)$	$n_a \xi / N$	$n_a(1-\xi+\xi/N)$	$\dfrac{n_a(1-\xi+\xi/N)}{n_a(1-\xi+\xi/N)+\sum_{j \neq a} n_j}$
$\xi = 1$	0	n_a / N	n_a / N	$\dfrac{n_a}{N} \Big/ \left[\dfrac{n_a}{N} + \sum_{j \neq a} n_j \right]$

Table V-3: Details about the number of asphaltene molecules

In crude oils, asphaltenes are mainly aggregated, hence $\xi = 1$. So, when a initial mixture is given with a known asphaltene molar fraction x_a, what is its relationship with the aggregated asphaltene fraction x_a^{agg} ? For $\xi = 0$, the definition of the asphaltene fraction induces that the mole number of asphaltenes is $n_a = \left(\frac{x_a}{1 - x_a} \right) \sum_{j \neq a} n_j$.

Once this expression is combined with the mole fraction of asphaltenes for $\xi = 1$, one gets:

$$x_a^{agg} = \frac{x_a}{N + (1 - N) x_a} \qquad \textbf{Eq V-21}$$

Using Eq V-20 and Eq V-21, the free asphaltene fraction is then:

$$x_a^{free} = \left(\frac{x_a}{K \left[N + (1 - N) x_a \right]} \right)^{\frac{1}{N}} \qquad \textbf{Eq V-22}$$

Let us focus on the fugacity calculations now.

$$\ln f_a^{agg}(x_a^{agg}) = \ln P + \ln \phi_a^{agg} + \ln x_a^{agg} \qquad \textbf{Eq V-23}$$

where ϕ_a^{agg} is the apparent fugacity coefficient of the aggregated asphaltenes and x_a^{agg} is their molar fraction

However, the fugacity of aggregated asphaltenes can not be calculated directly from the EOS contrary to the fugacity of monomers (the free asphaltenes). Nonetheless, asphaltene fugacities are equal, hence:

$$\begin{aligned} \ln \phi_a^{agg} &= \ln \phi_a^{EOS} + \ln x_a^{free} - \ln x_a^{agg} \\ &= \ln \phi_a^{EOS} + \left(\frac{1}{N} - 1 \right) \ln x_a^{agg} - \frac{1}{N} \ln K \\ &= \ln \phi_a^{EOS} + \left(\frac{1}{N} - 1 \right) \ln \left(\frac{x_a}{N + (1 - N) x_a} \right) - \frac{1}{N} \ln K \end{aligned} \qquad \textbf{Eq V-24}$$

One can wonder which mole fractions of asphaltenes should be considered for the fugacity calculations: the free or the aggregated one? φ_a^{EOS} represents the fugacity of the

asphaltenes in the free form since the critical parameters are the one of the monomer. This fugacity is calculated when there is no aggregation, i.e. when all the asphaltenes are free. Hence, the mole fraction used should be the total one. In this description, if the number of free asphaltene molecules is considered to be very small compared to the number of associated asphaltene molecules, the constant value of the constant K_m plays no role in the phase separation calculations since the last term of the previous equation is the same for both the oil phase and for the asphaltene rich phase.

As for the fugacity of the other components, it has to be modified because the number of molecules is changing due the aggregation. x_i^{free} represents the number of molecules $i \neq a$ before aggregation starts and x_i^{agg} after aggregation. Aggregation is assumed to be total.

$$x_i^{free} = \frac{n_i}{\sum_{j \neq a} n_j + n_a} \qquad \textbf{Eq V-25}$$

$$x_i^{agg} = \frac{n_i}{\sum_{j \neq a} n_j + \frac{n_a}{N}} \qquad \textbf{Eq V-26}$$

The fraction of free asphaltenes can now be written as:

$$\begin{aligned} x_i^{free} &= \frac{x_i^{agg}}{1 + N x_a^{agg} \left(1 - \frac{1}{N}\right)} \\ &= \left[1 + \left(1/N - 1\right) x_a\right] x_i^{agg} \end{aligned} \qquad \textbf{Eq V-27}$$

The fugacity of compound $i \neq a$ is:

$$\begin{aligned} \ln \phi_i &= \ln \phi_i^{EOS} + \ln x_i^{free} - \ln x_i^{agg} \\ &= \ln \phi_i^{EOS} + \ln\left(\left[1 + \left(1/N - 1\right) x_a\right] x_i^{agg}\right) - \ln x_i^{agg} \\ &= \ln \phi_i^{EOS} + \ln\left(1 + \left(1/N - 1\right) x_a\right) \end{aligned} \qquad \textbf{Eq V-28}$$

As last, the fugacity of the asphaltenes can be expressed:

$$f_a = P \cdot \phi_a \cdot x_a$$
$$= P \cdot \phi_a^{EOS} \cdot \left(\frac{x_a}{K\left[N + (1-N) x_a \right]} \right)^{\frac{1}{N}} \quad \textbf{Eq V-29}$$

If the value of the aggregation number *N* is large, the value of $x_a^{\frac{1}{N}}$ will be close to 1 and the value of the fugacity of asphaltene faction will not be sensitive to the dilution. Hence, the absence of dilution effect shown in Figure V-5 can be modelled by any EOS once the fugacity is modified that way.

3.2. Consistency tests

Any modification of the fugacity is likely to be dangerous since some basic relationships of thermodynamics should be valid no matter which model is used. Michelsen and Møllerup list the equations that should be valid (Michelsen and Møllerup, 2004). The first consistency test that was checked is:

$$\frac{\partial \ln \varphi_i}{\partial n_j} = \frac{\partial \ln \varphi_j}{\partial n_i} \quad \textbf{Eq V-30}$$

For our model, this relationship becomes:

$$\frac{\partial \ln \varphi_a}{\partial n_i} = \frac{\partial \ln \varphi_i}{\partial n_a} \quad \textbf{Eq V-31}$$

$$\frac{\partial \ln \varphi_a}{\partial x_i} \frac{\partial x_i}{\partial n_i} = \frac{\partial \ln \varphi_i}{\partial x_a} \frac{\partial x_a}{\partial n_a} \quad \textbf{Eq V-32}$$

Furthermore,

$$\frac{\partial x_j}{\partial n_j} = \frac{1 - x_j}{n_{total}} \quad \textbf{Eq V-33}$$

Hence:

$$\left(\frac{\partial \ln \varphi_a^{EOS}}{\partial x_i} - \frac{1/N - 1}{1 - x_i}\right)\frac{1 - x_i}{n_{total}} = \left(\frac{\partial \ln \varphi_i^{EOS}}{\partial x_a} - \frac{1/N - 1}{1 + x_a\left[1/N - 1\right]}\right)\frac{1 - x_a}{n_{total}} \quad \textbf{Eq V-34}$$

Since $\frac{\partial \ln \varphi_i^{EOS}}{\partial n_j} = \frac{\partial \ln \varphi_j^{EOS}}{\partial n_i}$, the previous equation is :

$$\left(\frac{1/N - 1}{1 - x_i}\right)\frac{1 - x_i}{n_{total}} = \left(\frac{1/N - 1}{1 + x_a\left[1/N - 1\right]}\right)\frac{1 - x_a}{n_{total}} \quad \textbf{Eq V-35}$$

$$1 = \left(\frac{1 - x_a}{1 + x_a\left[1/N - 1\right]}\right) \quad \textbf{Eq V-36}$$

$$\frac{1}{N} = 0 \quad \textbf{Eq V-37}$$

$$N = \infty \quad \textbf{Eq V-38}$$

The second consistency test is the Gibbs-Duhem equation:

$$\sum_i n_i \frac{\partial \ln \varphi_i}{\partial n_j} = 0 \quad \textbf{Eq V-39}$$

For our model, it can be written as :

$$n_a \frac{\partial \ln \varphi_a}{\partial n_a} + \sum_{i \neq a} n_i \frac{\partial \ln \varphi_i}{\partial n_a} = 0 \quad \textbf{Eq V-40}$$

$$n_a\left(\frac{\partial \ln \varphi_a^{EOS}}{\partial x_a} + \frac{1/N - 1}{x_a}\right)\frac{\partial x_a}{\partial n_a} + \sum_i n_i\left(\frac{\partial \ln \varphi_i^{EOS}}{\partial x_a} - \frac{1/N - 1}{1 + x_a\left(1/N - 1\right)}\right)\frac{\partial x_a}{\partial n_a} = 0 \quad \textbf{Eq V-41}$$

$$n_a\left(\frac{1/N - 1}{x_a}\right) + \left(-\frac{1/N - 1}{1 + x_a\left(1/N - 1\right)}\right)\left(n_t - n_a\right) = 0 \quad \textbf{Eq V-42}$$

$$n_t\left(1/N - 1\right) - \left(\frac{1/N - 1}{1 + x_a\left(1/N - 1\right)}\right)\left(n_t - n_a\right) = 0 \quad \textbf{Eq V-43}$$

$$n_t\left(1/N-1\right)-\left(\frac{1/N-1}{1+x_a\left(1/N-1\right)}\right)\left(n_t-n_a\right)=0 \qquad \textbf{Eq V-44}$$

$$\left(1/N-1\right)\left[n_t-\frac{n_t-n_a}{1+x_a\left(1/N-1\right)}\right]=0 \qquad \textbf{Eq V-45}$$

The two solutions are $N=1$ and $N=\infty$.

After checking only two of the consistency tests advised, unrealistic conditions were found. Hence, though this model is tempting and would solve some if the issues, it does not seem very wise to use it. However, the approach taking into account aggregation can be used with no modifications of the fugacity.

3.3. A second approach: the aggregation model

If one makes the same assumptions as for the previous approach, the mole fractions are modified due to the change of mole numbers. What if the system was considered to be composed of asphaltene aggregates and i compounds with the following molar fractions: $x_a^{agg}=\frac{x_a}{N+\left(1-N\right)x_a}$ and $x_i^{agg}=\frac{Nx_i^{free}}{N+\left(1-N\right)x_a}$? What about the thermodynamic model?

The properties of the asphaltenes are the ones of the monomer. Hence, modifications should be done at one point. As Heidemann and Prausnitz advised it, the a and b factors can be modified in order to take into account association (Heidemann and Prausnitz, 1976). They proposed the following mixing rules:

$$b_j=jb \qquad \textbf{Eq V-46}$$

$$a_j=j^2a \qquad \textbf{Eq V-47}$$

where the subscript j refers to the aggregate containing j molecules of the monomer.

Once the mole fractions are calculated as well the properties of the pure compounds, a regular multiphase flash can be used with no further modifications of the fugacities. Thus, the thermodynamic model would be consistent and aggregation would be taken

into account. However, "*(though it is) possible, it will probably give strange results*" (Michelsen, 2006).

3.3.1. The dilution effect

The mole fractions are affected by the asphaltene fraction and the aggregate number and it is interesting to investigate briefly their dependence. First, the fraction of aggregated asphaltenes is almost independent of the fraction of free asphaltenes when N is large enough (Figure V-15). As for the fractions of the other compounds, the key factor is the asphaltene concentration rather than the aggregate number. Indeed, for $x_a^{free} = 10^{-2}$ and x_i^{free} varying between 0.1 and 0.9, the deviation $\left(x_i^{agg} - x_i^{free}\right)/x_i^{free}$ reaches 1% for $N = 200$. However, for $x_i^{free} = 0.1$ and x_a varying between 10^{-7} and 0.1, deviations reach 11%. The deviation becomes significant (higher than 1%) when x_a^{free} is larger than $2 \cdot 10^{-2}$, regardless of the aggregate number.

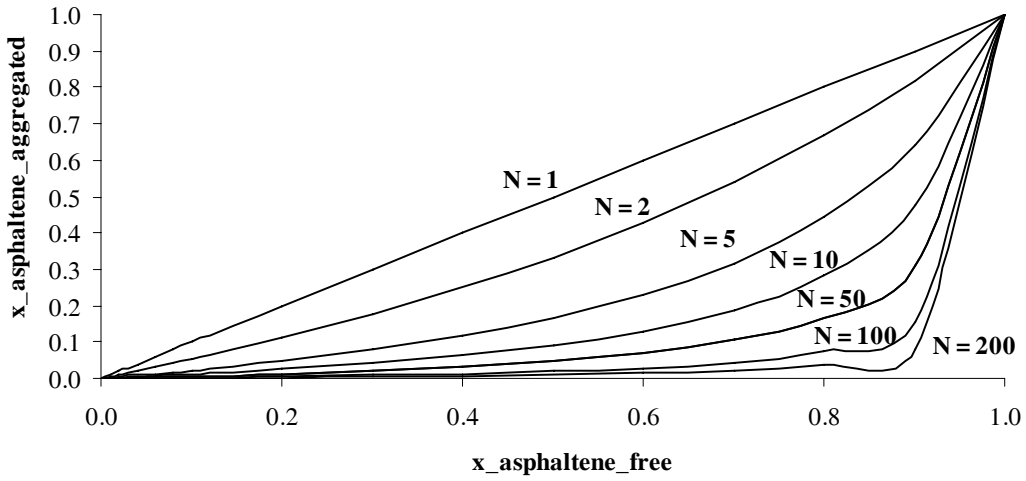

Figure V-15: Influence of the aggregate number N of the fraction of aggregated asphaltenes

The dilution effect can be rendered by this simple model as seen on Figure V-16. The system presented in paragraph 2.2 was tested with this model at the same conditions. Indeed the slope is much lower though the ratio $\left(m_{n-C7}/m_{toluene}\right)_{onset}$ varies from 0.02 until 0.48.

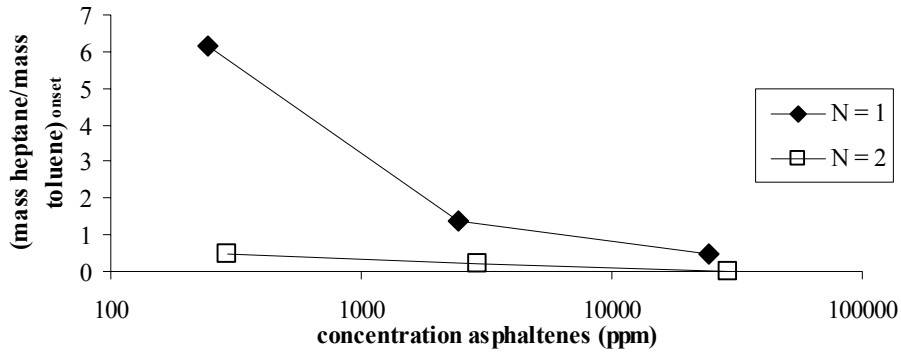

Figure V-16: Influence of dilution on the onset as function of the aggregate number

However, with a larger value of N, such variations would not be seen. Unfortunately, with the original critical parameters shown in Table V-2, asphaltenes are not soluble in pure toluene with N larger than 3. Hence, for the same system but with a slight modification $\left(T_c\left(asphaltenes\right)=1100\,K\right)$, the influence of N is more significant. Figure V-17 does indicate how sensitive the onset is with respect to the aggregate number. One may think that for higher values of N, the dependence to dilution is inexistent but, for this example, asphaltenes are not soluble in pure toluene for too large aggregates. In order to use larger values of N, one should study "smaller molecules", i.e molecules with smaller T_c and ω and larger P_c. Note that the influence of N becomes less important from $N=4$ here, hence large values of N are not necessarily required.

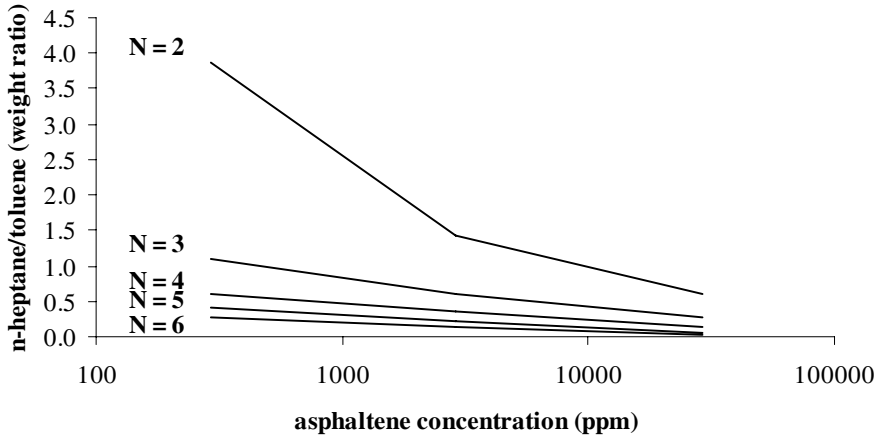

Figure V-17: Influence of the aggregate number on the onset of precipitation

3.3.2. Phase envelopes

The influence of the aggregate number on the phase envelope is of major importance since the pressure and temperature effects are the key issues. The system studied in Figure V-7 is tested here with $N = 2$. As seen in Figure V-18, the impact is huge, considering that the y-axis is a logarithmic scale. At 250 K, the onset pressure is 19 MPa for $N = 1$ and 490 MPa for $N = 2$.

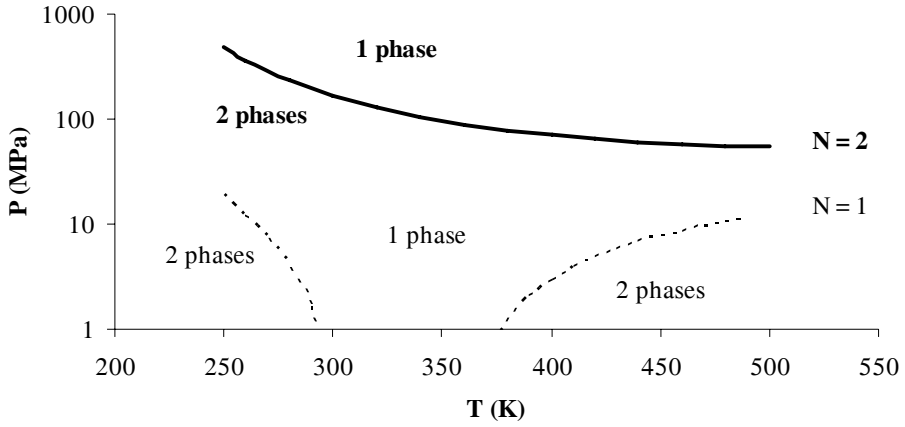

Figure V-18: Influence of the aggregate number on the phase envelope

The model predicts that aggregation destabilizes this system. Indeed, the one-phase region predicted with $N = 1$ is partly located in the two phase region predicted with $N = 2$. This model noticeably affects the phase envelope and, in order to fit experimental data, the critical parameters of asphaltenes have to be chosen with care.

Figure V-19 shows the phase envelope of the same asphaltene solution with or without aggregation and with different critical parameters for the asphaltenes. This figure aims at showing that similar phase envelopes can be predicted with different critical parameters and aggregation numbers. With a variation of the critical temperature from 1300 to 1134 K, the models with $N = 1$ and $N = 2$ give similar phase envelopes. If the critical pressure is modified as well, the right hand-side part of the curve is better fitted but the left-hand side part "disappears". If the acentric is slightly modified (from 3 to 2.993), a one-phase zone can be predicted between 300 and 340 K. With more intensive fitting, the curves are likely to be even more similar.

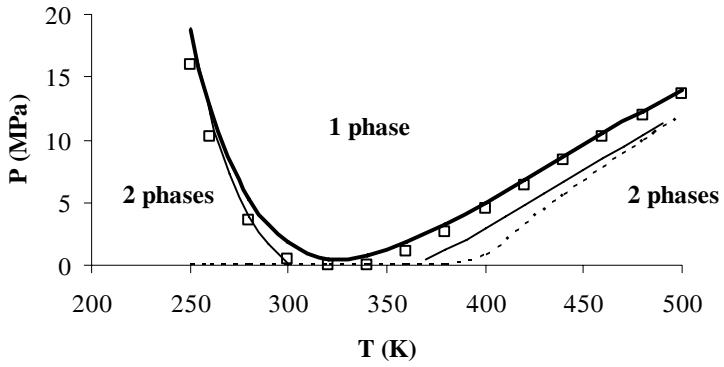

Figure V-19: PT-diagram and influence of the critical parameters (—, N = 1; —, N = 2 and Tc = 1132 K; ----, N = 2 and Tc = 1132 K and Pc = 6.9 atm; □, N = 2 and Tc = 1134 K and ω =2.993)

3.3.3. Gas injection

The system studied in paragraph 2.5 with CO_2 is investigated here with the aggregation model. As seen in Figure V-20, a simple modification of the critical temperature of asphaltenes is sufficient to get similar curves, even with an aggregate number of 3. Obviously and as it was said previously, the bigger the aggregate number, the smaller the critical parameters should be.

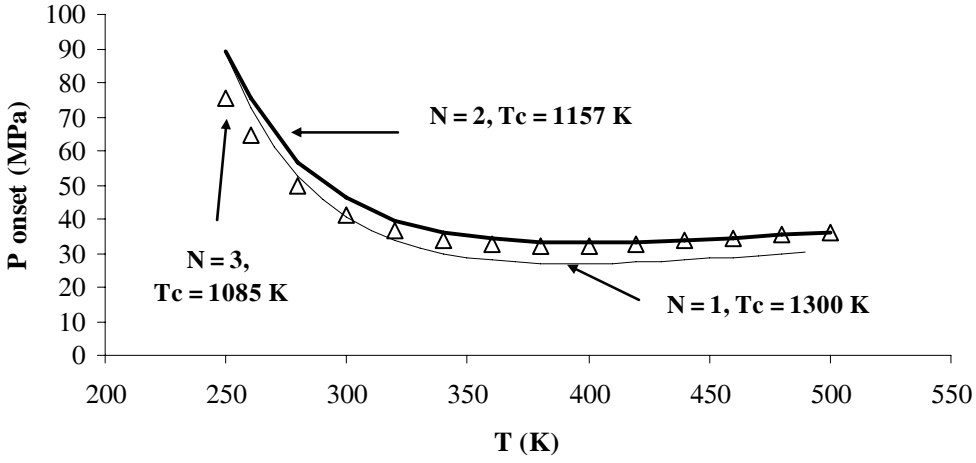

Figure V-20: PT-diagram with 10% CO_2

The influence of the aggregate number and the critical temperature on the bubble point is very limited. The aggregate number was varied from 1 to 6 at different critical temperatures and no difference was seen. As for the critical temperatures, it was varied

between 1000 and 1500 K at constant aggregate number $N = 2$ and the bubble point varied at the most of 0.1 MPa. The lack of influence of the asphaltene parameters can be expected since the gas phase is asphaltene-free.

However, studying a model system does not validate a model. Therefore, data reported in literature about a live oil were chosen and investigated (Jamaluddin et al., 2002). This set of data was chosen because the detailed composition of the oil until the C_{12}^{+} fraction is available as well as the phase envelope (bubble point and precipitation envelope). Gonzalez et al. (2005) modelled this system with PC-SAFT but only taking into account dispersion forces and with 7 pseudo-components (H_2S/CO_2, N_2, methane, light gases, saturates, aromatics + resins and asphaltenes).

The first step is the characterization. It was done using the in-house PVT software SPECS with the Pedersen characterization method. No chromatographic data were given for the molar distribution. The density of the C_{12}^{+} fraction was given. The number of total components was set to 25. Once it was done, the C_{51}^{+} fraction was divided into two: C_{51} and asphaltenes. The molar mass of asphaltenes was assumed to be 1000 g/mol and its molar fraction was calculated from the known weight fraction. Hence, the C_{51} molar fraction was calculated by subtraction. Interaction parameters were not set to zero. The default values given by SPECS were kept and are as follows:

- **Interactions with nitrogen**: $k_{ij}\left(N_2/CH_4\right) = 0.02$, $k_{ij}\left(N_2/C_2H_6\right) = 0.06$, $k_{ij}\left(N_2/X\right) = 0.08$ where X represents the remaining compounds with higher carbon numbers.
- **Interactions with carbon dioxide**: $k_{ij}\left(CO_2/CH_4\right) = k_{ij}\left(CO_2/H_2S\right) = 0.12$, $k_{ij}\left(CO_2/X\right) = 0.15$
- **Interactions with hydrogen sulfide**: $k_{ij}\left(H_2S/CH_4\right) = 0.08$, $k_{ij}\left(H_2S/C_2H_6\right) = k_{ij}\left(H_2S/C_3H_8\right) = 0.07$, $k_{ij}\left(H_2S/iC_4H_{10} \rightarrow nC_5H_{12}\right) = 0.06$, $k_{ij}\left(H_2S/C_6\right) = 0.05$

The remaining interaction coefficients are set to zero.

The second step is the use of the multiphase flash in order to plot the phase envelope. The different phases were differentiated according to their densities, i.e. the asphaltene phase is heavier than the oil phase. The compositions are not given here but the gas phase has no asphaltenes and the asphaltene phase is mainly composed of them.

The fitting procedure was done by hand. Indeed, an optimization routine combined with the multiphase flash appeared to be too time-consuming to program.

The acentric factor was set to a constant value to reduce the number of fitting parameters to three: $T_c^{asphaltenes}$, $P_c^{asphaltenes}$ and the aggregate number. A triplet was found to give proper results but other solutions are quite likely to give satisfying results as well (Table V-4).

Parameters	Value
Critical temperature (K)	1190
Critical pressure (atm)	8.4
Acentric Factor	3
Aggregation number	13

Table V-4: Critical constants and aggregation number of the asphaltenes

Figure V-21 shows the modelled phase envelope as well as the experimental points. The average absolute deviation is 8% for the onset curve and 14% for the bubble point curve.

In the original paper presenting the data, there is no mention of the lower onset curve (re-dissolution curve) but the model predicts one. Since re-dissolution is strongly linked to kinetics, further experiments would be necessary to be able to conclude whether the model is wrong or not. The experimental onset curve shows a minimum around 400 K whereas the model seems monotonous over the studied pressure range. However, the model did reach a minimum around 450 – 500 K because the onset pressures at 550 K is 5 bar higher than at 500 K. Other critical parameters were able to describe this minimum between 350-400 K ($T_c = 1320K$, $P_c = 7.2\ atm$, $\omega = 3.01$ and $N = 20$) but the deviation was much higher though the trend was correct.

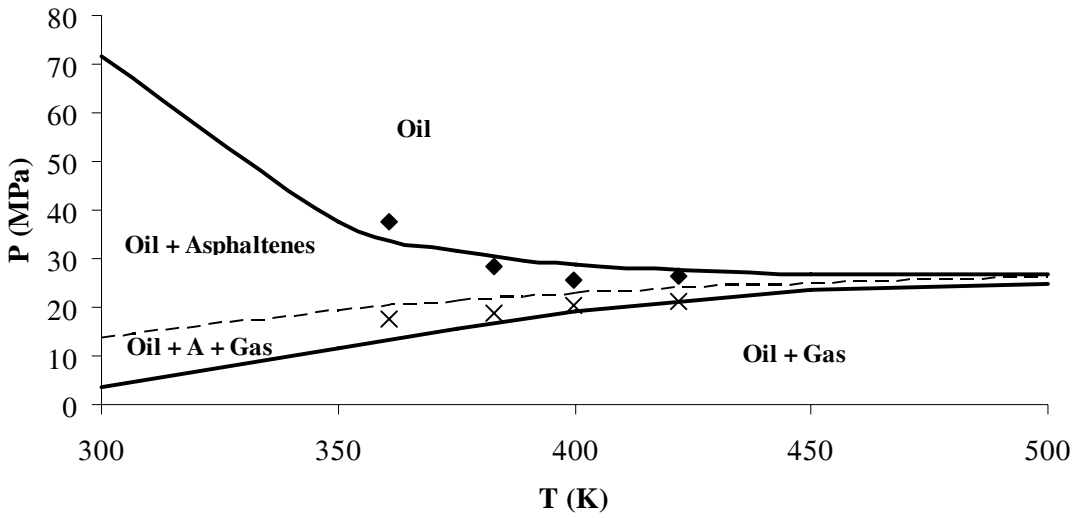

Figure V-21: Phase envelope of the Jamaluddin live oil (◆, experimental onset; —, onset with modified PR; ×, experimental bubble point; - - -, bubble point with modified PR)

Cubic equations usually describe properly bubble points but the fitting was only performed on the onset curve. Other characterization methods use the bubble point and they would probably give much better results for that matter. However, the intensive study of characterization procedures is the not the purpose of this work though it would be very interesting.

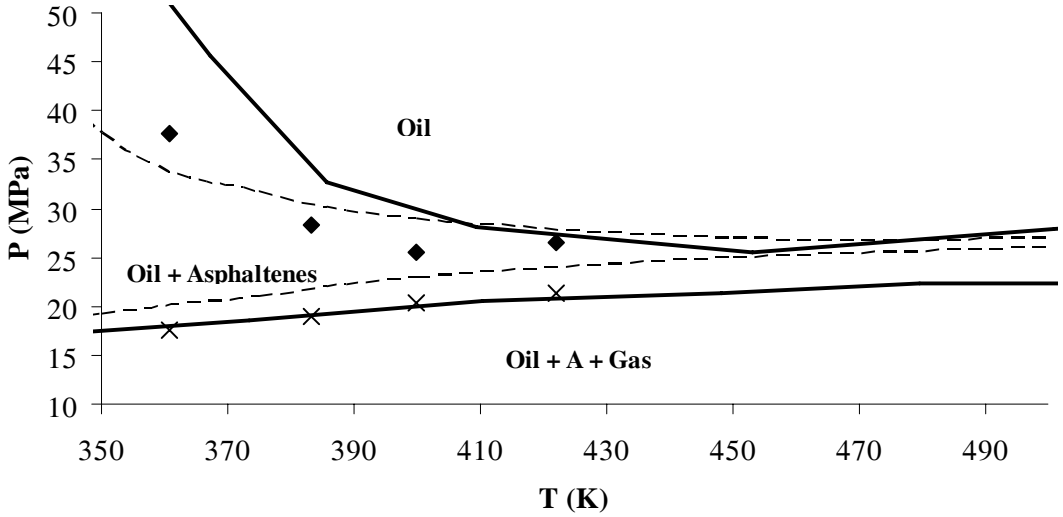

Figure V-22: modelling of asphaltene phase envelope (—, PC-SAFT; - - - , modified PR)

Figure V-22 compares the ability of PC-SAFT and the modified PR to describe the phase envelope. The upper curves represent the precipitation and the lower ones the bubble point. PC-SAFT describes the bubble point more satisfactorily but the onset curves are equivalent.

3.3.4. Conclusion about the aggregation model

This simple model taking into account the aggregation is based on the assumptions and the work of the TOTAL model but, instead of modifying the fugacities, the a and b parameters of the asphaltenes are modified as well as the initial molar fractions. The onset of precipitation is much less dependent on the concentration but the aggregate number cannot be too large otherwise the asphaltenes are not soluble anymore in pure toluene. As for phase envelopes, they can be similar to the ones predicted by the model without aggregation providing that the critical parameters are modified. The effect of gas injection can also be described properly.

When dealing with a crude oil, all the steps are source of improvement or errors:

- **The experimental data:** how were they obtained? Was the equilibrium reached? How was the onset determined? How was the oil stored? How was it recombined?
- **The composition**: is it correct? How trustful are the experiments? What about the asphaltene content? Which method was used? How is the heavy fraction analyzed?
- **The molar weight of asphaltenes**: in this work, the monomers were assumed to have a molar weight of 1000 g/mol. Since the asphaltene content of a crude oil is determined by weight, this parameter is important although, in the model presented in this work, the asphaltene fraction has less impact on the results due to the aggregation number.
- **The characterization procedure**: how many pseudo-components should be used? What is their influence? Which method should be applied? Which molar mass should be chosen for asphaltenes?
- **The interaction coefficients**: the Computer Modelling Group employed the interaction coefficients to "predict" asphaltene precipitation (Nghiem et al., 1993). What is their influence?

- **The fitting procedure**: since it was done by hand in this work, the model can obviously give better results with a proper fitting. Are there any "empirical rules" linking T_c, P_c, ω and N ?

If one seriously considers these few items, the words "prediction of asphaltene precipitation" merely sound utopian.

4. Conclusion

Asphaltene modelling has been quite intensive since the 80's. Many different approaches have been tried. The thermodynamic approach seems to be the appropriate one since it has strong experimental evidences.

The regular solution is simple and intuitive to use. All possible effects of temperature and pressure can be described depending on the input parameters of asphaltenes.

The cubic EOS describe properly phase envelopes but the behaviour with respect to dilution cannot be predicted.

The TOTAL model brings important improvements thanks to the aggregation number but, unfortunately, the modified fugacities do not seem to pass the consistency tests. However, using the same assumptions and only modifying the a and b parameters of asphaltenes, interesting results can be found such as a much lower dependence to dilution. This modification helps describing phase envelopes, providing that the critical parameters of asphaltenes are modified. Literature data were successfully fitted (within 10%) and the model is believed to perform better with a proper fitting procedure.

However, the sources of potential errors and "adjustments" are plethora and they make modelling a fragile tool with today's knowledge and understanding of asphaltenes.

Literature

Alboudwarej H., Akbarzadeh K., Beck J., Svrcek W.Y., Yarranton H.W., Regular Solution Model for Asphaltene Precipitation from Bitumens and Solvents, AIChE J. (2003), 49, 2948 – 2956

Andersen S.I., Speight J.G., Thermodynamic models for asphaltene solubility and precipitation, J. Petrol. Sci. Eng. (1999), 22, 53 - 66

Barton, A.F.M. CRC Handbook of solubility parameters and other cohesion parameters; CRC Press, 1991

Buenrostro-Gonzalez E., Lira-Galeana C., Gil-Villegas A., Wu J., Asphaltene precipitation in crude oils: theory and experiments, AIChE J. (2004), 50, 2552 - 2570

Cimino R., Correra S., Del Bianco A., Lockart T.P., Solubility and Phase Behaviour of asphaltenes in hydrocarbon media, Asphaltenes: Fundamentals and Applications, Sheu E.Y., Mullins O.C., Ed., Plenum Press, NY, 97 - 130 (1995)

Christensen A.A., Hadsbjerg C., Vestager-Tybjerg P.C., A study of the perturbed chain statistical associating fluid theory, Midterm Project: Technical University of Denmark, Department of Chemical Engineering, 2005

Diallo M.S., Strachan A., Faulon J.L., Goddard III W.A., Pet. Sci. Technol. (2004), 22, 877 – 899

Fahim M.A., Al-Sahhaf T.A., Elkilani A.S., Prediction of asphaltene precipitation for Kuwaiti crude using thermodynamic micellization model, Ind. Eng. Chem. Res. (2001), 40, 2748 – 2756

Fahim M.A., Andersen S.I., Tuning EOS Using Molecular Thermodynamics to Construct Asphaltene Deposition Envelope (ADE), Presented at the 6th International Conference on Petroleum Phase Behaviour and Fouling, Amsterdam, 2005

Griffith M.G., Siegmund C.W., Controlling compatibility of residual fuels oils, Marine Fuels (1985), 227 – 247

Gonzalez, D. L., Ting, P. D., Hirasaki, G. J., Chapman W.G., Prediction of Asphaltene Instability under Gas Injection with the PC-SAFT Equation of State, Energ. Fuel. (2005), 19, 1230 – 1234

Gupta A.K., A model for asphaltene flocculation using an equation of state, Master thesis, Department of Chemical and Petroleum Engineering, University of Calgary, 1986

Hansen C.M., Hansen Solubility Parameters: a user's Handbook, CRC press, 2000

Heidemann R.A., Prausnitz J.M., A van der Waals-type equation of state for fluids with asociating molecules, Proc. Natl. Acad. Sci. (1976), 73, 6, 1773 - 1776

Hirschberg A., deJong L.N.J., Schipper B.A., Meijer J.G., Influence of temperature and Pressure on asphaltene flocculation, paper SPE 11202, SPE J. (1984), 283 – 293

Jamaluddin, A.K.M., Joshi, N., Iwere, F., Gurpinar, O., An investigation of asphaltene instability under nitrogen injection, Proceedings of the SPE International Petroleum Conference and Exhibition of Mexico (2002), 427 – 436

Kawanaka S., Park S.J., Mansoori G.A., Organic deposition from reservoir fluids: a thermodynamic predictive technique, SPE Reservoir Eng. (1991), 6, 185-192

Kontogeorgis G.M., Voutsas E.C., Yakoumis I. V., Tassios D.P., Equation of state for associating fluids, Ind. Eng. Chem. Res. (1996), 35, 4310 - 4318

Knudsen L., Modelling of asphaltene precipitation, Master Thesis, Department if Chemical Engineering, Technical University of Denmark, 2001

Leontaritis K.J., Mansoori G.A., Asphaltene Flocculation during oil recovery and processing: a thermodynamic-colloidal model, SPE paper 16258, SPE International Symposium on Oilfield Chemistry, 4-6 February, San Antonio, Texas (1987)

Li M., Guo P., Li S., Modeling technique of asphaltene precipitation, SPE 70048 (2001)

Michelsen M., Møllerup J., Thermodynamic models: fundamentals and computational aspects, Tie-Line Publications, Holte, 2004

Michelsen M., Personal communication (2006)

Nghiem L.X., Hassam M.S., Nutakki R., George A.E.D., Efficient modelling of asphaltene precipitation, SPE 26642 (1993)

Porte G., Zhou H., Lazzeri V., Reversible description of asphaltene colloidal association and precipitation, Langmuir (2003), 19, 40 – 47

Rassamdana H., Dabir B., Nematy M., Farhani M., Sahimi M., Asphalt flocculation and deposition: I. The onset of precipitation, AIChE J. (1996), 42, 1, 10 - 22

Rogel E., Carbognani L., Density estimation of asphaltenes using molecular dynamic simulations, Energ. Fuel. (2003), 17, 378 – 386

Rogel E., Leon O., Contreras E., Carbognani L., Torres G., Espidel J., Zambrano A., Assesment of asphaltene stability in crude oils using conventionnal techniques, Energ. Fuel. (2003), 17, 1583 – 1590
Szewczyk V., Behar E., Compositional model for predicting asphaltenes flocculation, Fluid Phase Equilibr. (1999), 158, 459 – 469

Ting P.D., Hirasaki G.J., Chapman W.G., Modeling of asphaltene precipitation phase behaviour with the SAFT Equation of state, Pet. Sci. Technol. (2003), 21, 647 - 661

Verdier S., Andersen S.I., Determination of isobaric thermal expansivity of organic compounds from 0.1 to 30 MPa at 30 °C with an isothermal pressure scanning microcalorimeter, J. Chem. Eng. Data 48 (2003), 892 – 897

Verdier S., Andersen S.I., Internal pressure and solubility parameter as a function of pressure, Fluid Phase Equilib. 231 (2005), 125 – 137

Victorov A.I., Firoozabadi A., Thermodynamic micellization model of asphaltene from petroleum fluids, AIChE J. (1996), 42, 1753-1764

Wu J., Prausnitz J.M., Firoozabadi A, Molecular-thermodynamic framework for asphaltene-oil equilibria, AIChE J. (1998), 44, 5, 1188 - 1199

Wu J., Prausnitz J.M., Firoozabadi A., Molecular thermodynamics of asphaltene precipitation in reservoir fluids, AIChE J. (2000), 46, 1, 197 – 209

Zhou H., Total, Personal Communication (2005)

Zhou H., Porte G., V. Lazzeri, Personnal Communication (2005)

List of symbols

Latin letters

a	Attractive term of a cubic EOS
a_i	Activity of compound i
b	Co-volume
f	Fugacity
G	Gibbs energy
k_{ij}	Interaction parameter
K	Equilibrium constant
m	Temperature dependence of the solubility parameter
m	Mass
n	Mole number
N	Aggregation number
N_s	Number of binding sites
P	Pressure
R	Gas constant
T	Temperature
v	Mole volume
x	Molar fraction
Z	Compressibility Factor

Greek letters

α_P	Isobaric thermal expansivity
γ	Activity coefficient
δ	Solubility Parameter
κ_T	Isothermal compressibility

μ	Chemical potential
v_i	Stoichiometric coefficient of compound i
ρ	Density
φ	Volume fraction
φ	Fugacity coefficient
χ	Interaction parameter
ω	Acentric factor

Subscripts and Superscripts

a	Asphaltene
agg	Aggregates
c	Critical
CR	Critical
l	Liquid
r	Reaction
0	Reference/Standard

Chapter VI

Conclusion and Future Challenges

Table of Contents

1. Conclusion

This work aimed at getting more understanding about asphaltene stability especially in presence of gas. This section will summarize the different investigations and the main results.

1.1. Solubility parameter

Its definition was clarified. If pressure and temperature are to be taken into account, cohesive energy should be equal to the residual internal energy. The diversity of definitions in the literature induced many databases and, even for pure compounds, deviations up to 0.5 $MPa^{1/2}$ are common. The effect of temperature was studied in the literature. However, the definitions of cohesive energy highly influence the impact of temperature. It was tested with a cubic EOS on n-heptane, ethanol and toluene. On the contrary, the effect of pressure is not well studied in the literature. Pressure was found to influence cohesive energy and it should therefore be regarded as an important factor. Cubic EOS combined with experimental volumes turned out to calculate the total solubility parameter and not the sole dispersion term, as it was expected.

1.2. Characterization of crude oils

The solubility parameter of crude oils was measured using an alternative approach taking pressure into account: the internal pressure. It is determined indirectly with density measurements and scanning transitiometry. Pure compounds were investigated at 303.15 K and up to 30 MPa. An accuracy of 1 $MPa^{1/2}$ was found for hydrocarbons. It was also confirmed that internal pressure does not "measure" hydrogen bonding. This method was successfully applied to both dead and live oils. However, the accuracy required by modelling (0.1 $MPa^{1/2}$) could not be satisfied. The uncertainty of isothermal compressibility measurements is the main source of such a high deviation. The high-pressure calorimetry measurements also confirmed that bubble point can be determined by scanning transitiometry.

1.3. Solubility parameters of asphaltenes

A technique based on the regular solution theory and density measurements was applied to asphaltene solutions. Solubility parameters of two asphaltenes were determined at 303.15 K and 0.1 MPa. Three pairs of solvents were tested and one did not give satisfactory results. An average deviation of 0.4 $MPa^{1/2}$ was found. The dependence of δ_a with respect to temperature could be investigated and would be quite easy from an experimental point of view. The only required parameters would be the internal pressures and the solubility parameters of the solvents at the studied temperature. As for the dependence with pressure, larger samples would be necessary since the ISCO pump should be used.

1.4. Critical constants of asphaltenes

A novel approach using partial volumes and a cubic EOS was tested on asphaltene solutions. Partial volumes of asphaltenes are measured in three different solvents. Partial volume calculations are performed with a cubic EOS using the measured densities as inputs. The calculated and experimental partial volumes are fitted using the critical constants as adjustable parameters. The ability of this method to evaluate critical parameters is too poor for modelling (13% of deviation for pure compounds). A second technique based on NMR data was tested. The content in hetero-atom and the molar weight have a very strong influence on the calculated critical constants.

1.5. Asphaltene stability and gas injection

A novel high-pressure PVT cell developed at the University of Pau (France) was tested on several crude oils in presence of carbon dioxide and methane. The onset of precipitation was determined using isobaric filtration. The influences of pressure and temperature were determined. Temperature destabilized both crude oils with carbon dioxide. As for methane, its influence was tested on one crude oil only and temperature had a stabilizing impact. For all the systems studied, the higher the pressure, the more soluble the asphaltenes. Reversibility was detected for one crude oil only. The role of kinetics in such measurements has to be carefully studied though.

1.6. Asphaltene Stability and Calorimetry

Isothermal titration calorimetry was applied to asphaltene solutions and to crude oils. Precipitation induced by n-alkanes had no strong thermal effects. It seems that the energy of the broken bonds (asphaltene-solvent) is equivalent to the one of the created ones (asphaltene-asphaltene and solvent-solvent). As for precipitation caused by pressure depletion or by a variation of temperature, it had visible exothermic effects accompanied by an increase in apparent thermal expansivity (i.e. an increase in volume due to the creation of a new phase). It is similar to a second-order transition.

1.7. Modelling of asphaltene precipitation

Once the different models used in the literature had been listed, a cubic EOS was tested. The impact of critical parameters on the asphaltene precipitation curve was investigated. It confirmed that even a modification of 1% had a strong influence. A simple model taking into account aggregation and based on cubic EOS was tested. A reported asphaltene phase envelope could be successfully described. However, the determination of critical parameters and the potential sources of error and adjustments are so large that modelling of asphaltene fluid is not predictive with today's knowledge of asphaltenes.

2. Future Challenges

The new challenges for investigation are listed below and follow the structure of this thesis.

2.1. Characterization of crude oils and asphaltenes

- The solubility parameter could be calculated with an advanced EOS such SAFT. Both dispersion and association terms could be calculated separately providing that the residual energy can be divided in two parts. The influence of pressure and temperature could be investigated.
- A correlation linking thermal expansivity and critical temperature was found but could not be tested due to lack of time:

$$T_c = \left(\frac{\alpha_p(T)}{0.04314} \right)^{\frac{-1}{0.6410}} + T$$

Asphaltene solutions could be prepared in different solvents and their densities measured with respect to temperature. Using a volume mixing rule, the thermal expansivity of asphaltenes could be calculated assuming that there is no excess volumes. This correlation does not require any assumption about molar weight.

2.2. Asphaltene Stability and gas injection

- A well-known and characterized crude oil should be tested with several precipitants: n-alkanes, carbon dioxide, methane and nitrogen. The relationship “effect of temperature/nature of precipitant” should be closely investigated.
- Investigation of bottom-hole samples would be of great interest as well since they would be more representative.
- The reversibility issue should be studied and especially the lower onset curve. The laser device installed on the cell would greatly help.
- Several sizes of pores for the filter should be tried. Important information about the transition flocculation/precipitation might be obtained.

- The effect of nitrogen on asphaltene stability should be studied since it is reported as a precipitant.

2.3. Asphaltene precipitation and calorimetry

- The influence of the liquid in the reference cell should be investigated for the ITC experiments (mixtures toluene/heptane could be tried).
- ITC experiments should go on with more oils and asphaltene solutions. Higher precipitant contents should be tried.
- As for the model systems, well-known sterically stabilised colloids should be investigated. The signal obtained by flocculation of well-known systems would probably help interpreting the signals obtained with asphaltenes.
- The effect of temperature could be investigated.
- The HP calorimetry experiments should be combined with the filtration technique in order to have fewer doubts about the measured signals. It might be possible to establish a relationship between heat of precipitation and stability with respect to temperature.

2.4. Modelling of asphaltene precipitation

- The fitting procedure to obtain the critical constants and the aggregation number should be optimized.
- The influence of the characterization method should be tested.
- A model taking into account polydispersity should be studied since there is not a single aggregation number but a distribution.
- Critical parameters could be obtained by fitting titration experiments at atmospheric conditions on a dead oil. They could also be determined with the method developed in this work and compared to the ones fitted by the EOS. Then, the APE should be plotted and compared to the experimental one.

- Aggregation could be modelled as chemical reaction equilibrium following the recommendations given by Michelsen and Mollerup (2004). Then, this model may be combined with a multiphase flash.

2.5. Other studies

- SANS and SAXS should be applied to asphaltene solutions next to the onset of flocculation and precipitation.
- The influence of pressure and temperature on the state of aggregation should be followed by microscopy and image analysis.
- Precipitation by pressure depletions should be investigated in an accurate high-pressure pycnometer since there seems to be a change in volumetric properties.
- The size distribution is of interest, especially close to the onsets of flocculation and precipitation.
- APE of live oils could be determined using speed-of-sound following a procedure already applied to LLE (Lu et al., 1999) and onset of asphaltene precipitation at room conditions (Carrier et al., 2000).
- The differences between n-heptane induced precipitation and pressure/temperature-induced precipitation is of major interest. The fitting procedures in modelling are often based on n-heptane titrations. Then, the model is applied to live systems. It would be interesting to investigate whether or not these types of precipitations have a different nature, as the calorimetric studies of this work give to understand.
- The co-precipitation of waxes with asphaltenes at low temperature was briefly introduced. An analysis of the filtrate would be necessary to be sure that the onset of precipitation is only due to asphaltenes.

Literature

Carrier H., Plantier F., Daridon J.-L., Lagourette B., Lu Z., Acoustic method for measuring asphaltene flocculation in crude oils, J. Pet. Sci. Eng. (2000), 27, 111 - 117

Lu Z., Daridon J.L., Lagourette B., Ye S., Phase comparison technique for measuring liquid-liquid phase equilibrium, Rev. Sci. Instrum. (1999), 70, 2065-2068

Michelsen M.L., Mollerup J.M., Thermodynamic models: fundamentals and computational aspects, Tie-Line Publications, Holte, 2004

Ratzsch M., The calculation of critical temperatures of binary mixtures from thermal expansion coefficient, Chem. Tech.- Leipzig (1969), 21, 774 – 775

Appendixes

List of Appendixes

Appendix I-1: Modified IP 143 method to measure the asphaltene content of a crude oil

Day 1

1. Weigh off 5g oil in 500ml Erlenmeyer glass
2. Add 30ml of n-heptane/g oil and weigh the amount of n-heptane
3. Cover with aluminium foil
4. Blend on ultra sound water bath for 10-15 min.
5. Rest for 16-18 h in darkness

Day 2

1. Transfer the suspended mixture quantitatively to a glass filter (Pyrex ASTM 4-5.5 .F) with suction and wash with, n-heptane. This is done .by stopping suction, adding ca. 20ml n-heptane, let it be for a couple of minutes and start suction again. Continue till the washing liquid is colourless.
2. Put the filter on a small- suction flask and heat ca. 40ml toluene. The asphaltenes are now dissolved similar to the washing process above. Use as small an amount of toluene as possible.
3. The toluene is removed by rotational evaporation at 80°C.
4. The asphaltenes are transferred to a preparation glass with toluene – max. 10 mL - remember to tare the preparation glass.
5. The toluene is evaporated in a water bath at 60°C under a flow of nitrogen.
6. To remove the last toluene, the preparation glass is placed in a vacuum oven.
7. A drop of toluene is added to the preparation glass to moisten the asphaltenes and then 10 ml n-heptane are added. Mix on ultra sound bath for 10 min. and centrifuge for 15 min. Remove as much h-heptane as possible without removing any solids. Continue till liquid is colourless.
8. The asphaltenes are dried in a vacuum oven.

Appendix I-2: Intermolecular forces

Atoms and molecules can interact together leading to the formation of either a new molecule (reactive channel) or a molecular cluster (nonreactive channel). The latter is named noncovalent interaction. Entropy always plays a dominant role in noncovalent interactions and its change accompanying cluster formation is always negative; the $T\Delta S°$ entropy term is usually, at room temperature, comparable to the enthalpy term $\Delta H°$. The change of the Gibbs' free energy accompanying the formation of a cluster is thus close to zero. (Müller-Dethlefs and Hobza, 2000)

On the basis of perturbation theory, the total stabilization energy of noncovalent complex can be divided into various energy contributions. The electrostatic, induction, charge-transfer and dispersion terms form the dominant attractive contributions:

- **Polar (or electrostatic) interactions:** they are due to interactions between permanent multipoles and are interactions between an electronegative and an electropositive atom. They are significant when the dipole moment is larger than 1 D. Quadrupolar effects are much smaller but can be of some importance in special cases (CO_2 for instance).
- **Dispersion interactions:** they originate from the interaction between an instantaneous time variable multipole and an induced multipole. They are always significant.
- **Induction interactions:** they come from the interaction between a permanent multipole and an induced dipole. They are generally small and never exceed 7% of the total forces.
- **Charge transfer interactions**: The condition for the formation of the charge transfer complex requires that one system is a good electron donor and the other one a good electron acceptor. Charge transfer implies electron flow from the donor to the acceptor.

The **van der Waals forces** refer to the first three ones and not to the only dispersion interactions, as it is sometimes found in literature. The charge transfer interactions are

also called “specific forces” or “chemical forces” since they are connected to the theory of covalent bond.

But what about the hydrogen bonding? And the π–π interaction? Hydrogen bonding is due to charge-transfer from the lone pairs or π-molecular orbitals of the electron donor (proton acceptor) to the antibonding orbitals of the X-H bond of the electron acceptor (proton donor) (Müller-Dethlefs and Hobza, 2000). This is accompanied by a very small charge transfer that usually does not exceed 0.01 e ¯. Complexes with H-bonds are stabilized by electrostatic, induction and dispersion energy terms. As for the so-called “π–π interactions”, they are subject to discussion. Quoting Müller-Dethlefs and Hobza: “*These empirical rules are misleading and redundant. The position of π-charges as well as the π–σ charge splitting introduced in this theory is almost arbitrary. […] Instead of artificially introducing the σ and π charges, it is enough to recognize the role of molecular quadrupoles*”.

As for the repulsive term, called exchange-repulsion, it is connected with the overlap of occupied orbitals, prevents the subsystems from approaching too closely.

For non-simple systems, the effect of molecular structure and shape is often very large but no adequate tools are available for describing such effects in a truly fundamental way. Molecular simulation can help estimating such effects (Prausnitz et al., 1999).

The list of forces that has been done arises between molecules in the low-pressure gas phase. Interactions between two molecules in a solvent medium are described by what is called the potential of mean force that plays a major role in colloid science and in the physical chemistry of protein solutions. The essential difference is that the interaction between two molecules in a solvent is influenced by the molecular nature of the solvent but there is no corresponding influence on the interaction of two molecules in (nearly) free space. For example, for two solute molecules in a solvent, their intermolecular pair potential includes not only the direct solute-solute interaction energy but also any changes in the solute-solvent and solvent-solvent interaction energies. Further, solute

molecule often perturbs the local ordering of the solvent molecules. The energy associated with this perturbation depends on the distance between the two dissolved molecules and it produces an additional solvation force between them.

References

Müller-Dethlefs K., Hobza K., Noncovalent interactions: a challenge for experiment and theory, Chem. Rev. (2000), 100, 143 – 167

Prausnitz J.M., Lichtenthaler R.N., Gomes de Azevedo E., Molecular thermodynamics of Fluid-Phase Equilibria (3rd edition), Prentice Hall PTR, New Jersey, 1999

Appendix II-1: Influence of temperature on the solubility parameters of toluene and ethanol

Calculations were performed with PR EOS. Densities given by Cibulka and Zikova (1994) for ethanol and by Cibulka and Takagi (1999) for toluene. The DIPPR correlations were used for the saturated density and the heat of vaporisation.

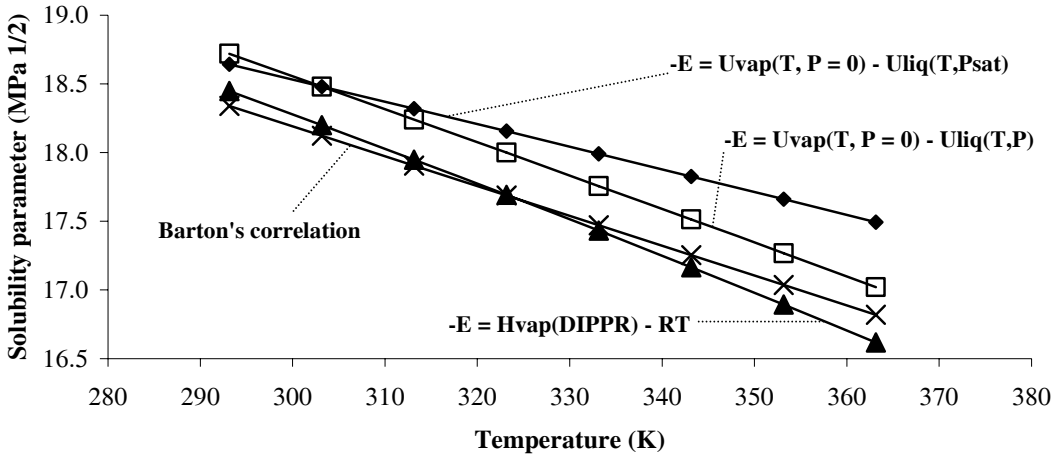

Figure 1: Solubility parameter of toluene at 0.1 MPa

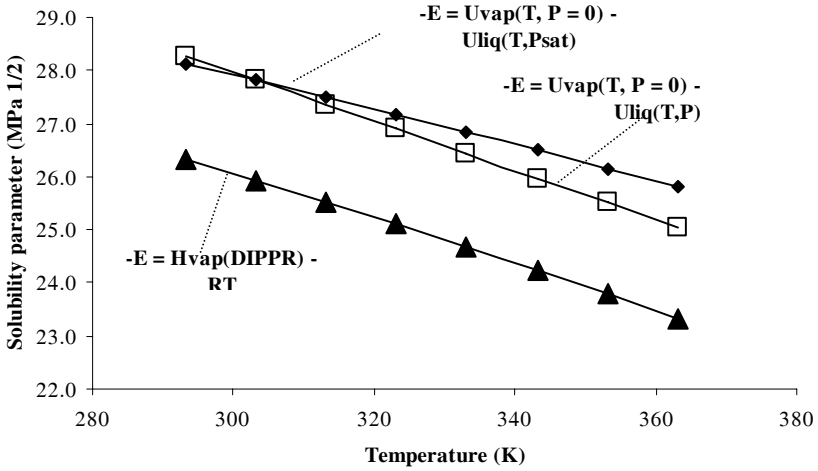

Figure 2: Solubility parameter of ethanol at 0.1 MPa

Cibulka I., Zikova M., Liquid densities at elevated pressures of 1-alkanols from C1 to C10. A critical evaluation of experimental data, J. Chem. Eng. Data (1994), 39, 876 – 886

Cibulka I., Takagi T., P-rho-T data of liquids: summarization and Evaluation. 5 – Aromatic hydrocarbons, J. Chem. Eng. Data (1999), 44, 411 - 429

Appendix II-2: Influence of pressure on the solubility parameters of toluene and ethanol at 303.15 K and up to 100 MPa.

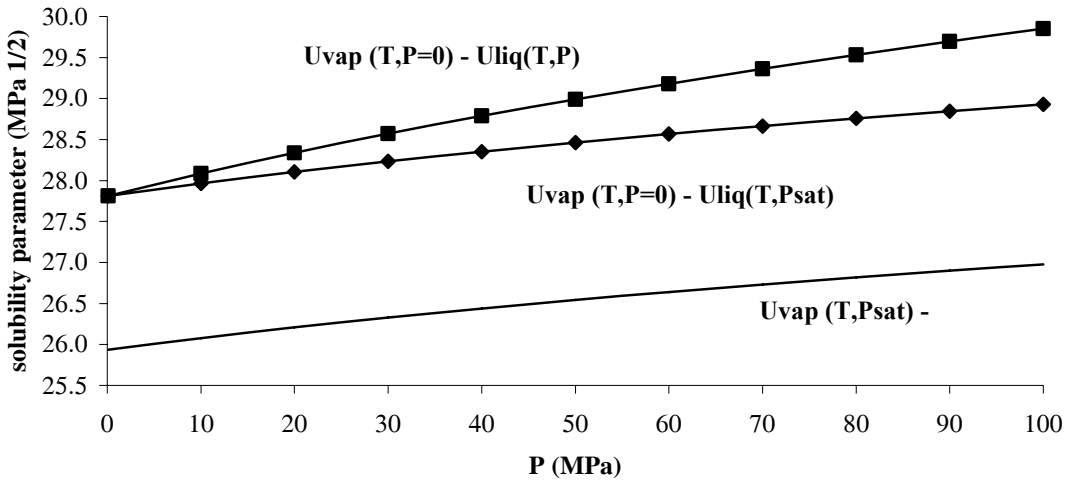

Figure 3: Solubility parameter of ethanol at 303.15 K

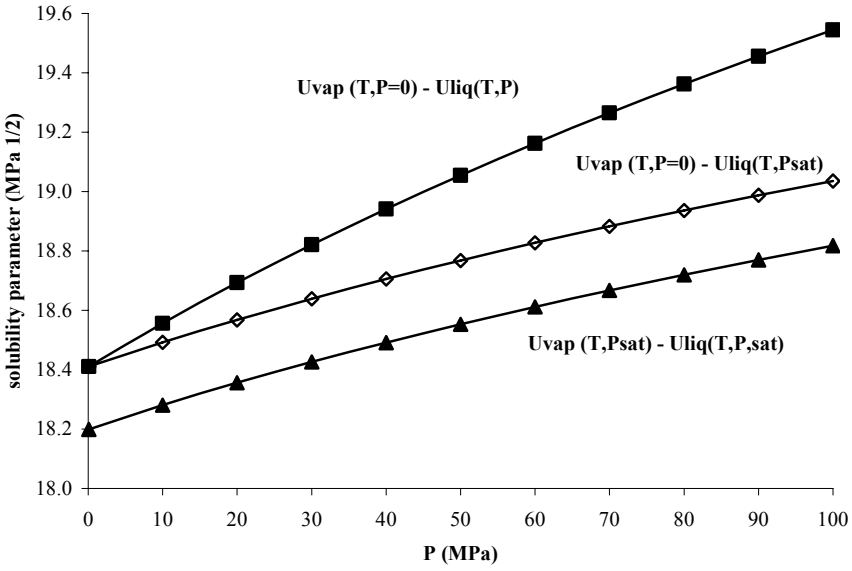

Figure 4: Solubility parameter of toluene at 303.15 K

Appendix II-3: Relationship between solubility parameter and internal pressure

The solubility parameter can be written:

$$\delta^2 = \frac{U^* - U}{V} \quad \textbf{(1)}$$

where U^* is the internal energy of the ideal gas and U the internal energy.

If the derivative with respect to V is taken, we have:

$$\left.\frac{\partial\left(\delta^2\right)}{\partial V}\right|_T = \frac{1}{V}\left(\frac{\partial\left[U^* - U\right]}{\partial V}\right)_T - \frac{\left[U^* - U\right]}{V^2} = \frac{1}{V}\left(\delta^2 - \pi\right) \quad \textbf{(2)}$$

Indeed, the internal energy of the ideal gas only depends on T.

Thus,

$$\left.\frac{\partial\delta^2}{\left(\delta^2 - \pi\right)}\right|_T = \left.\frac{\partial V}{V}\right|_T \quad \textbf{(3)}$$

Furthermore,

$$\left.\frac{\partial V}{V}\right|_T = -\left.\frac{\partial\rho}{\rho}\right|_T \quad \textbf{(4)}$$

Then, after integration on each side of the equation, it becomes:

$$\ln\left(\delta^2 - \pi\right) = A - \ln\left(\rho\right) \quad \textbf{(5)}$$

$$\ln\left[\left(\delta^2 - \pi\right)\rho\right] = A \quad \textbf{(6)}$$

$$\delta^2 = \pi + \frac{A'}{\rho} \quad \textbf{(7)}$$

Appendix II-4: Verdier S., Andersen S.I., Internal pressure and solubility parameter as a function of pressure, Fluid Phase Equilibr. (2005), 231, 125–137

Appendix 2-5: Verdier S., Duong D., Andersen S.I., Experimental determination of solubility parameters of oils as function of pressure, Energ. Fuel. (2005), 19, 1225 - 1229

Appendix II-6: Origin and purity of the chemical compounds

Compound	Origin compounds	Purity (wt. %)
methanol	JT Baker	> 99.8
n-heptane	Rathburn Chemicals	> 99
n-decane	Aldrich Chemie	> 99
toluene	Riedel de Haën	> 99
carbon disulfide	Rathburn Chemicals	
m-xylene	Merck-Schuchardt	> 99

Appendix II-7: Alexander's correlations

The three adjustable constants for SRK are given by:

$$a_c = 0.42747\, R^2 T_c^2 \,/\, Pc \qquad \textbf{Eq 1}$$

$$b = 0.0866\, RT_c \,/\, P_c \qquad \textbf{Eq 2}$$

$$m = 0.480 + 1.574\,\omega - 0.176\,\omega^2 \qquad \textbf{Eq 3}$$

These three parameters were correlated to NMR data, as explained below:

$$a_c^{1/2} = (-3.437 + 3.990/C^{1/2} + 2.5930\, C^{1/2} + 0.20437 H_{aro} + 0.04809 H_\alpha + 0.10936 H_\beta + 0.09500 H_\gamma - 0.2534 H_{aro}{}^{1/2} + 0.2176 H_\alpha)/(1 - 0.004973 H_{aro} + 0.0009645 H_\beta + 0.002973 H_\gamma) \qquad \textbf{Eq 4}$$

$$b = -0.1707 + 0.3929/C^{1/2} + 0.033131 H_{aro} + 0.020902 H_\alpha + 0.015881 H_\beta + 0.012906 H_\gamma - \left(0.10759 H_{aro} + 0.06224 H_\alpha + 0.03939 H_\beta + 0.02355 H_\gamma\right)/C \qquad \textbf{Eq 5}$$

$$m = -3.010 + 0.6621 C^{1/2} - 0.1256 H_\beta^{1/2} - 0.0425 H_\gamma^{1/2} + \left(2.223 H_{aro} + 1.388 H_\alpha + 1.316 H_\beta + 1.086 H_\gamma\right)/C \qquad \textbf{Eq 6}$$

However, heavy fuels containing hetero-atoms need corrections. Here, sulfur, oxygen and nitrogen are considered. In addition to the previous terms (determined from hydrocarbons), other terms are added:

$$b - b_{HC} = 0.00191(NH) + 0.03853(NH_2) + 0.01276 N_p H_{aro}/C + 0.00486(OH) + 0.02261 O_e + 0.02034 S \qquad \textbf{Eq 7}$$

$$a_c - a_{c,HC} = [2.189(NH) + 3.430(NH_2) + 2.246 N_p + 1.950(OH) 2.680 O_e + 2.674 S]^2 \qquad \textbf{Eq 8}$$

$$m - m_{HC} = 0.4026(NH) + 0.5389(NH_2) + 0.1064 N_p + 0.8935(OH) - 0.0445 O_e + 0.2545 S \qquad \textbf{Eq 9}$$

where:

C is the number of carbon atoms per number-average molecule

H_{aro} = number of hydrogen atoms bonded to aromatic carbon atoms PAM (Per Average Molecule);

H_{α} = number of hydrogen atoms bonded to aliphatic carbon atoms which are in turn bonded to aromatic carbon atoms PAM;

H_{β} = number of hydrogen atoms bonded to aliphatic carbon atoms which are not α and do not terminate a chain PAM;

H_{γ} = number of hydrogen atoms bonded to aliphatic carbon atoms which are not α and do terminate a chain PAM

Thus, we can obtain:

$$T_c = 0.202587\, a_c / (Rb) \qquad \textbf{Eq 10}$$

$$Pc = 0.01754\, a_c / b^2 \qquad \textbf{Eq 11}$$

ω is the smallest positive root of:

$$\omega = 4.47159 \pm 2.84091 (2.815396 - 0.704m)^{1/2} \qquad \textbf{Eq 12}$$

If $m > 3.999$, there will be imaginary roots of the above equation, i.e. no solution for ω.

Appendix II-8: Elemental analysis, Molecular weight and NMR data for various asphaltenes

sample	Mw (g/mol)	H_{aro}	H_{alpha}	H_{beta}	H_{gamma}	C_{aro}	C_{ali}
b1c780	7300	10.13	48	109.5	36.5	81.73	100
k1c7to10	4700	15.65	40	115	40	17.59	100
k1c7to20	3800	13.58	40	110	39	113.37	100
b1c7to20	9300	7.67	44.5	112	37.5	79.56	100
b1c725	2000	7.39	40	114	36	67.45	100
b1c760	5800	8.1	42.5	104.5	35	76.02	100
k1c760	5900	10.35	48	104	37	112.65	100
k1c780	6800	11.24	52	112	37	122.42	100
b1c7to10	5800	7.6	43	98	29	62	100
k1c725	4300	12.59	44	98	35	108.88	100

Table 1: Molecular weight and NMR data (VPO at 60C in pyridine for Mw)

sample	C	H	N	S	O
b1c780	80.8	7.9	1.8	7.0	2.5
k1c7to10	82.2	7.8	1.1	5.8	3.1
k1c7to20	82.4	8.0	0.9	8.4	0.3
b1c7to20	80.7	7.8	2.0	6.4	3.2
b1c725	80.8	8.3	1.6	7.1	2.2
b1c760	80.8	8.0	1.9	6.9	2.5
k1c760	82.2	7.5	0.9	6.4	3.0
k1c780	82.2	7.4	0.9	7.1	2.4
b1c7to10	80.9	8.1	1.9	7.0	2.2
k1c725	82.4	7.7	0.7	7.6	1.6

Table 2: Elemental analysis (LeoPharma)

Appendix III-1: Le Châtelier's Principle

Let us consider a component A in equilibrium between two phases.

$$A_\alpha \rightleftarrows A_\beta$$

At the equilibrium, the chemical potentials are equal:

$$\mu_A^\alpha\left(T,P,n^\alpha\right)=\mu_B^\alpha\left(T,P,n^\beta\right)$$

$$\mu_A^{\alpha,0}\left(T,P\right)+RT\ln\left[a_A\left(T,P,n^\alpha\right)\right]=\mu_A^{\beta,0}\left(T,P\right)+RT\ln\left[a_A\left(T,P,n^\beta\right)\right]$$

$$\left(\mu_A^{\beta,0}\left(T,P\right)-\mu_A^{\alpha,0}\left(T,P\right)\right)+RT\ln\left[\frac{a_A\left(T,P,n^\beta\right)}{a_A\left(T,P,n^\alpha\right)}\right]=0$$

$$\left(g_A^{\beta,0}\left(T,P\right)-g_A^{\alpha,0}\left(T,P\right)\right)+RT\ln K_A=0$$

$$\left[h_A^{\beta,0}\left(T,P\right)-h_A^{\alpha,0}\left(T,P\right)\right]-T\left[s_A^{\beta,0}\left(T,P\right)-s_A^{\alpha,0}\left(T,P\right)\right]+RT\ln K_A=0$$

$$\ln K_A=\frac{-\left[h_A^{\beta,0}\left(T,P\right)-h_A^{\alpha,0}\left(T,P\right)\right]+T\left[s_A^{\beta,0}\left(T,P\right)-s_A^{\alpha,0}\left(T,P\right)\right]}{RT}$$

Let us investigate the pressure and temperature effects on the equilibrium constant.

- **Temperature effect:**

$$\left.\frac{\partial\ln K_A}{\partial T}\right|_P=\frac{\Delta h_A^0}{RT^2}-\frac{1}{RT}\frac{\partial\Delta h_A^0}{\partial T}+\frac{1}{R}\frac{\partial\Delta s_A^0}{\partial T}$$

$$\left.\frac{\partial\ln K_A}{\partial T}\right|_P=\frac{\Delta h_A^0}{RT^2}-\frac{1}{RT}\left(\frac{\partial h_A^{0,\beta}}{\partial T}-\frac{\partial h_A^{0,\alpha}}{\partial T}\right)+\frac{1}{R}\left(\frac{\partial s_A^{0,\beta}}{\partial T}-\frac{\partial s_A^{0,\alpha}}{\partial T}\right)$$

$$\left.\frac{\partial\ln K_A}{\partial T}\right|_P=\frac{\Delta h_A^0}{RT^2}-\frac{1}{RT}\left(c_p^{0,\beta}-c_p^{0,\alpha}\right)+\frac{1}{R}\left(\frac{c_p^{0,\beta}}{T}-\frac{c_p^{0,\alpha}}{T}\right)=\frac{\Delta h_A^0}{RT^2}$$

$$\left.\frac{\partial\ln K_A}{\partial T}\right|_P=\frac{\Delta h_A^0}{RT^2}$$

This relationship is known as the Van't Hoff equation. If the reaction is endothermic, Δh_A^0 is negative, so the equilibrium shifts to its left side. If the reaction is exothermic, the equilibrium shifts to its right side.

- **Pressure effect:**

$$\left.\frac{\partial \ln K_A}{\partial P}\right|_T = \frac{1}{RT}\left[-\frac{\partial\left(h_A^{\beta,0}-h_A^{\alpha,0}\right)}{\partial P}+T\frac{\partial\left(s_A^{\beta,0}-s_A^{\alpha,0}\right)}{\partial P}\right]$$

Furthermore, we have:

$$\left.\frac{\partial h}{\partial P}\right|_T = v\left(1-\alpha_P T\right)$$

$$\left.\frac{\partial s}{\partial P}\right|_T = -\alpha_P v$$

where α_p is the isobaric expansivity and v is the molar volume

So, it becomes:

$$\left.\frac{\partial \ln K_A}{\partial P}\right|_T = \frac{1}{RT}\left[-v_A^{\beta,0}\left(1-\alpha_p^{\beta,0}\right)+v_A^{\alpha,0}\left(1-\alpha_p^{\alpha,0}\right)+T\left(-\alpha_p^{\beta,0}v_A^{\beta,0}+\alpha_p^{\alpha,0}v_A^{\alpha,0}\right)\right]$$

$$\left.\frac{\partial \ln K_A}{\partial P}\right|_T = \frac{1}{RT}\left[v_A^{\alpha,0}-v_A^{\beta,0}\right] = \frac{-\Delta v_A^0}{RT}$$

If Δv_A^0 is negative (smaller molar volume is phase β than in phase α), an increase in pressure will shift the equilibrium to the right side.

	Increase in T	**Increase in P**
$\Delta h_A^0 < 0$	$\leftarrow$	-
$\Delta h_A^0 > 0$	$\rightarrow$	-
$\Delta v_A^0 < 0$	-	$\rightarrow$
$\Delta v_A^0 > 0$	-	$\leftarrow$

In terms of asphaltene's solubility,

	Increase in T	**Increase in P**
$h_{precipitation} < 0$	Increase solubility	-
$h_{precipitation} > 0$	Decrease solubility	-
$v_A^{deposit} < v_A^{solution}$	-	Decrease solubility
$v_A^{deposit} > v_A^{solution}$	-	Increase solubility

Appendix III-2 : Verdier S., Carrier H., Andersen S.I., Daridon J.L., Study of pressure and temperature effect on asphaltene stability in presence of CO2, Energ. Fuel. (2006), to be published

Appendix IV-1: ITC experimental procedure

This procedure is very similar presented by Merino-Garcia in his PhD thesis since he was the first one to use the ITC equipment in our research group.

More details are available in: Merino-Garcia D., Calorimetric investigations of asphaltene self-association and interaction with resins, Ph.D. Thesis, IVC-SEP, Department of Chemical Engineering, Denmark, Technical University, Lyngby, Denmark, 2004

1. Preparation of the samples

Asphaltenes are photosensitive. Hence, asphaltenes and crude oils are stored in dark and dry places.

First, asphaltenes or crude oils are weighed as well as the appropriate solvent (mixture of toluene and heptane). Usually, 5 mL of sample are prepared and sealed. 1.5 mL is necessary for the injection.

Then, the sample is taken to the ultrasound treatment in order to dissolve faster the asphaltenes and/or to eliminate gas dissolved in the solvent. The vial containing the sample is sealed, a needle is placed on its top to enable gas to escape and the vial is placed in a Becher filled with water in the ultra-sound bath. The ultra sound treatment lasts 50 minutes. Once it is over, the needle is removed and the sealing cap changed.

2. Filling syringe

First, the solution that is going to be placed inside the cell is taken with a syringe. It is necessary to take 2 ml with the 2.5 ml-syringe. The bubbles inside the syringe must be removed. Some of the solution will be lost during the removal of the air bubbles. The volume needed is 1.5 ml, so the elimination of the gas bubbles has to be done carefully.

Once the syringe is filled, the solution is slowly injected inside the sample cell: the end of the syringe has to touch gently the bottom of the cell in order to remove the air. Then, the solution is injected slowly. If the vial still contains solution to perform more tests, it has to be sealed again right after taking the sample with the syringe. The white stopper is placed on top of the cells, to avoid any contamination of the

cell while preparing the syringe solution. This is the most delicate step of the preparation of the test. It is necessary to ask for some help, because the computer has to be used at the same time, and both hands are inside the glove box. The vial that contains the solution that will go in the syringe is unsealed and placed inside the calorimeter. It is as well necessary to have inside the glove box the 2.5ml-syringe and also a small rubber tube.

The syringe plug has to be in the OPEN position; that it achieved by pressing the button OPEN FILL PORT in the computer screen.

The rubber tube has to connect the 2.5ml-syringe to the upper connection of the syringe. The holder attached to the calorimeter is not suitable for the type of vials used, so the syringe must be hold with the left hand over the vial, making sure that at least the whole stirrer is dipped inside the solution. The right hand is used to hold the 2.5mlsyringe and this 2.5ml-syringe is used to suck carefully the solution from the vial into the syringe. In order to avoid wasting too much solution, it is a good idea to suck carefully until the level of liquid reaches the upper connection to the rubber tube. Once there, the person in charge of pressing the buttons in the computer has to press CLOSE FILL PORT. Right after that, the person in charge of the syringe has to suck again with the 2.5ml-syringe before the port closes totally, in order to remove the last bubble of air. It is important that there are no bubbles left, because if there are any, the signal will be distorted.

Then, the cell has to be refilled, by pressing the button PURGE-REFILL. This has to be done three times. Once this has been done, the rubber tube has to be disconnected, and the tip of the syringe must be cleaned with toluene because it has been in contact with the asphaltenes. Once the tip is clean, the syringe is carefully placed inside the cell.

3. Cleaning of the cell

The 2.5ml-syringe is used to clean the cell:

- First, remove the solution from the cell.
- Fill the 2.5-ml syringe with toluene and fill and empty the cell three times.
- Empty and fill again the 2.5ml-syringe with a new solution of toluene and repeat the refill another three times.
- Do it again. Normally, three times is enough, but if the concentration of asphaltenes was high, maybe it is necessary to repeat it once again.

- If the toluene is still not transparent, inject toluene in the cell. Start the ITC procedure and let the stirring on for a few hours.
- Once it seems clean, dry the cell with air, using the THERMOVAC.

4. Cleaning of the syringe

In the first step, a big vial (20 ml) is placed under the holder of the syringe, making sure there is enough toluene to cover the tip of the syringe. Press the button CLOSE FILL PORT (or UP 29 times) to suck the toluene. Press PURGE-REFILL a couple of times. Change the toluene solution and repeat the same procedure.

Then, press the button OPEN FILL PORT and take the syringe out of the glove box. Connect the rubber tube to the upper connection and the rubber tube to the 2.5mlsyringe, just as was done previously in the preparation of the test. Use the 2.5ml-syringe to suck cleaning toluene from a beaker, through the syringe, to finish the cleaning. Repeat this until the toluene that comes out is transparent.

5. Remarks

When the precipitation of AgCl was studied, the samples were also stored in the dark. The cleaning procedure was performed with distilled water.

The reference cell was filled with toluene for the experiments performed with asphaltenes, crude oils and n-heptane. It was filled with water + NaCl for the AgCl precipitation. The liquid filling the reference cell does indeed affect the signals.

Appendix IV-2: Precipitation of AgCl(s)

A solution of $AgNO_3$(aq) is added to a solution of NaCl(aq). A precipitate forms according to the following reaction:

$$Ag^+ + Cl^- \rightleftarrows AgCl(s) \qquad K = \frac{1}{K_s} = 10^{9.75}$$

The concentrations and volumes are C', V' for Ag^+ and C, V for Cl^-.

However, if the concentrations in Ag^+ is not sufficient, two complexes can be formed:

$$Ag^+ + Cl^- \rightleftarrows \{AgCl\} \qquad K' = \frac{1}{K_{d1}} = 10^{2.85}$$

$$Ag^+ + 2Cl^- \rightleftarrows \{AgCl_2\}^- \qquad K'' = \frac{1}{K_{d2}} = 10^{4.72}$$

The precipitate appears when the condition $[Ag^+][Cl^-] = 10^{-9.75}$ is filled.

The concentration in ions Ag^+ can be calculated as follows:

$$[Ag^+]_{total} = [Ag^+]_{free} + [Ag^+]_{complex1} + [Ag^+]_{complex2}$$

$$[Ag^+]_{total} \approx [Ag^+]\left(1 + \frac{[Cl^-]}{K_{d1}} + \frac{[Cl^-]^2}{K_{d1}K_{d2}}\right)$$

Furthermore, due to dilution,

$$[Ag^+]_{total} = \frac{C'V'}{V + V'}$$

Thus, the volume required in Ag^+ to start precipitation is:

$$V \approx \left(1 + \frac{[Cl^-]}{K_{d1}} + \frac{[Cl^-]^2}{K_{d1}K_{d2}}\right)\frac{V K_s}{CC'}$$

$[Cl^-]$ is assumed to be equal to C since the injected volume is small and the quantity of Ag^+ is little. After calculation with our system conditions (C=0.078 mol/L, V=1.5 mL, C'=0.048 mol/L), the minimum volume to inject is 75.8 μL. Without taking into account the complex formation, the volume is 75.5 μL.

Appendix IV-3: Enthalpograms of the precipitation of AgCl

The figure below shows some of the enthalpograms obtained during the titration of NaCl with $AgNO_3$. The large deviations between the different experiments are likely to be due to an improper cleaning of the cell.

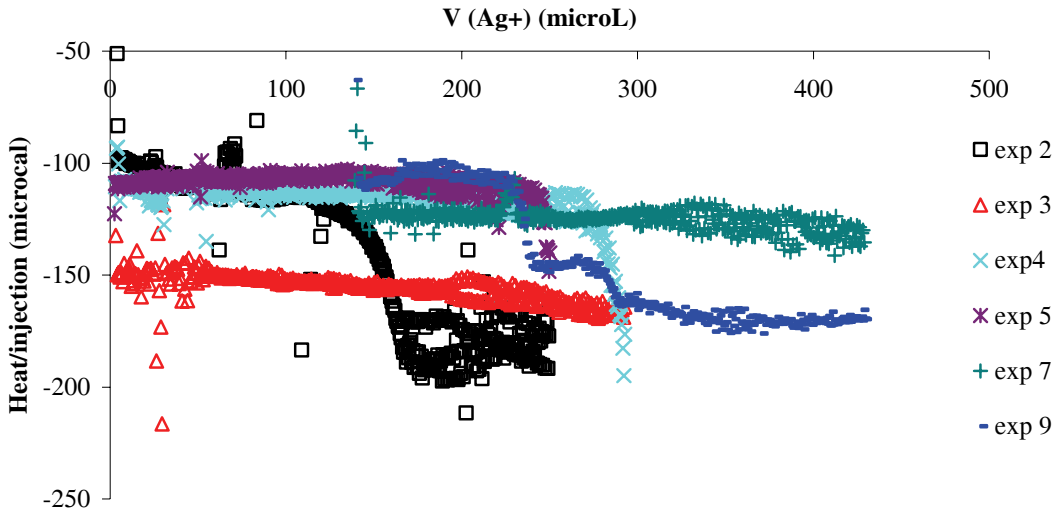

Figure 5: Enthalpograms of the titration of NaCl with AgNO3 at 303.15 K

Appendix IV-4: Enthalpograms of the precipitation of Boscan solutions

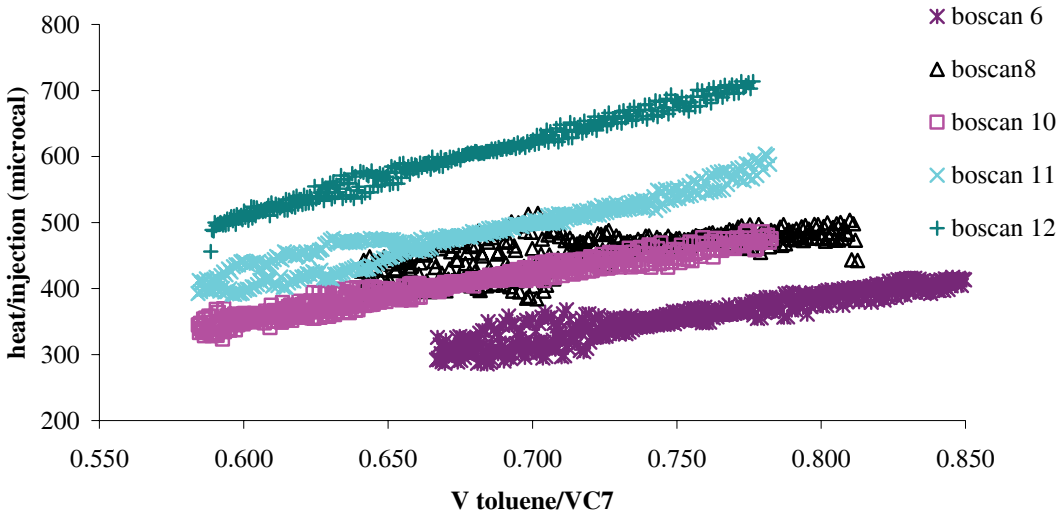

Figure 6: Enthalpograms of the titration with n-C_7 of Boscan solutions in a toluene/heptane mixture at 303.15 K (concentration of asphaltenes 1.4 g/L)

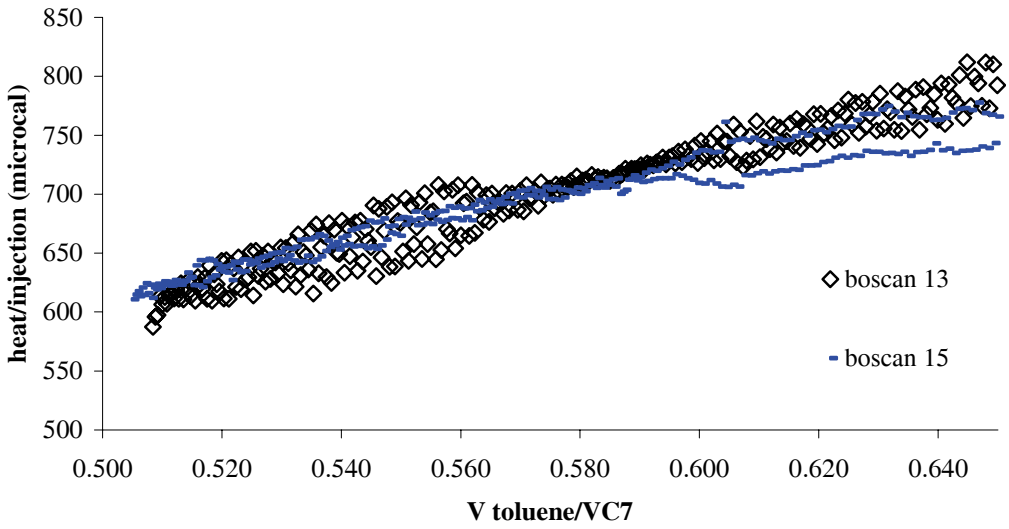

Figure 7: Enthalpograms of the titration with n-C_7 of Boscan solutions in a toluene/heptane mixture at 303.15 K (concentration of asphaltenes 10 g/L)